NASA TECHNICAL TRANSLATION

NASA TT F-803

(NASA-TT-F-803) DISTRIBUTION OF ENERGY IN THE SOLAR SPECTRUM AND THE SOLAR CONSTANT (Kanner (Leo) Associates) 253 P HC $6.50 CSCL 03B

N74-29259

Unclas H1/30 43764

JUL 1974 RECEIVED NASA STI FACILITY INPUT BRANCH

NASA TT F-803

DISTRIBUTION OF ENERGY IN THE SOLAR SPECTRUM AND THE SOLAR CONSTANT

by Ye. A. Makarova and A. V. Kharitonov

Nauka Publishing House
Moscow, 1972

NATIONAL AERONAUTICS AND SPACE ADMINISTRATION • WASHINGTON, D. C. • JUNE 1974

1. Report No.	2. Government Accession No.	3. Recipient's Catalog No.
NASA TT F-803		

4. Title and Subtitle	5. Report Date
DISTRIBUTION OF ENERGY IN THE SOLAR SPECTRUM AND THE SOLAR CONSTANT	June 1974
	6. Performing Organization Code
7. Author(s)	8. Performing Organization Report No.
Ye. A. Makarova and A. V. Kharitonov	
	10. Work Unit No.
	11. Contract or Grant No. NASw-2481
9. Performing Organization Name and Address	13. Type of Report and Period Covered
Leo Kanner Associates Redwood City, CA 90463	Translation
12. Sponsoring Agency Name and Address	14. Sponsoring Agency Code
National Aeronautics and Space Administration Washington, D.C. 20546	

15. Supplementary Notes

Translation of "Raspredeleniye energii v spektre Solntsa i solnechnaya postoyannaya," Nauka Publishing House, Moscow, 1972, pp. 1-288

16. Abstract

Information on the energy flux emitted by the sun and its spectral components is collected in the book. A critical review is given of research (including also work done by the book's authors) on the subject. Based on numerous measurements using different techniques, the most reliable value for the solar constant is derived, 1.95 cal/cm^2·min, or 136 mw/cm^2; also presented are mean-weighted data on the distribution of energy in the solar spectrum from 1400 angstroms to 0.3 mm. Individual chapters deal with the following topics: distribution of energy in the spectrum of the solar photosphere, methods of determining the solar constant, calculation of the attenuation of energy in the terrestrial atmosphere, and instrumental problems. The information presented reflects the status of the problem as of the end of 1971. Virtually none of the numerous theoretical models of the photosphere are discussed. The need for a new international spectrophotometric reference standard is stressed.

17. Key Words (Selected by Author(s))	18. Distribution Statement
	Unclassified - Unlimited STAR Category 30

19. Security Classif. (of this report)	20. Security Classif. (of this page)	21. No. of Pages	22. Price*
Unclassified	Unclassified	253	$6.50

*For sale by the National Technical Information Service, Springfield, Virginia 22151

DISTRIBUTION OF ENERGY IN THE SOLAR SPECTRUM AND THE SOLAR CONSTANT

/2*

Ye. A. Makarova and A. V. Kharitonov

ANNOTATION

Raspredeleniye energii v spektre Solntsa i solnechnaya postoyannaya /Distribution of Energy in the Solar Spectrum and the Solar Constant/, Makarova, Ye. A., and Kharitonov, A. V., Main Editorial Board of Physics and Mathematics Literature of the Nauka Publishing House, 1972, 288 pp.

Information on the flux of energy emitted by the sun and its spectral components is collected in the book. A critical review is given of research (including also work done by the book's authors) on the subject.

Based on numerous measurements using different techniques, the most reliable value for the solar constant is derived, 1.95 cal/cm^2 · min, or 136 mw/cm^2, and also mean-weighted data on the distribution of energy in the solar spectrum from 1400 angstroms to 0.3 mm. Individual chapters deal with the following: distribution of energy in the spectrum of the solar photosphere, methods of determining the solar constant, calculating the attenuation of energy in the terrestrial atmosphere, and equipment problems.

Figures: 61, Tables: 33.

* Numbers in the margin indicate pagination in the foreign text.

PRECEDING PAGE BLANK NOT FILMED

In the Memory of Vasiliy Grigor'yevich Fesenkov

FOREWORD /5

The brilliant progress of space navigation has brought about, in particular, an unexpectedly great interest in investigations of classical astrophysics such as the determination of the solar constant and the study of the distribution of energy in the spectra of the sun and other stars. Investigations of the distribution of energy in the solar spectrum undertaken by Langley and Abbot early in this century were extremely laborious and cumbersome and were "not effective." Nonetheless, during 1965-1970 about 100 studies directly related to this subject were completed; this is much more than had been undertaken during the 60 years before the beginning of the "space age." And many series of observations were made beyond the earth's troposphere, on aircraft, balloons, rockets, and satellites.

The unusual rise in the number of studies on a subject that is generally not so popular is accounted for by the necessity of solving several problems, quite concrete and sometimes far removed from astrophysics. For example, in calculating the thermal balance of a spacecraft and the number of silicon photocells needed to power its equipment, one must know quite accurately the distribution of energy in the solar spectrum. Still, the disparity between individual series of observations is as much as 10-20 percent, which in the estimate of M. P. Thekaekara yields an error in determining the efficiency of photocells of as much as 2 percent, and about 10 percent error -- in the fraction of energy absorbed by a given paint with which the spacecraft is coated; this indeterminacy costs quite dearly in performing space flights.

Precise information on the spectral components of the flux /6 of solar radiation, especially in the ultraviolet (UV) region is essential in solving several geophysical problems associated, for example, with processes occurring in the upper layers of the earth's atmosphere, and in the infrared (IR) region -- in studying the thermal balance of the terrestrial atmosphere.

Finally, revising data on the distribution of energy, especially in the far UV and IR spectral regions lets us build a

PRECEDING PAGE BLANK NOT FILMED

more faithful model of the solar atmosphere -- the foundation of solar astrophysics.

We estimate that at the present time about ten reliable series of direct determinations of the solar constant and about 30 reliable series of direct determinations of energy distribution can be used (cf. Chapters Two and Five). The paramount problem is how to use the series: whether to select the "best" one series and to adopt it as the standard in each category, or else to derive mean values, considering as far as possible the reliability of the series, and to regard this mean as being the most dependable?

As for direct determinations of the solar constant, it is evidently quite clear that one can use only mean values. In fact, such measurements, possible in principle only as the result of observations at high altitudes, were made on different absolute scales (cf. Chapter Two), none of which we have the right to give a preference for, all the more so in that it is precisely the mean of these independent determinations that augments the reliability of the end result.

The situation is more involved when we deal with the distribution of energy. Some of the authors directly undertaking this kind of investigation assume that it is precisely their series that must be regarded as the most reliable and used as the standard. But owing to the extreme laboriousness and many steps of the reductions needed to arrive at results in absolute units over a wide spectral region, the majority of the results, even if not all, are fraught with explicit or implicit systematic errors (cf. Chapter Five). By the irony of fate, it is precisely the results that aspire to be unique that contain explicit systematic errors, that is, one can indicate the Table number and the spectral region where these data cannot be used. This applies, for example, to one of the best observational series taken in Europe by D. Labs and H. Neckel, and in the United States by the Thekaekara group. Even going beyond the bounds of the terrestrial troposphere, simultaneous observations, and a single spectral photometric standard used in five series of the Thekaekara group did not eliminate systematic wavelength-dependent discrepancies, for which an explanation cannot be found. /7

Therefore we believe that the most reliable and maximally accurate data can be obtained only by a weighted averaging of an adequate number of the best observational series. We cannot base our conclusion on any single series, however methodologically advanced it appears and whatever the internal precision it has, since there is never a complete guarantee that the result does not contain some unrevealed systematic error. When we have a large group of measurement series, possible systematic errors of each series emerge as random errors and are significantly cancelled out after averaging.

We will attempt to give the fullest possible critical review of investigations made of the total energy flux emitted by the solar photosphere, its spectral components (Chapters Two and Five), and associated data on the function of the darkening of the solar disk toward its limb and the fraction of energy emitted in Fraunhofer lines (Chapter Four). By averaging the best results, we hope that we have derived the most reliable numerical characteristics of solar emission, which can be recommended as a kind of "standard". Information of this kind cannot be obtained without allowing for the losses of light in the terrestrial atmosphere (Chapter One). Naturally, we have had to also examine methods of absolute spectral photometry used not only in solar, but also in stellar research (Chapter Three).

Our main goal is to gather facts; we virtually deal with none of the numerous theoretical models of the photosphere (the abundance of models reflects, in our view, inadequate reliability and inadequate detail of factual data).

Information gathered in this book reflects the status of the problems of interest to us as of approximately the end of 1971. By the time of the book's publication (end of 1972), only three works had appeared /415-417/ on the solar spectrum, and here involving only the UV and IR ends of the solar spectrum. The new reviews by Thekaekara /418/ and Tousey (in the collection /420/) are based on the same primary sources as the previous reviews /157, 378/. In contrast, a stream of studies related to measurement techniques, setting up of reference standards, and so on, is steadily growing; being unable to enumerate all journal articles, we will mention only several works that have a summary nature. Directly related to the content of Chapters One to Three and Five are the books /419-422/ and the article /423/; the problem of setting up reliable IR reference standards is discussed in /424/.

The sharp decline in the number of works directly dealing with the flux of solar emission, compared with the average number of works over the preceding 5 years, given the simultaneous increase in the number of "auxiliary" investigations, confirmed our conclusions that it is essential to improve the precision of measurements by one order of magnitude in order to refine data on the energy radiated by the sun (see "Conclusions"), which probably will require about 10 years.

The foregoing lets us take the liberty to state that this review has been compiled in time and that the mean "standard" data on the flux of solar radiation presented at the end of the book can scarcely require substantial changes in the immediate future.

Doubtless, this publication -- the first of its kind as far as we know -- is admittedly marked by numerous shortcomings. The authors will be very grateful to readers for the critical comments and suggestions.

We are happy to be able to express our gratitude to Professors M. P. Thekaekara, A. Drummond /deceased/, and K. Ya. Kondrat'yev, and to Drs. D. Heath, and G. A. Nikol'skiy for valuable discussion on a number of essential questions and for making available preprints of publications difficult to acquire. We are grateful to N. I. Kozhevnikov, A. B. Delone, G. A. Krakhmal'nikova, E. A. Lapina, and A. V. Kurchakov, whose counsel and remarks we have utilized.

Moscow-Alma-Ata
November 1971,-October 1972

Ye. A. Makarova and
A. V. Kharitonov

TABLE OF CONTENTS

	Page
Annotation	iii
Foreword	v
Table of Contents	ix
Introduction	1
Chapter One. Attenuation of Radiation in the Terrestrial Atmosphere and Its Calculation	6
1. Introductory remarks	6
2. Superposition principle and Bouguer's law. Cases of their violation	8
3. Scattering of light in the terrestrial atmosphere	14
4. Absorption of light in the terrestrial atmosphere	21
5. Practical determination of the transmission coefficient and monitoring the stability of optical properties of the atmosphere	34
Chapter Two. Determination of the Solar Constant	41
1. Introductory remarks	41
2. Instruments used in measuring the total flux of solar radiation	44
3. Methods of determining the solar constant used by the Smithsonian Institution	51
4. Measurements of solar constant outside the earth's troposphere	54
5. Variability of the sun as a star	74
Chapter Three. Instrumental Problems in Absolute Spectrophotometry	80
1. Introductory remarks	80
2. Temperature scale	84
3. Model of an absolute blackbody as a primary spectrophotometric reference standard and other techniques of energy calibration	90
4. Secondary spectrophotometric standards	98
5. Fourier spectrometer	106
Chapter Four. Effect of Limb Darkening of the Solar Disk and the Effect of Absorption Lines on the Distribution of Energy in the Solar Spectrum	119
1. Limb darkening	119

Chapter Four /continued/
2. Intensity of solar radiation in the continuous and integrated spectra, coefficients of conversion between these spectra 124
3. Variations in equivalent line widths from solar disk center to limb. Corrections for absorption lines for the entire disk 128
4. Integral "line blanketing" effect 132

Chapter Five. Distribution of Energy in the Spectrum of the Solar Photosphere 133
1. First investigations of the distribution of energy in the solar spectrum 135
2. Distribution of energy in the photospheric spectrum in the region 0.3-3 microns 141
3. Rocket region of ultraviolet emission of the solar photosphere, 1400-3000 angstroms 169
4. Infrared spectrum of the photosphere, 3-300 microns 184
5. Mean data on the distribution of energy in the spectrum of the quiet photosphere in the region 1400 angstroms - 0.3 mm 201

Conclusions 207

Tables of Mean Data 212

References 222

INTRODUCTION

The goal of this book is to present information, as substantiated and reliable as possible, on the total flux of energy emitted by the solar photosphere, and on the spectral components comprising this flux, in other words, to present the distribution of energy in the spectrum of the quiet photosphere.

The very concept "photosphere" is somewhat vague; according to M. Minnaert /1, page 80/, "this consists of the solar layers that are the direct source of virtually all solar radiation we observe." We supplement this definition by noting the fact that is of fundamental importance for all that follows, namely that in the photosphere temperature (as well as density) decreases in the direction toward outer layers.

The apparent indeterminacy of the localization of the photospheric layer disappears if we consider that the coefficient of absorption for radiation emanating from the solar interior and, therefore, the opacity of the solar plasma -- are enormous, so that the thickness of the layer emitting virtually all the flux energy is negligibly small and does not exceed 0.001 solar radius, which is no more than 400 km. The solar limb distinctly visible in the continuous spectrum is thus its photosphere and it determines the visible dimensions of the sun.

In referring to the flux of energy emitted only by the photosphere, we thus limit ourselves to the spectral region of investigation that ranges from ~1400 angstroms to roughly 0.2 to 0.5 mm. Outside this intervalthe photosphere is unobservable, since the optical thickness of the upper layers of the solar atmosphere -- the chromosphere and the corona -- increases rapidly for $\lambda < 1400$ angstroms and $\lambda > 0.2$-0.5 mm, wholly covering the photosphere from the observer. The temperature gradient of these layers has a sign that is opposite to the photospheric layer sign: the temperature increases with altitude.

Approximately 99.999 percent of the total flux of solar electromagnetic radiation departs from the photosphere, and this flux is quite time-constant; while it does vary, it does so by not more than tenths of a percent (cf. Chapter Two), in spite of the existence in the photosphere of active formations (spots, flares, and faculae) and the cyclicity of solar activity. /10

The remaining fraction of the flux, even though representing only 0.001 percent of the total value, nonetheless plays a most important role in processes occurring in the terrestrial atmosphere under the effect of solar radiation. Its components, on the one hand, far UV radiation, extending to hard x-ray irradiation, and on the other -- radio emissions -- are characterized by the fact that they react strongly to the extent of activity in the underlying photosphere. Characteristics of processes in the chromosphere and the corona that give rise to intense emission in the far spectral regions and the effect of this radiation on the terrestrial atmosphere have been dealt with in numerous interesting monographs, to which we refer the reader /2-8/.

For convenience of the further presentation, let us enumerate several astronomical (and physical) concepts used in the text[1] that are vital to the subject. All the following applies to the quiet photosphere.

The continuous spectrum of the photosphere (continuum). In the propagation of radiation from the solar interior toward the solar surface, the interaction of radiation with the solar plasma occurs to a considerable extent via nonquantized free-free and free-bound transitions, which ultimately leads to the formation of quanta of arbitrary frequencies -- to the continuous spectrum.

Owing to the presence in the photospheric spectrum of absorption lines, the true continuous spectrum is not accessible to observation in all wavelength regions. In sections where the lines are numerous and their wings overlap, we will use a concept of a "quasi-continuum". The quasicontinuum is constructed as the /11

[1] Only the most fundamental definitions and concepts essential here are presented, due to shortage of space. While we do deal with the physical processes determining these concepts, we do so only very schematically. Complete information, generally essential for an understanding of the text, can be found by the reader in monographs and handbooks. Thus, the physical characteristics of the sun have been collected, for example, in /9-12/, astrophysical concepts -- in /11-16/, and a description of physical processes occurring in plasma generally and the solar plasma in particular -- in /17, 14, 15/.

envelope of spectral points relatively free of absorption lines (spectral windows -- cf. Section 2, Chapter Four). The intensity of the quasi-continuum is less than or equal to the intensity of the true continuous spectrum.

The line (Fraunhofer) spectrum is produced in quantized bound-bound transitions of atoms and ions of the solar atmosphere; the coefficient of absorption of the plasma increases sharply in the corresponding frequencies, and absorption lines are formed against the background of the continuous spectrum.

The integrated spectrum is the actually observed solar spectrum, in which absorption lines are visible against the background of the continuous spectrum. The intensity of this spectrum depends strongly on the width of the pass band of the spectral instrument (or on the wavelength range in which averaging is carried out), while the dependence is weak for the continuous spectrum (with the exception of singular points -- the limits of the absorption series of individual elements. We refer to a fundamental aspect; in practice a very high spectral resolution is essential to reveal the quasi-continuum, especially at $\lambda < 4300$ angstroms; cf. Section 1, Chapter Three).

The distribution of energy in the photospheric spectrum, in other words, the dependence of radiation intensity on wavelength, is determined by the ratio between the coefficient of emission $\epsilon(\lambda)$ and the coefficient of absorption $\chi(\lambda)$ of the solar plasma. Kirchhoff's law is applicable to each elementary volume:

$$\frac{\varepsilon(\lambda)}{\varkappa(\lambda)} = f(\lambda, T). \tag{1}$$

The condition of local thermodynamic equilibrium is observed in the quiet photosphere and we have

$$f(\lambda, T) = B(\lambda, T),$$

where $B(\lambda, T)$ is Planck's function:

$$B(\lambda, T) = \frac{2hc^2}{\lambda^5} \cdot \frac{1}{e^{\frac{hc}{\lambda kT}} - 1} = \frac{C_1}{\lambda^5} \cdot \frac{1}{e^{\frac{c_2}{\lambda T}} - 1}. \tag{2}$$

The coefficient χ is determined principally by the absorption by negative hydrogen ions. /12

For the entire photosphere the transfer equation takes account of the overall action of elementary volumes lying along the line of sight. As a result, to the first, very rough approximation, the distribution of energy in the photospheric spectrum will be described by Planck's function at temperatures close to the effective temperature.

The effective temperature characterizes the total radiation of the solar surface, integrated over all wavelengths; it is defined as the parameter of the Stefan-Boltzmann law, which is a consequence of Planck's law:

$$B(T)=\frac{\sigma}{\pi}T_{\text{eff}}^{4} \qquad (3)$$

Since the sun as a whole is not in a state of complete thermodynamic equilibrium, the concept of "temperature" is not single-valued. In addition to the effective temperature, we will use two more "temperatures" /18/.

The spectrophotometric temperature T_S is the T value at which the shape of the Planck curve (2) best approximates the shape of the energy distribution curve.

The brightness temperature T_b characterizes the monochromatic intensity (brightness) of the radiator; it is equal to the temperature of an absolutely black body with the same monochromatic brightness. The T_b of the photosphere varies along the spectrum by more than 30 percent (cf. Table 28).

Below we present a list of the main symbols, and also the values of the physical and astronomic constants used in this book.

1. $I_\lambda(0)$ is the intensity of radiation from the center of the solar disk (erg/cm^2 · sec · sterad · cm), that is, of the radiation emanating along the normal to the photospheric layers.

$I_\lambda(\theta)$ is the intensity of radiation emanating at the angle θ to the normal.

$F_\lambda = \frac{1}{\pi}\int_{\omega} I_\lambda(\theta)\cos\theta\, d\omega$ is the disk-averaged intensity of solar radiation (erg/cm^2 · sec · sterad · cm).

$S_\lambda = \pi(R_\odot^2/\Delta^2)F_\lambda$ is the monochromatic illumination produced by the sun at the mean earth-to-sun distance Δ ($R_\odot$ is the solar radius) (erg/cm^2 · sec · cm).

$S_0 = \int_0^\infty S_\lambda d\lambda$ is the solar constant (erg/cm^2 · sec; cal/cm^2 · min; w/cm^2). /1

The symbol I_λ usually refers to the continuous spectrum (continuum) and F_λ refers to the integrated spectrum. In some special cases of departure from this rule, we insert the superscript "c" as the continuum, "i" -- as the integrated, "d" -- disk, and "ce" -- center.

2. Several astronomical and radiation constants are as follows[2]:

Δ = 1 a.u. = 149,600 · 10^6 m (astronomical unit),
c = 299,792.5 · 10^3 m/sec (speed of light),
h = 6.62559 · 10^{-27} erg · sec (Planck's constant),
k = 1.38054 · 10^{-16} erg/° K (Boltzmann's constant),
σ = 5.6698 · 10^{-5} erg/cm^2 · sec · ° K^4 (Stefan-Boltzmann constant),
$c_1 = 2hc^2$ = 1.1910 · 10^{-5} erg · cm^2/sec (first radiation constant),
c_2 = hc/k = 1.43879 cm · ° K (second radiation constant),
T_{Au} = 1337.58° K (melting point of gold), and
1 cal = 4.1840 J = 4.1840 · 10^7 erg = 4.1840 w · sec.

[2] Cited from decisions of the International Astronomical Union, 1964 /19/ and the International Committee on Measures and Weights, cf., for example, /20/.

CHAPTER ONE /14

ATTENUATION OF RADIATION IN THE TERRESTRIAL ATMOSPHERE AND ITS CALCULATION

1. Introductory Remarks

At the present time it has been established that the earth's atmosphere extends to altitudes of upwards of a thousand kilometers. Its density gradually decreases and at high altitudes fluctuates as a function of solar activity, increasing during the maxima of the latter. The upper limit of the atmosphere is not denoted physically: the high rarefied gaseous formation called the geocorona extends up to 10,000-20,000 km from the earth's surface, gradually intergrading into interplanetary space.

Physical conditions of atmosphere vary very decidedly with altitude; depending on how they vary, the atmosphere will be divided into a number of layers. The division into layers can differ, depending on which parameter is taken as the criterion of division. The arrangement of layers is illustrated with Figure 1, taken from the Spravochnik of Yu. A. Glagolev /21/. In turn, the Spravochnik data are based on the recommendations of the International Union of Geodesy and Geophysics (1953), extensively revised in subsequent studies, and the so-called SMA -- standard models of the atmosphere -- constitute the generalized results of these investigations. The SMA provide mean values of physical parameters of the atmosphere at different altitudes, based on analysis and averaging of a great deal of observational material in which local and temporal variations of a random nature are smoothed out. The standard 1964 USSR model of the atmosphere (SMA USSR) is used in the Soviet Union, confirmed as GOST /State Standard/ 4401-64 as the fundamental document for various design projects.

Table 1 gives a brief summation of variation with altitude of several mean parameters of the atmosphere according to the SMA USSR (the data are cited from /21/).

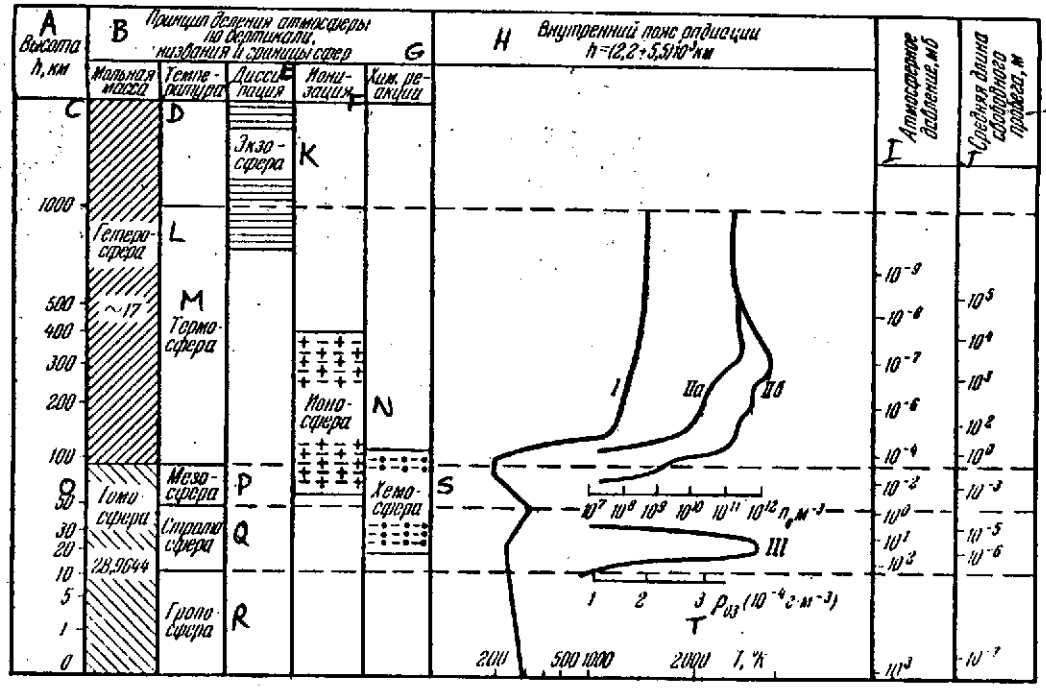

Fig. 1. Scheme of vertical structure of atmosphere. I -- Air temperature (° K), IIa and IIb -- concentration of electrons at night a) and in the daytime b), and III -- density of ozone.

KEY:
- A -- Altitude, h, km
- B -- Principle of division of the atmosphere along the vertical, names and bounds of spheres
- C -- Molar mass
- D -- Temperature
- E -- Dissipation
- F -- Ionization
- G -- Chemical reactions
- H -- Inner radiation belt
- I -- Atmospheric pressure, millibars
- J -- Mean free path length
- K -- Exosphere
- L -- Heterosphere
- M -- Thermosphere
- N -- Ionosphere
- O -- Homosphere
- P -- Mesosphere
- Q -- Stratosphere
- R -- Troposphere
- S -- Chemosphere
- T -- ρ_{ozone} (10^{-4} g · m^{-3})

TABLE 1. VARIATION WITH ALTITUDE OF SEVERAL PHYSICAL PARAMETERS OF THE ATMOSPHERE ACCORDING TO SMA USSR /16

Altitude h, km	Temperature, t, °C	Density, ρ, 10^{-3} g/cm^3	Pressure, P, millibars
0,0	+ 15,00	1,2250	1013,25
0,5	+ 11,75	1,1672	954,53
1,0	+ 8,50	1,1117	898,76
1,5	+ 5,25	1,0582	845,66
2,0	+ 1,99	1,0066	794,98
3,0	— 4,51	$9,0941 \cdot 10^{-1}$	701,25
4,0	— 11,02	$8,1942 \cdot 10^{-1}$	616,56
5,0	— 17,52	$7,3654 \cdot 10^{-1}$	540,45
8,0	— 37,01	$5,2591 \cdot 10^{-1}$	356,48
10	— 50,00	$4,1357 \cdot 10^{-1}$	264,91
11	— 56,49	$3,6485 \cdot 10^{-1}$	226,90
20	— 56,49	$8,8870 \cdot 10^{-2}$	55,269
30	— 42,80	$1,7901 \cdot 10^{-2}$	11,836
40	— 15,49	$4,0003 \cdot 10^{-3}$	2,9586
50	+ 0,85	$1,0754 \cdot 10^{-3}$	$8,4581 \cdot 10^{-1}$
60	— 19,75	$3,3162 \cdot 10^{-4}$	$2,4121 \cdot 10^{-1}$
70	— 54,00	$9,2747 \cdot 10^{-5}$	$5,8343 \cdot 10^{-2}$
80	— 88,15	$2,0979 \cdot 10^{-5}$	$1,1141 \cdot 10^{-2}$
90	— 88,15	$3,4733 \cdot 10^{-6}$	$1,8444 \cdot 10^{-3}$
100	— 63,93	$5,3993 \cdot 10^{-7}$	$3,2411 \cdot 10^{-4}$
200	+ 953,61	$3,6109 \cdot 10^{-10}$	$1,3633 \cdot 10^{-6}$
300	+1084,8	$3,3531 \cdot 10^{-11}$	$1,5939 \cdot 10^{-7}$

/Commas in numbers are equivalent to decimal points in American usage./

Details on interesting processes and phenomena occurring in atmospheric layers can be found in numerous literature sources, for example /22-36/.

In conclusion, let us dwell on the concepts of altitude of a homogeneous atmosphere. For each given locality with elevation h above sea level, we designate the altitude of a standard isothermal gaseous layer whose density is equal to the density of the air at sea level, and whose pressure is the actual pressure at elevation h. The altitude of a homogeneous atmosphere H depends on temperature t and for sea level is equal to the following values /9/:

t, °C	—30	—15	0	+15	+30
H (0), km	7.113	7.552	7.991	8.430	8.869

Ordinarily, the value of H for 0° C is used for all kinds of calculations.

2. Superposition Principle and Bouguer's Law. Cases of Their Violation /17

One of the fundamental principles of optics formulated at the very dawn of its inception is the superposition principle.

It states that different light rays in their propagation usually do not interact with each other. To compel them to interact one must take special measures ensuring, for example, their coherence. But in natural conditions ... "everyday experience shows us that the action of light beams is independent, that is, the effect wrought by a single beam does not depend on whether other beams act simultaneously or whether they have been eliminated. Thus, if light from a broad landscape strikes the objective lens of a camera, then by obstructing access to some of the light beams, we do not change the images yielded by the remaining beams" (G. S. Landsberg /37, page 14/). In other words, "... for light waves the perturbation (at a given point and a given instant of time) produced upon passage of a series of waves is equal to the algebraic sum of the perturbations produced by each wave separately" (Ditchburn /38, page 46/).

This formulation is quite general: intensifying and weakening of light observed in an interference pattern, which represents a special case of the algebraic sum of perturbations, do not contradict it.

The superposition principle determines the nature of the attenuation of light when passing through matter. Actually, suppose a beam of rays with intensity I passes through a layer of material with thickness dl. We can represent the beam as a set of "elementary" rays with intensity i, for each of which the attenuation di is proportional to i:

$$di = -i\varkappa dl. \tag{4}$$

Since by the superposition principle the propagation and action of "elementary" rays do not depend on each other, the parameter $\varkappa$ cannot depend on their "number", that is, on the intensity of the entire beam I, but is only a characteristic of the medium, /18 where in the general case $\varkappa = \varkappa(l)$. For the entire beam we will have

$$dI(\lambda) = -I(\lambda)\varkappa(\lambda, l)\,dl, \tag{5}$$

whence

$$I(\lambda) = I_0(\lambda)e^{-\int \varkappa(\lambda, l)\,dl}. \tag{6}$$

The law of the attenuation of light expressed by equation (6) was first formulated in 1729 by the eminent French physicist Pierre Bouguer in his work "Experiment on the Gradation of Light" and subsequently more extensively in "Optical Treatise on the Gradation of Light" /39/. This law has been justly referred to as Bouguer's law, although it is sometimes called the Bouguer-Lambert law and the "Bouguer-Lambert-Beer" law in honor of the physicists also involved with problems of the attenuation of light in various media.

Bouguer's law and, therefore, the superposition principle underlying it have withstood, in the words of A. A. Gershun, "the most severe experimental verification" /40/.

With the aid of simple ingenious devices, S. I. Vavilov succeeded in 1920 in verifying the validity of Bouguer's law by varying the density of light flux from $2.5 \cdot 10^{-12}$ erg/cm^2 · sec to $2 \cdot 10^8$ erg/cm^2 · sec /41/. The index of attenuation $\chi(\lambda, l)$ remains independent of light flux when the density of the latter is varied by nearly 20 orders of magnitude!

Equation (6) enables us to determine several optical characteristics of a medium. The quantity $\chi(\lambda, l)$ is called the index of attenuation, and the quantity

$$\tau(\lambda) = \int \chi(\lambda, l)\, dl \tag{7}$$

is called the optical thickness of the medium. The index of attenuation is the optical thickness calculated per linear unit of the path length. Incidentally, sometimes the index $\chi(\lambda)$ is calculated per unit not of length, but of mass or volume of the material along the path of the beam (unit cross-section), and sometimes even per single molecule; in the latter case the index of attenuation is called the cross-section of attenuation. /19 Often one uses the concept "decimal coefficient (index) of attenuation"

$$\chi_{10}(\lambda, l) = 0.4343\chi(\lambda, l). \tag{8}$$

The concepts "index of attenuation" and "optical thickness" are employed also for the terrestrial atmosphere as a light-attenuating medium. The optical thickness of the atmosphere in the vertical direction is distinguished:

$$\tau(\lambda, 0) = \int_{h_0}^{H} \chi(\lambda, h)\, dh \tag{9}$$

and the optical thickness of the atmosphere in the direction toward a point with zenith distance z:

$$\tau(\lambda, z) = M(z) \int_{h_0}^{H} \chi(\lambda, h)\, dh. \tag{10}$$

Integration is performed with respect to the altitude, h_0 is the altitude of the observer, and H is the upper bound (arbitrary) of the atmosphere. The quantity

$$M(z) = \frac{\tau(\lambda, z)}{\tau(\lambda, 0)}, \tag{11}$$

which is the ratio of the optical thicknesses of the atmosphere in the direction with zenith distance z and in the vertical

direction, is called the atmospheric, or air, mass. If the atmosphere consisted of plane-parallel layers and if we could neglect refraction, then the following equality would be valid:

$$M(z) = \sec z, \tag{12}$$

that is, the atmospheric mass to the first approximation does not depend on wavelength. This function derives from the refractive curvature of an inclined ray in the atmosphere and is very weak, since the index of refraction of air differs only slightly from unity and changes only slightly with wavelength. Taking account of refractive effects and the curvature of the earth leads to a highly complicated form of the function M(z), which has to be modified even further as data on physical conditions in the upper atmospheric layers are revised. However, the difference /20 between true M(z) values and sec z becomes actually perceptible only for large z. Thus, when $z < 70^\circ$, it does not exceed 0.7 percent, when $z = 73.2^\circ$ it is 1 percent, when $z = 80^\circ$ it is 2.9 percent, and so on. Therefore, in reducing observations made at $z < 70^\circ$, we can quite properly use the values M(z) = sec z. The function M(z) has been tabulated more accurately by Bemporad /42/ His tables are reproduced, in particular, in /43, pages 507-510/.

The air mass determined by formula (11) does not depend, to the first approximation, on which elevation above sea level and to which atmospheric pressure observations are made, since both optical thicknesses $\tau(z)$ and $\tau(0)$ are approximately proportional to the physical mass $\int_{h_0}^{H} \rho(h)\,dh$ of a column of air of unit cross-sectional area, that is, the atmospheric pressure at level h_0. In this sense the air mass determined by expression (11) must be regarded as "relative", $M_{rel}(z)$. Still, sometimes the concept of "absolute" air mass is used in actinometry, especially in aircraft and balloon observations /44/:

$$M_{abs}(z) = \frac{\tau(z, h)}{\tau(0, 0)} = \frac{P(h)}{P(0)} \cdot \frac{\tau(z, h)}{\tau(0, h)} = \frac{P(h)}{P(0)} M_{rel}(z), \tag{13}$$

being the ratio of the optical thickness of the atmosphere above level h in the direction with zenith distance z to the vertical optical thickness above sea level (here P(h) and P(0) are pressures).

An important characteristic of a light-attenuating medium is its transmission coefficient $p(\lambda)$. It is the ratio of the intensity of a beam of rays passing through the medium to the intensity of the initial arriving beam.

We can readily obtain the following expression from formulas (6) and (7):

$$p(\lambda) = \frac{I(\lambda)}{I_0(\lambda)} = e^{-\tau(\lambda)}. \tag{14}$$

In the case of the terrestrial atmosphere, the term "transmission coefficient" applies only to the vertical direction. The expression is obvious for other zenith distances: /21

$$I(\lambda, z) = I_0(\lambda)\, p(\lambda)^{M(z)} = I_0(\lambda)\, e^{-\tau(\lambda) M(z)}. \qquad (15)$$

Equations (5), (6), and (15) are strictly valid only for monochromatic radiation, which is in fact noted by specifying the wavelength λ. But if a heterochromatic radiation flux is observed, and λ_1 and λ_2 are the limits of its spectrum, attenuation of this flux in the medium will be described by the integral of expression (6). In particular, we will have the following for attenuation in the atmosphere:

$$\int_{\lambda_1}^{\lambda_2} I(\lambda, z)\, d\lambda = \int_{\lambda_1}^{\lambda_2} I_0(\lambda)\, e^{-\tau(\lambda) M(z)} d\lambda = \int_{\lambda_1}^{\lambda_2} I_0(\lambda)\, p(\lambda)^{M(z)}\, d\lambda. \qquad (16)$$

Equation (16) shows that if the optical thickness of the medium varies with wavelength, the law of exponential attenuation of light in a medium (Bouguer's law), remaining valid for each monochromatic component of the flux of radiation, ceases to be satisfied for the entire heterochromatic flux as a whole. The function in this case is more complicated.

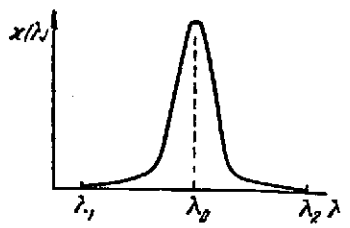

Fig. 2. In explanation of the formation of Forbes' effect

To clarify, let us examine an example taken from a book by K. Ya. Kondrat'yev /44/. Suppose the heterochromatic flux with spectral limits λ_1 and λ_2 passes through a medium that is homogeneous with constant density, undergoing highly selective absorption with its maximum at λ_0 (Fig. 2).

Even at the very outset of the optical path, radiation with wavelength close to λ_0 will be weakened to the extent that its contribution to the total flux will be negligible. Further attenuation of the total light flux will occur now only through a decrease in the radiation of other wavelength accounted for by the band wings, that is, more slowly than at the beginning of the optical path. In other words, change (decrease) in the effective attenuation index χ along the path of the ray is observed for a heterochromatic flux of radiation in a homogeneous medium. This phenomenon is called the Forbes effect. /22

The Forbes effect also occurs in the terrestrial atmosphere. The "mean" transmission coefficient of the atmosphere for rays of any celestial body at the zenith distance z is defined by the expression

$$p_{av} = \left[\frac{\int_{\lambda_1}^{\lambda_2} I_0(\lambda)\, p(\lambda)^{M(z)}\, d\lambda}{\int_{\lambda_1}^{\lambda_2} I_0(\lambda)\, d\lambda} \right]^{\frac{1}{M(z)}} \qquad (17)$$

We can easily see that the transmission coefficient depends on M(z), increasing with increase of the latter. By the definitions of N. N. Kalitin, when M varies from 2 to 3, p_{av} becomes 0.843, and when M varies from 9 to 10, p_{av} = 0.907.

The Forbes effect is the greater, the more intensely $p(\lambda)$ changes near the maximum intensity of the radiation received by the instrument, and special caution must be manifested for observations in the true absorption bands (ozone, oxygen, CO_2, and H_2O; cf. Section 4). As a rule, the bands have a complex fine structure consisting of numerous narrow lines, sometimes with developed "wings". The attenuation index in the central regions of these lines and in the intervals between them can differ by tens of times. Therefore in making observations within the bands each time one must investigate the applicability of Bouguer's law, taking two factors into account: the structure of the observed absorption band and the width of the instrument's pass band. This problem is examined, in particular, by Elzasser (cf., for example, /44, 45/) and is presented in close detail in Chapter Four of a book by R. Goody /24/. The following cases, for example, can be encountered:

1. The pass band of an instrument $\Delta\lambda$ is so narrow that within it the attenuation index can be assumed constant or linearly varying -- Bouguer's law is satisfied.

2. The pass band of the instrument $\Delta\lambda$ is quite broad, and in it several fine structure lines somewhat different in intensity are included, so that the attenuation index varies over $\Delta\lambda$ very strongly and irregularly -- as a rule, Bouguer's rule is not satisfied. /23

3. The pass band $\Delta\lambda$ is quite broad, it includes several fine structure lines, but of identical intensity and separated by intervals such that the course of the attenuation index over $\Delta\lambda$ can be represented by a sinusoidal periodic curve. Bouguer's law can be satisfied in this case.

4. The absorption band is not physically separated into fine structure (for example, for a very significant abundance of the absorbing agent). Depending on the specific conditions of the experiment, here Bouguer's law may or may not be satisfied; in solving the problem, a great deal of caution is required.

For completeness of our presentation, we must point out several other cases in which Bouguer's law is violated, besides the Forbes effect. In the past 10-15 years the possibility has arisen of producing beams of radiation with enormous, previously unachieved energy density, using lasers. Thus, ruby lasers emit energy from several tenths of a joule to hundreds of joules in the form of pulses of duration 10^{-3} to 10^{-8} sec, achieving power ratings of up to 10^9 w and higher /46/. The limiting density of energy that can be achieved per square centimeter of ruby laser surface is 10^{11} w/cm^2 /47, 48/. The beam intensity can be augmented still further by several orders of magnitude by employing focussing optics and can be brought to $10^{13} - 10^{14}$ w/cm^2, that is, 12-13 orders of magnitude above the maximum values in the experiments of S. I. Vavilov. At energy densities that are this high, new effects are observed, indicating that in these conditions the superposition principle is not satisfied, and in particular, the scattering of "light by light" takes place. Further, the intensity of the electrical field in the electromagnetic wave becomes comparable with intra-atomic fields confining electrons in atoms. As the result processes of multiphotonic absorption, for example, take place, depending on the radiation intensity along with combination scattering and other phenomena, which are studied by the fairly new field of nonlinear optics[3]. An extensive special literature deals with lasers and nonlinear optics, to which we refer interested persons, for example, /46-51/. /24

3. Scattering of Light in the Terrestrial Atmosphere

In contrast to true absorption, light is scattered without energy exchange on a macroscopic scale[4] between the radiation and the scattering medium; it amounts only to the transformation of the directions of incident light quanta.

Scattering of light in media has been investigated by numerous outstanding physicists. An account of these investigations as applied to the terrestrial atmosphere is well described in an article by G. V. Rozenberg /52/. A formula for molecular scattering in a physically wholly homogeneous medium, agreeing with experiment and observations and fully explaining the blue color of the daytime sky, was derived near the end of the past century by the British physicist Rayleigh. This conclusion was based on the representation of light as elastic oscillations of the ether, and based on the electromagnetic theory. Rayleigh's theory is presented in numerous sources, in particular, in close detail in

[3] The occurrence of certain nonlinear effects at high luminous flux densities was predicted by S. I. Vavilov (cf. /41/, pages 438-440).

[4] This exchange occurs on the scales of individual atoms; the atoms are excited, but then lose energy.

books by N. M. Shtaude [53] and M. V. Vol'kenshteyn [54], and also, for instance, in [32, 34, 44].

Rayleigh reasoned thusly. Under the effect of incident light, forced oscillations of internal oscillators are produced in gas molecules. If the molecules were fixed, secondary electromagnetic radiation produced by the molecular oscillators would be strictly coherently incident primary radiation. In this case allowance for the interference of secondary waves would lead to the scattering of light necessarily not occurring, and the luminous flux would completely preserve its initial direction. However, the thermal motion of molecules disturbs the coherence of secondary and primary radiation; here the main role is played by the Doppler effect, which displaces the phase of secondary oscillations. As a result, the interference pattern is strongly modified and scattered light appears. /25

Subsequently, L. I. Mandel'shtam criticized Rayleigh's theory with respect to the mechanism by which scattered light is formed. The theory would be valid if in a volume of space comparable in dimension with λ^3 a few molecules would be present. But under normal conditions in air this space contains $\sim 5 \cdot 10^6$ of these molecules in the volume λ^3 for $\lambda = 6 \cdot 10^{-5}$ cm.

In 1907 L. I. Mandel'shtam showed [55] that in this case it is all the same whether individual molecules or elementary volumes of matter with dimensions much smaller than λ^3 are regarded as the scattering agents. But in the latter variant it does not matter at all whether the molecules are moving within the volume or not, since the volumes themselves are fixed, destruction of coherence cannot occur, and scattered light cannot take place.

L. I. Mandel'shtam demonstrated that the scattering of light is due only to the optical inhomogeneities of the medium, that is, due to change in the index of refraction from one point in the medium to another, and not by individual molecules as Rayleigh thought.

In 1908 the Polish scientist M. Smoluchowski explained the nature of the formation of these optical inhomogeneities. He showed that due to the chaotic nature of thermal molecular motions in a medium inevitably density flucuations must arise, that is, regions where at a given instant the number of molecules is smaller than or larger than the mean number. The smaller the dimensions of the region, the more probable are the significant fluctuations. At sites where these fluctuations take place the index of refraction, dependent on the density of the medium, changes, and the initiated optical inhomogeneities lead to the scattering of light.

The study by M. Smoluchowski [56] referred only to the critical state of matter at which density fluctuations are extremely great and the matter becomes turbid. But his idea was soon

(1910) utilized by A. Einstein [57], who produced the theory of the molecular scattering of light in gas. The term "molecular scattering" used currently must be understood in the sense that even though the scattering agents are not molecules, these agents [2] are formed due to the thermal motion of molecules.

The formula for the index of attenuation $\chi_R(\lambda)$ of light in air caused by a molecular or, as it is often called, Rayleigh scattering, is of the form

$$\chi_R(\lambda) = \frac{32\pi^3 (n-1)^2}{3N\lambda^4} \cdot \frac{6+3\rho_n}{6-7\rho_n}. \qquad (18)$$

Here n is the index of refraction of air, and N is the number of molecules per cm^3. Under normal conditions, $N = 2.687 \cdot 10^{19}$ cm^{-3}. The fact that N appears in the denominator of expression (18) should not be surprising, since $(n - 1) \alpha N$, and ultimately $\chi_R(\lambda)$ is proportional not to 1/N, but to N.

The first factor in formula (18) was derived by Rayleigh himself; the second factor, numerically equal to 1.061, was introduced by Kabann to allow for the anisotropy of molecules with the further refinement of scattering theory (cf., for example, [58]). The quantity $\rho_n = 0.035$ is the so-called "depolarization factor" of molecules. By formula (18), the index of attenuation due to Rayleigh scattering is inversely proportional to the fourth power of wavelength. This is an explicit function. But the formula also has a small implicit dependence of χ_R on wavelength in terms of the index of refraction of air n. If we take the function $n(\lambda)$ into account, in the denominator the exponent at λ will be ~ 4.15 instead of 4.

In order to obtain the optical thickness caused by Rayleigh scattering for the entire atmosphere over some level h, the value $\chi_R(\lambda)$ must be multiplied by H(h) -- the altitude of the homogeneous universe for the level h, $\tau_R(h) = \chi_R \cdot H(h)$ [5].

Table 2 presents the cross-sections and index of attenuation of Rayleigh scattering, and also the optical thickness and transmission coefficient of a Rayleigh atmosphere over sea level, according to the very comprehensive calculations by R. Penndorf [59].

---

[5] The altitude of a homogeneous atmosphere for level h is usually estimated by using the ratio $H(h) = H(0) \cdot P(h)/P(0)$, where $H(0) \approx 8$ km is the altitude of the homogeneous universe for sea level; to calculate the ratio of pressures at the corresponding altitudes, P(h)/P(0), we can use, for example, the data in Table 1.

TABLE 2*. CROSS-SECTION $\sigma_R(\lambda)$ AND INDEX OF ATTENUATION $\chi_R(\lambda)$ OF RAYLEIGH SCATTERING FOR DRY AIR IN NORMAL CONDITIONS, OPTICAL THICKNESS $\tau_R(\lambda)$, AND TRANSMISSION COEFFICIENT $P_R(\lambda)$ OF RAYLEIGH ATMOSPHERE AT SEA LEVEL FOR 0° C

/27

λ, μ	$\sigma_R(\lambda)$ (cm^2)	$\chi_R(\lambda) \cdot 10^5$ cm^{-1}	$\tau_R(\lambda)$	$P_R(\lambda)$
0,20	$3,551 \cdot 10^{-25}$	954,2	7,625	$0,488 \cdot 10^{-3}$
0,25	$1.258 \cdot 10^{-25}$	338,2	2,703	$0,670 \cdot 10^{-1}$
0,29	$6,568 \cdot 10^{-26}$	176 5	1,410	0,244
0,30	$5,676 \cdot 10^{-26}$	152,5	1,219	0,296
0,31	$4,933 \cdot 10^{-26}$	132,6	1,060	0,347
0,32	$4,309 \cdot 10^{-26}$	115,8	0,9254	0,396
0,34	$3,334 \cdot 10^{-26}$	89,59	0,7159	0,489
0,36	$2,622 \cdot 10^{-26}$	70 45	0,5630	0,570
0,38	$2,091 \cdot 10^{-26}$	56,20	0,4491	0,638
0,40	$1,689 \cdot 10^{-26}$	45,40	0,3628	0,695
0,42	$1,380 \cdot 10^{-26}$	37,08	0,2958	0,745
0,44	$1,139 \cdot 10^{-26}$	30,60	0,2445	0,783
0,46	$9,482 \cdot 10^{-27}$	25,48	0,2036	0,817
0,48	$7,961 \cdot 10^{-27}$	21,40	0,1710	0,843
0,50	$6,735 \cdot 10^{-27}$	18,10	0,1446	0,865
0,55	$4,563 \cdot 10^{-27}$	12,26	0,09797	0.908
0,60	$3,202 \cdot 10^{-27}$	8,604	0,06875	0,933
0,70	$1,713 \cdot 10^{-27}$	4,605	0,03680	0,964
1,00	$4,065 \cdot 10^{-28}$	1,092	0,008726	0,991
2,0	$2,519 \cdot 10^{-29}$	0,6770	0,000541	0,999
5,0	$6,434 \cdot 10^{-31}$	$0,1729 \cdot 10^{-2}$	0,0	1,000
10,0	$4,020 \cdot 10^{-32}$	$0,1080 \cdot 10^{-3}$	0,0	1,000
20,0	$2,512 \cdot 10^{-33}$	$0,6751 \cdot 10^{-5}$	0,0	1,000

* TRANSLATOR'S NOTE: Commas represent decimal points.

In addition to molecular scattering, the scattering of light by aerosols plays a major role in the atmosphere.

The classification of atmospheric aerosols and the participation of particles of a given size in processes within the atmosphere are shown in Fig. 3, taken from a book by Ch. Yunge /36/. The finest particles ($r \leq 0.1$ micron) are called Aitken particles. Particles with sizes from 0.1 to 1.0 μ are classified as large particles, and those with size $r > 1.0$ μ -- as giant particles.

Aerosols are contained in virtually all atmospheric layers. /28
In the troposphere their mean concentration falls off rapidly with altitude, being reduced roughly by one order of magnitude with ascent from sea level to 2 km. Near the upper tropospheric limit one observes the concentration minimum, then relatively moderate growth, due to the presence of the layer of stratospheric aerosol, with a concentration maximum at the altitude of 19-20 km.

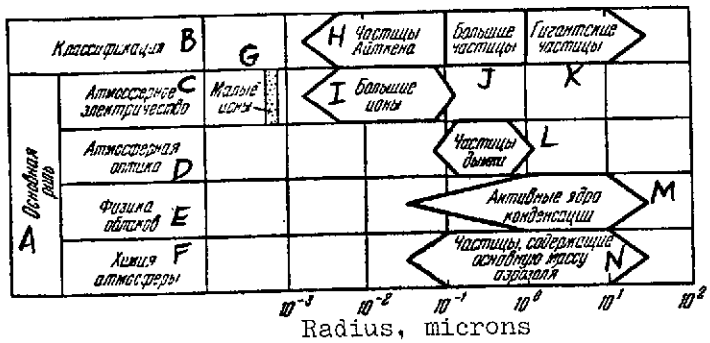

Fig. 3. Classification of aerosols and the role of particles of different sizes in processes within the atmosphere

KEY: A -- Main role
B -- Classification
C -- Atmospheric electricity
D -- Atmospheric optics
E -- Cloud physics
F -- Atmospheric chemistry
G -- Small ions
H -- Aitken particles
I -- Large ions
J -- Large particles
K -- Giant particles
L -- Smoke particles
M -- Active condensation nuclei
N -- Particles containing the bulk of the aerosol

N. M. Shtaude /53/, based on an analysis of twilight glow proposed to be existence of an aerosol layer at the altitude of 80-100 km. Later, A. Ye. Mikirov /60/, on measuring the brightness of the twilight sky at an altitude of about 100 km with a photometer carried aloft on a rocket, shows that the aerosol concentration maximum in the mesosphere is at the altitude 85-92 km. Estimates of density lead to values of the order of 10^{-16} g/cm^3, which exceeds the density of the dust component of interplanetary space by many orders.

The aerosol layer in the mesosphere evidently consists principally of the disintegration products of meteoritic bodies.

In the standard atmosphere the distribution of aerosols with altitude is accepted as following the data of L. Elterman /61/; cf. also /62, 63/. Details of research on atmospheric aerosol can be found in monographs by R. Caidle, /28/. Ch. Yunge /36/, G. V. Rozenberg /32/, and other works.

The theory of light scattering by dust particles was formu- /29
lated in 1908 by Mie. Its detailed presentation is found in the already-cited book by Ye. M. Shtaude /53/. The Mie theory was revised and advanced by several authors, in particular, by G. V. Rozenberg and K. S. Shifrin, in whose monographs /32, 64/ one can find modern treatments of light scattering by aerosols.

If one does not resort to complicated mathematical treatment, qualitatively the theory of light scattering, simplest for

the case of spherical dielectric particles, leads to the following results:

1. The main parameter characterizing the scattering ability of particles is the quantity $\alpha = 2\pi r/\lambda$, where r is the particle radius; thus, α is the particle size with respect to the wavelength of the scattered radiation.

2. If the parameter α is sufficiently small ($\alpha < 0.07$-0.1), the intensity of scattered light is proportional to α^4, or $1/\lambda^4$, that is, fine particles (for visible light they must be of the order of 0.01 μ) scatter light according to Rayleigh's law.

3. With increase in parameter α, the intensity of scattered light acquires a more complicated dependence on it. This function can be characterized by the so-called "efficiency factor" $K(\alpha)$, which shows by how many times the extinction caused by a particle is larger than the geometric screening caused by it; if σ_α is the index of attenuation calculated per particle, $K(\alpha) = \sigma_\alpha/\pi r^2$.

4. The curves of the dependence of efficiency factor K on α are similar to the curves shown in Fig. 4, taken from /32/, where $K(\alpha)$ is represented for particles with indices of refraction n = 1.33 (water droplets) and n = 1.50.

5. With increase in the index of refraction, "large" maxima and minima of function $K(\alpha)$ shift along the abscissae axis and the height of the large maxima increases (Fig. 4). The fine structure (a kind of "rippling") of function $K(\alpha)$ is caused by interference phenomena. Its influence on the overall pattern of aerosol scattering is very slight.

6. With increase in particle size, regardless of the particle's index of refraction, the efficiency factor $K(\alpha)$ tends to a constant, 2. This reflects the fact that particles that are large in comparison with wavelength carry out neutral scattering of light. /30

Detailed calculations of $K(\alpha)$ according to Mie theory for particles with indices of refraction n ≈ 1, 1.33, 1.40, 1.44, 1.48, and 1.50 were made by R. Penndorf /65/.

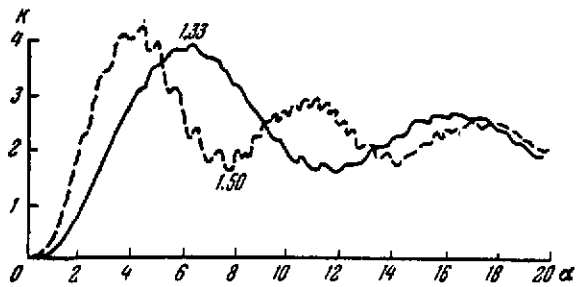

Fig. 4. Dependence of efficiency factor K of aerosol scattering on $\alpha = 2\pi r/\lambda$ for spherical dielectric particles with indices of refraction 1.33 and 1.50

In actual conditions different-sized particles are present

in the atmosphere; their averaged action leads to the aerosol index of attenuation $\chi_\alpha \propto 1/\lambda^m$, where $0 < m < 4$, in most cases. Large particles scattering light neutrally or with minimum wavelength dependence cause the "whiteness" of the sky, which is the more intense, the larger these particles. Since even for the same point on the ground the content of aerosols in the air and their distribution by size vary as a function of weather or other factors, where sometimes these changes take place over intervals of only several hours it should not cause amazement that since the optical thickness of the atmosphere $\tau(\lambda)$ and the transparency coefficient $p(\lambda)$ are highly inconstant. Not only do their absolute values vary, but also to some extent the form of their wavelength dependence. All this makes the reduction of observations difficult. When absolute values of radiation fluxes of heavenly bodies are determined, terrestrial atmosphere (for ground observations) and the instability of its optical parameters are key causes of reduced accuracy. /31

Light scattering, Rayleigh and aerosol types, causes the continuous (over the spectrum) attenuation of radiation, while true absorption occurs in bands, where the index of attenuation varies strongly within a band. The difference between extinction caused by scattering and that caused by absorption becomes especially when we compare Fig. 5 with Figs. 7 and 8. The first of these shows the mean values of the actual observed transparency coefficient and Rayleigh transparency coefficient values in the region 3200-6600 angstroms. Here the extinction is produced mainly by scattering, and the transparency coefficient varies quite smoothly. In the second and third figures are shown the recordings of the solar spectrum in the IR region. The abrupt "troughs" of intensity are caused by bands of true absorption in the terrestrial atmosphere.

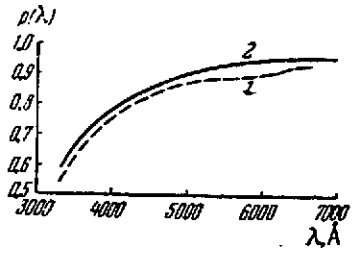

Fig. 5. Mean value of the transparency coefficient of the terrestrial atmosphere as a function of wavelength in the region 3200-6600 angstroms:
1 -- for the Tien-Shan station of the State Astronomical Institute imeni P. K. Shternberg (3000 m)
2 -- Rayleigh transparency coefficient for an altitude of 3000 m

The values of optical thickness of different origins, that is, caused by scattering by given agents and caused by absorption, are additive quantities. Therefore from the total observed optical thickness one can isolate the aerosol component according to the equality

$$\tau(\lambda) = \tau_R(\lambda) + \tau_a(\lambda) + \tau_u(\lambda). \qquad (19)$$

/π = abs, absorption/

The optical thickness of the Rayleigh atmosphere $\tau_R(\lambda)$ for a given location remains virtually unchanged (its variations associated with atmospheric pressure can be neglected in the actual calculations). But the optical thickness caused by absorption $\tau_\pi(\lambda)$ can be calculated from the content of the absorbing agent.

A parameter called the "turbidity factor" is often used in actinometry /45, 66/. In the visible spectral region it principally characterizes aerosol scattering and shows by how much the actual atmosphere differs from the ideal atmosphere, that is, an atmosphere in which extinction is caused only by Rayleigh scattering and absorption in gases whose content remains unchanged. /32

4. Absorption of Light in the Terrestrial Atmosphere

1) Composition of the terrestrial atmosphere. The composition of the dry (free of water vapor) and clean (free of aerosols) gaseous shell around the earth is given in Table 3 (according to /62/). The mean molecular weight of this atmosphere is 28.9644 on the C^{12} isotope scale (that is, the molecular weight of C^{12} is taken as 12.0000). This atmospheric composition is invariant up to an altitude of 90-95 km. Numerous attempts to detect in the lower layers -- the troposphere and stratosphere -- the segregation of gases by altitude in accordance with their molecular weights, as should occur according to Dalton's law on partial pressures, have been unfruitful. It was concluded that atmospheric gases are completely mixed owing to turbulent motions up to an altitude of 90-95 km. Diffuse separation begins only above 100 km: heavy gases concentrate beneath light gases.

The main atmospheric constituents up to an altitude of 90 km are molecular nitrogen and oxygen. Higher, the dissociation of O_2 begins under the effect of ultraviolet solar radiation: even at an altitude $\sim$ 200 km there is more atomic oxygen than molecular, and molecular oxygen is virtually absent at an elevation of 500 km. The energy of dissociation of the N_2 molecule is higher than for the O_2 molecule, and the concentration of atomic nitrogen is small up to an altitude of 500 km /62/.

As the result of diffusion processes, helium and hydrogen become the principal components of the upper atmosphere. Above 3000 km the hydrogen content predominates over the helium content, and the atmospheric composition approximates the composition of interplanetary space.

The dissipation of gases in the earth's air shell begins, on the average, in the years of maximum solar activity at an altitude $\sim$ 600 km.

TABLE 3.* NORMAL CHEMICAL COMPOSITION OF CLEAN DRY AIR NEAR SEA LEVEL, ON THE C^{12} ISOTOPE SCALE

/33

Gas Component	Symbol	Content, by % by volume	Molecular wt.
Nitrogen	N_2	78,084	28,0134
Oxygen	O_2	20.9476	31,9988
Argon	Ar	0,934	39,948
Carbon dioxide	CO_2*)	0,0314	44,00995
Neon	Ne	0,001818	20,183
Helium	He	0,000524	4,0026
Krypton	Kr	0,000114	83,80
Xenon	Xe	0,0000087	131,30
Hydrogen	H_2	0,00005	2,01594
Methane	CH_4*)	0,0002	16,04303
Nitrogen oxide	N_2O	0,00005	44,0128
Ozone	O_3*)	Sum. 0—0,000007 Win. 0—0.000002	47,9982
Sulfur dioxide	SO_2*)	0—0,0001	64,0628
Nitrogen dioxide	NO_2*)	0—0,000002	46,0055
Ammonia	NH_3*)	Traces	17,03061
Carbon monoxide	CO*)	Traces	28,01055
Iodine	I_2*)	0—0,000001	253,8088

*) The content of these gases can vary widely from place to place and with time.

Translator's Note: Commas represent decimal points.

Positive and negative ions and electrons are formed in the upper atmosphere due to processes of photoionizations on exposure to solar radiation. The highest absolute ion concentration is observed at the altitude of 300-400 km, where it is of the order of 10^6 cm^{-3}, and the total number of atmospheric particles is several orders higher. At higher altitudes the absolute concentration decreases, but the ratio of the number of ions to the total number of particles climbs.

The physical properties of the atmosphere up to an elevation of 200 km are quite stable, while at higher altitudes density and temperature vary as a function of the level of solar activity and from day to night; the changes are the greater, the higher the layers.

2) Variable constituents of the earth's gaseous shell. /3
Complete mixing of gases up to an altitude of 90 km is quite well performed for so-called "permanent" gases of the terrestrial atmosphere, whose content can be regarded as invariant. However, some of the gases noted in Table 3 with an asterisk either are variable in content for certain reasons (for example, CO), or else do not obey the law of total mixing (for example, ozone). Though these variable components comprise a negligible fraction of both the volume and the mass of the earth's atmosphere and have practically no effect on its mean molecular weight, it is precisely

these components that to a larger extent are responsible for the absorption of radiation in the earth's atmosphere, and the variability of their content gives rise to additional difficulties in recording atmospheric extinction. Below are given brief characteristics of the variable constituents.

a) Carbon dioxide gas, CO_2. The content of gas CO_2 is quite constant in the atmosphere, on the average; however, locally over a given locality it can vary by ~ 50 percent depending on from where the air mass came: whether it passed over an ocean, forest, fields, deserts, and so on; these changes are caused by the circulation of CO_2 in the biosphere and its interaction with sea water. In the near-earth layer the content decreases by day and increases by night. There are also seasonal fluctuations. They are most appreciable in the Arctic where the mean CO_2 content in April is 0.0317 percent, and 0.0309 percent in August. The secular growth in the carbon dioxide content caused by human activity is beyond question: at the end of the 19th century CO_2 represented 0.028 percent by volume, while in 1960 its fraction rose to 0.033 percent. This secular variation can be substantial for climate, since the infrared bands of CO_2 significantly inhibit thermal radiation of the earth, with a maximum in the range 8-13 μ. Owing to the increased CO_2 content, the temperature of the atmosphere currently increases by 1° per century; predictions have been made that with the current rate of increase in industrial activity the mean atmospheric temperature in the next 500 years will climb by 12°, which will lead to catastrophic thawing of the ice shields of the earth.

b) Ozone, O^3. Ozone is contained in the air in negligible quantity, less than $4 \cdot 10^{-5}$ percent by volume. Nonetheless, the thermal balance and the thermal structure of the atmosphere are to a larger extent controlled by ozone, since it is one of the principal absorbers of electromagnetic radiation in the atmosphere. The ozone layer absorbs about 1.5 percent of the total flux of the sun's rays, principally in the range 2300-3000 angstroms (the Hartley band). Due to this absorption, a noticeable temperature maximum is formed in the upper reaches of the ozonosphere: the temperature can be +44° C at an altitude of 50 km, but on the average (according to the SMA USSR) it is +0.85° C, while if ozone is absent it would be roughly -45° C. Along with molecular oxygen, ozone serves as a "shield" protecting the biological life on earth from the damaging effect of ultraviolet radiation. /35

The principal region of ozone formation is a layer 10-15 km thick, with its middle at an altitude of ~23 km over the equator and 30 km in higher latitudes. Ozone forms from the action of solar ultraviolet radiation on oxygen molecules; its concentration is controlled by photochemical reactions forming and breaking down O_3 /25, 26, 34-36/. The ozone layer has a quite well-defined upper limit: 90 percent of the total amount of ozone lies below

35 km and 99 percent -- below 45 km. However, traces of ozone have been detected at altitudes up to 70 km.

Changes in the ozone content in the upper layer of the ozonosphere above 30 km follow the changes in the influx of solar radiation over the course of a year. Below 25 km large fluctuations in the ozone content are observed, caused by circulatory processes in the atmosphere. There is little ozone in the troposphere, $6 \cdot 10^{-11}$ g/cm^3, which is roughly one-tenth of its content in the maximum-concentration layer ($4 \cdot 10^{-10}$ g/cm^3). And since the density of air at a 23-km altitude is $4.54 \cdot 10^{-2}$ percent of its density at sea level (according to the SMA USSR), therefore the relative ozone concentration increases by more than a factor of 100 at this altitude.

The total ozone content over the equator averages 0.240 cm, increasing to 0.380 cm in the upper latitudes (the thickness of the ozone layer at normal pressures and temperature). The total ozone content reflects the circulation pattern in the lower /3(
stratosphere. The distribution of ozone is constant only in the equatorial belt and is most variable in the polar regions. The ozone content maximum commences in spring, and the minimum -- in autumn; the fluctuations are approximately sinusoidal and are about 0.200 cm in amplitude. Regular diurnal fluctuations in the ozone amount are evidently absent, however irregular changes in a day can amount to 20-25 percent, and the maximum limits of change over the entire globe are very large: from 0.07 to 0.70 cm.

c) Water vapor is the most variable constituent of the atmosphere and the main cause of the depletion of solar radiation in the earth's troposphere. The H_2O content varies as a function of atmospheric circulation and temperature drops and increases sharply with rise in the latter.

The water vapor content in the troposphere decreases rapidly with altitude. Whereas at the earth's surface it averages 10 g/kg (10 g H_2O per kg of dry air), in the tropopause it falls to several thousandths g/kg. The temperature drop is the main reason for this decrease. But the relative humidity in the troposphere remains virtually unchanged with altitude, at about 50 percent.

The decrease in the H_2O content continues above the troposphere up to the frost point $\sim -83^\circ$ C at an altitude of 14-16 km. Above this, in the stratosphere, a certain increase in the water vapor concentration is observed; it reaches a value ~ 0.05 g/kg at the altitude 24-25 km. Still, the total amount of water vapor above the troposphere is very small: layers lying above the troposphere contain no less than 10 percent of the entire mass of the earth's gaseous shell, and not more than 0.1 percent of the total amount of water vapor.

The water vapor content in the surface layer can vary virtually within the same enormous limits as from the base of the troposphere to the tropopause: in the region of Verkhoyansk, for example, it varies from 10 g/kg in summer to $2 \cdot 10^{-3}$ g/kg in winter (in severe frosts), that is, by nearly four orders. Unfortunately, the exceptional dryness of the air observed in winter in the surface layer does not mean that at a given locality there is appreciably less water vapor overall throughout the entire atmospheric column. Owing to the severe temperature inversion accompanying strong frosts and windless days, humidity /37 increases rapidly with altitude along with temperature rise. As a result, the water vapor content in the column of air over a locale of observation (near Verkhoyansk) decreases in exceptional cases by only one order /67/ compared with regions that have normal surface humidity (for example, central Russia). This decrease in overall moisture content very slightly improves the atmospheric transparency at $\lambda = 300\ \mu$. For $\lambda \approx 1$ mm where the index of attenuation is smaller, transparency improves more appreciably, and it was noted in /67/ that Eastern Siberia is promising for the organization of millimeter-range observations.

However, a more effective method of reducing extinction due to water vapor is to take observations at high altitudes above sea level. In mountains, it is possible even at an elevation of about 3 km to measure the flux of solar radiation in the "spectral windows" of the submillimeter and millimeter ranges /68-71/, since the total absorption over the observation station proved to be several times, and even one order of magnitude less than at sea level (cf. Table 5).

In addition to the appreciable irregular changes in water vapor content caused by circulatory processes in the atmosphere (shift of air masses is also associated with change in the temperature stratification), noticeable, quite regular fluctuations in moisture content are observed in the atmospheric column over an observation locale. For example, in mountainous regions the amount of precipitated water in the spring-summer period can vary by a factor of 2 in the course of a day /72-73/. Therefore, if one determines the atmospheric transparency by Bouguer's method (Section 5) over a wide range of the visible spectrum, in addition to Forbes' effect, errors can occur of several percent owing to change with time in the observations of equivalent widths of the H_2O absorption bands. For the same reason the optical thickness of the atmosphere in the "spectral windows" of the submillimeter range can vary by a factor 1.2-1.3.

All the foregoing shows how difficult and, of prime importance, unreliable is an estimation of extinction in the terrestrial atmosphere in those spectral regions where absorption in the water vapor bands plays a key role. The most reliable method /38 of avoiding this indeterminacy is to make observations outside the earth's troposphere.

d) Oxides of nitrogen, NO and NO_2. The presence of negligible amounts of nitrogen oxides plays no appreciable role whatever in the attenuation of solar radiation for observations taken on plains where absorption by these oxides is suppressed by incomparably more intense absorption, principally in the bands of water vapor and molecular oxygen. However, even at an altitude of about 3 km, it is found that owing to the reduced absorption by water vapor absorption in the NO and NO_2 bands becomes appreciable /74/, and the more so, the higher the altitude at which the observations are made.

The content of NO and NO_2 oxides is variable, since it is associated with photochemical reactions determined by the far UV emission of the sun, whose intensity increases when flares are present on the sun. Nitrogen oxide and dioxide form in the chemosphere at altitudes from 50-60 to 160 km, where the principal processes of the oxygen-nitrogen cycle occur. It is estimated that NO and NO_2 result from reactions of atomic nitrogen with oxygen (O and O_2). Atomic nitrogen at altitudes up to 160 km is formed mainly due to predissociations (dissociations from an excited state).

3) Absorption in the terrestrial atmosphere and "spectral windows". The range of currently measured electromagnetic emission from the sun, from gamma-rays with wavelengths of hundredths of an angstrom to meter radiowaves, occupies the region of frequencies from 10^{20} to 10^6 Hz, which is more than 46 octaves. Most of this range is blocked off for terrestrial observations, mainly owing to the molecular absorption of solar radiation in the earth's atmosphere. There are two main "windows" of relative atmospheric transparency in which solar radiation can penetrate: in the optical range from 3000 angstroms to $\sim 4\ \mu$ and in the radio range, occupying the wavelength interval from several millimeters to ~ 30 m. The "optical window" is narrow; it encompasses less than 4 octaves out of the 46; however, fortunately for biological life on earth it is precisely this window that accounts not only the solar radiation maximum arrives, but also from the energy standpoint virtually all solar radiation, since 98 percent of the solar constant "is formed" in the wavelength range 3000 angstroms $< \lambda < 4\ \mu$.

The "radio window" is much broader than the optical window; it occupies about 11 octaves, nearly one-fourth of the entire range of radiation received. Observations taken within the limits of this window provide much important and interesting information about physical conditions and processes occurring in the upper regions of the solar atmosphere; however, the fraction of total solar energy accounted for by this "window" is negligible -- less than 0.001 percent of the solar constant.

There are other, much less broad and less "transparent" "windows" in the terrestrial atmosphere, but we will refer to these below, in passing as we describe several characteristics of atmospheric absorption.

Absorption in the terrestrial atmosphere, as already indicated, occurs mainly in molecular bands owing to the fact that molecules have quantized energy values of rotational and oscillatory motions and electron energies. In addition, dissociation of molecules and their ionization on exposure to high-frequency solar radiation is responsible for the continuous (not quantized) absorption of the latter, localized mainly in the far ultraviolet. Spectroscopy of atoms and molecules is well presented, for example, in the books /75-79/.

Let us consider in more detail absorption in various wavelength ranges.

a) The region $\lambda < 3000$ angstroms. Absorption is caused mainly by molecules of oxygen, nitrogen, and ozone. Molecular nitrogen and oxygen absorb in the spectral region from 200 to 2600 angstroms. Some of these molecules dissociate at high altitudes; the atoms formed absorb radiation with $\lambda < 900$ angstroms. A small fraction of oxygen atoms upon collision with O_2 molecules forms ozone molecules O_3. The abrupt break in the observed solar spectrum at 3000 angstroms is caused by absorption in the O_3 band, called the Hartley band, which extends to 2100 angstroms and has a maximum at 2550 angstroms. Much weaker absorption bands of ozone, the Huggins, embrace the interval 3400-3000 angstroms. The absorption coefficients of ozone have been reliably determined by Inn and Tanaka /80/ and Vigroux /81/. Fig. 6 gives /40
the altitudes up to which 50 percent of radiation extends following propagation along the vertical /82/. All absorption is determined by ozone between λλ 3000 and 2100 angstroms, and from 2000 to 1300 angstroms absorption is mainly caused by oxygen in the Schuman-Runge bands, intergrading into the continuous spectrum. Beginning at 1300 angstroms in the short-wave side radiation is absorbed by the continuum of molecules and atoms of nitrogen and oxygen. Sharp maxima at 31 and 23 angstroms are caused by the limits of absorption of the K-shells of N and O atoms.

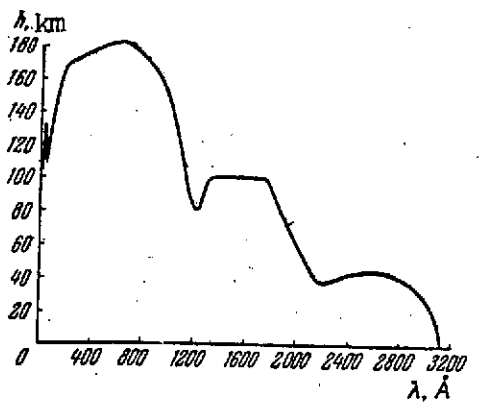

Fig. 6. Altitudes up to which 50 percent of solar radiation extends (for propagation along the vertical)

Absorption of solar radiation for wavelengths smaller than 3000 angstroms is so intense that observations of this radiation from the earth surface is practically impossible; no allowance for absorption has any effect. Only lifting instruments above levels schematically shown in

Fig. 6 enables us to measure solar emission in this spectral region. Absorption in the Huggins bands is not as great and permits ground observations followed by allowance for extinction using tables /80-81/ for a known ozone content in the atmosphere.

b) Photographic spectral region, 0.3-1.3 μ, is bounded on the one side by absorption in the ozone band at 0.3 μ, and on the other side -- by the water vapor band at 1.38 μ. The principal absorption bands of atmospheric gases accounted for by this spectral region are presented in Table 4, covering the interval 0.34-17 μ. In this table intensity I is given on a five-division scale, based on the possibility of resolving the fine structure of the band for different air masses. Thus, in the region 3400-5700 angstroms of the band intensities I are so faint that they are noticeable only at large zenith distances of the sun. /41

Weak Chappuis bands, lacking well-defined structure, and with their absorption maximum at λ 6020 angstroms [6] are localized in the interval 4500-6500 angstroms. When observations are taken at stations on a plain with dusty atmosphere, these bands are masked by intense scattering at aerosols and are not noticeable on the curve of the transparency coefficient $p(\lambda)$. But for observations taken in mountain observatories they are easily visible, since the curve $p(\lambda)$ near 6000 angstroms plainly slopes downward (cf. Fig. 5 and data in /83/).

The red bands of oxygen are induced in the electronic transitions of O_2 molecules. Their fine structure lines are very narrow, therefore they are sometimes used to determine the instrumental profile of spectral instruments. Investigation of these bands led to the discovery in the earth's atmosphere of the oxygen isotopes O^{17} and O^{18}. Data on these bands are collected in the works /84-86/.

Water vapor bands in the visible region are faint (cf. Table 4), but intensify appreciably with movement into the IR region. The strong band Ψ lies at λ 1.4 μ, nearly completely absorbing solar radiation. The band Ψ is easily visible in one of the first recordings of IR spectra of the sun taken by Langley in 1900 (Fig. 7). The form of the spectrum, depth and width of the H_2O lines in bands naturally depends strongly on the amount of water vapor in the atmosphere.

For ground observations in this region, and all the more so in the far IR region, one has to select the "windows" of relative

[6] The decimal coefficient of attenuation at the maximum χ_{10} is 0.06 cm^{-1}, while it is 1 cm^{-1} in the Huggins band at λ 3100 angstroms. For details, cf. /80-81/, and also, for example, /25, 34, 35/.

transparency between the telluric lines, using atlases and catalogs of the solar spectrum and other investigations /87-95/, and allowing for the resolving power of the spectral instrument with which the observations are made. /42

c) The region 1.4-5.5 μ. Three very intense bands with $\lambda\lambda$ 1.87, 2.66-2.77, and 4.51-4.63 μ are in this region; absorptions of H_2O, CO_2, and N_2O (cf. Table 4) overlap in these bands. Fowle called these bands Ω, X, and Y. The H_2O band is quite strong at λ 3.17 μ. This region contains also many fainter bands and lines of various molecules. In particular, in the interval 2.15-2.45 μ about half of all telluric lines belong to methane; the methane band is quite strong at 3.31 μ. In the intervals 2.1-2.3 and 2.9-5.5 μ the weak N_2O and CO bands have been identified. The ozone band λ 4.75 μ in ground observations is practically entirely masked by the H_2O, CO_2, and CO lines. Finally, one must take note of several bands belonging to molecules of the isotopes HDO, $C^{13}O_2^{16}$, $C^{12}O^{16}O^{18}$, and so on. This spectral region borders the long-wave side with the strong H_2O band at λ 6.27 μ.

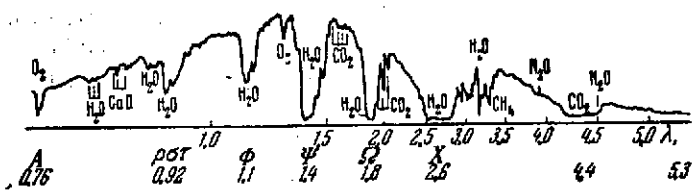

Fig. 7. Reproduction of one of the first recordings of the solar spectrum in the infrared region obtained by Langley in 1900

d) The region 7-25 μ. To illustrate absorption in the terrestrial atmosphere in this and the preceding region, Fig. 8 presents a recording of the solar spectrum from 3 to 13 μ, taken from /73/. The recording was made at an altitude of 3100 m with relatively low water vapor content, and nonetheless the H_2O band centered at 6.27 μ completely absorbs incident solar emission. The 7-25 μ region can be divided into two sections. The first section, 7-13 μ, is bounded on the short-wave side by the 6.27 μ band. The broad wings of this band make the transparency of /43 the atmosphere highly variable, depending on the water vapor content, even between 7 and 8 μ. On the long-wave side the section is bounded by the most intense carbon dioxide gas band with its center at 15 μ. CO_2 bands with centers at 9.39 μ and 10.4 μ and the ozone band centered at 9.6 μ are located in the section. However, in spite of the presence of intense absorption bands, the 8-13 μ section is a window of relative transparency of the earth's atmosphere in the infrared region. This window is particularly interesting, since it is precisely in this spectral interval that the maximum of proper terrestrial emission and most of the outgoing radiation lie. The narrow interval at λ 11.1 μ is the interval that is most free of absorption, but there

also the index of attenuation (decimal) reaches values of 0.10-0.12 cm^{-1} in the wings of the water vapor bands (that is, per cm of precipitated water). The interval at λ 11.1 μ is used for ground determinations of the extra-atmospheric intensity of solar radiation and serves as an important "reference point" in the infrared region [73, 96].

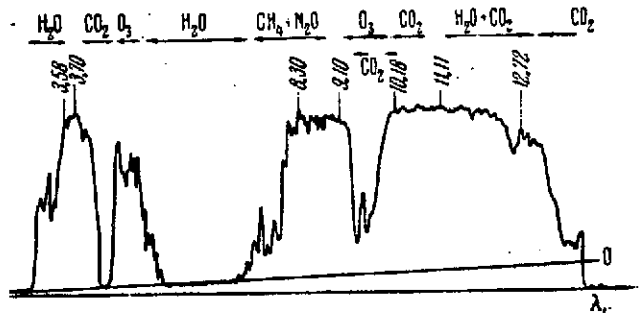

Fig. 8. Reproduction of tracing of solar spectrum in the 3-13 μ region, obtained by coworkers at Leningrad State University at Mt. Terskol (3100 m above sea level), with sun's altitude ~ 34°. The "spectral windows" in which the measurements were made are marked with vertical strokes and the wavelength is indicated (μ).

The second section of this region is 15-25 μ; atmospheric absorption here is strong. On the short-wave side the section is bounded by the CO_2 band at λ 15 μ, then comes one more CO_2 band at 16.2 μ, and a NO_2 band with its center at 17.0 μ. On the long-wave side radiation is entirely absorbed by the water vapor band centered at 23.73 μ. With an instrument of adequate resolving power, narrow windows of relative transparency can be selected in this section, for example, at 20.15 μ and 20.40 μ. The intensity of solar radiation in these wavelengths was measured, in particular, in the work [97] for a 0.25 μ pass band of a monochromator (spectral resolution).

e) Far infrared, submillimeter, and millimeter spectral regions. Atmospheric absorption increases strongly and quite smoothly in the section 23-40 μ, and at wavelengths longer than 40 μ it becomes complete (for tropospheric observations). Total absorption is produced mainly owing to water vapor and extends up to λ 345 μ. The atmosphere passes only 5 percent of incident radiation in the center of the "spectral window" at λ 345 μ -- and for observations taken in the mountains, also a negligible (0.2 cm) moisture content. Even when the H_2O content is increased to 0.3 cm, this "window" is completely locked. /46

The spectral region from 7 to 400 μ has been described in detail, with good resolving power, by Farmer and Key [94], who made observations in the Bolivian Andes at 5300 m.

TABLE 4.* LIST OF MOLECULAR BANDS AND LINES IN THE ATMOSPHERIC ABSORPTION SPECTRUM BETWEEN 0.34 and 17 μ

Wave nr, cm^{-1}	λ, μ	Molecule	I	Wave nr, cm^{-1}	λ, μ	Molecule	I
29400	0,3400	O_2	1	10329	0,9681	H_2O	3
20940	0,4774	O_4	1	10284	0,9724	H_2O	2
18394	0,5436	H_2O	2	9834	1,017	H_2O	2
17495	0,5714	H_2O	1	9366	1,067	O_2	2
17384	0,5750	O_3	1	9000	1,111	H_2O	3
17324	0,5770	O_4	1	8807	1,135	H_2O	4
17248	0,5796	O_2	3	8762	1,141	H_2O	3
17023	0,5872	O_3	1	8273,9	1,209	H_2O	3
16899	0,5915	H_2O	3	8273,7	1,209	H_2O	3
16898	0,5918	H_2O	2	7882	1,268	O_2	3
16822	0,5942	H_2O	2	7445	1,343	H_2O	4
16605	0,6020	O_2	1	7250	1,379	H_2O	5
15900	0,6288	O_2	3	7201	1,388	H_2O	4
15892	0,6290	O_4	1	6973	1,434	CO_2	4
15832	0,6314	H_2O	2	6871	1,455	H_2O	4
15671	0,6379	O_2	3	6775	1,475	H_2O	3
15348	0,6513	H_2O	1	6503	1,54	CO_2	2
14523	0,6884	O_2	4	6350	1,57	CO_2	3
14494	0,6897	$O^{16}O^{17}$	1	6228	1,61	CO_2	3
14486	0,6901	$O^{16}O^{18}$	2	6076	1,64	CO_2	2
14343	0,6970	O_2	2	6005	1,67	CH_4	3
14319	0,6981	H_2O	3	5861	1,71	CH_4	1
14221	0,7032	H_2O	2	5775	1,73	CH_4	1
13831	0,7227	H_2O	3	5331	1,87	H_2O	5
13828	0,7232	H_2O	2	5235	1,91	H_2O	4
13653	0,7324	H_2O	3	5132	1,95	CO_2	3
13120	0,7620	$O^{16}O^{18}$	3	5100	1,96	CO_2	4
13119	0,7620	$O^{16}O^{17}$	2	5046	1,98	$C^{13}O_2^{16}$	2
13118	0,7621	O_2	4	5042	1,98	$C^{12}O^{16}O^{18}$	1
12966	0,7710	O_2	2	4978	2,01	CO_2	4
12565	0,7955	H_2O	3	4965	2,02	CO_2	3
12408	0,8059	H_2O	2	4905	2,04	$C^{12}O^{16}O^{18}$	2
12151	0,8226	H_2O	3	4887	2,05	$C^{13}O_2^{16}$	3
12140	0,8237	H_2O	2	4853	2,06	CO_2	4
11813	0,8465	H_2O	2	4808	2,08	CO_2	3
11032	0,9061	H_2O	3	4791	2,09	$C^{12}O^{16}O_2^{18}$	1
10869	0,9200	H_2O	3	4748	2,10	$C_{12}O_2^{16}$	1
10613	0,9419	H_2O	4	4735	2,11	N_2O	1
10600	0,9434	H_2O	3	4667	2,14	H_2O	3
				4630	2,16	N_2O	1

* Translator's Note: Commas represent decimal points.

TABLE 4. LIST OF MOLECULAR BANDS AND LINES IN THE ATMOSPHERIC ABSORPTION SPECTRUM BETWEEN 0.34 AND 17 μ /CONCLUSION/

Wave nr, cm^{-1}	λ, μ	Molecule	I	Wave nr, cm^{-1}	λ, μ	Molecule	I
4546	2,20	CH_4	3	2224	4,51	N_2O	4
4420	2,26	N_2O	2	2161	4,63	H_2O	4
4390	2,28	N_2O	1	2143	4,67	CO	3
4313	2,32	CH_4	3	2130	4,69	CO_2	3
4260	2,35	CO	1	2105	4,75	O_3	3
4216	2,37	CH_4	3	2093	4,79	CO_2	3
4123	2,43	CH_4	3	2077	4,81	CO_2	4
3756	2,66	H_2O	5	2057	4,87	H_2O	3
3714	2,69	CO_2	5	1933	5,18	CO_2	3
3657	2,74	H_2O	4	1595	6,27	H_2O	5
3613	2,77	CO_2	5	1556	6,43	H_2O	3
3481	2,87	N_2O	3	1403	7,14	HDO	4
3366	2,97	N_2O	3	1306	7,66	CH_4	4
3151	3,17	H_2O	4	1285	7,78	N_2O	4
3019	3,31	CH_4	4	1167	8,54	N_2O	3
2823	3,55	CH_4	3	1064	9.39	CO_2	3
2798	3,57	N_2O	3	1043	9,6	O_3	4
2724	3,67	HDO	3	961	10,4	CO_2	3
2600	3,85	CH_4	3	792	12,6	CO_2	3
2564	3,91	N_2O	3	741	13.5	CO_2	3
2462	4,06	N_2O	3	720	13,9	CO_2	3
2349	4,26	CO_2	5	667	15,0	CO_2	5
2283	4,38	$C^{13}O_2^{16}$	3	618	16,2	CO_2	3
2260	4,42	N_2O	2	589	17,0	N_2O	3

Absorption of solar radiation in the submillimeter and millimeter spectral regions is determined chiefly by water vapor and oxygen; H_2O absorption is especially intense for wavelength shorter than 0.9 mm. Submillimeter and millimeter spectral regions have been studied nearly exclusively by radio-astronomical methods. A review of absorption studies in this range as of 1961, containing a compilation of spectral "windows" was made by Williams and Chang /95/. The following spectral "windows" are indicated in the interval up to 1 cm: 0.44; 0.59; 0.71; 0.81; 3.2; 4.3; and 8.5-8.9 mm.

A large series of studies both experimental and theoretical in nature on the absorption spectrum of the terrestrial atmosphere in this wavelength range was conducted at the Gor'kiy Radiophysical Institute. These studies broadly supplement our information on absorption coefficients in the spectral "windows" in the submillimeter and millimeter regions. Thus, L. I. Fedoseyev et al. /68, 69/ measured absorption in the "windows" at λλ 0.87, 0.873, 1.06, 1.16, 1.19, 1.2, 1.26, 1.3, 1.45, and 1.8 mm; the observations were made at high elevations.

A study by A. G. Kislyakov and K. S. Stankevich /70/ provides a broad compilation of measured absorption coefficients of water vapor and oxygen in the wavelength from 0.2 mm to several centimeters. A review of studies on the same subject, both experimental and theoretical, and provided with a bibliography, was carried out by S. A. Zhevakin and A. P. Naumov /98/. A comparison of calculated and experimental absorption coefficients of water vapor and other agents for the broad wavelength range from 10 μ to 10 cm is given in the dissertation of A. P. Naumov /99/; also /47 given is a list of the spectral "windows" for this spectral region. Calculated and experimental absorption coefficients of water vapor differ by an average factor of 1.5-2. Finally, we must recall that as already noted, A. G. Kislyakov and A. P. Naumov /74/ found that for high-elevation observation stations it is not only absorption by water vapor and oxygen that is substantial in the submillimeter and millimeter ranges, but also absorption by the "small admixtures" NO, N_2O, NO_2, and CO.

TABLE 5.* OPTICAL THICKNESS OF ATMOSPHERE PRODUCED BY WATER VAPOR IN THE CENTRAL WAVELENGTH OF THE RELATIVE SPECTRAL WINDOWS OF THE FAR IR AND SUBMILLIMETER SPECTRAL REGIONS

h, km / λ, mm	τ_{H_2O} for $\rho = 7{,}5$ g/cu.m summer (290 °K)			τ_{H_2O} for $\rho = 1$ g/cu.m winter (270 °K)		
	0	4	8	0	4	8
0,038	83	5,8	0,41	12,8	0,9	0,064
0,042	93	6,5	0,46	14,3	1,0	0,071
0,046	196	13,7	0,98	30,6	2,14	0,153
0,054	207	14,5	1,03	31,8	2,22	0,159
0,061	216	15,1	1,08	33,2	2,32	0,166
0,07	320	22,4	1,6	49,4	3,45	0,247
0,073	207	14,5	1,03	32	2,24	0.16
0,12	340	23,8	1,7	52,4	3,66	0,26
0,152	176	12,3	0,88	27,1	1,9	0,135
0,164	370	25,9	1,85	57,0	4,0	0,28
0,2	93	6,5	0,46	14,3	1,0	0,071
0,22	108	7,6	0,54	16,6	1,16	0,083
0,29	98,2	6,9	0,49	15,1	1,06	0,075
0,32	41,4	2,9	0,207	6,38	0,45	0,032
0,34	32	2,24	0,16	4,92	0,34	0,025
0,36	22,2	1,55	0,111	3,42	0,24	0,017
0,45	18,6	1,3	0,093	2,86	0,2	0,014
0,65	17	1,19	0,085	1,62	0,183	0,013
0,74	6,2	0,43	0,031	0,95	0.066	0,0048
0,86	3,1	0,217	0,015	0,48	0,034	0,0024

* TRANSLATOR'S NOTE: Commas represent decimal points.

The results of radioastronomical studies in the millimeter and submillimeter wavelength ranges (as of the end of 1969) are summed up most completely in a review article by A. G. Kislyakov /71/, provided with a very long bibliography (more than 300 entries). In particular, the review compiles information on absorption in the terrestrial atmosphere in this spectral region. Table 5, taken from the review, gives optical thicknesses of the atmosphere caused only by water vapor in the relative spectral windows of the submillimeter range. The data were obtained by calculation; their accuracy is ±30-50 percent; they apply to three values of elevations above sea level (0, 4, and 8 km) for summer and winter conditions. /48

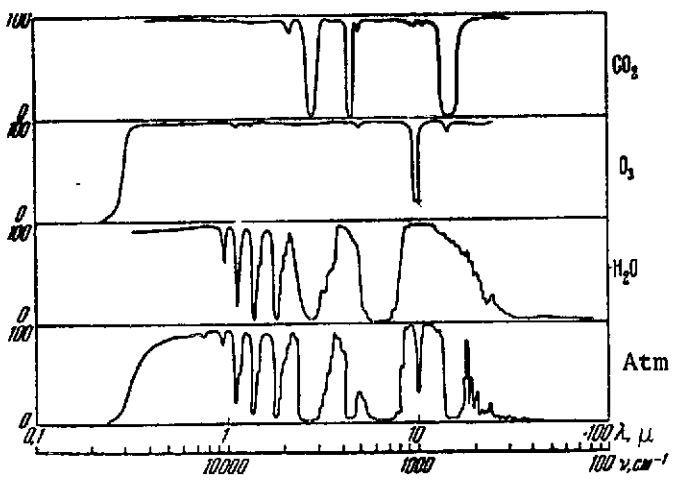

Fig. 9. Scheme of arrangement of principal absorption bands and relative spectral windows of the atmosphere in the region 0.1-100 μ

On passing over to the centimeter range, a broad spectral "radio-window" of the earth's atmosphere begins at 2-3 mm (cf. above) /99/.

In concluding this section, we present Fig. 9, taken from /97/; it schematically shows the arrangement of the principal absorption bands and the relative spectral windows of the atmosphere in the region 0.1-100 μ. This figure together with Table 5 clearly shows that in the atmosphere inclusively to wavelength 2-3 cm there are no "clean" "spectral windows", with the exception of the interval 3600-5500 angstroms, where the extinction is caused only by scattering. This is the situation for ground observations, but even at altitudes of 12-13 km, that is, right at the end of the troposphere we can count 15-20 "windows" completely free of absorption (and with significantly reduced extinction due to scattering). /49

5. Practical Determination of the Transmission Coefficient and Monitoring the Stability of Optical Properties of the Atmosphere

Formula (15) derived from Bouguer's law leads to a very simple method of determining the transmission coefficient, called the Bouguer method. By taking the logarithm of (15), we have

$$\lg I(\lambda, z) = \lg I_0(\lambda) + M(z) \lg p(\lambda). \qquad (20)$$

This equality shows that the dependence of lg $I(\lambda, z)$ on $M(z)$ is linear; lg $p(\lambda)$ is the slope of the corresponding line and lg $I_0(\lambda)$ is the free term of its equation. Hence the method itself is obvious: a heavenly body, for example, the sun or a fixed star is observed several times at different zenith distances; in practice it is essential that $M(z)$ be varied by 1.5-2. Here it is postulated that during the time of observations the optical properties of the atmosphere and, in particular, the transmission coefficient, remain unchanged. Then one plots a graph of lg $I(\lambda, z)$ as a function of $M(z)$, which is called the Bouguer line. For its confident execution all we need is five to eight points. Its slope allows us to determine lg $p(\lambda)$, and extrapolation to the intersection with the Y axis, that is, extrapolation to $M(z) = 0$, yields the logarithm of the extra-atmospheric value of the flux, $I_0(\lambda)$.

Bouguer's method is simple, graphic, and independent of the nature of extinction (scattering or absorption). But its use is restricted in two cases. The first restriction is associated with conditions under which Bouguer's law is satisfied for the attenuation of light. In particular, the Forbes effect represents /50 a danger for the method, as does the scattering of light of higher orders. The latter amounts to the "scattered" quantum having some probability of experiencing one more or several scatterings when there is a large optical thickness, and as a result acquiring a direction coinciding with the direction of the direct rays. Scattering of higher orders leads to the apparent violation of Bouguer's law, since one cannot experimentally separate double and triple scattered radiation travelling in the "forward" direction from residual, unscattered rays of the initial beam. Therefore, for example, due to scattering of higher orders the observed solar brightness near the horizon decreases with increase in z somewhat more slowly than would be expected by formula (15) derived from Bouguer's law. The use of the Bouguer method in these conditions gives an overstated $p(\lambda)$.

The restrictions on the Bouguer method associated with the Forbes effect and with multiple scattering have been studied closely and can be easily circumvented. Thus, by taking observations only in quasimonochromatic rays (in all spectrophotometric work), one can avoid the Forbes effect, and scattering of higher orders begins to have a perceptible effect only for quite large values of the atmospheric mass $M(z)$ [7].

[7] These values differ for observations taken at different wavelengths. The Bouguer method can be used without risking scattering of higher orders when $M(z) \cdot \tau(\lambda) < 6\text{-}7$ /32, pp. 193-195/.

A much greater danger of errors and difficulty in practical execution of the Bouguer's method stems from the second restriction: the method leads to trustworthy results only if the optical properties of the atmosphere are kept constant throughout the observation period. And the observations themselves for determining $p(\lambda)$, by necessity must be quite protracted; in practice they take 2 to 4 hours. During this time optical conditions of the atmosphere can change even when the sky is completely clear. Rapid and abrupt changes in transmission associated, for example, with the appearance of near-noon haze leads to a violation of the linear course of $\lg I(\lambda, z)$ as a function of $M(z)$. These observations are usually not processed. The linear dependence of $\lg I(\lambda, z)$ on $M(z)$ is the essential criterion for the atmosphere being stable during the observation period. But this criterion is insufficient. /51

Often slow, extremely smooth and monotonic changes in $p(\lambda)$ occur. With monotonic change in transparency, Bouguer lines remain straight, but their slope changes, and as a result the $p(\lambda)$ values determined prove to be imaginary. One can easily see that with improvement in transparency observations of setting bodies will yield overstated $p(\lambda)$ values, and observations of ascending bodies will yield understated $p(\lambda)$ values, and when transparency is improved the opposite results are forthcoming. This problem has been analyzed in detail by V. B. Nikonov /100/. Even earlier this disadvantage of the Bouguer method was noted by Abbot. Several methods of determining "instantaneous" values of the transparency coefficient applicable even when the atmosphere is unstable were devised. But the "nocturnal" methods /100-102/ are not suitable by day, and the day /103-105/ methods based on characteristics of light scattering are valid only for those wavelength regions where there is no true absorption and for specific air mass values. Therefore, in undertaking absolute spectrophotometry of the sun, astronomers are compelled to select the hours when the atmospheric properties are stable and when the Bouguer method can be employed. And the selection of a period in which the atmosphere is stable is made by means of auxiliary monitoring observations, which are conducted in parallel with the main, spectrophotometric observations. Unfortunately, this choice is executed, so to speak, after the event: first observations are made, and then, by processing the monitoring observations one can find which portion of the principal observations are amenable to mathematical treatment (sometimes all observations on a specific day have to be rejected).

To monitor the stability of the optical properties of the atmosphere in the visible region, often one must take observations of the solar aureole [8]. The method was proposed in 1933 /52

/footnote 8 on following page/

by Academician V. G. Fesenkov [107]. Essentially, the method amounts to the following. A special instrument, the aureole photometer designed by V. G. Fesenkov is used for the monitoring observations. This instrument's field of view covers the circular zone around the sun with an external diameter of 1.5-3°. When making aureole observations, one shields the radiation receiver against the direct and diffracted solar rays with two screens. The instrument reading in this case is proportional to the aureole brightness B_{au}. By rotating the handle, the screens can be rapidly removed and then the instrument gives a reading at the sun, that is proportional to the solar brightness, $B_\odot$. The effect of the light flux from the aureole can be neglected in this case, since it is at least one thousand times weaker than the direct flux from the sun. When the latter is being recorded, a neutral light filter is added to the instrument(simultaneously with removal of the screen), affording attenuation of several hundreds of times, therefore the reading ratio $B_{au}/B_\odot$ is not equal to, but only proportional to the ratio of the corresponding brightnesses.

V. G. Fesenkov showed that if the optical properties of the atmosphere are unchanged, and the scattering of higher orders does not play a key role, the ratio $B_{au}/B_\odot M(z)$, called the relative aureole, varies in proportion to the air mass, that is, the relative aureole as a function of M(z) with stable atmospheric properties must yield a straight line, which on being extrapolated to M(z) = 0 must pass through the origin of coordinates. The latter is related to the fact that for a zero air mass, that is, in the absence of an atmosphere, the aureole disappears. But if one plots $B_{au}/B_\odot M(z)$ on the graph, then as a function of M(z) it yields a straight line parallel to the X axis.

Variation in the atmospheric optical properties leads to violation of the linearity of the quantities cited, where the V. G. Fesenkov criterion is marked by very high sensitivity. According to Ye. V. Pyaskovskaya-Fesenkova [103] and G. F. Sitnik [108], lines of the relative aureole are more sensitive by more than one order to disturbances in optical properties of the atmosphere than are Bouguer lines (Fig. 10). /53

The high sensitivity of the method of monitoring atmospheric transparency using measurements of relative aureoles is accounted

---

8 In most cases the sky brightness at small angular distances from the sun (1-3°) is much greater than farther off from the sun; this brightening of the sky is the circumsolar aureole. It is caused by the fact that in aerosol scattering, especially by large particles, most of the scattered quanta acquire a direction forming a relatively small angle with the main flux. The aureole brightness at a distance of 1-1.5° from the sun is of the order of 10^{-3} - 10^{-4} times the brightness of the solar disk [106].

for quite simply. Change in transparency is strongly related to variation in the atmospheric content of large aerosol fractions, mainly large particles. But a coarse aerosol, as already noted, scatters light predominantly in directions forming small angles with the direction of the main beam. The indicatrix [9] of aerosol scattering is very elongated. Let us now assume that the content of coarse aerosols will increase, and that more than one-thousandth of it will begin to be abstracted from the direct beam of solar radiation. The Bouguer line point will be displaced in the ratio $(1.001)^{M(z)}$, that is, by $0.001 \cdot M(z)$ of its ordinate. And the energy abstracted from the direct flux will be distributed mainly within the aureole owing to the elongatedness of the indicatrix. The brightness of the aureole will, in order of magnitude, be 10^{-3} of the brightness of the solar disk, but the area of the /54
aureole will be roughly ten times greater than the visible area of the disk. Hence we can easily see that this additional scattering of 10^{-3} direct sun rays will lead to an increase in the aureole brightness of roughly one-tenth, that is, the increment in the aureole brightness will exceed by more than one order the displacement of the Bouguer point.

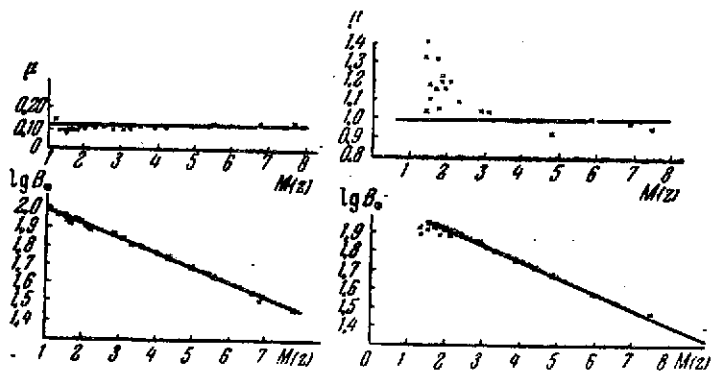

Fig. 10. Bouguer lines (lower) and relative-aureole lines corresponding to them $\mu = B_{au}/B_{\odot}M(z)$ (upper) for stable (at left) and unstable (at right) atmosphere, optically speaking

The most characteristic example of solar spectrophotometry undertaken with constant monitoring of the optical properties of the atmosphere by parallel observations with aureole photometer is the series of studies made at the Astrophysics Department of the State Astronomical Institute imeni Shternberg /GAISh/ under the supervision of G. F. Sitnik /109-112, 83/. During observations taken at Kuchino near Moscow (150 meters above sea level), G. F. Sitnik deemed suitable for use in further mathematical processing only those groups of observations taken on a large spectrophotometer for which simultaneous determinations of $B_{au}/B_{\odot}M(z)$ yield fluctuations of not more than 9 percent during the

[9] The indicatrix of scattering $f(\theta)$ is a function that is proportional to the probability that a quantum will be scattered at an angle θ to the direction of the main beam.

time period corresponding to the change in the solar air mass by two units (the observation usually began at z $\approx 75^{\circ}$). Of the 172 days of observations in 1948-1955, one-third proved to be stable /108/.

Instrumental measurements of the relative aureole are quite necessary when taking observations from a lowland site. In the mountains, at an elevation of 2000-3000 meters and higher where the air is much purer, sometimes so-called "aureole-free days" occur when the aureole is so weak that it cannot be seen with the eyes [10]. On these days observations of an aureole photometer are not mandatory; visual estimates of the "aureole-free status" are sufficient. The transparency coefficient remains unchanged from one day to another within the limits of 1 percent. This was verified by Ye. A. Makarova /83/ at the Tien-shan Station of the GAISh (3000 m elevation), and was also noted by D. Labs and H. Neckel /113/ in observations taken of the International Station Jungfraujoch (3650 m).

Ye. V. Pyaskovskaya-Fesenkova /103/ generalized the criterion of the stability of atmospheric optical properties and showed /55
that not only the relative aureole, but also the ratio of the brightness at any point in the sky at the solar almucantar to the brightness of the solar disk is a linear function of the air mass and in some cases can be used in monitoring. In addition, Pyaskovskaya-Fesenkova and her colleagues /103-105/ in the atmospheric optics department of the Astrophysical Institute of the Kazakh SSR Academy of Sciences developed several methods of determining the transparency coefficient, based on measuring light scattered by the atmosphere. These include methods of determining the maximum aureole, the brightness of several points in the celestial dome polarization of sky light, and so on. They yield transparency coefficients that agree well with those found by the Bouguer method in the case of stable atmospheric properties. But unfortunately, these methods are derived mainly for the visible spectral region for those wavelength where there is no true absorption, and some of them are valid only for values of the optical thickness that do not exceed specific limits.

In studies made in the IR region where it is not scattering, but true absorption that is substantial, and the instability of extinction is mainly due to the variable water vapor constant, to monitor the stability of atmospheric optical properties one must, in parallel with spectrophotometric observations, determine the H_2O content. An example is the observations of Koutchmy and Peyturaux /97/. Monitoring of the moisture content is undertaken optically, most often based on the equivalent width of one of the following bands: $\rho\sigma\tau$ (λ 0.94 micron or Φ (λ 1.2 microns), which

[10] In Rayleigh scattering no aureole is formed, since the Rayleigh indicatrix is very slightly elongated.

is determined with a photometer provided with filters centered on the band and its neighboring sections, or from records of the solar spectrum.

In concluding the section, we must, together with Ye. V. Pyaskovskaya-Fesenkova /103/, note that the concepts "constancy of atmospheric transparency and "invariancy of atmospheric optical properties" are quite conditional; minor variations in transparency of the fluctuation type evidently occur continually in the atmosphere. They then pose a natural limit to the accuracy of determining the transparency coefficient, which is about 1 percent under favorable conditions.

CHAPTER TWO /56

DETERMINATION OF THE SOLAR CONSTANT

1. Introductory Remarks

Measurement of solar radiation is one of the tasks of actinometry -- the scientific discipline lying at the interface between astrophysics and geophysics and dealing with the radiative energy of the sun and its transformation under natural conditions. We will not deal with most of the actinometric problems and methods, which are quite fully presented in monographs concerned with actinometry proper (for example, /44, 45, 58, 66, 114/), but we will examine only several problems associated with the determination of the solar constant S_0.

Commonly, the year of the birth of actinometry is taken as 1837, when Pouillet in France undertook the first attempt to determine the solar constant and obtained the value $S_0 = 1.79$ cal/cm^2 · min.*

N. N. Kalitin /66/ presents the summary of results of solar constant determination over nearly 100 years, beginning with Pouillet and ending with the work of V. G. Fesenkov (1931). The solar constant based on these data "changed" by more than twofold, from 1.79 to 4.0 cal/cm^2 · min, which in no way reflects the actual changes in S_0.

The problem of true fluctuations in the solar constant, that is, the problem of whether the sun is a variable star, remains thus far a matter of discussion and will be explored below. Leaping ahead, we note that if S_0 had undergone changes, these will be very small, not more than tenths of a percent.

Determinations of the solar content made in the 1930's to the 1960's afford a much smaller scatter of S_0 values. They are collected in Table 6. Extratropospheric determinations are not included in the table; they are considered separately.

* Translator's Note: In the year 1838, Pouillet determined the solar constant as 1.7633 calories per square centimeter per minute.

However, even measurements made in recent decades do not afford the desired precision: deviations in some independent results amount to ±3-4 percent. Therefore the problem of investigating and precluding sources of errors continues to be urgent up to the present time.

Measurement of total illumination produced by the sun is a difficult task; in its resolution the observer encounters the following problems (not to speak of the numerous technical difficulties in undertaking the experiment):

TABLE 6.* RESULTS OF SOLAR CONTENT DETERMINATIONS MADE IN THE 1930'S TO 1960'S /57

Year	Author	cal/cm^2·min	Remark
1923—1952,	Abbot et al.	1,94	
1932	Lincke	1,94	
1934—1935	Mulders	1,95	
1938	Unsold	1,90	
1940	Moon	1,90	d.e.
1949	Schatzman	1,97	
1949	Shuepp	1,96—2,03	
1950	Allen	1,97	
1951	Auren	1,97	
1951	Fritz	1,97	
1951	Houghton	1,97	
1951	Nicolet	1,98	d.e.
1952	Georgi	1,98	
1954	Johnson	2,002	d.e.
1955	Unsold	1,96	
1956	Stair & Johnson *)	2,05	d.e.
1958	Allen	1,99	
1967	Sitnik	2,076	d.e.
1967	Makarova&Kharitonov	2,03	d.e.
1968	Labs and Neckel	1,958	d.e.
1968	Stair and Ellis	1,95	d.e.
1969	Makarova&Kharitonov	1,98	d.e.

*) Based on a more recent publication /151/, this study /149/ is admitted by Stair himself as being erroneous.

* TRANSLATOR'S NOTE: Commas represent decimal points.

1. A radiation receiver nonselective over a fairly wide wavelength range must be built in order that sections of the solar spectrum outside this interval introduce a negligibly small fraction of energy into the solar constant.

2. Attenuation of light in the terrestrial atmosphere must be determined and allowed for. /58

Let us look at the first problem. Usually thermal action of radiation is utilized in actinometric instruments. These are first of all devices in which radiation heats water, thaws ice, causes a

bimetallic strip to bend, and so on. Secondly, thermoelectric radiation receivers are widely employed: thermoelements and bolometers. In both cases the instrument's response does not depend on the spectral composition of the radiation absorbed. However, we must be convinced that the surface of the working element in the instrument facing the sun has identical absorptivity for all wavelengths, and we must also experimentally verify that the instrument is nonselective overall. This verification is a quite delicate experimental procedure. Cases are known when the selectivity of receivers was detected which by concept could not be selective. Thus, Abbot rejected his 1916-1918 observations on detecting the selectivity of the bolometer used (related, probably, to the inadequate "blackening" of its working surface).

The problem of the nonselective absorption of radiation by the instrument is solved in principle, evidently, optimally in devices modeling an absolute black body (cf. Chapter Three). In particular, Abbot's water pyrheliometer and Voloshin's ice pyrheliometer, the helical radiometer, and so on, are so constructed (cf. Section 2).

The complexity of the second problem -- taking account of the attenuation of radiation in the terrestrial atmosphere -- has been discussed at length in the first chapter. Let us recall here that the Forbes effect does not permit extra-atmospheric values of total illumination from the sun to be determined only from actinometric observations, without bringing in additional data, in any case, in terrestrial research. Therefore, solar observations using nonselective actinometric instruments must be paralleled by spectrophotometric observations intended to explore the spectral transparency of the atmosphere and the distribution of energy in the solar spectrum and to calculate, on the basis of these data, the attenuation of the integrated radiation flux. This is the scheme of the method developed and used /59
at the Smithsonian Institution. In the past decade the second difficulty in determining the solar constant has been significantly reduced and eliminated altogether in individual cases, since it has become possible to carry actinometric instruments beyond the terrestrial atmosphere or at least beyond the troposphere (cf. Section 4).

Let us return again to Table 6. The results noted in the remarks with the letters d.e were not obtained from measurements of the total solar radiation using actinometric instruments, but by employing data on the distribution of energy in the solar spectrum and by integrating them. This determination approach is in principle quite correct, but is also difficult, since one must have reliable data on spectral illumination produced by the sun or else on its spectral brightness expressed in absolute energy units over a wide wavelength range.

Values of the solar constant derived by R. Stair and R. Johnston /115/, Sitnik /116/, D. Labs and H. Neckel /113/, and by

Stair and Ellis /117/ were based on their own series of absolute [11] measurements of the spectral distribution of solar energy.

Early in the 1950's M. Nicolet /118/ and F. Johnson /119/ derived independently of each other the distribution of energy in the solar spectrum by relying on the averaging of the results of several series of measurements performed during this time. By integrating S_λ values, Nicolet and Johnson obtained S_0 values of 1.98 and 2.002 cal/cm^2 · min, respectively. In similar fashion, the authors of /120/ derived the value S_0 = 2.03 cal/cm^2 · min in 1967.

Nicolet's result was recommended in the International Handbook on Radiation Measurements for the International Geophysical Year as the "final" value of the solar constant. Johnson's result, as well as the method of its derivation, was regarded as most correct for several years. However, both these results as well as the value given in /120/ are now already much out-of-date, since /60 many new measurements of the distribution of energy in various regions of the solar spectrum have been undertaken since then. An attempt to re-examine the 1967 data on the distribution of energy in the solar spectrum and the derivation on this basis of a revised S_0 was undertaken by us late in 1969 /121/. We will return to the problem of deriving the solar constant from the distribution of energy in the solar spectrum in Chapter Five.

2. Instruments Used in Measuring the Total Flux of Solar Radiation

Numerous instruments for measuring solar radiation are described in detail in books on actinometry by K. Ya. Kondrat'yev /45/, N. N. Kalitin /66/, Yu. D. Yanishevskiy /114/, and so on. Instruments used in measuring the solar constant during high-altitude flights (on aircraft, balloons, and spacecraft) are described in /112-126/.

Most of the specifically actinometric instruments measure energy in relative units and cannot yield solar constant values directly, without comparison with a calibrated instrument. We will describe very briefly several of the instruments, preferably those in which energy is measured in absolute units: most provide results in the International Pyrheliometric Scale, some in the International Thermodynamic Scale, and finally, some in the absolute electrical scale. The fact that here we have direct measurements of the solar constant made in three different absolute scales

[11] Each of these authors supplemented his results in the long-wave and short-wave directions of the spectrum by using data of other measurements; these other measurements were usually taken in relative units. Naturally, these supplements did not change the absolute S_0 values.

is doubtless of fundamental importance. By comparing measurements taken on independent scales one can estimate how reliable the solar constant value is and what is the probable systematic error of determination.

Principal actinometric instruments

The Angstrom compensation pyrheliometer. The main element of the instrument consists of two (as completely identical as possible) blackened manganin plates. One of the plates is shaded /61 and the other is illuminated by the sun. Electric current is passed through the shaded plate compensating for heating of the sun-illuminated plate. Equality of the heating of plates makes it possible for certain electric circuit parameters to determine the illumination produced by solar rays. The Angstrom pyrheliometer is marked by systematic errors caused by the somewhat different conditions of heating of both strips. According to /114/, measured illumination values are understated by 1.1 percent owing to these errors. Their exact estimate is difficult. In reducing readings of compensation pyrheliometers to the International Pyrheliometric Scale of 1956, it was decided to increase their readings by 1.5 percent.

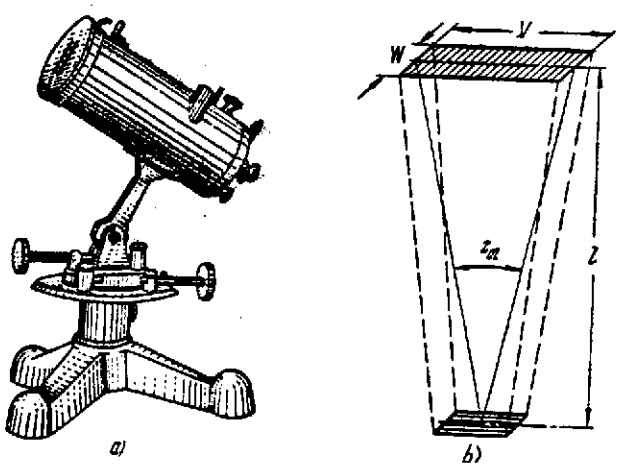

Fig. 11. Angstrom pyrheliometer: a) general view; b) scheme of aperture angles

Another source of error in pyrheliometers of this type is the instrument's geometry. Slit diaphragms of the pyrheliometer (Fig. 11) admit along with solar radiation also some fraction of the solar aureole, but different fractions for different directions and with strong dependence on the sky conditions. All this complicates a comparison of network actinometric instruments which usually have a circular entrance diaphragm with reference /62 standard instruments. Even for comparisons made in high-altitude conditions with the sky clear, the aureole distorts their results and data must be extrapolated to the zero turbidity factor, which of course reduces the accuracy of observed absolute values of the solar radiation flux.

In addition, even reference standard pyrheliometers at different laboratories have somewhat different geometries; for example, the aperture angles z_{0i} with respect to the length of the entrance strip (Fig. 11 b) for the pyrheliometers at the Eppley laboratory and the Leningrad State University, reproducing the 1956 scale, are 10.5° and 16.8°, respectively, though as to strip width the angles coincide and are 4.1°.

Nonetheless, owing to its simplicity and operating reliability, the Angstrom pyrheliometer invented in 1895 is the principal international reference standard of the 1956 Pyrheliometric Scale. Reference standard instruments with which the remaining actinometric instruments are compared are stored at Davos (Switzerland) and Uppsala (Sweden).

The Abbot water-flow pyrheliometer served as the principal reference standard instrument at American actinometric stations before establishment of the 1956 International Pyrheliometric Scale. Now, evidently, it has been displaced by the Angstrom pyrheliometer. The concept of the instrument based on modeling an absolute black body was proposed by W. A. Michelson as early as the beginning of the 1900's and was first built by Abbot in 1913. In this pyrheliometer solar radiation passing through the entrance diaphragm impinges in a cavity with a conical bottom. Typical dimensions of the cavity are roughly one order of magnitude larger than the diaphragm diameter; the outer surface is continually bathed with water. The difference in the water temperatures before and after streaming over the cavity is the measure of radiation intensity. The water-flow pyrheliometer also has a systematic error: its readings are overstated by about 2 percent /114/. Therefore, to convert to the 1956 scale conversion factors of water-jet pyrheliometers, that is, the American pyrheliometric scale, are reduced by 2 percent.

These pyrheliometers are instruments that are absolute in the sense that the conversion factors for converting from directly measured quantities: the current strength in the Angstrom pyrheliometer and the difference in water temperatures in the Abbot pyrheliometer, to the measured radiative energy -- are found by laboratory means in the case of reference standard instruments, without comparing pyrheliometers with other instruments measuring radiation. But the calibration of working instruments used in daily observations is conducted by comparing them with reference standards, which is done periodically.

These two instruments determine the pyrheliometric scale.

The Yanishevskiy thermoelectric actinometry at the present time is the main instrument used to measure the flux of direct solar radiation at USSR actinometric stations. A system of zigzag-connected thermocouples, whose "hot" junctions are connected to a blackened silver disk heated by the sun is employed in this device /114/.

The Yanishevskiy actinometer is a relative instrument. The conversion factor for determining radiation on an absolute scale is found by comparison with readings of a calibrated pyrheliometer. The factor increases with temperature, therefore its temperature dependence must be investigated.

Instruments used in measuring the solar constant at higher altitudes.

In addition to the standard Angstrom pyrheliometer and the Yanishevskiy actinometer, whose descriptions are given above, several other instruments are employed:

A series of multichannel radiometers was developed at the Eppley Laboratory of the Drummond group [123-125]. In particular, a 12-channel radiometer is extensively used in flights. A high-sensitivity low-inertia nonselective thermocouple, which is a flat wire wound in spiral form, serves as the radiation receiver in this device. Two channels with fields of view 5 and 15° are used to measure the total flux of solar radiation with a precision of 0.5-1 percent. The channels are protected with a double quartz window. By means of two glass filters, orange and red, the fluxes /64 of solar radiation with $\lambda \geqslant 5300$ angstroms and $\lambda \geqslant 6900$ angstroms are separated in two other channels, with a precision of measurement 1-2 percent. The remaining eight channels are intended essentially for spectral measurements: the regions 2390-7000 and 3550-9630 angstroms are covered by means of narrow-band interference filters in different versions of the radiometers. The radiometer is calibrated on the 1956 International Pyrheliometric Scale (cf. below) by comparison in high-elevation conditions with the primary Eppley Laboratory pyrheliometers, which in turn are tied in to the standard pyrheliometer stored at Davos. Tying in of the radiometer is performed each time before and after a flight. The precision of pyrheliometric scale reproduction is 0.1-0.2 percent. The stability and reproducibility of the radiometer signals are checked under conditions that are close to those of outer space -- in a vacuum chamber (10^{-5} atm) at the temperature of liquid nitrogen -- and also in normal atmospheric conditions. Solar energy is simulated with a xenon-mercury arc lamp; all 12 radiometer channels are illuminated at the same time.

Cone radiometer [122]. In this instrument electric current is passed through a 0.05 mm thick wire wound in the form of a cone. The base of the cone is oriented toward the light source, and the conical surface is blackened. The absorptivity of the black coating is taken as 0.9945. The cone is enclosed in a vessel whose internal temperature is kept constant: it is filled with liquid nitrogen. When the working surface is illuminated the temperature and resistance of the wire change; the changes are compensated in a Wheatstone bridge circuit, which makes it possible to measure. The detector block and the vessel filled with liquid nitrogen are

enclosed in a vacuum chamber with a sapphire window which has no absorption bands in the region 0.2-6 microns. The aperture angle of the radiometer is approximately 5.5°; at this field of view the flux from the solar aureole at an altitude of 11.58 km is $5 \cdot 10^{-4}$ of the solar flux, according to calculations based on the data in /61/.

The cone radiometer is an absolute instrument; it is calibrated on the absolute electrical scale.

The Hy-Cal normal-incidence pyrheliometer /122/. A thin metal /65
disk coated with a special (Hy-Cal) graphite coating with high radiativity serves as the detector in this instrument. The detector is mounted in a cylindrical copper block with a quartz window that admits the spectral region from 0.2 to 3.5 microns. The block is placed at the bottom of a wide tube with a circular opening; the aperture angle is 4°. The strength of the direct current induced in the disk on exposure to radiation varies linearly as a function of the intensity of incident radiation all the way up to values of two solar constants. This pyrheliometer is calibrated on the thermodynamic scale with respect to the radiation of an absolute black body.

When several versions of pyrheliometers and actinometers are examined, one is struck by the fact that they differ greatly in geometrical parameters. There are virtually no two types of instruments that are geometrically wholly identical. Even Angstrom reference standard pyrheliometers at different laboratories, as already noted, receive different angular sections of the sky around the sun. This disparity is by no means as innocuous for results obtained in the pyrheliometric scale as might appear at first glance. From the estimate of Angstrom /127/, the zone of the solar aureole, intersected by the pyrheliometer with a 5° aperture angle when atmospheric conditions at sea level are good, yields a radiation flux representing from 1 to 3 percent of the flux of direct solar radiation. Even if the transmission coefficient is constant during the observations, the error in solar radiation measurements caused only by the aureole can be 0.3 percent, according to /127/.

V. I. Golikov investigated closely the problem of the effect that the solar aureole has on the results of measuring radiation as a function of geometrical characteristics of actinometers /128/. Fig. 12 gives the dependence of the vignetting factor $F(\beta, \infty)$ for an infinitely removed source on its angular dimensions, expressed in the aperture number of the instrument β, for different pyrheliometers. In the absence of vignetting $F(\beta, \infty) = 1$. The function $F(\beta, \infty)$, which is an analogy of the "instrumental profile", differs widely even for the instruments most commonly /66
used in the actinometric network. The dependence of the calculated "aureole correction" Λ as a function of a quantity that is proportional to the air mass and the scattering coefficient of

the atmosphere is shown in Fig. 13 for three instruments. The aureole correction Λ is equal to the ratio of the energy flux received by the actinometer only from the solar aureole to the flux received only from the solar disk. Aureole corrections for different instruments vary by several-fold, which naturally limits the precision of calibration of working instruments based on reference standard instruments in the pyrheliometric scale, all the more so in that the geometry of the reference standard Angstrom pyrheliometers themselves at different laboratories is not the same. Therefore in determining the solar constant the instruments can be more or less reliably compared with each other only when the atmosphere is exceptionally clear. Thus, recently in the Soviet Union, in Armenia a comparison was made of working pyrheliometers of the Eppley Laboratory (A. Drummond) and Leningrad University (K. Ya. Kondrat'yev and G. A. Nikol'skiy) at an elevation of about 1500 m. It was found that the discrepancy /67
between the Eppley pyrheliometer (No 8420) readings, closely tied in with the reference standard pyrheliometer stored at about Davos (Switzerland) and the readings of the LGU /Leningrad State University/ pyrheliometer (No 575) tied in to the Stockholm reference standard amounted to about 2.9 percent for a turbidity factor of $\beta = 0.08$, and 2 percent for $\beta = 0.051$, and when extrapolated to zero cloud cover the ratio of the fluxes measured was 1.0035 ± 0.001, that is, deviation of the scales does not exceed 0.3-0.4 percent. The extrapolation procedure doubtless is not desirable for absolute measurements.

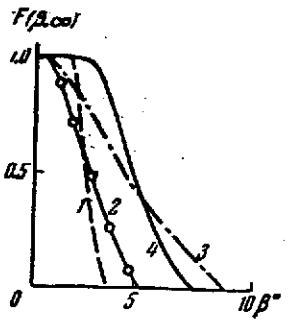

Fig. 12. Dependence of the vignetting factor $F(\beta, \infty)$ on the aperture angle β in degrees for the following pyrheliometers:
1 -- Eppley
2 -- silver-disk; and for the following actinometers:
3 -- Lincke-Foyssner
4 -- Yanishevskiy

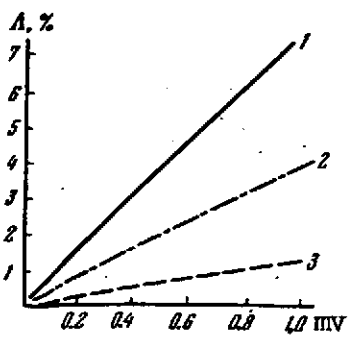

Fig. 13. Dependence of aureole correction Λ on the product of the atmospheric mass and the scattering coefficient of the atmosphere for:
1 -- Yanishevskiy actinometer
2 -- Angstrom pyrheliometer with a 50 mm tube
3 -- Angstrom pyrheliometer with a 150 mm tube (Smithsonian instrument)

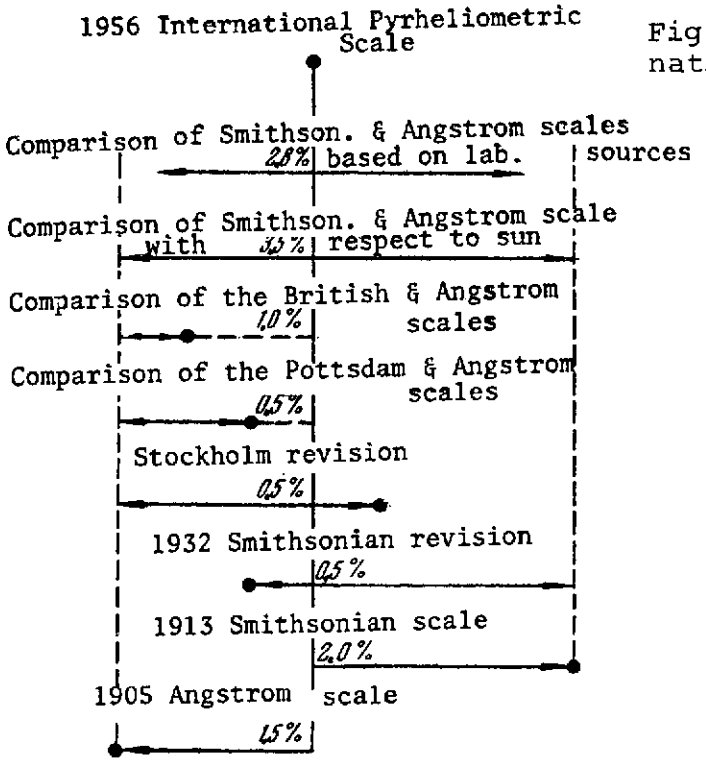

Fig. 14. Differences between national pyrheliometric scales

All of the above-noted facts: difference in the geometry of instruments, effect of solar aureole on comparison results, difficulties in determining corrections associated with individual features of instruments, and the like, have led to the fact that pyrheliometric scales in different countries differ somewhat between each other. The differences between national scales are very graphically illustrated by Fig. 14, taken from the study of Thekaekara /130/. /68

The problem of the specific causes for the discrepancy between individual scales is extremely hard to clarify and is not often resolved. Thus, it has not been possible to discover the reason for the 1 percent discrepancy between the Smithsonian and Stockholm revised scales. The currently adopted 1956 International Pyrheliometric Scale (IPS) was established as the mean between them.

One must hope that in the near future the annoying disparity of geometrical parameters of actinometers and, in particular, reference standard pyrheliometers will be cleared up, and thus will also be cleared up the reason for the by no means justified understating of accuracy and reliability of pyrheliometric comparisons.

Observations made at high altitudes on the electrical and thermodynamic scales, with corrections for the aureole, obviously are not needed, since the aureole outside the earth's troposphere is virtually absent, and reference standardization of instruments in a laboratory is not burdened with the aureole correction. One can assume that these scales -- electrical and thermodynamic -- being scales for general-physical measurements will subsequently displace from use the pyrheliometric scale developed specifically for solar constant determinations.

3. Methods of Determining the Solar Constant Used by the Smithsonian Institution

In determining the solar constant from ground observations, the most successful method is the one proposed as early as the end of the 19th century by S. Langley [131] and receiving further development and extensive use in the work of C. Abbot and his coworkers. It is appropriate to mention that Abbot and his colleagues (L. Aldrich, F. Fowle, and V. Hoover) devoted about 70 years to the problem of determining the solar constant, performing enormous methodological, observational, and organizing work. In all, the Smithsonian Institution made several tens of thousands of individual determinations of S_0, published, for example, in [131, 132]. /69

Two instruments were used simultaneously: a pyrheliometer and a spectrobolometer. The latter recorded the integral spectrum of the entire solar disk in the interval from ~0.34 to ~2.4 microns with very low resolution.

The concept of the method was as follows. Solar observations were made with different air mass values M and simultaneously spectrobolograms and pyrheliometer readings were obtained. Since the bolometer is nonselective, the spectrobologram -- after correction for absorption of radiation in the optics of the instrument, which was carefully investigated, showed the distribution of energy in the solar spectrum e_λ (M) in relative units (instrument readings).

An envelope was drawn with respect to the gaps between the most intense telluric bands; it showed what these spectrobolograms would be if the telluric bands were absent. Forty ordinates of the spectrobolograms in selected wavelengths were extended beyond the atmosphere by the Bouguer method, and the resulting envelope e_λ (0) provided the extra-atmospheric distribution of energy in the solar spectrum expressed in the same spectrobolometer readings.

Further, the areas under these spectrobolograms were determined. First the areas Σ_M and Σ_0 were found under their envelopes for atmospheric masses M and beyond atmospheric limits, respectively.

Then the sums Σ'' of the areas of all telluric bands were subtracted from the Σ_M values. Finally, the following corrections were added to the Σ_0 areas: K_u for the nonobservable ultraviolet radiation, and K_i -- for the infrared, K_u and K_i are extra-atmospheric values of the corrections. Let us assume $K_u + K_i = \delta_0$. For rigor in our line of reasoning, we must also add a small correction δ_M to Σ_M. It is dictated by the fact that spectrobolograms embrace a narrower spectral region, roughly from 0.34 to 2.4 microns, then is received by the pyrheliometer: radiation in the interval 0.30- /70
0.34 micron and in the region $\lambda > 2.4$ microns (in the transmissiion windows) strikes the latter.

Thus, if P_M is the pyrheliometer reading at the moments of observation with the spectrobolometer and Δ is the distance from the earth to the sun expressed in fractions of the mean distance, the solar constant will be determined by the obvious formula

$$S_0 = \frac{\Sigma_0 + \delta_0}{\Sigma_M - \Sigma' + \delta_M} \frac{P_M}{\Delta^2}. \qquad (21)$$

The mean value of the solar constant obtained from the many years of observations by Abbot and his colleagues is 1.94 cal/cm^2 min in the 1956 International Pyrheliometric Scale [12].

The corrections K_i and, especially, K_u are the source of considerable indeterminacy in ground determinations of the solar constant. Before rocket observations were made, when the correction K_u was determined one always had to make certain assumptions. At the Smithsonian Institution the correction K_u was determined on the basis of the assumption that the sun radiates in the region $\lambda < 3000$ angstroms as an absolute black body, with $T = 6000^\circ$ K. The Planckian curve corresponding to this temperature was artificially distorted by the absorption lines presumed at $\lambda < 3000$ angstroms; the overall values of their equivalent widths were obtained by extrapolating the corresponding data for $\lambda > 3000$ angstroms.

---

12 The mean value of the solar constant obtained in the Smithsonian Institution as the result of 30 years of observations and published in a study by Aldrich and Hoover /133/ was 1.946 cal/cm^2 · min. Subsequently it was found that this result is understated by 1.8 percent compared with the 1913 Smithsonian Scale, which in turn is overstated (cf. Fig. 14) compared with the 1932 Smithsonian Revised Scale. After introducing the corrections described in detail by Johnson /119/, values of S_0 = 1.934 cal/cm^2 · min in the 1932 scale and 1.94 cal/cm^2 · min in the 1956 International Pyrheliometric Scale were obtained.

As for the correction K_i, the situation is somewhat better, since one can even from the earth's surface record solar radiation quite far toward the long-wave side (in the atmospheric windows of the earth's atmosphere). In determining the correction K_i at the Smithsonian Institution, a spectrophotometer was used with a rock salt prism, which permitted recording the solar spectrum with low dispersion all the way to λ 10.9 microns. /71

The indeterminacy of the corrections K_u and K_i is aggravated even further by the fact for different particular instruments of the same model, even when the same observational measurement is used, the limits between the observed and nonobservable sections of the spectrum fall at different wavelengths. Thus, at the Smithsonian Institution the short-wave limit of spectrobolograms is displaced from 0.340 to 0.370 micron, and the long-wave limit -- from 2.3481 to 2.8 microns /113/.

Various arbitrary assumptions in determining the corrections K_u and K_i, and also the "mobility" of their limits led to the fact that for different workers concerned with determining the solar constant from the earth's surface, the correction K_u varied from 3.4 to 6.1 percent, and the correction K_i -- from 2.0 to 3.8 percent of the observed flux derived beyond the atmospheric limits, that is, of the Σ_0 in formula (21).

The Abbot method described, called the "long" method, has two key drawbacks:

1. The necessity of making extended observations during the day in order to be able to plot Bouguer lines. As a result, during each day not more than two independent determinations of S_0 can be made -- based on ante-meridian and post-meridian solar observations.

2. The high sensitivity of the method to slow changes in atmospheric transparency during the observational period. Abbot selected locations with very good astronomical conditions in organizing his stations (California, Chile, and Egypt), but there was no monitoring of the stability of optical properties or sampling for analysis of only those observations which were made with an optically stable atmosphere. Therefore, results can be burdened by errors whose origins are explained in Section 5, Chapter One; the errors can be systematic in nature and are not cancelled out upon averaging even of a very great deal of observational material, if at the observational sites the change in the atmospheric optical properties is regular in nature over a period of days. This problem was examined in a study by G. F. Sitnik /134/. /72

In 1919 Abbot proposed another method of determining the solar constant, which he called the "short" method. Based on a wealth of observational material obtained with the "long method,"

Abbot found empirical functions between the brightness of the solar aureole and the water vapor content in the atmosphere, on the one hand, and between the atmospheric transparency coefficient at different wavelengths -- on the other. The brightness of the aureole was determined by him with a special instrument -- the pyranometer, and the water vapor content was determined from the equivalent width of the telluric band $\rho\sigma\tau$ measured on spectrobolograms. Thus, having one observation each made on the pyrheliometer, spectrobolometer, and pyranometer, one can find the S_0 value. In the course of a day independent determinations of S_0 can be made, each of which is less affected by the instability of atmospheric conditions than with the long method. Therefore, while in the long method the probable error of a single determination is 0.9 percent, in the short method it is lowered to 0.4 percent. (We are speaking of the internal convergence of results; systematic errors associated with scale error and other general factors are not under discussion.)

The "short" method of Abbot, like the "long" method, is not free of disadvantages. First of all, it is not wholly independent, since the empirical relationships postulated as its basis are derived on the basis of using the "long" method, which was employed, as already remarked, without monitoring the stability of atmospheric optical properties. Another disadvantage of the "short" method has been analyzed in detail by Academician V. G. Fesenkov. He showed that one can imagine a situation when for the same water vapor content and for the same attenuation of light due to scattering, the brightness of the solar aureole will change. This change can be caused by changes in the composition of aerosols, which soon is reflected in the shape of the scattering indicatrix. As a result, "from the stability of the aureole one can conclude that the atmospheric transparency index is constant, but conversely, one cannot not yet estimate the corresponding changes in transparency based on changes in the brightness of the aureole" /135/.

4. Measurements of the Solar Constant Outside the Earth's Troposphere /73

As stated above, using only actinometric instruments it is impossible to directly measure the solar constant from the bottom of the terrestrial atmosphere even under high-elevation conditions. Naturally, as soon as the technical possibility of carrying instruments beyond the earth's atmosphere or even beyond the limit of the troposphere appeared since the early 1960's, attempts were made at the direct determination of the solar constant; reliable results were obtained beginning in 1965. The instruments were lifted on special aircraft to altitudes of 11-13 km, on balloons -- to 30-33 km, and on rockets, spacecraft, and satellites -- virtually beyond the terrestrial atmosphere. At the present time, a total of more than 10 independent determinations of the

solar constant have been made in the USSR and the United States, based on approximately 80 series of very expensive observations from high altitudes.

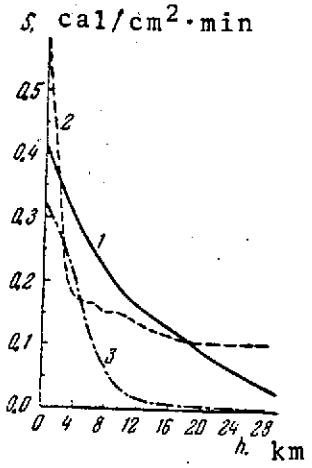

Fig. 15. Role of various factors in the attenuation of the total flux of solar radiation for different altitudes:
1 -- Rayleigh scattering
2 -- Aerosol scattering
3 -- Extinction caused by absorption by polyatomic gases

Fig. 15 taken from /136/ shows the role of various factors in the attenuation of the total flux of solar radiation for different altitudes.

At elevations of 11-13 km the instruments are carried beyond the limits of the troposphere; below remains about 80 percent of the main gases of the atmosphere and 99.9 percent of water vapor /122/. Under these conditions it is possible to determine the extra-atmospheric value of this solar constant without spectral observations, since the Forbes effect is significantly reduced, and the main absorber of IR radiation, water vapor, remains below the instrument. But the effective thickness of the layer of ozone absorbing radiation /74
from $\lambda < 3000$ angstroms is nearly the same at this altitude as at sea level (therefore curve 3 of Fig. 15, showing the extinction due to the absorption by all gases is noticeably above zero for the altitude of 10-12 km).

At "balloon" altitudes (32-33 km) ~99 percent of the terrestrial atmosphere /137/ and the layer of the maximum concentration of ozone molecules is beneath the instrument, though one must still allow for absorption in the upper section of the ozone layer and in intense lines such as, for example, the CO_2 line at λ 4.3 microns, and in addition, aerosol scattering still remains appreciable /136, 138/.

Only observations taken from rockets and satellites are entirely free of the effect of the terrestrial atmosphere.

Direct measurements of the solar constant from rockets and spacecraft

1. Rocket observations of the Drummond group. The first direct measurement of the solar constant made outside the earth's atmosphere was carried out by the Drummond group /124, 125, 139-142/

and is the result of the combined work of two scientific research laboratories in the United States -- the Eppley and the Jet Propulsion Laboratories. This first step in outer space actinometry was made on 17 October 1967. A 12-channel radiometer (section 2) was lifted by a X-15 rocket to an altitude of 82 km. The measurements were made outside the rocket, that is, without a supplementary window. Thus, the readings of the two radiometer channels measuring the total flux of solar radiation had to be corrected only for absorption in the quartz window of the radiometer and a correction had to be introduced adjusting the solar constant for the mean earth-sun distance [13]. The solar constant measured during this flight was 136.1 mw/cm^2 or 1.95 cal/cm^2 · min (cf. Table 8).

2. Results of determining the solar constant on the spacecraft Mariner VI and Mariner VII. In 1969 two series of solar constant measurements were carried out during the flight of the spacecraft Mariner VI and Mariner VII to Mars at a distance of more than 20,000 km from the earth /143/. The results were based on measurements with an active-cavity radiometer, transmitted via telemetry to the earth. The layout of the active-cavity radiometer is given in Fig. 16 /126/. The radiometer scale as well as the scale of the cone radiometer (Section 2) was calibrated in absolute electrical units. In spite of the fact that the distance between the Mariner VI and Mariner VII was enormous, still the results of measurements taken during several weeks proved to be very close to each other, and the solar constant based on these determinations was 135.2 mw/cm^2 or 1.940 cal/cm^2 · min (cf. Table 11).

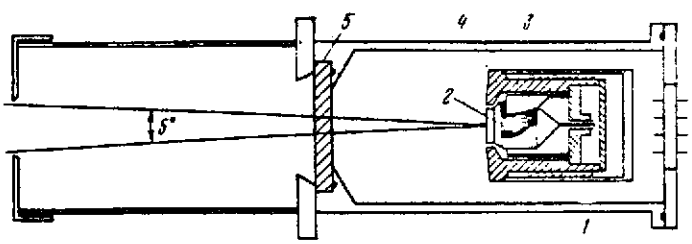

Fig. 16. Scheme of active-cavity radiometer used to determine the solar constant on the spacecraft Mariner VI and Mariner VII, and also in the work /126/
1 -- Silvered cavity blackened internally (cavity) detecting the radiation
2 -- gold foil covering the cavity winding being heated with electricity
3 -- electrical winding monitoring the T of the cavity
4 -- heat-insulating space
5 -- quartz window

[13] This correction appears in the formula for the determination of the solar constant, therefore in the following all data will be presented with allowance for this correction, without additional qualifications.

Balloon measurements

1. Observations of Leningrad University. Though the first determination of the solar constant in outer space was undertaken by the Drummond group in 1967, the priority of direct measurements of the solar constant undoubtedly belongs to the group of scientists /76 at Leningrad University headed by K. Ya. Kondrat'yev. This group developed and built an involved complex of instruments and equipment for measuring the solar radiation flux as well as the radiation regime and various characteristics of the terrestrial atmosphere /144-146/. The complex was first carried by balloon in 1961 to an altitude of about 32 km, and by 1970 a total of 28 ascents were made; the results are summarized in the works /136, 137/, and also /147/. During the balloon ascent direct solar radiation was measured with a Yanishevskiy actinometer. The instrument was placed in a hermetic chamber with a quartz window cutting off radiation at $\lambda > 3.7$ microns. On the short-wave side radiation from $\lambda < 3000$ angstroms is absorbed by ozone.

The temperature of the chamber shell was regularly measured to introduce corrections to the thermoelement readings. Recording of residual extinction in the terrestrial atmosphere and determination of extra-atmospheric values of solar radiation flux were carried out with the classical Bouguer method; here it was assumed that at an altitude of 32 km the Forbes effect can be neglected:

$$\lg S'_M = \lg S'_0 + M \lg p, \qquad (22)$$

where S'_M and S'_0 are the solar radiation fluxes in the spectral region 0.3-0.7 micron at the observational altitude and beyond the limits of the earth's atmosphere, respectively. The transmission coefficient p of the atmosphere determined in this way for one of the ascents (No 23, Fig. 17) given the condition of a clean and optically stable atmosphere was subsequently used in processing the results of all the remaining ascents. In determining the solar constant, the following had to be allowed for: 1) radiation with $\lambda < 0.3$ micron not reaching the receiver owing to absorption in the ozone layer (in its upper section), and 2) radiation with $\lambda > 3.7$ microns cut off by the quartz window of the instrument. The ultraviolet correction for balloon observations was taken as 0.014 cal/cm^2 · min, and the infrared correction was taken as 0.020 cal/cm^2 · min.

The results of determining the solar constant obtained during the ascents of the balloons in the period of 1962-1967 are shown in Fig. 17, taken from the work /137/. The Wolf numbers characterizing solar activity are plotted on the X axis, and on the Y axis are plotted the solar radiation flux values beyond the terrestrial atmosphere, in cal/cm^2 · min. /77

Upon analyzing these results, K. Ya. Kondrat'yev and G. A. Nikol'skiy concluded that the most realistic maximum solar constant

value is 1.94 cal/cm2 . min. The same value was observed for Wolf numbers of the order of 80-100. With increase and decrease in Wolf numbers, the solar constant drops by 2-2.5 percent. The precision of absolute values is determined by three factors: 1) the precision of introducing the correction that allows for variation in the actinometer's sensitivity with temperature, about 0.8 percent; 2) the precision of calibrating the instrument on the 1956 pyrheliometric scale, about 0.5 percent; and 3) the precision of corrections for radiation not measured by the actinometer — about 0.2 percent. Thus, the maximum possible error is approximately 1.5 percent. /7

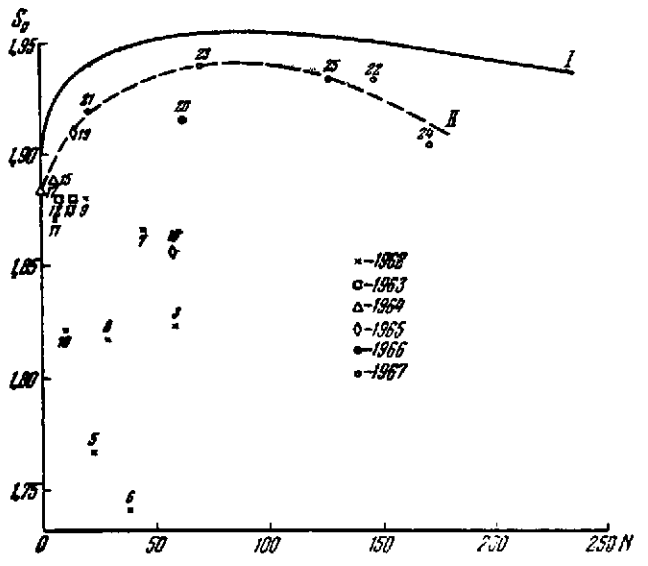

Fig. 17. Results of altitude determinations of the solar constant obtained by the Leningrad State University group. The Wolf numbers N characterizing the relative number of spots are plotted on the X axis, and the solar constant S_0 values are plotted on the Y axis, in cal/cm^2 . min.
I -- Angstrom's 1922 results;
II -- the average course proposed by the authors. Ascents made in different years are denoted with symbols.

In discussing the precision of results, the problem of the error caused by extrapolating actinometer readings beyond the limits of the terrestrial atmosphere remains unexplored.

Even though about 99 percent of the mass of the principal gases remains below the instrument in balloon observations, nonetheless the variable aerosol component of the atmosphere sometimes markedly reduces the solar radiation flux, which can be readily seen from the data of K. Ya. Kondrat'yev and G. A. Nikol'skiy, shown in Fig. 17. Most of the points lie much below the value of 1.94 cal/cm^2 . min, adopted as the most probable maximum solar constant value. It is difficult to assume that the solar constant itself changed so appreciably and erratically; this distribution of points is evidently a consequence of the fact that in extrapolating observations beyond the limits of the earth's atmosphere, data on extinction in it were used that were determined for a single day with good transparency. In this case, it follows from formula (22)

that for days with worse transparency we obtain understated extra-atmospheric values of the solar constant.

By comparing their results with the data on the contamination of the terrestrial atmosphere due to atomic bomb tests at high altitudes (cf., for example, the works /148-150/) and with ground pyrheliometric observations made in India /151/, K. Ya. Kondrat'yev and G. A. Nikol'skiy suggested that the lowest values of the solar energy flux, for 1962 (ascents Nos 3, 5-11) are in all probability due to the series of explosions of large atomic bombs /137/. This same conclusion about the effect of atomic explosions in the atmosphere was also reached by the foremost scientist determining the solar constant, Abbot. According to the data of Kuroda et al. /150/, and V. G. Fesenkov /152/, atomic explosion products will move as a cloud that will circle the globe several times before they are completely assimilated. The approximate period of rotation of the cloud for the middle latitudes is of course very roughly, about 22 days. The understated value of the 1965 results (ascent No 18) is accounted for, in the view of the authors /137/, by atmospheric contamination following the eruption of the Taal volcano in 1965. /79

The actual extra-atmospheric solar constant value itself must not, naturally, depend on how dusty the terrestrial atmosphere is. Numerous understated results shown in Fig. 17 are evidently due to the systematic error in the processing of observations owing to the use of an overstated transparency coefficient instead of the actual coefficient on days with poor transmission.

Accordingly, doubt is cast on the suggestion by K. Ya. Kondrat'yev and G. A. Nikol'skiy of the strong dependence of the solar constant on Wolf numbers, that is, on the solar activity phase, within the limits 2-2.5 percent. Since there is no objective criterion of what caused the understating of the results -- whether it was the low atmospheric transparency or the actual decrease in solar radiation flux, this function appears to be poorly substantiated. We can more properly suggest that the results shown in Fig. 17 represent the lower limit of the true value of the solar constant. Angstrom, with whose data /153/ the results of the work /137/ were compared, recently drew the same conclusion, that all the so-called "fluctuations" in the solar constant are a consequence of unreliable allowance for extinction in the terrestrial atmosphere /127/. The problem on the "variability" of the sun will be discussed in detail below, in Section 5.

2. The balloon observations of Denver University. These observations were made by the Murcray group /138,154/ over a period of three days: in June 1967, and January and April 1968, at altitudes of about 31 km. The solar constant was measured with two Eppley-Angstrom pyrheliometers (Angstrom pyrheliometers improved in the Eppley laboratory). They were compared in high-elevation conditions with standard pyrheliometers of the Eppley

laboratory, and these latter were "tied in" to the primary instrument reproducing the 1956 International Pyrheliometric Scale. The mean square-root error of the tie-in of the working instruments to the pyrheliometric scale was less than 0.2 percent.

During the ascents, the pyrheliometers were placed in a double thermostat, due to which there was no need to make correction for variation in ambient temperature. The pyrheliometer readings were recorded on magnetic tape and simultaneously transmitted by telemetry to a ground command station. When the observations were analyzed it was found that the readings of one of the pyrheliome were distorted by systematic error; in the end, the final result were based on only readings of the second, correctly working pyrheliometer. Two corrections were made in the data obtained with the same instrument: 1) for absorption in the quartz window of the pyrheliometer for $\lambda > 4$ microns, the correction was taken as 0.017 cal/cm^2 · min [14]; and 2) for residual absorption in the ozone layer and attenuation of the aerosol component /15/. This latter correction was calculated in accordance with the standard Elterman model /61/ for the spectral region from 0.2 to 4 microns. The calculated residual extinction at an altitude of 31 km is 0.035 cal/cm^2 · min. Thus, the overall correction to the pyrheliometer readings is 0.052 cal/cm^2 · min.

TABLE 7. RESULTS OF BALLOON OBSERVATIONS OF THE MURCRAY GROUP

Date	Illumination from sun, S, cal/cm^2·min	
	at 31 km altitude	outside atm.
June 1967	1.867	1.919
January 1968	1.848	1.900
April 1968	1.865	1.917

The mean value of illumination from the sun for each of the three balloon flights at the altitude ~31 km S" is given in the second column of Table 7. The last column gives the solar constant values S_0, that is, the correction of 0.052 cal/cm^2 · min is taken into account.

Murcray maintains that during the summer and spring balloon flights the aerosol component was present in slight amounts, while during the January 1968 flight the balloon never

[14] Even though the window admits radiation up to ~4.5 microns however owing to the CO_2 absorption line that is intense even at an altitude of 31 km, at 4.3 microns, the radiation is practically cut off near 4 microns.

went beyond the limits of the aerosol layer. On this basis the understated solar constant value in January 1968 is not taken into consideration by this author, and the mean value of the solar constant is assumed to be 1.919 cal/cm^2 · min.

The Denver authors estimated the accuracy of the result as 0.4 percent; in their view, it is determined by the accuracy of the tie-in to the pyrheliometric scale. However, the observations of the Murcray group evidently are burdened with a systematic error caused by the fact that the actual extinction of the terrestrial atmosphere brought about by the aerosol layer localized over the "balloon altitudes" was not taken into account.

K. Ya. Kondrat'yev and G. A. Nikol'skiy, on comparing the data of their own balloon observations /137/ with the results obtained by the Murcray group, noted that, for example, in June 1967 both groups measured the solar constant virtually simultaneously, and measurements at the altitude of 31 km yielded the same value with a precision up to 0.1 percent: 1.884 cal/cm^2 · min is the result of Denver University and 1.886 cal/cm^2 · min is the result of Leningrad State University (corrections are introduced only for absorption in the quartz windows of the instruments). Still, extrapolation beyond the limits of the terrestrial atmosphere gives a solar constant of 1.919 and 1.938 cal/cm^2 · min, respectively; the deviation is 1 percent, which evidently can be explained only by the different methods allowing for the residual atmospheric extinction.

Calculated values of the extinction caused by the aerosol component, based on the standard model of the atmosphere, proved to be understated compared with the actual values. Fig. 18, taken from /136/, presents the dependence on altitude of the aerosol coefficient of attenuation of radiation according to the standard model /61/, and the mean value of measurements made during the ascent of balloons undertaken by the Leningrad State University group (Rayleigh scattering and absorption in the ozone layer are excluded). As we can see from the plots, the acceptable /82 agreement of observations and calculations is maintained up to altitudes of 8 km; for higher altitudes the aerosol component proves to be more substantial than follows from the standard model of the atmosphere. Beginning at 9-10 km, the observed coefficient of aerosol attenuation is approximately one and a half orders of magnitude higher than the calculated value.

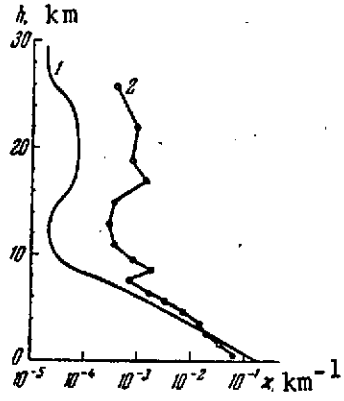

Fig. 18. Altitude dependence of aerosol index of the attenuation of radiation in the atmosphere:
1 -- according to the standard model
2 -- according to the observational data of K. Ya. Kondrat'yev and G. A. Nikol'skiy (mean value from several spectral intervals)

Evidently, we can justifiably assume that the lowest solar constant obtained by the Murcray group, compared with the data of the K. Ya. Kondrat'yev group, for equal values of solar radiation flux at the altitude of 31 km, is due to the systematic error caused by the fact that attenuation of light by the aerosol layer lying above the balloon was insufficiently accounted for. Therefore, we will assume that the data of the Murcray group must be increased by ~ 1 percent and the mean solar constant value from its determinations must be 1.935 cal/cm^2 · min.

3. Balloon observations of the Jet propulsion Laboratory (United States). The laboratory measured the solar constants not only on spacecraft, rockets, and aircraft, but also on balloons (Willson /155, 126/). In August 1968 observations were made with active-cavity radiometers (see Fig. 16) raised on a balloon to an altitude of 24 km. The radiometers were calibrated in absolute electrical units just as the instruments installed on spacecraft, however the solar constant obtained in the work of Willson /155/ proved to be much higher than all the remaining altitude determinations -- 139.0 mw/cm^2 or 1.99 cal/cm^2 · min. Later, reductions were introduced into the data: the new value was 137.0 mw/cm^2 or 1.96 cal/cm^2 · min; it remained still above /8 all the other values. Wilson believes that the International Pyrheliometric Scale gives results that are understated by 2.2 percent compared with the other absolute scales /126/.

Determinations of solar constants made on aircraft

1. The Drummond group undertook determinations of the solar constant also on aircraft at altitudes of 11-15 km, outside the earth's troposphere. During 1966 to 1968 a total of 28 successful flights were made; the results of 14 of these were selected for analysis /124, 125, 139-141/. As in observations made on rockets, the measurements were carried out with a 12-channel radiometer. In B-57 aircraft the cabin pressure was equal to the external pressure, therefore the observer could sight the radiometer on the sun in a through hole, without

protective aircraft shielding window. On the CV-990 aircraft the additional absorption in the window had to be taken into account. Several characteristics of the flights and the results of the measurement of the solar radiation flux undertaken by the Drummond group are given in Table 8 /141/.

As already remarked, all 12-channel radiometers were calibrated on the International Pyrheliometric Scale. Besides calibration work described in Section 2, standard Angstrom pyrheliometers to which the radiometers were tied in were compared during November 1969 to February 1970 with the primary pyrheliometers of the British National Physical Laboratory and the Canadian National Council on Scientific Research. The agreement of instrument readings was maintained within the limits of several tenths of a percent /141, 156/. Comparison with Soviet pyrheliometers tied in to the Stockholm standard was made in June 1970, and as already noted, the deviation of pyrheliometer readings when extrapolated to the zero turbidity factor also does not exceed several tenths of a percent.

TABLE 8. RESULTS OF ALTITUDE MEASUREMENTS OF SOLAR RADIATION FLUX (EPPLEY LABORATORY AND JET PROPULSION LABORATORY, US)

/84

Year	Month	Ascent vehicle, number of observ. series, ascent alt., km	Total solar rad. flux, mw/cm^2	Solar rad. flux, mw/cm^2		Wolf numbers
				UV & visible reg. $\lambda < 6070$ Å	IR reg. $\lambda > 6070$ Å	
1966	July-August	B-57B aircraft; 2; 11.5-15	135.8	48.8	87.0	60
1967	March	B-57B aircraft; 4; 11.5-15	136.0	48.7	87.3	86
1967	October	CV-990 aircraft; 1;11.0-12.5	136.2	48.9	87.3	60
1968	July	CV-990 aircraft; 3; 11.8	135.9	48.9	87.1	93
1968	July-August	CV-990;3; 12.5	135.8			
1966—1968	Average from aircraft ascents		135.95	48.8	87.2	
1967	October	X-15 rocket; 1 78-83	136.1	48.6	87.4	60
Mean averaged from rocket and aircraft data			136,0 (±0,1%) *)	48.8	87.7	

*) The mean square-root error of the weighted mean, equal to ±0.1 percent, characterizes only internal agreement of actual measurements

TABLE 9. CORRECTIONS ALLOWING FOR THE EFFECT OF THE TERRESTRIAL ATMOSPHERE ON THE RESULTS OF AIRCRAFT OBSERVATIONS BY THE DRUMMOND GROUP (IN PERCENTAGES OF MEASURED FLUX)

Type of correction \ Date and altitude of flight, km	22 October 1967 12	July 1968 11.8	July-August 1968 12.5
1. Rayleigh scattering	2,2	3,0	2.8
2. Ozone	2,0	2,4	2,5
3. Water vapor	0,3	0,5	0,2
Overall correction	4,5	5,9	5,5
Overall correction reduced to zenith	4,5?	5,4	5,1

The results of the aircraft observations corrected for absorption in the quartz windows of the instruments, and for the CV-990 aircraft also for absorption in their windows -- had corrections introduced that allow for the attenuation of light in the upper layers of the terrestrial atmosphere (above the troposphere). Table 9, based on the works /124, 141/, present corrections for three flights of the CV-990 aircraft. The contents of ozone and water vapor were determined from ground observations and also during flights; on the basis of these determinations the fractions of solar radiation fluxes (in percentages) absorbed by ozone and by water vapor were found. Allowing for extinction due to scattering was limited to calculating attenuation caused only by Rayleigh scattering. The air mass at which the observations were made was 1.1 in 1968; 0.5 percent must be subtracted to place the correction on a unit mass basis. Thus, corrections introduced by Drummond can be conditionally called theoretical. A comparison of the experimentally determined attenuation of light for the altitudes ~12 km with calculated values will be made below, when we discuss the works of the Thekaekara group.

Table 8 presents a compilation of all altitude determinations /86 of the solar constant made by the Drummond group. The mean value from rocket and aircraft observations is 136.0 mw/cm^2 or 1.950 cal/cm^2 · min with an error of 1.7 percent /141, 142/. The last column of the table gives the Wolf numbers of sunspots for the observation days. The dependence of the solar constant on the sun's activity phase was not detected from these data.

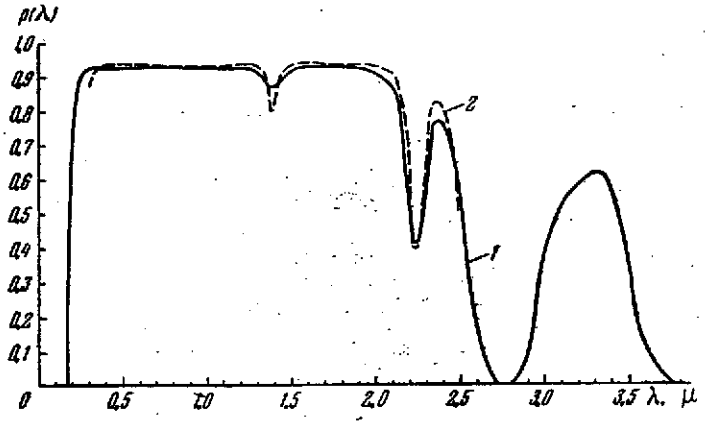

Fig. 19. Transparency coefficient of quartz (dynasil) aircraft window 25 mm thick.
1 -- Thekaekara-Winker determination (calculation and observations)
2 -- Arvesen data

2. The Thekaekara group from the Goddard Space Flight Center organized /122, 142, 157/ a broad complex investigation of solar radiation flux on a CV-990 aircraft. From 3 to 19 August 1967 six flights were made at an altitude of 11.58 km. Five instruments for measuring the solar constant and seven -- for spectral studies in the region from 0.3 to 15 microns -- were placed on board the aircraft. Sighting of all instruments on the sun was carried out during the flight within the limits 0°.5, which with the provision of an integrating sphere at the instrument entrance was quite adequate. Of the five instruments intended to measure the total flux, observations were successfully performed with four. /88
Certain characteristics of instruments and results are given in Table 10 /122/.

In interpreting observations made with all instruments, the following determinations were common to all: 1) zenith distance of the sun and air mass at the instant of observation and 2) transparency coefficients of aircraft windows as a function of wavelength, which were determined experimentally and calculated theoretically /158/. Fig. 19 presents the transparency coefficient of a quartz (dynasil) window 2.5 cm thick for the wavelength range to 3.8 microns inclusively. The absorption bands of quartz, which are insignificant for small thicknesses, intensely attenuate radiation in thick aircraft windows.

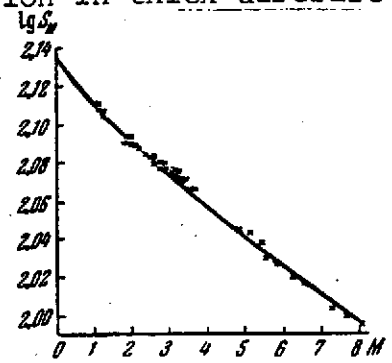

Fig. 20. Dependence of the logarithm of total solar radiation flux lg S_M (S_M is expressed in mw/cm^2) on air mass M at altitude 11.58 km

TABLE 10. INSTRUMENTS AND RESULTS OF SOLAR CONSTANT MEASUREMENTS BY THE GODDARD CENTER, AUGUST 1967, ALTITUDE 11.58 KM

Experimenter	Instrument	System of absolute units	Material & trans. reg. of aircraft window, microns	Nr. of observation days and nr. of series	Corr. for extinction in terr. atm., reduced to zenith %	Values of solar constant & observational error, mw/cm^2
1. Kruger Winker Ward	Cone radiometer	Electrical	Infrasyl 0.3—4	6; 67	5.3	135.8±2.4 (1.8%)
2. McNutt Riley	Hy-Cal pyrheliometer	Thermodynamic	Infrasyl 0.3—4	4; 170	4.7	135.2±2.2 (1.6%)
3. McNutt Riley	Angstrom pyrheliometer No 6618	Pyrheliometric	Infrasyl 0.3—4	5; 154	5.6	134.3±2.6 (1.9%)
4. Duncan	Angstrom pyrheliometer No 7635	Pyrheliometric	Dynasyl 0.3—4	4; 42	8.4	134.9±4.0 (3%)
Weighted mean from all determinations						135.1±2.8 (2%)

Also studied was the content of certain gases in the aircraft galley. The water vapor content varied within the limits 0.7 to 1.4 microns of precipitable water per m of route (over the aircraft it varied within the limits from 12 to 18 microns in the atmosphere). The relative content of permanent atmospheric gases was as follows: O_2, N_2, and Ar was the same as in normal conditions. However, the CO_2 content, which usually in normal conditions is ~ 0.0314 percent proved to be several times greater in the aircraft, sometimes it is as much as 10 times more.

Below are presented brief characteristics of the methods used in observations and in processing results for individual instruments.

a) Cone radiometer. The instrument has been described earlier (cf. Section 2). It records the solar radiation flux S_M directly in milliwatts; Fig. 20 presents by means of points observed values of lg S_M as a function of air mass M for six days of observations. Owing to the Forbes effect, this function /89 is not linear: the points corresponding to larger M yield a "smoother" curve (cf. Section 2, Chapter One). In order to extrapolate observed lg S_M values, in spite of the Forbes effect, beyond atmospheric limits, the following procedure was used. Total fluxes S_M were represented by the sum of the terms

$$\lg S_M = \lg \sum_{i=1}^{20} f_i T_i p_i^M, \qquad (23)$$

where p_1 is the interval number, f_i is the relative fraction of solar energy in the i-th interval, T_i is the transparency coefficient of the optic (aircraft window) in the i-th interval, and T_i is the transparency coefficient of the terrestrial atmosphere in the interval with number i. Corrections were introduced into the first and last terms of this sum for the unobservable radiation at $\lambda < 0.295$ micron absorbed by ozone, and from $\lambda > 4$ microns completely cut off by the aircraft window; the overall correction was 2 percent of total radiation flux.

The family of curves lg S_M was calculated as a function of M for different p according to expression (23), where p was not varied for all spectral interval, but only for the interval from 1.2 to 1.6 microns, in which the intense water vapor band occurs (λ 1.40 microns). Thus, the variation in p in this interval apparently corresponded to the change in H_2O content. Values of the transparency coefficient determined with a Perkin-Elmer monochromator installed on the same aircraft were used in the second approximation. The transparency coefficients were selected for intervals containing water vapor bands at $\lambda\lambda$ 1.4, 1.9, and 2.7 microns.

Since f_i represents the relative fractions of solar radiation, the resulting family of calculated curves can shift along the Y axis, by attaining the optimum coincidence of one of them with experimental points (as shown in Fig. 20). The intersection of this curve with the Y axis yields the unknown value [15] of the solar constant lg S_0.

The mean weighted value of the solar constant for all the determinations with the cone radiometer is 135.8 mw/cm^2 ($\pm$ 2.4 mw/cm^2 or 1.8 percent). The principal sources of error which make roughly equal contributions are the following: absolute calibration of the radiometer, determination of the transparency coefficient of the atmosphere, determination of the transparency coefficient of the aircraft window, and the instrumental errors of the measurements per se. /9

b) the Hy-Cal pyrheliometer (cf. Section 2). The pyrheliometer signals were recorded on magnetic tape at the frequency of 5 times a second; a computer averaged them over a period of 10 seconds. Over the entire 4 days of observations 170 such averaged readings were obtained. Extrapolation beyond the terrestrial atmosphere was carried out by the same technique as for the cone radiometer. The intersection of the curve describing the function lg S_M with the Y axis gives a solar constant of 135.2 mw/cm^2 ($\pm$ 2.2 mw/cm^2 or 1.6 percent).

c) and d) Angstrom compensation type pyrheliometers No 6618 and No 7635 (cf. Section 2). The aperture angles of these pyrheliometers are $4^\circ.2 \times 10^\circ.6$. Extrapolation beyond the atmospheric limits was also carried out by the method described for the cone radiometer. Solar constant values were found to be, respectively, 134.3 $\pm$ 2.6 and 134.9 $\pm$ 4.0 mw/cm^2. The greater error for the No 7635 pyrheliometer was due to the fact that during its calibration relative to the standard instruments in high-elevation conditions (Table Mountain in California) and then in the Eppley laboratory it was found that instrument readings were not stable enough.

The mean weighted solar constant based on all the determinations of the Goddard Center group is 135.1 $\pm$ 2.8 mw/cm^2 or 1.936 $\pm$ 0.041 cal/cm^2 · min (cf. Table 10). The weights were taken as inversely proportional to the mean square-root error of the result obtained with each instrument.

---

[15] Obviously, even though this is not directly stipulated in the text /122/, with this procedure which can be conditionally called the Bouguer method, corrections for unobservable radiation from $\lambda < 0.295$ micron must be made for the experimental points (instrument readings). Introducing corrections for absorption in the aircraft window cutting off IR radiation is stipulated for all the instruments.

It is of interest to compare the corrections for extinction in the earth's atmosphere at the altitude ~12 km based on calculations (of the Drummond group, last row in Table 9) with corrections empirically determined by the "Bouguer method" (Thekaekara group; the next to the last column in Table 10). As we /91
can see from the table, both methods, the theoretical determination of corrections, and the empirical extrapolation of observed data to zero air mass showed that the solar constant is roughly 5 percent (with a precision to 0.5 percent) greater than the total illumination produced by the sun at the altitude of 12 km, reduced to M = 1. The corrections agree quite well with each other, with the exception of the data of the No 7635 Angstrom pyrheliometer [16]. The agreement of the corrections obtained by the various methods evidently shows that on the observation days the aerosol component in the stratosphere over the aircraft was so negligible that it made no appreciable contribution to extinction; Drummond /124, 140/ specifically checked this. However, as shown by comparisons of balloon observations of the K. Ya. Kondrat'yev and Murcray groups, we cannot always neglect the aerosol component, which is quite time-variable; we must either estimate its effect or else use the Bouguer method, as was done by the K. Ya. Kondrat'yev and Thekaekara groups. Even at altitudes of 30 and more kilometers, the aerosol component can make the solar constant value too low by 1 percent, and sometimes much more.

Mean value of the results of direct determinations of the solar constant at high altitudes

The Committee on Solar Electromagnetic Radiation was set up in the United States in 1969, under the chairmanship of Thekaekara /141, 142, 157/; the goal of the Committee was to arrive at the most reliable values of the solar constant as well as the distribution of energy in the solar spectrum for engineering purposes. Data on the distribution of energy will be discussed below, in Chapter Five.

The Committee critically evaluated methods used in each of the experiments and examined the results and the various sources /92
of error. Ground observations were completely excluded from final data, since all ground determinations of recent years (cf. Table 6) were obtained by integrating the distribution curves, containing several sources of error: the standards of spectral emission vary from author to author; extrapolation to zero air

---

[16] The correction for this instrument is more than one and half times greater than for the remaining instruments. Evidently, this result must not be taken into account, for as noted in /122/, the instrument readings were not stable enough.

mass was very difficult and indeterminate owing to the highly inconstant water vapor content in the atmosphere; and estimating UV- and IR-spectral ends incapable of being measured from the earth's surface is unreliable. Of the altitude observations, the Committee did not give consideration to Wilson's data /155/, since the cause of the relatively high solar constant obtained in this work is unclear. Most Committee members believe that the remaining 56 determinations made on the International Pyrheliometric Scale, and several results obtained in the electrical and thermodynamic scales are sufficient for deriving a reliable solar constant value. Table 11 gives the sources and results on which the determination of the mean constant was based, along with the weights assigned to each result, and the mean value itself. The weights were given based on estimates and critical remarks of Committee members, where the maximum weights are assigned to those results based on the largest number of observations. High weight values are also given to determinations made on the electrical and thermodynamic scales.

The proposed solar constant value is 135.3 mw/cm^2 or 1.940 cal/cm^2 · min. On the average, the deviation of individual determinations listed in Table 11 from this mean is $\pm$ 1.9 mw/cm^2 or 0.027 cal/cm^2 · min, that is, about 1.5 percent.

The weights that the Committee assigns to individual observations, as is always the case in such instances, are quite subjective and arbitrary. Let us attempt to somewhat re-evaluate them, by conforming with the critical discussion of the observational results presented above.

To data of whose reliability there is any reason to doubt we will assign the weight 1. There are three such results. These are Murcray's balloon observations, corrected by 1 percent in this book based on a comparison of the data of K. Ya. Kondrat'yev [17]. /9
The observations of Duncan and Webb performed with the No 7635 Angstrom pyrheliometer are not reliable enough. For these observations, extrapolation beyond the earth's atmosphere at an altitude of 11.58 km requires corrections of 8 percent of the flux observed per unit air mass, while the correction must be about 5 percent for all the remaining data of the Goddard Center, as well as the Eppley laboratory. Finally, Willson's data that were not given consideration by the Committee were also assigned the weight 1. These recent results raised doubt, since they are strongly overstated relative to the remaining solar constant values.

---

[17] Accordingly, in deriving the mean weighted value carried out by the authors of this book (cf. last line in Table 11), Murcray's data were taken as 134.9 $\pm$ 2 mw/cm^2 or 1.935 cal/cm^2 · min.

TABLE 11. COMPILATION OF SOLAR CONSTANT DETERMINATIONS AT HIGH ALTITUDES

Authors & Sources	Organization	Method and system of absolute units	S_0, mw/cm^2	ΔS, mw/cm^2	S_0, cal/cm^2.min	Weights	
						US rad. comm.	Book's authors
Murcray [138,154]	Denver Univ.	Balloon, Eppley pyrheliometer, Pyr. System	133.8	0.6	1.919	4	1
McNutt, Riley [122]	Goddard Center	Aircraft, Ang. pyrheliometer No 6618, Pyr. Sys.	134.3	2.6	1.926	3	2
Duncan, Webb [122]	Goddard Center	Aircraft, Ang. pyrheliometer No 7635, Pyr. Sys.	134.9	4.0	1.935	3	1
McNutt, Riley [122]	Goddard Center	Aircraft, Hy-Cal pyrheliometer, El.	135.2	2.2	1.939	8	3
Plamondon [143]	Rocket Lab.	Mariner, radiometer, El. Sys.	135.3	2.0	1.940	10	4
Kondrat'yev et al. [137]	Leningrad Univ.	Balloon, actinometer, Pyr. Sys.	135.3	1.4	1.940	10	2
Kruger [122]	Goddard Center	Aircraft, cone radiometer. Therm. Sys.	135.8	2.4	1.947	8	3

TABLE 11. COMPILATION OF SOLAR CONSTANT DETERMINATIONS AT HIGH ALTITUDES [Conclusion]

Authors & Sources	Organization	Method and system of absolute units	S_0, mw/cm^2	ΔS, mw/cm^2	S_0, cal/cm^2·min	Weights: US rad. comm.	Weights: book's authors
Drummond et al. /139-141/	Eppley and Rocket Lab.	Rocket, aircraft, radiometer, Pyr. Sys.	136.8	1.3	1.952	10	4
Willson /126, 155/	Rocket Lab.	Balloon, radiometer, El. Sys.	137.0	2.0?	1.960	—	1
Weighted mean of the US Committee			135.3	1.9	1.940		
Weighted mean of present book's authors			135.5	2.0	1.943		

*) Table 11 presents the following abbreviations: Pyr. Sys.= Pyrheliometric System of Units; El. Sys. = Electrodynamic System of Units; Therm. Sys. = Thermodynamic System of Units. In converting mw/cm^2 to cal/cm^2·min, the US Solar Radiation Committee adopted the mechanical equivalent of heat J as equal to 4.1840 j/cal, according to /195/. Here the joule is the absolute joule, the calorie is the thermochemical calorie. In Soviet literature the values are J = 4.1868 j/cal /129/. Given the prevailing measurement precision, this difference in J has practically no effect on solar constant values. The conversion of our spectrophotometric S_0 was done with J = 4.1868 j/cal.

For the rest, the weights are distributed according to the following reasoning. Most observations were made on the pyrheliometric scale. Still, observations on other scales, electrical and thermodynamic, as already noted, are of fundamental importance to establish the true solar constant, all the more so in that sometimes doubt is cast on the reliability of the determination of the pyrheliometric scale itself, whose precision of reproducibility is doubtless lower than the other two scales. Therefore the weights of the pyrheliometric observations were adopted, if there were no special reasons for changing it, as 2, and the observations made on the electrical and thermodynamic scales would give a weight of 3. A weight was added to observations made outside the earth's atmosphere that did not require reductions for extinction; thus, the results obtained on the Mariner spacecraft were given a weight of 4. To the results of the Drummond group, although they were also made on the pyrheliometric scale a weight of 4 was assigned, since in addition to the aircraft data, they also included rocket data.

The mean weighted value of the solar constant in this distribution of weights, the supplementing of Willson's data, and the 1 percent correction of Murcray's data proved to be practically the same; the deviation was 0.1 percent for the mean error (deviation from the mean value) of about 1.5 percent (Table 11): S_0 = 135.5 mw/cm^2 or 1.943 cal/cm^2 · min.

Thus, the presently available series of solar constant determinations at higher altitudes is quite long and homogeneous enough in order that a reliable mean can be obtained from it for practically any reasonable distribution of weights and even when adding to it a result appreciably different from the mean. /96

However, it must be noted that still there is no complete certainty that the derived mean is altogether free of systematic errors. Moreover, there is some ground to assume that this mean is only the lower limit of the possible solar constant value. Discussion of the method by which the results of altitude observations were processed showed that even at "balloon altitudes" the calculated extinction value in the terrestrial atmosphere cannot always be used. Evidently, the actually existing aerosol component sometimes can lead to understating the measured S_0 value by 0.5-1 percent, and possibly even by a greater understatement, which is discussed in detail in the works of the Kondrat'yev group /136, 137/ and is graphically illustrated by Figs. 15, 17, and 18.

The conclusion suggests itself to the effect that in all the altitude determinations of the solar constant, up to the balloon flight altitudes inclusively (~ 30 km), one must experimentally determine the correction for atmospheric extinction in the earth's atmosphere for each observation day, for example, by the technique used by the Thekaekara group /122/.

Unfortunately, it is not possible to evaluate the systematic errors of this kind in studies already completed, since the initial observation data, with rare exceptions, were not published.

We must, however, note that in available rocket observations that were not deliberately burdened with this systematic error we are discussing, the true constant value must not appreciably exceed the mean derived in Table 11 and must lie below the value obtained by Johnson /119/, 2.00 cal/cm^2 · min. The mean solar constant derived from altitude measurements conducted before 1970 is ~ 3.1 percent below Johnson's value.

The spectrophotometric solar constant derived by us from the mean-weighted distribution of energy in the solar spectrum is 1.969 cal/cm^2 · min = 137.4 mw/cm^2 (cf. Section 5, Chapter Five). The final solar constant value proposed in this book is the mean weighted value from direct and spectrophotometric determinations: S_0 = 1.95 cal/cm^2 · min = 136 mw/cm^2 (cf. Conclusions). /97

5. Variability of the Sun as a Star

The problem of the variability of solar radiation has been discussed now for many decades. Hypotheses on the noticeable changes in the influx of solar heat on the earth have repeatedly been resorted to in explaining fluctuations of climate of both modern as well as past geological epochs.

Let us at the very outset refine the statement of the question. We made estimates of the effect of spots, faculae, and flares on total solar radiation; it was found that the effect is negligible. Let us also estimate the effect of bursts of radio-emission and fluctuations in short-wave radiation.

Less than 10^{-7} of the entire solar energy is accounted for by fraction of radiation from the quiet sun with $\lambda > 1$ mm (cf. Chapter Five). The most intense bursts during which emitted energy is increased up to 10^5 times take place in the meter range. If these bursts had encompassed the entire spectrum with $\lambda > 1$ mm, then they would have results only in a 1 percent change in the solar constant; but the actual changes are at least one order of magnitude less (since the spectral region of the bursts is much narrower).

Similarly, emission over the entire short-wave spectral region from $\lambda < 1200$ angstroms is not more than $6 \cdot 10^{-7}$ of the total solar energy. Therefore the intensification of X-ray ($\lambda < 100$ angstroms) and gamma ($\lambda < 0.1$ angstrom) radiation which usually accompanies strong flares and reaches a level of $10^5 - 10^6$ times cannot cause fluctuations in the overall solar radiation by more than a fraction of a percent.

Thus, it appeared that all estimates of the effects of possible changes in solar activity on the total flux of energy emitted by the sun would lead to the conclusion that the solar constant must not vary by more than a fraction of a percent. However, it can be assumed that, for example, for reasons unknown to us temperature fluctuations of the entire photosphere take place. /98
Only long-term well-organized measurements of the total flux of solar radiation can decisively solve the question as to how "variable" is the solar constant.

To discover and measure possible fluctuations in S_0, it has often been suggested to use observations of the bodies in the solar system /159-161/. In studying fast variations covering small intervals of time, this method has some advantages. Its basis, the precise and regular determination of stellar magnitudes of planets or satellites, can be carried out by comparing these heavenly bodies with stars that lie at closely similar angular distances and for closely similar air mass values. The effect of atmospheric extinction here is virtually excluded and high observational precision can be achieved. In particular, in the work /161/ carried out as far back as the 1920's, stellar magnitudes of Jupiter's satellites were determined with the precision of $0^m.004$ - $0^m.005$. Nonetheless, these studies are more properly methodological in nature. Episodic observations /159-161/ conducted over several weeks of time revealed no changes in the overall solar radiation exceeding the limits of error of the determination of stellar magnitudes.

The most prolonged series of observations made of Uranus and Neptune, begun in 1950, has been carried out at the Lowell Observatory /162-164/. These studies note the change (increase) in the brightness of both planets during this period of time from 1950 to 1966. After reduction to identical sun-earth-planet distances, the amplitude of brightness changes was found to be $0^m.02$ - $0^m.03$, which corresponds to a 2-3 percent change in the solar constant. Along with the planetary observations, regular observations were made of stars in several spectral classes, including 16 solar-type stars. These 16 stars revealed no changes in brightness greater than $0^m.004$ - $0^m.008$. The precision of observations was estimated to be $\pm$ $0^m.003$ /164/. Changes in the brightness values of Uranus and Neptune are regarded by the authors of the works /162-164/ to be realistic and attributable to change in solar radiation. But other investigators /165/ doubt that the Lowell observations show evidence of change in solar radiation. Even the authors of the work /164/ themselves admit that changes in the Uranus brightness are possibly associated with darkening of its surface from the equator to the /99
poles. Recently Rakosch made a new reduction of these observations /166/. He reached the unexpected conclusion that the solar brightness changes with a period of 27-29 days with an amplitude smaller than $0^m.01$.

The absence of an agreed view as to Lowell observations evidently is due to the fact that by necessity they had to be subjected to different reductions. Owing to the reductions the precision and advantages of short-period observations of planets and satellites, referred to above, were lost. In particular, it is difficult to provide color system constancy over a period of 15-16 years to avoid aging of the photomultiplier, light filters, and aluminum films on the telescope mirrors, and change in their spectral properties, and also to preserve precision (at $\pm 0^{m}.003$, /164/) in moving from, with planetary motion, some comparison stars to others.

In this respect, the remark by A. S. Sharov /167/ that in making studies such as /162/ -- of the catalog type, it is very difficult to reliably establish for heavenly bodies the variability of brightness with small amplitude (hundredths of a stellar magnitude) -- appears valid.

In recent years much attention has been given to possible fluctuations of the solar constant and their comparison with characteristics of solar activity, in altitude determinations of S_0. These studies are examined closely in the preceding section; here it remains only to repeat the conclusion that even modern altitude observations do not give indisputable proof that changes in total solar radiation exceeding the limits of measurement error (0.1-0.3 percent) exist.

Finally, we must turn to the long-term determinations of the solar constant conducted at the Smithsonian Institution under the leadership of Abbot /132/. Devising the "short method" aimed, in particular, at obtaining as large as possible a number of individual solar constant determinations with the goal of discovering its short-periodic fluctuations. In order to cancel out or at least to reduce possible errors associated with the imprecise allowance for atmospheric extinction and associated with fluctuations in this quantity, Abbot organized observations of several stations separated from each other by many thousands of kilometers (North and South America, Africa). Simultaneous /100
fluctuations in results of S_0 measurements at all stations must, in Abbot's view, prove that there are actual changes in total solar radiation.

The simultaneous fluctuations in the results of different stations were actually sometimes observed, with an amplitude of about 1-2 percent. Abbot himself attributed a solar origin to them, calculated their period, and sought various correlations, for example, between changes in S_0 and meteorological elements /168/.

However, Abbot's view that these results of simultaneous observations taken at stations remote from each other proved the existence of true fluctuations in S_0 met objections. Thus, V. G. Fesenkov /135/ noted that systematic differences

between the results of individual stations in general are of the same order as the assumed fluctuations in the solar constants. From this he concluded that even though solar constant determinations were reduced by Abbot to a high degree of perfection and precision attainable in the ground pyrheliometric measurements, actual fluctuations in this quantity still lie within the limits of observational error.

Sometimes the Smithsonian Institution noted appreciable reductions in the solar constant immediately after passage of large groups of spots across the central meridian of the sun. For example, a 6 percent reduction in solar radiation was recorded on 23 March 1920 a day after the passage of a large spot. In describing this reduction, N. N. Kalitin /66/ observed that even these phenomena still do not prove that there are actual changes in the total solar radiation, since the intensifying of its short-wave radiation usually accompanying the manifestations of solar activity could have led to an appreciable reduction in the transmission of the upper atmospheric layers over the entire globe, caused, for example, by an increase in the ozone content.

Finally, we must bear in mind that there can be global disturbances in atmospheric transparency associated with eruptions of volcanoes, large forest fires, encounters of the earth with meteor swarms, and in the past two decades -- also related to technological factors, for example, explosions of atomic and hydrogen bombs (cf. Section 4). /101

Recently A. Angstrom /127/ re-examined anew the entire enormous material of the Smithsonian observations of the solar constant from the standpoint of the possibility of detecting its variability. In his earlier work /169/, Angstrom, and then later Lundblad -- mathematically -- /170/examined the problem of possible deviations from Bouguer's law and their effect on the errors of determining the solar constant and the transparency coefficient using Abbot's long method (cf. Section 3). If during observations of the intensity of solar radiation beyond the atmospheric limits I_λ and atmospheric transparency p_λ change simultaneously, then from Bouguer's law there follows a relationship that relates these changes:

$$M\frac{\partial p_\lambda}{p_\lambda} = -\frac{\partial I_\lambda}{I_\lambda}. \qquad (24)$$

Based on this relationship, Lundblad investigated the reliability of the Smithsonian determinations of the variability of the solar constant in 1909-1911 (/132/, Vol. III) and reached the categorical conclusion that all the observed changes in the solar constant are not real.

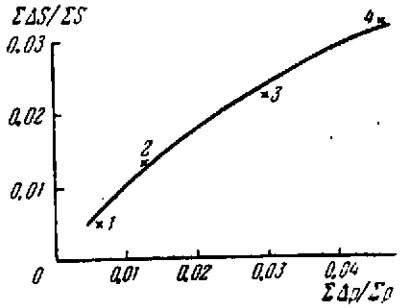

Fig. 21. Dependence of fluctuations in solar constant on fluctuations in transmission for different observation stations:
1 -- Montezuma, 1921-1930
2 -- Mount Wilson, 1911
3 -- Bassur, 1911
4 -- Bassur, 1912

Recently Angstrom [127] examined the entire wealth of the Smithsonian observations /132/ of the solar constant by the long as well as by the short method. Initially the mean values of fluctuations in the transpaency $\Sigma\Delta p/\Sigma p$ were compared with the mean values of fluctuations in the solar constant $\Sigma\Delta S_0/\Sigma S_0$ for observations performed by the long method. It was found that these quantities are very closely correlated with each other, as shown in Fig. 21 plotted /102 for the stations on Mount Wilson and on Bassur, where transparency experienced quite intense fluctuations, and in Montezuma where transparency was very stable. The explicit relationship between deviations in individual values of the solar constant with respect to the mean and analogous deviations in the transmission coefficient from the mean is obvious. By investigating separately the same dependence only for the Montezuma station with stable atmospheric transparency Angstrom found that

$$\frac{\Sigma\Delta S_0}{\Sigma S_0}=0.0028+0.37\frac{\Sigma\Delta p}{\Sigma p},$$

that is, if $\Delta p \to 0$, then $\Sigma\Delta S_0/\Sigma S_0 \to 0.0028$.

By comparing further results obtained by Abbot by the long as well by the short method, Angstrom found that the quantity $\Sigma\Delta S_0/\Sigma S_0 \approx 0.00245$, that is, close to the just-presented estimate of the long method. Finally, Angstrom presents results of the most precise comparisons of standard Angstrom pyrheliometers conducted by Rodhe /171/ in high-elevation and exceptionally stable conditions (low temperature gradients and absence of wind). It was found that estimating the errors of the comparison factor Ω gives the following relationship: $\Sigma\Delta\Omega/\Sigma\Omega = 0.0023$. Thus, if the variability in the solar constant is reduced to conditions of stable atmospheric transparency in practice it agrees with the error of the most precise pyrheliometric measurements and is 0.2 percent of the measured quantity. But if the solar constant does change, then it does by no more than 0.2 percent, and these changes can not be detected by the pyrheliometric method. The truly enormous series of observations by the Smithsonian Institution, covering nearly half a century, serve as the foundation for this conclusion and make it, most likely, irrefutable. By the irony of fate, Langley and Abbot, undertaking

these investigations early in 1900, in presenting their difficulty, complexity, and previously unprecedented requirements on experimental precision quite clearly, anticipated the directly opposite conclusion; they were convinced that the solar constant varies as a function of the solar cycle and that this could be easily revealed by accurate measurements.

CHAPTER THREE /103

INSTRUMENTAL PROBLEMS IN ABSOLUTE SPECTROPHOTOMETRY

1. Introductory Remarks

Separating monochromatic components of a radiation flux of complex composition can be done in different ways using spectral equipment of different types. In prism and diffraction spectrographs and spectrometers, a spatial separation of rays with different wavelengths is carried out; spatial separation is also performed by echelle spectrographs by Fabry-Perot etalons, and by Lummer-Gehrcke plates; here also we can include light filters of various kinds. Most widely used at present are instruments with prisms and gratings. There are many modifications of their designs. A quite extensive literature deals with them, for example, /13, 37, 38, 43, 172-187/, therefore we will not dwell on them here.

Fabry-Perot etalons and Lummer-Gehrcke plates cannot be used in studying extended spectral regions, since they have a highly restricted region of dispersion /174/. We will also exclude them from our consideration.

In addition to instruments affording a spatial separation of components, in recent years devices segregating monchromatic components of radiation on the basis of selective modulation have appeared: the SISAM /180/ and the Fourier spectrometer, most interesting and promising, which has already gained quite wide acceptance in the spectrophotometry of the sun, planets, and stars. The Fourier spectrometer and a comparison with it of various kinds of spectral devices are taken up in Section 5.

In all spectral instruments without exception light losses occur, which depend generally on wavelength. When taking them into account in absolute spectrophotometry, one of two methods can be used, examined by A. Unsold /13/ and analyzed in detail by /10
G. F. Sitnik /109/.

The first method makes use of a nonselective radiation receiver (bolometer, thermoelement, radiometer, and so on). The spectral curve $I(\lambda)$ obtained at the output of the instrument equipped with this receiver can be represented as [18]

$$I(\lambda)\Delta\lambda = qE(\lambda)P(\lambda)\frac{d\lambda}{dl}\Delta l, \tag{25}$$

where $E(\lambda)$ is the illumination given by the test source at the spectrometer slit, $P(\lambda)$ is the transmission of the optics, and the factor $(d\lambda/dl)\Delta l$ allows for possible variation in dispersion with wavelength.

Finally, the coefficient q is determined by the receiver's sensitivity (it does not depend on wavelength!) and by several geometric factors: the area of the entrance slit, and so on.

Inserting into curve $I(\lambda)$ corrections for light losses in the optics and reducing it to a normal dispersion basis, we obtain the distribution of energy in the spectrum of the source, expressed in relative units:

$$e(\lambda) = \frac{I(\lambda)\Delta\lambda}{P(\lambda)\frac{d\lambda}{dl}\Delta l} = qE(\lambda). \tag{26}$$

Finally, by calibrating the receiver on an energy scale, we can determine q and obtain $E(\lambda)$ -- the distribution of energy in the spectrum of the source, expressed in absolute energy units.

Thus, the following are essential in applying this method: a) investigate the transmission of the optics; b) determine the dispersion of the spectral instruments; and c) undertake the energy calibration of the (nonselective) receiver. A classical example of the use of this method is to be found in works of the Smithsonian Institution, conducted under the supervision of Abbot (cf. Section 3, Chapter Two).

The second method is based on a comparison of the spectrum of the test source with the spectrum of a reference source whose energy distribution is known. The comparison is made by means of the same optical system and receiver. In this case /105

$$E_{test}(\lambda) = \frac{I_{test}(\lambda)}{I_{ref}(\lambda)}E_{ref}(\lambda) \quad . \tag{27}$$

[18] In order not to encumber the formula, we omit the factor that corresponds to atmospheric extinction. Taking this phenomenon into account, described in Chapter One, is identical in the case of both spectrophotometric methods.

By comparing (27) and (26), we easily see that all difficulties related to transmission of the optics, nonuniformity of dispersion, and sensitivity of the receiver are automatically eliminated by this method. However, a new requirement appears -- building a reference standard source of radiation with known distribution of energy in its spectrum. For the visible and near-visible spectral regions, this requirement means the necessity of making a model of an absolute black body, which is the primary reference standard of spectral distribution emitting in accordance with Planck's formula. Here we have distinct technical difficulties: ensuring equilibrium conditions within the model, determining model temperature, and so on, so that in terms of work load the second method scarcely affords an advantage compared with the first. However, the possibility of using any radiation receivers is a major and indisputable advantage of the second method, since the most sensitive receivers are, as a rule, selective. It is precisely because of this that comparison of the spectrum of a test source with the spectrum of the reference standard is the fundamental spectrophotometric method used in astrophysical as well as laboratory studies. As far as we know, besides the work of Abbot and Pettit /188/, all remaining investigations of the distribution of energy in the solar spectrum and also in stars have been carried out using the second method, therefore in individual sections of this book we will examine the problems of modeling an absolute black body and tying it in the temperature scale.

Let us briefly deal with the requirements imposed on dispersion and the resolving power of the spectral equipment in absolute solar spectrophotometry. If we set the goal of securing data on the integrated spectrum, that is, on the intensities of radiation averaged for sections of 10, 50, or 100 angstroms, regardless of whether they apply to the continuum or to lines, the dispersion /106
and resolving power of the instrument can be moderate: it suffices for the instruments to segregate spectral intervals two to three times smaller than the averaging intervals. However, of particular interest is the continuous spectrum, which corresponds to intensities at wavelength free of absorption lines. Finding such sections is quite involved, especially in the short-wave region, where $\lambda < 4300$ angstroms. As we can see in the famous atlases of Minnaert [189] and Bruckner /190/, often these relatively free sections are quite narrow, amounting to fractions of an angstrom. In recent years solar spectrophotometry has made use of instruments in which, in addition to high resolving power, double monochromatization of rays has been achieved and high spectral purity has been attained (for example, /191, 192/). The spectrograms recorded with these instruments exhibit spectral details unresolved in the above-cited atlases, probably because they were blurred with scattered instrumental light. Finally, in studying the true continuum much difficulty is caused by allowing for the depression due to the extended wings of the intense lines, such as the Balmer, H and K lines, and others, and allowing for the superpositioning of the

wings of neighboring lines. All this shows that to study the continuous solar spectrum, at least in the short-wave region, $\lambda < 4300$ angstroms, instruments with high dispersion and resolving power are essential; the resolving power must be superior to that exhibited in atlases /189, 190/, that is, it must be not less than $(5-10) \cdot 10^4$ with a negligible level of scattered instrumental light.

The necessity of high angular and spectral resolution compelled observations on tall tower type and horizontal solar telescopes with a system of coelostat mirrors. The latter together with the principal mirrors of the telescope forming the solar image can lead to marked polarization of light. Both the degree of polarization, which can be as much as 5 percent and higher, as well as the orientation of the primary oscillations vary as a function of the angle of incidence of the rays on the coelostat mirror; in addition; the degree of polarization can depend on wavelength. Moreover, virtually all spectral equipment polarizes light, and in general they do so also selectively in terms of wavelength. In particular, maximum polarization on a diffraction grating lies at the wavelength $\lambda = 0.7\ d \cdot \cos \alpha$, where d is the grating constant and α is the angle of incidence of the rays on it, and the maximum polarization is as much as approximately 50 percent. Ignoring these effects in absolute spectrophotometry can be a source of serious errors; here we cannot indicate general recommendations to take these effects into account; each system: telescope-spectral equipment must be investigated under conditions of the specific method employed (the solar positions and the layout of the standard source). Incidentally, the maximum possible error introduced by polarization effects is in general smaller when the spectrophotometric standard is used, than in the first method of absolute spectrophotometry.

In conclusion let us take up the subject of photoelectrical recording of spectra compared with photographic recording. Referring those readers interested in details to the specialized literature /43, 172, 182, 183, 193, 194/, we note that the photoelectric method is much more convenient: as a rule, it affords the linear dependence of readings on the signal; the quantum yield for the photocathodes is two orders higher than for photographic plates; finally, photoelectric receivers: photoelements and photomultipliers afford precision of individual measurements that is roughly one order higher than photography provides.

However, use of photomultipliers in spectrophotometry with classical prism or diffraction spectrometers requires scanning of the spectrum, followed by recording it from point to point. As a result, only a small fraction of the radiation of the source under study acts on the photoreceiver at each given instant, not more than 1 percent, and often much less.

At the same time, owing to the panoramic feature of the photographic plate, simultaneously the entire spectral region studied or a significant fraction of it can be recorded. Therefore, in spite of the high quantum yield of photocathodes, in making spectral observations, especially of extended wavelength regions and with high resolution, the photographic method can prove much more efficient than the photoelectric method.

2. Temperature Scale

/108

The scale for measuring temperature (in degrees) must not depend on the specific properties of a specific thermometric body and on which of its characteristics varying with temperature -- length, volume, pressure, brightness, etc. — is used to measure the latter. It is extremely difficult to construct such a scale. To do this, we must use the most general physical laws, which are independent of specific substances.

As shown in the mid-19th century by W. Thomson (Lord Kelvin), the temperature scale satisfying this requirement can be constructed based on the Carnot cycle /195/. Suppose that as a result of this cycle an amount of heat Q_1 is removed from a heater at initial temperature T_1, and of this amount Q_2 is transmitted to a cooler ("heat sink") at temperature T_2, and the quantity $Q_1 - Q_2$ is converted into work. The following equality is valid for the Carnot cycle:

$$\frac{Q_1}{Q_2}=\frac{T_1}{T_2}, \tag{28}$$

which also defines the thermodynamic temperature scale. The Carnot cycle enables us not only to establish by means of equality (28) the ratio of any two temperatures, but also specifies the zero of the temperature scale (absolute zero): this is the temperature T_2 of the cooler at which the efficiency η of a Carnot engine

$$\eta=\frac{Q_1-Q_2}{Q_1}=\frac{T_1-T_2}{T_1} \tag{29}$$

will be unity (for any T_1).

The thermodynamic temperature scale is physically the most well-grounded, however it can be directly determined only theoretically, since we cannot build such an ideal heat engine operating by reversible processes that would reproduce this scale over its entire range /195/. Still there are methods /196-201/ that allow us to reproduce, with good approximation, sections of this scale [19] /109 in particular, the gas thermometer method for the interval from ~10 to 1337.58° K (the freezing point of gold) and the absolute black body method -- for temperatures above 1337.58° K.

/Footnote 19 on following page/

Using an ideal gas in a thermometer based, for example, on the Charles law[20] -- the linear variation of gas pressure with the temperature at constant volume -- would afford a thermodynamic scale in the "pure form." However all real gases differ from the ideal gas, which leads to some deviations of the gas thermometer scale from the thermodynamic scale. But these deviations can be made very small if the real gas in the gas thermometer is present under conditions (low pressure and specific temperature interval) for which it is quite close to the ideal gas. Moreover, deviations of a real gas from an ideal gas can be allowed for by special corrections. By taking all necessary precautionary measures, one can achieve a very close approximation to the thermodynamic scale. For example, in the All-Union Scientific Research Institute of Metrology a precision of about 0.01° was attained in using a gas thermometer to determine the equilibrium temperatures between solid and liquid cadmium and tin /203/:

$$t_{Cd} = 321.110 \pm 0.013\,^{\circ}C, \quad t_{Sn} = 231.95 \pm 0.01\,^{\circ}C.$$

These error values take into account the nonideality of the thermometric gas (nitrogen), as well as to other known error sources [21].

Research on gas thermometry is technically extremely involved /110 and gas thermometers are highly unsuitable for preservation and reproduction of the temperature scale. Therefore in 1927 at the Seventh General Conference on Weights and Measures, the International Practical Temperature Scale (IPTS) was adopted, which provides for other standard methods of reproducing temperature. The IPTS is based on natural reference points. The temperatures of equilibrium states as follows are used as these points: equilibrium between solid, liquid, and gaseous phases (triple point), equilibrium between solid and liquid phases (melting or freezing

---

19 Modern methods of obtaining the lowest possible temperatures from 0.02 to 0.00085° K -- and in the future even lower temperatures -- have been described in an interesting article by O. Lounasmaa /202/.

20 In 1887 the International Committee on Measures and Weights concluded that it is most convenient and advantageous to use precisely Charles' law in constructing a gas thermometer:

$$p = p_0(1 + \alpha t), \qquad V = \text{const.} \tag{30}$$

21 Hydrogen and helium are the closest to the ideal gas, however, they can be used only in measuring low temperatures below 80-100° C, since at higher temperatures these gases diffuse through the walls of the container (made of any material). The nitrogen gas thermometer is used to measure higher temperatures, all the way to the freezing point of gold.

point), and equilibrum between liquid and gaseous phases (boiling point) of various chemically pure substances (not more than 0.0002 - 0.001 percent impurities is allowed). Standardized instruments (thermocouple, resistance thermometers, and so on /204-207/) and interpolation formulas are provided for interpolating between reference points in different temperature intervals; the interpolation formulas relate temperature and the quantity being directly recorded (thermo-emf, resistance, and so on).

Temperature values are assigned to two reference points a priori. In this way the magnitude of a degree and the zero-point of the scale are specified. Before 1960 the melting point of ice (0° C) and the boiling point of water (100° C) served this purpose; in 1960 they were replaced with the absolute zero of the temperature scale and the triple point of water, to which t = 0.01° C exactly was assigned (273.16° K). The degree of the thermodynamic and the International Practical scale following 1960 was defined as 1/273.16-th of the temperature interval between these "primary" points mentioned above. Temperatures of the remaining reference points were determined with a gas thermometer and by other techniques with maximum care.

The Resolution on the IPTS adopted in 1927 was in effect up to January 1949 when the revised scale, known as IPTS-48 came into effect. IPTS-48 was revised in 1960. In 1968 a Resolution on IPTS-68 significantly improved compared with IPTS-48 was adopted. Based on new measurements with much improved gas thermometers, more exact temperature values were assigned to the principal /11
reference points on the IPTS-68, and in addition five new points in the low-temperature region were included in it.

The reference points of the IPTS-48 and IPTS-68 are listed in Table 12 /204, 205, 208, 20/. The stability of temperature in reproduction and the maximum possible simplicity and ease of reproduction served mainly as the criterion for their selection. For example, the freezing points depend less on atmospheric pressure than due the boiling points and therefore do not require especially careful (and moreover standardized!) barostatting carried out with quite cumbersome equipment, for which "each assembly ... can be a source of significant errors" /209/. Therefore, for example, the boiling point of sulfur in IPTS-68 was replaced with the freezing point of zinc; it was stated /208/ that "the freezing point of tin with the assigned value t_{68} = 231.9681° C can be used instead of the boiling point of water."

Of greatest importance for high temperatures is the freezing point of gold, which is at the limit of the use of gas thermometer and absolute black body methods. The latter method based on extremely general physical laws theoretically enables us to plot a scale, thermodynamic and practical, independently of the gas thermometer scale, by using as reference points

in determining the degree, for example, absolute zero and the triple point of water. However, in practice this construction is impossible and the scale of an absolute black body is "coupled" at the freezing point of gold to the gas thermometer scale.

Up to the 1950's the numerical value of the freezing point of gold (1063.0° C) adopted also in the IPTS-48, was based on work done as far back as 1900-1910 by Holborne, Day, and Sosman /205/. From the mid-1950's to the early 1960's new determinations were made of this temperature using much improved gas thermometers in a number of countries. We must particularly note investigations that pioneered with this technique, conducted in our country by specialists of the All-Union Scientific Research Institute of Metrology /VNIIM/ under the supervision of A. N. Gordov and I. I. Kirenkov /197, 210-212/. The results they obtained with two gas thermometers: 1064.54 ± 0.2 and 1064.36 ± 0.2° C /197/ and their proposals along with the works of Moser (FRG, /213/), Oishi et al. (Japan /214/), and others were the basis for the re-examination of the IPTS made in 1968, when the following value was adopted (cf. Table 12): /112

$$t_{Au}=1064.43\ ^{\circ}\mathrm{C}.$$

We introduce a correction corresponding to the revision of T_{AU} in all the results of absolute measurements of the distribution of energy in the solar spectrum made before 1968, which we have used.

The temperature scale above the freezing point of gold is defined from the equation

$$\frac{B_1(\lambda)}{B_2(\lambda)}=\frac{(e^{c_2/\lambda T_2}-1)}{(e^{c_2/\lambda T_1}-1)}=n, \qquad (31)$$

where $B_1(\lambda)$ and $B_2(\lambda)$ are the intensities of radiation by a black body at wavelength λ and temperatures T_1 and T_2, and where the initial temperature is

$$T_{\text{ini}}=T_{Au}=1337{,}58\ ^{\circ}\mathrm{K}.$$

In conclusion, let us describe two methods of extrapolating upwards of 1337.58° K used in the Soviet Union to obtain high-temperature reference standards and, which is especially important to us, reference standards of the spectral distribution of radiant energy.

I. The method employed in the VNIIM /215, 216/.

The freezing point of gold is fixed with the model of an absolute black body. The power regime for the lamp is selected so that its monochromatic brightness is equal to the value for a black body in the freezing of gold. The lamp power regime found is recorded.

The brightness values are compared with a spectropyrometric unit (SP) in which employing a double monochromator virtually eliminates the effect of scattered light, and a photoelectric modulator permit equality of brightnesses to be attained with very high precision.

Thus, the brightness of an absolute black body at the freezing point of gold is "extrapolated" for a number of wavelengths to sample lamps. Further operations are carried out with these lamps.

TABLE 12.* MAIN REFERENCE POINTS OF INTERNATIONAL PRACTICAL TEMPERATURE SCALES OF 1948 AND 1968

Equilibrium state	Assigned Temperatures			
	by IPTS-48		by IPTS-68	
	T, °K	t, °C	T, °K	t, °C
Triple point of equilibrium hydrogen	—	—	13,81	—259,34
Boiling pt. of eq. hydrogen at 333.306 mb (25/76 standard atm.)	—	—	17,042	—256,108
Boiling pt. of eq. hydrogen (at normal pressure)	—	—	20,28	—252,87
Neon boiling pt.	—	—	27,102	—246,048
Oxygen triple pt.	—	—	54,361	—218,789
Oxygen boiling pt.	90,18	—182,97	90,188	—182,962
Water triple pt.	273,16	0,01	273,16	0,01
Water boiling pt.	373,15	100	373,15	100
Sulfur boiling pt.	717,75	444,6	—	—
Zinc freezing pt.	—	—	692,73	419,58
Silver freezing pt.	1234	960,8	1235,08	961,93
Gold freezing pt.	1336	1063	1337,58	1064,43

Remarks. 1. Save for the triple points and one point of equilibrium hydrogen (17.042 °K), assigned temperatures are actual for equilibrium states at the pressure 1013.25 mb (normal atm.). 2. Water must have the isotopic composition of sea water.

* Translator's Note: Commas represent decimal points.

The equality of the lamp brightness and the black body brightness in the freezing of gold enables us to assume that the brightness temperature of the lamp at a given wavelength is 1337.58° K. However, we recall that values of different kinds of temperature (brightness, spectrophotometric, and so on /18/) agree only in an absolute black body for conditions of thermodynamic equilibrium. A lamp ribbon is not an absolute black body; its emissitivity is less than for an absolute black body and moreover this difference in emissitivities varies with wavelength. In this regard two aspects are of interest: 1) When the brightness temperature of the ribbon is T_{br} [br=brightness], its temperature measured, for example, with a gas thermometer, will be higher. 2) The power regime of the lamp to which the brightness of a black body is transferred in the freezing of gold is different at different wavelengths. However, both these factors will play no role subsequently, since all our setting up of reference standards will be based solely on the brightness temperature, and individually at each wavelength. /114

After the brightness of the black body at the "gold point" is transferred to the lamp (which we will denote with L_g /g="gold" point/), an auxiliary lamp L_{aux} /aux = auxiliary/ and a brightness doubling device (PU) are used; the latter device enables us to separate the beam from the lamp Laux arriving at the SP into two completely identical portions and to send to SP either one portion or the other, or both together (Fig. 22).

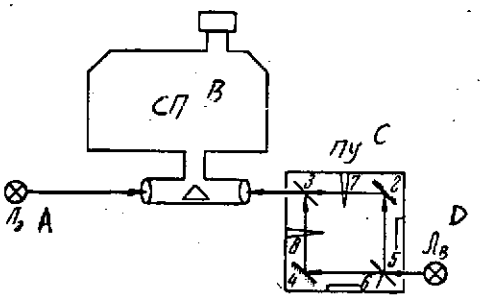

Fig. 22. Diagram of device for extrapolating temperature from T_{Au} used at the VNIIM
1 and 3 -- beam splitters,
2 and 4 -- mirrors,
5 and 6 -- shutters,
7 and 8 -- optical wedges for pression flux flattening

KEY: A -- L_g
B -- SP
C -- PU
D -- L_{aux}

The temperature is extrapolated in stages: /115

1. The "gold point" regime is established at the L_g lamp.

2. At the L_{aux} lamp the regime is selected so that its brightness when observed at the SP through any one channel of the instrument PU is equal to the brightness of the lamp L_g. This lamp L_{aux} regime is recorded.

3. Both channels are opened in the PU device. At the recorded lamp L_{aux} regime, the current in the lamp L_g is increased until

SP shows that the brightness of L_g equals the brightness of L_{aux} observed through the two channels. The new incandescence regime of L_g is recorded.

Obviously, the brightness temperature T_2 of lamp L_r in the second regime is determined by equality (31) with n = 2. The procedure of doubling can be repeated several times and thus temperatures to about 2000° K can be attained.

The advantage of this method with splitting of brightness lies in the fact that the photoelectric system in SP operates as a null instrument establishing each time the equality of light fluxes. In this way errors associated with the nonlinearity of the photoreceiving and recording equipment and also with the instability of its sensitivity are eliminated.

II. In contrast to the VNIIM, at the Kuchino Astrophysical Observatory of the GAISh, an actual model of absolute black body was heated to high temperatures, under the supervision of G. F. Sitnik /217, 218/. First the black body was heated to the "gold point" and at the instant of gold wire melting, the monochromatic brightness of the black body was recorded in several wavelengths. After the brightness measurements at the gold point, the black body model was placed on a more intense power regime; when the temperature stabilized, the monochromatic brightness was again measured at the same wavelengths. The new temperature can be easily determined by formula (31) by setting $T_1 = T_{Au}$ in it.

The advantage of this method is that in contrast to a lamp, the model of an absolute black body serves not only as the reference standard for brightness temperature, but also -- since thermodynamic equilibrium is achieved in its cavity to a high approximation -- all other kinds of temperatures whose numerical values in this case coincide.

3. Model of an Absolute Black Body as a Primary Spectrophotometric /1 Reference Standard and Other Techniques of Energy Calibration

Although in nature there are no materials or dyes that would entirely absorb radiation striking them over the entire wavelength range, theoretically one can build the model which would be as arbitrarily close to the ideal absolute black body, and since it will emit according to Planck's law, it can be used as a primary spectrophotometric reference standard. Suppose we have an enclosed cavity with a small opening much smaller than the characteristic dimensions of the cavity. A ray entering this opening can exit only after diffuse reflections and if the opening is relatively small, the ray will be so weakened that absorption can be regarded as total, and the cavity itself with the opening can be regarded as a model of an absolute black body.

Construction of this model must satisfy three paramount conditions. Let us consider them, following [217-227].

1. If the cavity is closed, and its walls are at an identical temperature everywhere, emittance within the cavity will be in equilibrium with the walls. The opening in the cavity through which a certain amount of radiation continuously escapes disturbs the equilibrium conditions. The disturbance can be characterized by how much the absorption coefficient χ of the model differs from unity. The appropriate estimates made first as early as 1895 were subsequently often repeated and revised for different cavity shapes and with allowance not only for purely diffuse, but also partially mirror reflection at its walls [219, 220, 222-225]. The simplest expression for χ is obtained for a spherical model and for purely diffuse reflection. Then if $r = 1 - \rho$ is the coefficient of reflection of the internal surface of the cavity, ρ is its absorption coefficient, $s = \pi d^2/4$ is the area of the opening, and l is the cavity diameter, then

$$\chi = 1 - r\frac{s}{\pi l^2} - \ldots \approx 1 - \frac{r}{1-r}\frac{s}{\pi l^2} = 1 - \frac{r}{1-r}\frac{d^2}{4l^2}. \qquad (32)$$

In the works cited it was shown that the effect of the shape of the model and the presence of partial mirror reflection has a very small effect on χ, and formula (32) is wholly suitable for estimating the "blackness" of the cavity, for example, of a cylindrical form. Fundamental in ensuring the "blackness" of the model is the requirement that the opening be relatively small in dimensions and that r is not large. /117

Table 13 illustrates the effect of various opening dimensions and reflection coefficient r values of the walls on the "blackness" of the model. The table gives the l/d values which at different r values ensure the absorption coefficients χ of the model equal to 0.999 and 0.998. The calculation was based on formula (32).

With a suitable l/d, one can construct an absolute black body even using material with the reflectivity of freshly fallen snow (0.95)!

We must note that all the reasoning presented along with Table 13 is valid when the wavelength is much smaller than the dimensions of the opening and of the cavity itself. Even in the submillimeter spectral region the blackness of models of "usual" size and design decreases owing to the effect of diffraction.

2. Temperature uniformity within the cavity must be ensured. G. F. Sitnik calculated [221, 222] that if the brightness of an absolute black body at the melting point of gold must /118

TABLE 13.* RATIO OF THE PARAMETERS OF AN ABSOLUTE BLACK BODY MODEL

Coefficients for cavity walls		1/d values required	
reflection, r	absorption, p	For χ = 0.998	For χ = 0.999
0,95	0,05	48,7	68,9
0,60	0,40	13,7	19,4
0,50	0,50	11,2	15,8
0,40	0,60	9,1	12,9
0,20	0,80	5,6	7,9
0,10	0,90	3,7	5,3
0,05	0,95	2,6	3,6
0,02	0,98	1,6	2,3

* TRANSLATOR'S NOTE: COMMAS REPRESENT DECIMAL POINTS

be reproduced with a precision of 0.1 percent, the temperature gradient within the cavity must not exceed 2 deg/cm. By using various procedures, one can achieve greater uniformity of the temperature field; thus, it is shown in /216, 227/ that a furnace field uniformity of $\pm 1^{\circ}$ over a 10 cm length can be achieved.

3. Since the melting (freezing) point of gold [22] is the main reference point of the IPTS for high temperatures, one must be able to reliably fix this point when working with a model of an absolute black body.

Models of an absolute black body of various designs have been developed. In some cases the model is made in the form of a crucible of graphite or other material, which is immersed in molten gold, and the vessel containing the gold is placed in an electric heating oven. When the slowly cooled metal freezes (or melts), the emittance of the model is recorded. Here the

[22] In some studies the determination of the temperature of an absolute blackbody employed as a spectrophotometric reference standard is made not based on equilibrium points fixed in the IPTS, but for example, using calibrated platinum-platinum-rhodium thermocouples /228, 229/ or resistance thermometers /146/. These blackbodies cannot be regarded in the full sense as primary reference standards, since their temperature is coupled to the IPTS by means of another instrument, though the coupling itself is reliable and in principle wholly correct, for the Resolution on the IPTS provides for various interpolational instruments (thermocouples, resistance thermometers) to attain temperatures intermediate between the principal points of the IPTS (Section 2).

uniformity of the temperature is easily ensured, and the duration of the quasi-equilibrium state of gold can be brought to 40-45 min /220/, which greatly facilitates measurements. The disadvantages of the method are as follows: a) it is impossible to extrapolate to higher temperatures by heating the model itself, as was done by G. F. Sitnik /222, 217, 218/; b) a great deal of gold (not less than 0.5 kg, according to /220/) is required; and c) blackbody radiation exits vertically upwards.

In recent years the method of the horizontal crucible /220, 216/ has been used in the VNIIM for calibrating lamps; its layout is shown in Fig. 23. A hermetically enclosed space embracing the emitting vessel on all sides is filled with gold. According to /216/, one installation requires 125, and another 180 grams of gold. In this way the third disadvantage of the vertical crucible method is eliminated and the second disadvantage is markedly reduced; the first disadvantage persists; however, the method of high temperature reference standardization employed in the VNIIM does not require heating of the actual model of an absolute blackbody above the "gold point" (Section 2). /119

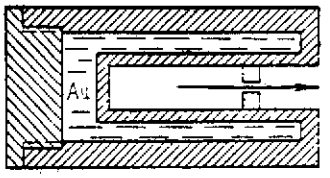

Fig. 23. Layout of the horizontal crucible device used in the VNIIM in modeling an absolute blackbody

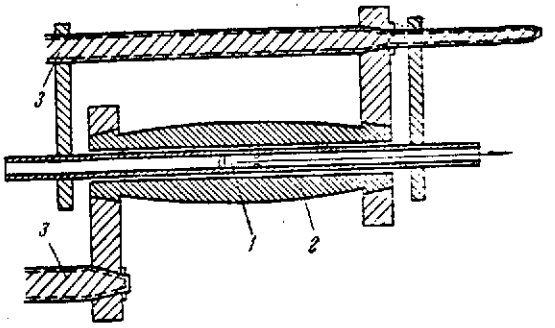

Fig. 24. Layout of the model of an absolute blackbody constructed at the Kuchino Astrophysical Observatory
1 -- Emitting cavity
2 -- graphite heating tube
3 -- current-conducting copper bus bars cooled internally with water

Fig. 24 shows the layout of the model of an absolute blackbody built at the Kuchino Astrophysical Observatory of the GAISh under the supervision of G. F. Sitnik /217/. The external heating tube has walls of variable thickness in order to compensate for large heat losses at the ends of the internal (emitting) tube and to ensure a uniform temperature field near the middle of the latter. This same effect can be achieved by using several heater windings with turns of variable density. The profiles of the heating tubes (different for different model temperatures) are calculated ahead of time and then are refined experimentally. The "gold point," that is, the furnace power regime and the emittance of the model /120

at the melting point of gold is fixed at the moment of melting of a gold wire stretched between the electrodes of a thermocouple placed in the emitting cavity. Melting of the wire breaks the thermocouple circuit. This moment can be easily recorded, but as has been validly noted by G. F. Sitnik /217/, it is necessary to have the melting taken place with the furnace operating regime on a quasi-steady state basis in order to avoid errors. In this sense the crucible method is more convenient owing to the thermal inertia of the relatively large mass of gold around the emitting cavity.

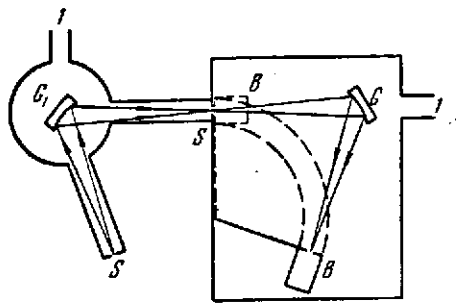

Fig. 25. Scheme of device for investigating the efficiency of concave grating (G) operating in vacuum ultraviolet. SG_1C -- auxiliary monochromator, B -- radiation receiver, 1 -- connections with vacuum pump.

The highest-temperature blackbody model known to us, built at the Kuchino Astrophysical Observatory, was heated to 2750° K /218/. Heating to higher temperatures is difficult, since any material that can be used for cavity walls and heater elements then loses its strength. All models built permit standardization in the ultraviolet up to $\lambda \approx 2500$ angstroms, inclusively. This /12
is wholly adequate for ground observations, but observations taken in the rocket ultraviolet raise new problems. Blackbody models with $T \leqslant 3000°$ K are unsuitable for standardization in the region $\lambda < 2500$ angstroms, since their radiation here is very weak [23]. One has to develop and use new methods of standardization.

Several of these methods provide for separate calibration of the receiver and the investigation of the transmission of the spectrometer and the other optics used, that is, return to the first method of absolute spectrophotometry (Section 1).

In vacuum ultraviolet spectral devices with convex gratings are used most extensively. In this case measuring these spectrometer transmissions reduces to determining the properties of the grating. The layout of the device for investigating the efficiency of gratings in Seyi-Namioki monochromators is shown in Fig. 25.

[23] By calculation based on Planck's formula, one can easily see that if T = 3000° K, the intensity of blackbody radiation in the transition from λ 3000 angstroms to λ 2000 angstroms falls off by a factor of 386, and in the transition to λ 1000 angstroms -- now by a factor of 10^7.

We will deal very briefly with the problem of calibrating receivers, referring interested readers for details to the excellent monograph /179/ provided with extensive bibliography.

1. Thermocouple method. The receiver can be calibrated in absolute or relative units by comparing its readings with the readings of a deliberately nonselective receiver, for example, a thermocouple or a thermopile. Absolute calibration of thermocouples can be conducted in the most convenient (visible) spectral region based on the model of an absolute blackbody (or by other techniques).

The difficulty of calibrating light receivers, for example, photomultipliers, using a thermocouple lies in the fact that their sensitivities differ by many orders. The thermocouple must be illuminated with an intense flux ; but in obtaining a reading from the calibrated receiver this flux must be considerably weakened, and must be weakened in a quite specific ratio (in absolute calibration).

2. The phosphor method. A phosphor is selected for which /122
a) luminescence is excited by ultraviolet radiation over wide wavelength range, and the long-wave portion of this interval overlaps with the region where calibration by the classical method is possible; b) luminescence occurs in a narrow interval of the visible (or generally classical) spectral region, and the luminescent wavelength is independent of the spectral composition of the exciting radiation; and c) the quantum yield of luminescence is known (it is best if it remains unchanged with wavelength). By depositing this phosphor on the light window of an ordinary photomultiplier, one can compare without impediment radiation fluxes of different wavelengths with each other -- radiation in the same spectral region always falls on the photocathode of the photomultiplier.

Sodium salicylate is used most often as this phosphor, preserving a constant quantum yield, close to unity, in the wavelength range 400-3400 angstroms /179/. Many studies deal with the properties of this phosphor and its applications, for example, /230-232/; a detailed bibliography is given in Chapter Four of the book /179/. Use is also made of the tungstates of magnesium and calcium, and other phosphors, in particular, organic (lumogens), whose long-wave sensitivity cutoff is 4600 angstroms /194, 230/.

Luminescence is to a large extent isotropic, therefore only part of it strikes the photomultiplier cathode. This severely reduces the overall quantum yield of the system: phosphor plus PEM /photoelectric multiplier/, nonetheless the system remains more sensitive than thermal receivers.

3. Thermophosphors. Certain substances, here $CaSO_4$ (Mn) is the most well-known and widely used, exhibit properties of

storing energy of ultraviolet (and also x-, gamma-, and beta-) radiation. The phosphor $CaSO_4$ (Mn) is sensitive to radiation at wavelengths shorter than 1500 angstroms /179/, and its sensitivity maximum lies at 1030 angstroms. If after exposure to short-wave radiation this thermophosphor is heated to 180° C, it will luminesce in the green region with maximum at 5000 angstroms. The total energy emitted by the phosphor during the entire heating period (light sum) is proportional within wide limits to the /123
energy of short-wave radiation incidence on it. The light sum does not depend either on the heating regime or on the irradiation regime; the stored energy can be preserved for a long time, therefore thermophosphors are highly convenient for absolute measurements and comparison of radiation fluxes differing by several orders. In particular, $CaSO_4$ (Mn) is suitable in the region from 1 to 1300 angstroms /179, 234/ and is widely used in the USSR /233, 234/ and the United States /235/ in rocket observations of short-wave solar radiation.

A disadvantage of thermophosphors is the dependence of their absolute quantum yield on processing technology; therefore in absolute measurements each specimen must be calibrated, for example, using a thermocouple.

4. Photochemical reactions. The quantum yield of a number of photochemical reactions: formation of ozone, decomposition of carbon dioxide gas, ammonia, uranyl oxalate, decomposition of nitrous oxide with the formation of N_2O_2 and NO, and other reactions -- is well known. It remains constant over wide wavelength intervals, and the reactions themselves can be used as detectors of ultraviolet radiation with known absolute sensitivity. A specific disadvantage of this method is the cumbersomeness of the equipment.

5. Ionization chambers and Geiger counters. These receivers developed mainly for research in high-energy physics were successfully employed for absolute measurements of far ultraviolet and x-ray emission of the sun /236/. As follows from theoretical and experimental (for example, /231, 237/) studies, the quantum yield of the ionization of inert gases beginning at the wavelength of the ionization threshold is unity and is independent of λ. If, moreover, we know the absorption coefficient of the gas filling the chamber and several other corrections (for absorption in the "window" and so on), then we can determine the intensity of monochromatic emission from the strength of the ionic current. Using ionization chambers filled with xenon and other inert gases, one can record radiation with $\lambda \leqslant 1022$ angstroms; nitrogen oxide, xylene vapor, and certain other compounds are used for the longer-wave /124
region with $\lambda \lesssim 1300$ angstroms.

Geiger counters are extensively used in the region $\lambda < 300$ angstroms. Their absolute calibration reduces (since in concept

the counter must record each quantum striking it) to the determination of a number of corrections: for absorption in the entrance "window", for miscalculations and spurious pulses, and so on. The calibration method is described in detail, in particular, in the works /238, 239/, where problems of design, adjustment, and investigation of the monochromator for the x-ray spectral region are also discussed.

6. Use of a pair of emission lines with a common upper level. Suppose we have two lines, λ_1 and λ_2, and any element, where λ_1 lies in the vacuum ultraviolet, and λ_2 -- in the visible (or in general in the "classical") spectral region. If both lines are caused by a transition from a common upper level, then if the following three conditions are satisfied: a) there is no self-absorption for both lines; b) the levels of their fine structure are resolved, and for the unresolved levels the population is proportional to statistical weights; and c) the ratio of the transition probabilities A_1 and A_2 is known -- then λ_1 can serve as a radiation reference standard. The brightness B_1 of the source of this line is calculated as follows:

$$B_1 = B_2 \frac{\lambda_2}{\lambda_1} \cdot \frac{A_1}{A_2}. \qquad (33)$$

To use this formula, one must determine simultaneously with the recording of the line λ_1 the brightness B_2 of line λ_2.

The pair of lines method has an indisputable advantage over the other above-cited methods, since it permits setting up a reference standard light source and calibrating not only the radiation receiver, but also the spectral equipment. Use of the method is expanding /240/, in spite of two drawbacks: first of all, it provides calibration only at specific wavelengths, and not over an entire spectral region. This poses some danger if the characteristics of instruments, for example, with prisms and lenses, vary rapidly over the spectrum. Secondly, an instrument for recording lines in the classical region must operate simultaneously with the short-wave spectrometer; here sighting of the same source location with both instruments must be ensured.

7. Use of a synchrotron as a radiation source with known energy distribution appears highly promising. As shown by numerous theoretical (for example, /241, 242/) and experimental (/243-245/, and so on) studies, the distribution of energy in the spectrum of electron bremsstrahlung radiation in a synchrotron depends only on electron energy. The intensity of radiation is proportional to the number of electrons in the beam. Therefore, both the relative and absolute distribution of energy in synchrotron radiation (oriented along the tangent to the electron orbit) can be calculated if we know the energy of electrons and their beam density. Fig. 26 presents a family of the distribution

/125

curves for the intensity of bremsstrahlung radiation for electron beams at different energies. Synchrotron radiation can be used as a standard not only in the rocket ultraviolet region, but also in the classical wavelength range -- as a reference standard altogether independent of absolute blackbody models. At the International Symposium on Spectrophotometry in Netherlands (June 1969), the method of calibration using the synchrotron was singled out along with the pair of lines method as one of the most promising. Both methods were evidently able by then to ensure a 20 percent precision of calibration in the rocket ultraviolet region /240/.

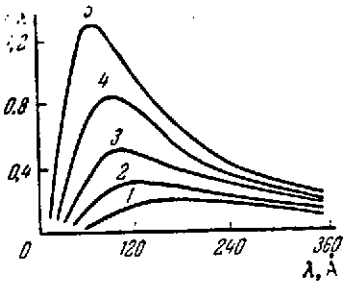

Fig. 26. Relative distribution of energy in the spectrum of synchrontron radiation for different beam electron energies:
1 -- 240 Mev
2 -- 260 Mev
3 -- 280 Mev
4 -- 300 Mev
5 -- 320 Mev

4. Secondary Spectrophotometric Standards

Primary spectrophotometric standards: absolute blackbody model and all the more so the synchrotron are cumbersome devices, therefore it is difficult to compare them directly with the sun, stars, /126 and other objects. Ordinarily, secondary standards -- radiation sources carefully calibrated based on the primary standards -- are used in spectrophotometric practice.

The principal requirement imposed on the sources is high stability and reproducibility of radiation.

The following are used as secondary standards: incandescent lamps, gas discharge lamps, positive crater of carbon Voltaic arc, fluorescent powders excited by ultraviolet radiation of a mercury lamp (at the line λ 2537 angstroms), permanent-action phosphors with radioactive excitation, and Cerenkov radiation sources.

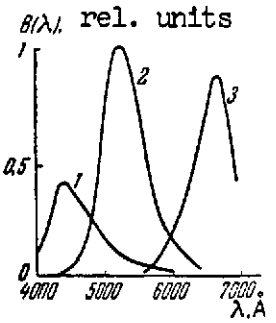

Fig. 27. Spectral distribution of the luminescence of various phosphors when excited with beta-radiation of Sr^{90}:
1 -- ZnS-Ag
2 -- ZnSCdS-Cu
3 -- ZnSCu

A description and comparison of several of these light sources with each other are given in a work by G. Kinley /246/, and also in Section 23 of a book by D. Ya. Martynov /182/.

Let us briefly characterize these light sources, beginning with the weakest.

The relative distribution of energy in the spectra of fluorescent powders and phosphors depends on their compositions; as an example, Fig. 27 presents the luminescence spectra of several substances excited with the beta-radiation of Sr^{90}, according to /247/. By selecting mixtures of various salts, a spectral curve most suitable for each specific problem can be obtained.

The theory of the Vavilov-Cerenkov effect has been presented in detail in the work /248/. The total energy emitted by an individual particle with charge e and velocity v along a path of 1 cm is given by the expression

$$E=\frac{e^2}{c^2}\int\limits_{\beta\cdot n(\omega)>1}\omega\left(1-\frac{c^2}{v^2n^2}\right)d\omega. \qquad (34)$$

Here $\omega = 2\pi c/\lambda_0$ is the circular frequency of radiation (λ_0 is the wavelength in vacuo), n is the index of refraction of the medium, and $\beta = v/c$. The condition for the domain of integration given under the sign of the integral is simultaneously also the condition for the production of Cerenkov radiation: the particle velocity v must be greater than the phase speed of light c/n in the given medium. /127

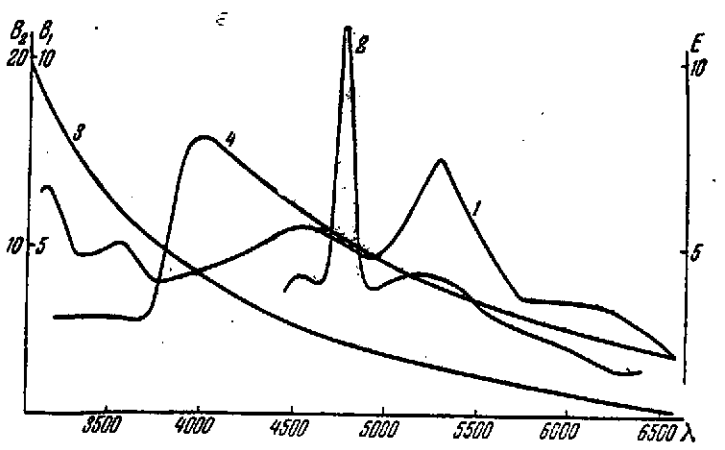

Fig. 28. Spectra of the Chalonge fluorescent source (scale B_1, relative units) -- 1; of phosphor (scale B_2, 10^2 erg/cm^2·sec·sterad·cm) -- 2; of Cerenkov radiator (scale B_1) -- 3; of Vega (scale E, 10^{-3} erg/cm^2·sec·cm) — 4.

We can easily see that the emission dE of an individual particle in the wavelength range $d\lambda$ will be

$$dE=\frac{f(v,\ n)}{\lambda^3}d\lambda, \qquad (35)$$

where f(v, n) is some function of v and n and is very small, only in terms of the index of refraction n dependent on λ. The relative distribution of energy in the spectrum of the Cerenkov radiator will approximately obey the law $1/\lambda^3$, which makes the Cerenkov radiator a highly convenient standard for comparison with hot stars (spectral classes O, B, and A, Fig. 28).

Usually Sr^{90} is used as the source of fast electrons to produce Cerenkov radiation; this isotope together with Cs^{137} is employed also in exciting phosphors used as spectrophotometric standards [247, 249]. /12

The absolute brightness of fluorescing powders, phosphors, and Cerenkov radiators depends on the excitation intensity; it cannot be made very high, therefore these light sources are used only in spectrophotometry of stars and other "nocturnal" objects.

To illustrate, Fig. 28 gives the spectra of the fluorescing Chalonge source [250], Cerenkov radiator [251], phosphor [249], and for comparison the spectral illumination produced by Vega (stellar magnitude $V = 0^m.04$, spectral class A0V) beyond the terrestrial atmosphere.

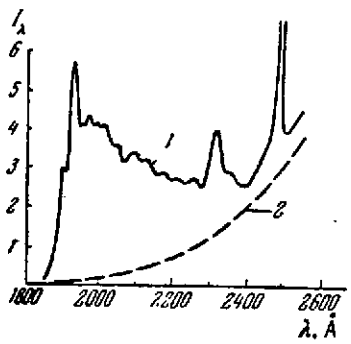

Fig. 29. Spectrum of positive crater of carbon arc (1) and blackbody at T = 3800° K (2). Break in arc spectrum at λ 1950 angstroms is caused by total absorption in a 120 cm thick layer of air

The Voltaic arc was used in spectrophotometry of the sun by Fabry and Buisson [252] and Plaskett [253], and also recently by Dunkelman and Scolnik [254] and Labs and Neckel (Chapter Five). Owing to its brightness and high temperature ($\sim 400^\circ$ K)*, the positive crater of the carbon arc is widely used as a secondary standard in studying the "rocket" ultraviolet. Most of the data obtained by the US Naval Research Laboratory in this spectral region is in one way or the other calibrated based on the carbon arc (Section 3, Chapter Five). Fig. 29 shows the distribution of energy in the spectrum of the positive crater of a carbon arc according to the study [255].

Detailed information on various incandescent and gas discharge lamps used in spectrophotometry is found in the studies [256, 257]. Gas discharge lamps with certain advantages, in particular, enormous radiation intensity, up to 20 kw and higher, and intense emission in the ultraviolet, in general do not have sufficiently /1 stable glow; in many of them something like nonchromatic flickerings occur, during which the distribution of energy is maintained

* Translator's Note: Should be $\sim 4000^\circ$ K.

nearly constant, but the overall intensity changes somewhat. This kind of instability is a certain hazard in recording spectra on photoelectric scanning instruments. Therefore for spectrophotometric purposes gas discharge lamps are used only in special cases, for example, in the ultraviolet spectral region where the emission of incandescent lamps is too faint. Hydrogen and deuterium lamps and tubes have gained wide acceptance (for example, the domestically produced VSFU-3, DU-1, DVS-40, DVS-25, and DOFU-3), yielding high-temperature and at the same time quite stable radiation in the short-wave spectral region, which is convenient to compare with the emission of hot stars (cf. Figs. 31 and 33).

On the other hand, gas discharge lamps have gained the broadest application in modeling extra-atmospheric solar emission, where limited instability poses no danger, and the important thing is to obtain general and spectral illumination values that are equal to solar values. This problem arose owing to the needs of astronautics -- to test the behavior of various materials and coatings exposed to continuous illumination, to determine the efficiency of solar batteries, to develop closed ecological systems in which material is recycled, and so on /258, 259/.

Numerous studies deal with problems of modeling solar radiation, for example, /260-264/. In particular, the study /262/ presents a comparison with the sun of various gas discharge lamps in terms of relative distribution of energy; the works /263,264/ describe very intense solar radiation simulators, with a beam diameter of more than 2 meters. Fig. 30 shows a comparison of spectral illumination from the sun and from the simulators /264/.

Incandescent lamps are also used in simulating solar radiation, but usually only in those cases when it is required to obtain the same general illumination, independently of the distribution of energy in the spectrum.

Though some incandescent lamps were developed and calibrated only for use as standards of general (total) radiation /229/, it is precisely the incandescent lamps that are most broadly /130
accepted secondary spectrophotometric reference standards. Let us examine them in greater detail.

There are two versions of lamp calibration: based on brightness and based on flux (illumination) at a fixed distance. The first version is used when the lamps are intended to determine spectral intensity (brightness) of individual details of the object under study, for example, the center of the solar disk. In this case the supplying optical system (telescope) must stand in front of the spectral apparatus; the optical system forms the image of the test object in the plane of the entrance diaphragm (slit) of the spectrometer. The second version is used for more limited problems, for example, in measuring illumination produced by the entire solar disk. These problems do not require a supplying telescope.

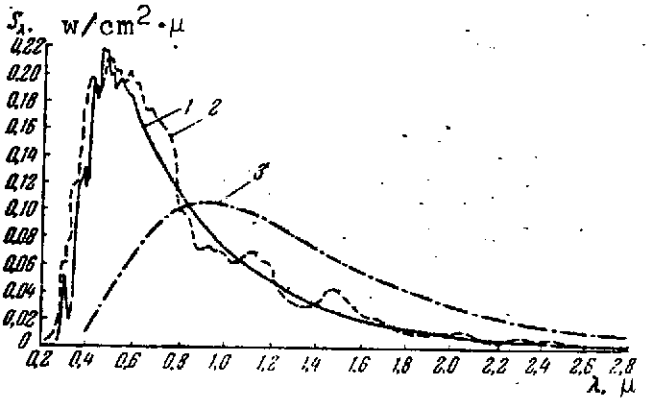

Fig. 30. Simulation of extra-atmospheric illumination produced by the sun (1), by a xenon gas discharge lamp (2), and by an incandescent lamp (3). Both lamps yield integral illumination equal to the sun's (at a given distance from the radiation receiver).

In lamps intended for calibration in terms of brightness, the brightness of a glowing body must be as identical as possible at all points. For this purpose, usually one employs so-called ribbon lamps, whose incandescent body is a broad (up to 2.6 mm) tungsten ribbon. At the operating incandescence regime for the most successful types of these lamps, which sometimes have to be specially selected from an entire lot, the central portion of the ribbon (± 1-3 mm from the center) has a constant brightness with the precision better than 1 percent /265, 266/. /13

Ribbon lamps built by Phillips and especially our domestically produced lamps of models SI6-40, SI6-100, SI8-200, and SI10-300 have gained wide renown. Incandescent lamps SI8-200, SI10-300, and the VSFU-3 hydrogen gas discharge lamps are shown in Fig. 31. Also produced are model SI-16 lamps, externally very similar to SI8-200 lamps. Sometimes the lamps are provided with an uviol /ultraviolet-transmitting glass/ window. The SI10-300 lamp was developed on the initiative of the VNIIM and is used there as a temperature reference standard /215, 216/.

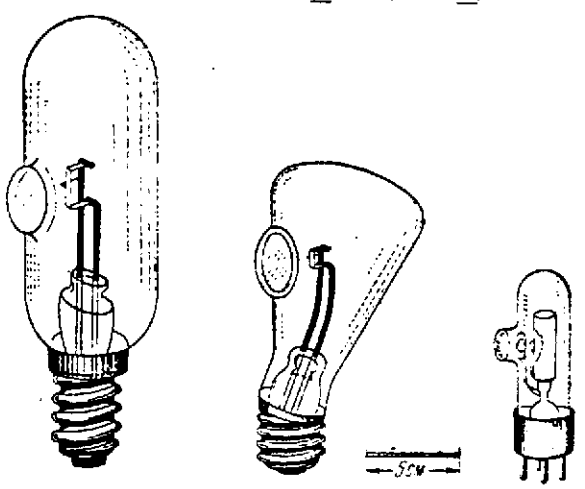

Fig. 31. Domestic ribbon type incandescent lamps. Left to right: SI10-300, SI8-200, and VSFU-3 hydrogen gas discharge.

When working with ribbon (and also with other) lamps, one must bear in mind the errors that can be introduced by the flashing formed at the rear wall

of the lamp bulb. Its brightness is as much as 10 percent of the ribbon brightness. Its effect is most successfully eliminated in domestic lamps with conical bulbs, for example, SI8-200 (Fig. 31). In these lamps, the emission of the flashing is diverted upwards /132 from the line of sight perpendicular to the plane of the ribbon.

A special procedure for mounting temperature lamps has been developed in the VNIIM in order that sighting of the central portion of the ribbon be executed with respect to the normal. A precision of 1 percent is achieved, which permits not only standardizing the effect of flashing (incidentally, in normal sighting it is covered by the ribbon itself), but also eliminating the effect of possible departures from Lambert's law and polarization effects. A thin wire rod (index) present within the SI10-300 lamp is used. It lies in the plane of the ribbon, opposite its center. A cross drawn on the rear wall of the lamp bulb serves as a second point for fixing the line of sight. The location for it is found by the shadow method using an autocollimator /267/. When the lamp is observed in a pyrometer (or in a telescope), the index and the cross must be brought into alignment.

In American research on solar spectrophotometry, often lamps are calibrated in terms of illumination produced by them at a fixed distance. Different kinds of incandescent lamps from 1000 to 5000 w used by the Eppley Laboratory and the Goddard Space Center as standard radiation sources are shown in Fig. 32. They are described in the studies /268, 269/. Also in these sources are to be found the results of their calibrations -- monochromatic illumination values in $mw/cm^2 \cdot$ microns produced by the lamp at distances of 40, 50, or 100 cm.

The advantage of this calibration method lies in the possibility of using lamps with incandescent bodies of any shape and with arbitrary distribution of brightness, since the illumination produced by the lamp as a whole is measured. In most lamps described in /268, 269/ the incandescent body is spiral. A disadvantage of calibration based on illumination is the necessity of precisely determining the distance to the lamp.

When celestial bodies are compared with a lamp, a certain difficulty arises related to the fact that all celestial bodies are practically infinitely remote compared with the focal length of the telescope. Refocusing the telescope from the celestial object to the lamp is undesirable in principle (the similarity of light beams is disturbed) and is often technically /133 infeasible. Following possibilities remain open: either to use a collimator mirror and to investigate its coefficient of reflection, or else to move the lamp to a distance that is 100-200 times greater than the telescope's focal length (in practice, 1-2 km) in order that the lamp appears as an "artificial star", or to use an integrating sphere or other averaging device at

the entrance of the spectral apparatus. The reflectivity of the mirrors and the actual path of the mirrors over the spectrum can be extremely dissimilar /100, 270, 271/, therefore in each case each collimator mirror must be investigated separately.

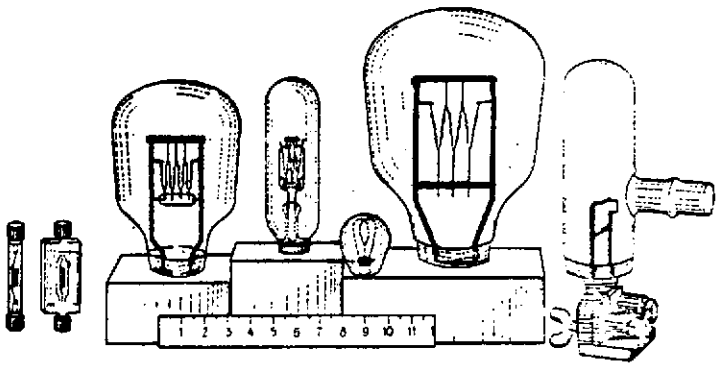

Fig. 32. American incandescent lamps used as spectrophotometric standards. From left to right: model EP1 (1000 w), HT (1000 w), E2K (2000 w), ETK (1000 w), EK carbon filament lamp (5000 w), and GE ribbon lamp, 30A/T24/17.

The second approach -- the "artificial star" -- is difficult to employ for solar spectrophotometry, since the emission flux from the lamp is very faint at a great distance. But it is widely used in stellar observations /272, 273/. When it is put into effect, one must determine precisely the distance from the lamp to the telescope and take allowance for the attenuating effect of air, which over a path of 1-2 km becomes appreciable. A certain difficulty of the second method is the removing to a great distance not only of the lamp, but also of the power sources and the power regulating devices, that is, the equipment of the auxiliary working station.

The integrating sphere is extremely convenient for comparing /134 the sun with a lamp calibrated in terms of flux and is widely used in American observations (cf. Chapter Five).

When working with any lamp, it is quite necessary to ensure that its power supply is most carefully stabilized. The incandescence current or the voltage at the lamp must be kept constant with the precision of at least one order of magnitude greater than the required radiation stability. The most exact and reliable method of monitoring lamp power is to measure the difference in the potentials at its base by means of a potentiometer with a normal second-class element /274/.

If for some reason lamp calibration can be done only in a narrow spectral region, then to determine the radiation at other wavelength one can use Kirchhoff's law in conjunction with data on the spectral emittance of tungsten. A technique for determining emittance is described, for example, in a monograph by V. A. Petrov /275/. However, emittance depends heavily on the technology of fabricating the tungsten ribbon and can vary

from specimen to specimen, therefore this method is less precise than the direct calibration of the lamp over a wide spectral region.

The temperature of incandescent lamps used as standards usually does not exceed 3000° K, though tungsten melts at 3650° K. Heating a lamp to higher temperatures, highly desirable for ultraviolet investigations, is quite hazardous, since it leads to the intense ageing of the lamp and in particular, to the precipitation of vaporizing tungsten at the lamp bulb and to a reduction in its transmission.

This disadvantage is eliminated in halogen lamps gaining acceptance in recent years. A certain amount of iodine or other halogen is introduced into them; the halogen compels tungsten atoms volatilizing from the incandescent body to execute a unique kind of turnover /276/ and to return from the walls of the bulb back to the incandescent body. Clouding does not occur, and the lamp can be heated to 3500° K. However, they must be used as standards with some caution, since the tungsten atoms returned by the iodine are precipitated in colder places of the incandescent body, resulting in the possible redistribution of the body's thickness and brightness. Characteristics of certain domestic and American halogen lamps are given in the works already cited /256, 257, 268, 269/. /135

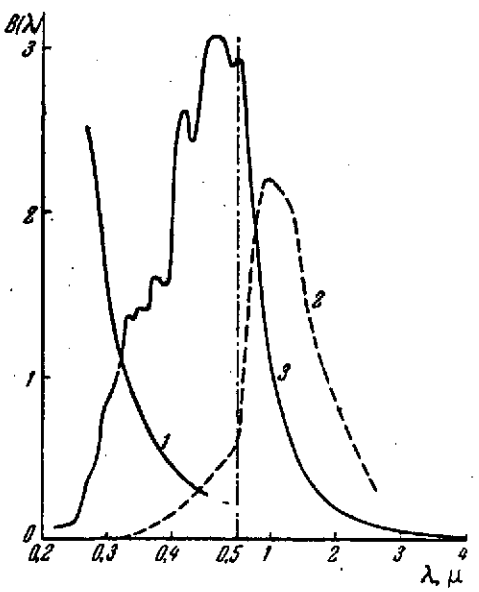

Fig. 33. Spectral brightness of the VSFU-3 hydrogen gas-discharge lamp (1), of the central region of the ribbon in a SI-16 lamp (2), and of the solar disk (3, integral spectrum). The B scale is used for (1) (10^9 erg/cm^2·sec·sterad·cm); for (2) -- (10^{13} erg/cm^2·sec·sterad·cm); and for (3) -- (10^{14} erg/cm^2·sec·sterad·cm).

As an illustration, Fig. 33 shows the distribution of energy in the spectra of the sun and the VSFU-3 and SI-16 reference standard lamps. The large difference in the course of the curve for the sun and for the lamps occasions additional difficulties in absolute spectrophotometry.

These procedures of investigating the distribution of energy in the spectra of celestial bodies and laboratory sources

unfortunately have not been standardized in the sense that there are no reference standards -- depositories of energy distribution -- that are comparable on an international scale and confirmed by international conventions. Though Planck's law for the radiation of an absolute blackbody is universal to the highest degree, as we have seen the designs of specific blackbody models have significant differences. The transition from the intensity of radiation at the melting point of gold to higher temperature radiation values is carried out in different ways. The principles and designs of secondary spectrometric standards differ greatly. /136

Whether the differences, especially in the designs of blackbody models and in the methods of extrapolating to temperatures above the melting point of gold, lead to errors can be definitively clarified (just as the size of errors can be estimated) only by comparison, directly via intermediate light sources, or the different models and methods with each other. These comparisons have been made, but infrequently and in limited scope. Thus, Labs and Neckel /113/ compared the results of calibrating lamps at several national laboratories. But studies on the comparison of spectrometric reference standards of all or most metrological establishments of the world have not been carried out. A comparison of temperature lamps in a number of countries (USSR, Great Britain, Australia, The Netherlands, FRG, and Japan), whose results are given in /277/ was made with the aim of investigating and improving reference standard-depositories of the temperature scale, but not the spectral distribution of radiation. Still, this task appears to be quite important; its significance grows owing to the expansion of spectrophotometric work in various wavelength regions, therefore it is desirable to call the attention of the different metrological establishments to this undertaking.

5. Fourier Spectrometer

The theoretical possibility of using a twin-wave interferometer for spectrophotometry at a high resolving power was well known to Michelson (and to other physicists) even at the very outset of the 20th century /278/. But lacking computers for high-speed Fourier transforms, Michelson was unable to use interferometers for the general spectroscopic problem area: studies of spectra with arbitrary and quite complex structure and energy distribution. He was limited only to analyzing particular cases: the fine structure of individual lines with several components of differing intensities /279, 280/. He undertook the mechanical modeling of interferograms using a specially designed, highly ingenious harmonic analyzer (a description and layout is given in /279/). These first experiments showed that the twin-wave interferometer can yield enormous spectral resolution, unattainable /137

with prismatic instruments and achievable only with difficulty by means of large diffraction gratings.

The modern method of Fourier spectrometry, exhibiting in addition to high resolution, also other important advantages, gained development mainly at the end of the 1960's in the works of P. Fellgett and H. Gebbie in Great Britain /281-283/, P. Jacquinot and the husband and wife J. and P. Connes in France /284-286/, and J. Strong in the United States /287-288/. A fairly extensive literature deals with Fourier-spectrometry -- cf., for example, the books and reviews /289-295/.

Several interesting investigations of this method have been undertaken in our country /296-302/. The first Fourier-spectrometer built by the Soviet optical engineering industry under the model IP-69 is described in /303/ (cf. also /180/).

Below we present the main principles and operating features of the Fourier-spectrometer.

Let us examine the Michelson interferometer, shown schematically in Fig. 34 [24].

The intensity recorded by receiver D will be determined by the phase difference induced as one beam traverses the path BM_1B, and the others -- the path BM_2B.

Suppose the path difference BM_1B-BM_2B is represented by Δ and suppose that strictly monochromatic radiation with wavelength λ enter diaphragm A. Oscillations defined by the following equations will be added at point D: /138

$$y_1 = a\cos 2\pi\left(\frac{c}{\lambda}t + \frac{\Delta}{\lambda}\right), \tag{36}$$

$$y_2 = a\cos 2\pi\frac{c}{\lambda}t. \tag{37}$$

The resultant oscillation will be

$$y = y_1 + y_2 = 2a\cdot\cos\pi\frac{\Delta}{\lambda}\cdot\cos 2\pi\left(\frac{c}{\lambda}t + \frac{\Delta}{2\lambda}\right). \tag{38}$$

---

[24] In addition to the interferometer with a crossed ray path many other optical layouts of the twin-wave interferometer can be built. Some are shown in Figs. 34 and 35 of a book by Michelson /279/. However, in describing them Michelson noted that the "crossed" interferometer constructed according to the scheme shown in Fig. 34 is the most convenient.

Its amplitude is $A = 2a \cdot \cos \frac{\Delta}{\lambda}$, and the intensity of radiation proportional to the square of the amplitude is given by the expression

$$I = I_0 \cos^2 \pi \frac{\Delta}{\lambda} = \frac{I_0}{2} + \frac{I_0}{2} \cos 2\pi \frac{\Delta}{\lambda}. \quad (39)$$

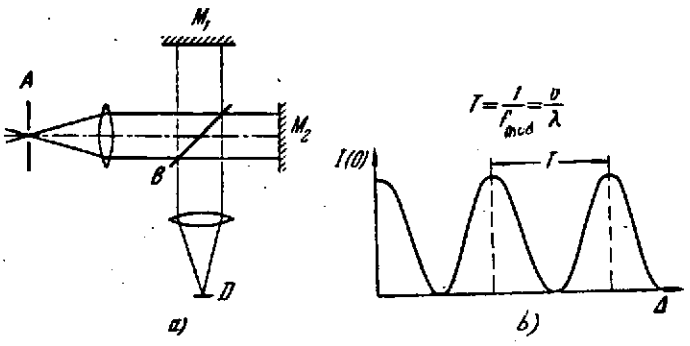

Fig. 34. Layout of Michelson interferometer (a) and interferograms of monochromatic radiation with wavelength λ (b)

Imagine that one of the interferometer mirrors, for example, M_1, moves uniformly at the rate v along the direction BM_1, remaining all the time parallel to its initial position. In this case the path difference $\Delta = vt$ and equation (39) will be rewritten as

$$I(\Delta, \lambda) = \frac{I_0(\lambda)}{2} + \frac{I_0(\lambda)}{2} \cos 2\pi \frac{v}{\lambda} t \quad (40)$$

or

$$I\left(\frac{\Delta}{c}, \nu\right) = \frac{I_0(\nu)}{2} + \frac{I_0(\nu)}{2} \cos 2\pi\nu \frac{v}{c} t. \quad (41)$$

The intensity of light at point D will experience oscillations /139 with frequency

$$f_{mod} = \frac{v}{\lambda} = \nu \frac{v}{c}, \quad (42)$$

in other words, the radiation leaving the interferometer will be modulated by 100 percent, according to cosine law; the modulation frequency f_{mod} is determined by formula (42). The receiving-recording system traces a cosinusoid similar to that shown in Fig. 34 b.

Suppose that radiation with a complex spectral composition ("white light") enters the interferometer. It is the result of the superpositioning of an infinitely large number of individual monochromatic radiations, each of which will be modulated with its own frequency at the interferometer output. The receiving-recording apparatus traces a complex interferogram, which is the

superpositioning of cosinusoids, whose frequencies are given by formula (42), and the amplitude is proportional to the intensities $E(\lambda)$ of the radiation at the corresponding wavelength. The proportionality factor is determined by the receiver's sensitivity and by the light losses in the interferometer optics, and in principle formulating it is similar to the procedure for classical instruments, therefore in the following we will not mention it. We can write

$$F(\Delta)=\int_0^\infty E(\lambda)\,d\lambda+\int_0^\infty E(\lambda)\cos 2\pi\frac{\Delta}{\lambda}\,d\lambda \tag{43}$$

or

$$F\left(\frac{\Delta}{c}\right)=\int_0^\infty E(\nu)\,d\nu+\int_0^\infty E(\nu)\cos 2\pi\nu\frac{\Delta}{c}\,d\nu. \tag{44}$$

The first term in these expressions describes the constant component of the interferogram. It is not of interest for a further analysis, and in certain Fourier spectrometers it simply is not received by the receiving-recording apparatus. Further, the function F must be symmetrical, in physical significance, relative to the Y axis (that is, it must not change when Δ is replaced by $-\Delta$). Therefore /140

$$F_1\left(\frac{\Delta}{c}\right)=\int_0^\infty E(\nu)\cos 2\pi\nu\frac{\Delta}{c}\,d\nu=\int_{-\infty}^\infty E(\nu)\cos 2\pi\nu\frac{\Delta}{c}\,d\nu. \tag{45}$$

The expression is the representation of the interferogram F_1 (the variable portion of the interferogram F) with a Fourier integral. The function $E(\lambda)$ of interest to us -- the distribution of energy in the spectrum of the source under study -- can be obtained by applying to (45) a Fourier transform, that is, by carrying out the mathematical procedure of the spectral analysis of the function F_1:

$$E(\nu)=2\int_{-\infty}^\infty F_1\left(\frac{\Delta}{c}\right)\cos 2\pi\nu\frac{\Delta}{c}\,d\left(\frac{\Delta}{c}\right). \tag{46}$$

As an example, Fig. 35 presents the interferogram of Saturn's disk and its interpretation /304/.

The detailed analysis of the operation of a Fourier-spectrometer made in the sources cited reveals the following properties of this spectrophotometric method:

1) The maximum resolving power is determined by the maximum path difference Δ_m:

$$R_{\underset{\text{theor}}{}} = \frac{\lambda}{\delta\lambda} = \frac{\Delta_{\nu}}{\lambda}. \qquad (47)$$

2) To achieve this resolving power (R) one must measure on the interferogram ordinates at 2R equidistant points. The large volume of calculations essential in obtaining $E(\nu)$ with high resolution was the main obstacle to progress in Fourier-spectrometry before the appearance of high-speed electronic computers with large memory capacity.

The advantage of the Fourier-spectrometer over other spectral apparatus lies in the following:

A. Simultaneous radiation of all wavelengths of the spectral interval under study is incident at the receiver. In ordinary methods this is carried out if a photographic plate is used as the receiver. But most other radiation receivers require spectral scanning. As a result, the receiver records the /14
spectrum successively, from point to point; at each given moment only a small fraction (1 percent and less) of the radiations studied strikes the receiver, and the remaining energy is not used (cf. Section 1).

Simultaneous exposure of the receiver to radiation in all wavelengths in a spectrometer with the Fourier transform, or, in other words, an increase in the recording time of each individual spectral element affords a particularly great advantage in the infrared spectral region. All known infrared-radiation receivers have high intrinsic noise (receiver noise), whose value is independent of the incident flux, to the first approximation. Receiver noises in the IR region are much greater than fluctuations in the radiation flux caused by the quantum nature of the radiation flux ("photon noise"). In these conditions simultaneous recording affords the advantage of the signal-to-noise ratio by a factor of $\sqrt{t/\delta t}$, where t is the recording time for the entire spectrum and δt is the recording time for an individual spectral element in an equivalent scanning spectrometer. In the visible spectral region where high-quality low-noise photomultipliers can be used, this advantage becomes less. An exact analysis is /1
quite difficult, since one must allow for many factors. In the limiting case when only photon noises are present, proportional to the square root of the total incident flux, and if all spectral elements are of comparable intensity, the signal-to-noise gain no longer holds.

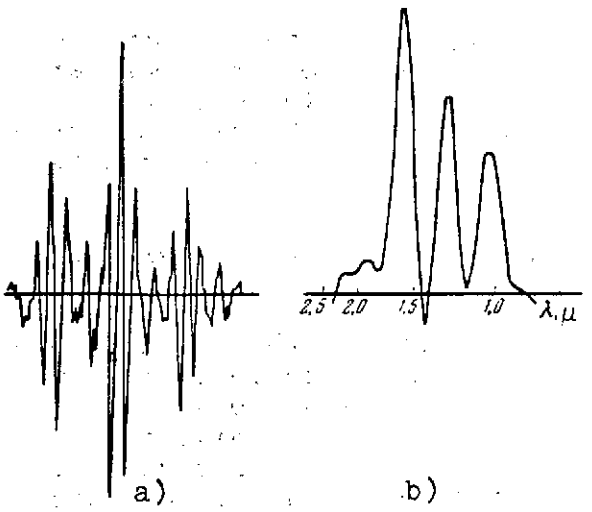

Fig. 35. Interferogram (a) of Saturn's disk and its interpretation (b)

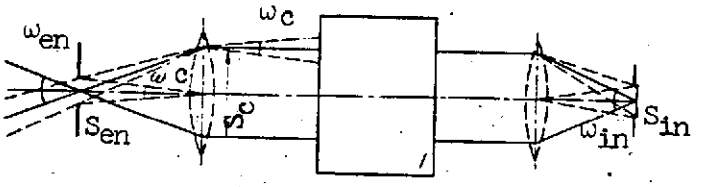

Fig. 36. Explanation of the concept "geometrical factor of spectral instrument." The product of the cross-section area S of a beam of rays by the solid angle ω within which the beam is propagated remains constant; 1 -- dispersing element

B. Large geometrical factor. Let us clarify this concept. In the investigation of the continuous spectrum, the flux $\Delta\Phi$ in the interval $\Delta\lambda$ incident at the spectrometer receiver will be (cf. Fig. 36)

$$\Delta\Phi = B_{so}(\lambda) \cdot \bar{S}_{en} \cdot \omega_{en} P(\lambda) \Delta\lambda, \tag{48}$$

where $B_{so}(\lambda)$ [so = source] is the brightness of the radiation source, S_{en} [en = entrance] is the area of the entrance diaphragm (slit), ω_{en} is the solid angle of the entrance pupil, and $P(\lambda)$ is the transmission of the optics.

In optical theory it is proven that if one neglects losses, then when a beam of monochromatic rays traverses any optical system a product of its cross-section S by the solid angle ω within which it is propagated is preserved unchanged for any transformations of this beam in the system -- reflections, refractions, collimations, and so on [25].

In particular /14

$$S_{en}\omega_{en} = S_{c}\omega_{c} = S_{in}\omega_{in} = S\Omega = \text{const}. \tag{49}$$

The quantity $S\,\Omega$ is called the geometrical factor of the instrument.

Let us compare geometrical factors for an ordinary spectrometer with grating and for a Fourier-spectrometer with identical resolving power.

a. Spectrometer with grating

$$(\Omega S)_{p} = \delta\gamma\vartheta DH\cos\alpha, \tag{50}$$

where $d\gamma$ and θ are the angular widths and lengths of the entrance slit, D and H are the linear dimensions of the grating, and α is the angle of incidence of the rays at the grating.

The grating of this spectrometer can provide the resolving power

$$R_{\text{theor}} = \frac{\lambda}{\delta\lambda} = Nk = \frac{D\sin\alpha}{\lambda}; \tag{51}$$

here N is the number of rulings /of the grating/ and k is the order of the spectrum. We find the width of the entrance slit $\delta\gamma$ from the formulas for angular dispersion and the resolving power of the grating; obviously, it must correspond to the maximum-resolving interval $\delta\lambda$:

$$\delta\gamma = \frac{k\delta\lambda}{b\cos\alpha} = \frac{\lambda}{D\cos\alpha}. \tag{52}$$

---

25 This follows, in particular, from the law of the conservation of energy. Actually, a radiation flux passing through an area S from a source with brightness B, which upon being observed from S subtends the solid angle ω, is $B\omega S$. Since B characterizes the radiation source and remains unchanged when the parameters of the optical system are varied, and the absence of energy losses is assumed in the optical system, for conservation of energy of the flux it is necessary that ωS = const.

Substituting into (50), we get

$$(\Omega S)_p = \lambda\theta H. \tag{53}$$

b. Fourier-spectrometer. The maximum angular dimensions of the entrance diaphragm of a Fourier-spectrometer, that is, the solid angle by which it is visible from the principal point of the entrance collimator objective (similar to the angle ω_c in Fig. 36), are determined by the condition that a phase difference equal to λ is induced between the axial and inclined rays. Analysis shows that

$$\Omega = \frac{2\pi}{R_{\text{theor}}} = \frac{2\pi\lambda}{\lambda_x}. \tag{54}$$

Suppose the cross-section of a collimated beam in a Fourier-spectrometer is the same as in a spectrometer with a grating and is determined by the dimensions D · Hcos α. In this case /144

$$(\Omega S)_f = \frac{2\pi}{R_{\text{theor}}} DH\cos\alpha. \tag{55}$$

The resolving power of the Fourier-spectrometer must by our condition equal the resolving power of the grating; substituting in (55) its expression from (51), we get

$$(\Omega S)_f = \frac{2\pi\lambda H}{\operatorname{tg}\alpha} \tag{56}$$

and, dividing (56) by (53),

$$\frac{(\Omega S)_F}{(\Omega S)_p} = \frac{2\pi}{\theta\operatorname{tg}\alpha} \approx 10^2. \tag{57}$$

Usually in spectrometers with gratings θ does not exceed 0.1, but α varies within $10\text{-}40^\circ$ from which it is clear that the geometrical factor of a Fourier-spectrometer is approximately two orders greater than that for classical instruments.

C. The optical component of a Fourier-spectrometer can in principle operate just as efficiently in any wavelength range. It has none of the specific details of the prism, grating, and filter types, which will limit the spectral region of its application. In specific cases its application is restricted mainly by receivers and to much smaller extent by the properties of the reflective coatings of the mirrors and beam splitter.

The main drawback of the Fourier-spectrometer is the neccesity for quite cumbersome calculations to transform the interferogram into a spectral curve. Another disadvantage is represented by

the extremely high requirements imposed on the quality of mirrors and on motion of one of them, which must not have skewing. Here the relative precision required is of the order of the requisite resolution.

Various modifications of the Fourier-spectrometer scheme have been developed. Fig. 37 shows the Fellgett scheme [281, 289], in which more complete utilization of light is achieved than in the classical Michelson interferometer. The entire flux entering the interferometer strikes the receiver, and none of the is reflected toward the source side. Fig. 53 in Chapter Five presents the scheme together with calibration devices used by Eddy, Lena, and McQueen in solar observations in the submillimeter region. /14

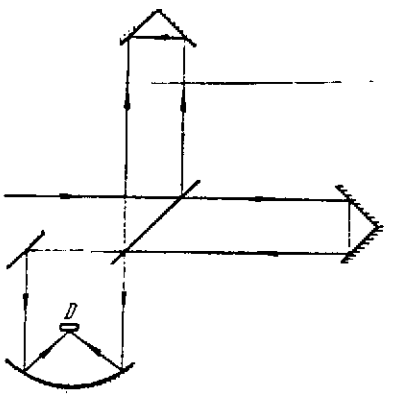

Fig. 37. Scheme of Michelson interferometer improved by Fellgett. It provides more complete use of the entering light flux

Finally, Fig. 38 shows the scheme of a polarization type Fourier-spectrometer. The concept of the application of polarization devices for modulating radiation at frequencies that are wavelength-dependent was first put forth by the Soviet optical physicist N. G. Bakhshiyev [305]. Fourier-spectrometers of the polarization type afford a smaller resolution than Michelson interferometers, but they have greater mechanical stability.

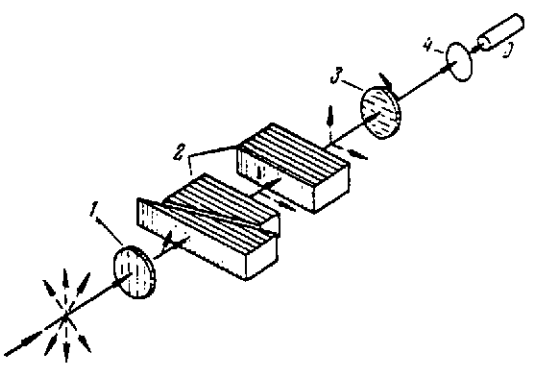

Fig. 38. Scheme of polarization type Fourier-spectrometer.
1 -- polarizer
2 -- Soleil compensator
3 -- analyzer
4 -- objective

Let us compare spectral instruments of various types with each other. In our comparison we will start from the fact, as noted by P. Jacquinot, that the "best method is the one which affords investigation of more spectroelements with higher resolving power over a short time with a less bright source" [290]. /14

The most general criteria for the comparison of spectral instruments were proposed by B. A. Kiselev and P. F. Parshin [306, 180], which we will in fact follow. Let us make the following two assumptions:

a) The precision is determined only by the ratio N of the signal to the mean-square-root noise value. Other sources of errors associated with the practical execution of the scheme (misadjustment, nonlinearity, and other errors of the recording apparatus, and so on) will be neglected by us.

b) The actual limit of resolution $\Delta\lambda$ is equal to the theoretical $\delta\lambda$ and is equal to the spectral width of the exit slit (in scanning instruments).

Obviously, the total number of spectral elements $\delta\lambda$ recorded by the instrument is

$$Z=\frac{\lambda_2-\lambda_1}{\delta\lambda}=\frac{tm_1}{\delta t}, \qquad (58)$$

where $\lambda_2 - \lambda_1$ is the operating range of the instrument, and m is the number of simultaneously recorded elements (for ordinary scanning spectrometers, m = 1).

The solid angle Ω is related to the resolving power $R = \lambda/\delta\lambda$ of the instrument by a relationship of the form

$$\Omega=p\frac{\delta\lambda}{\lambda}, \qquad (59)$$

where p is the parameter that is instrument-dependent.

Further, all radiation receivers can be divided into two classes, based on noise properties [193]:

a) Receivers in which intrinsic noise depends on the area of the working surface, but does not depend on the size of the incident light flux (bolometers, and so on); let us call them thermal receivers. In these the equivalent noise intensity $w_{e.n.}$ [e.n. = equivalent noise] is proportional to $\sqrt{S_{in}}$; they are characterized by the threshold sensitivity $D = 1/w_{e.n}$ and the normed sensitivity threshold $D^* = \sqrt{S_{in}}/w_{e.n}$.

b) Receivers in which intrinsic noise depends on the signal value (photomultipliers, and the like). Here the noise is determined mainly by the small shot effect (fluctuations in the number of emitted electrons) and therefore $w_{e.n} \propto \sqrt{\Phi}$, where Φ is the total light flux striking the receiver. We refer to these receivers as quantum receivers. /147

In spectrophotometry the signal-noise ratio $N \propto \sqrt{\delta t}$, for receivers of both types.

With the foregoing, we can write the following expressions for N in instruments with receivers of different classes:

$$N_т = \Phi D^* \sqrt{\frac{\delta t}{S_{ir}}} \tag{60}$$

and

$$N_ф = D' \sqrt{\frac{\Phi \delta t}{m_2}}; \tag{61}$$

here D' is the sensitivity of the quantum receiver, and m_2 is the number of elementary fluxes with spectral interval $\delta\lambda$ simultaneously incident at the receiver and determining its noise intensity. In ordinary spectrometers, $m_2 = 1$; for the Fourier-spectrometer $m_1 = m_2 = z$.

Substituting (60) and (61) the values $\Phi(\lambda)$ from (48) and referring to (49), (58), and (59), we get for instruments with thermal receivers

$$N_т = B(\lambda) D^* P(\lambda) \delta\lambda \sqrt{pStm_1 \frac{\omega_{in}}{\lambda z} \delta\lambda} \tag{62}$$

and for instruments with quantum receivers

$$N_ф = D' \delta\lambda \sqrt{B(\lambda) P(\lambda) pStm_1 \frac{1}{m_2 \lambda z}}. \tag{63}$$

Taking the second power of both equalities and transferring the free parameters of the instrument (those that the experimenter can modify depending on the spectral recording problem: N, λ, $\delta\lambda$, z, and t) to the left-hand side, and transferring the "hard" parameters determined by the instrument design -- to the right side, we get Q -- the desired criteria for comparing spectral apparatus of different types, expressed in terms of the recording parameters or in terms of the hard instrument parameters. The criteria Q also characterize the efficiency of the instruments, more precisely -- their limiting capabilities. For instruments with thermal receivers

$$Q_т = \frac{N_т^2 \lambda z}{\delta\lambda^3 t} = [B(\lambda) D^* P(\lambda)]^2 m_1 p \omega_{in} S, \tag{64}$$

and for instruments with quantum receivers

/ 14

$$Q_ф = \frac{N_ф^2 \lambda z}{\delta\lambda^2 t} = B(\lambda) D'^2 P(\lambda) \frac{m_1}{m_2} pS. \tag{65}$$

TABLE 14.* APPROXIMATE COMPARISON OF THE EFFICIENCIES OF THE VARIOUS TYPES OF SPECTRAL INSTRUMENTS

Type of instrument	Expressions for P	Parameter values (mean; max. in ( )) P, ster	S, cm²	T	m_1	m_2	ε_i, ster	$\frac{Q_T}{[B(\lambda)D^*]^2}$ *)	$\frac{Q_S}{B(\lambda)D^{*2}}$ *)
Spectrometers with Littrow prisms	$2\theta\frac{d\lambda}{\lambda^3}\frac{d\lambda}{dn}$ **)	0,01 (0,04)	50 (100)	0,5	1	1	1	0,12 (1)	0,25 (2)
Spectrometers with Littrow gratings ***	$2\theta\sin\beta$ **)	0,1 (0,15)	100 (500)	0,35 (0,50)	1	1	1	1,2 (20)	3,5 (38)
Fabry-Perot etalon ***	2π	6,28	20 (50)	0,2 (0,7)	1	1	1	5 (150)	25 (220)
SISAM ***	2π	6,28	100 (500)	0,2	1	100 (1000)	1	64 (320)	12
Fourier-spectrometer, after Michelson	2π	6,28	100 (900)	0,5	100 (200)	100 (200)	1	16000 (280 000)	300 (9500)

*) The quantities

$$\frac{Q_T}{[B(\lambda)D^*]^2} = P(\lambda)^2 m_1 p^{m_2} S$$

and

$$\frac{Q_S}{B(\lambda)D^{*2}} = P(\lambda)\frac{m_1}{m_2} pS \quad (\mathrm{cm}^2\cdot\mathrm{sterad})$$

derived from (64) and (65) characterize only the limiting capabilities of instruments realized for the most favorable conditions. **) In calculations the following values are adopted: $\theta = 0.005$ (0.1), $\frac{1}{\lambda^3}\left(\frac{d\lambda}{dn}\right) = 0.1$ (0.2), and the diffraction angle $\beta = 30°$ (60°). ***) These instruments are considered without preliminary monochromator.

* TRANSLATOR'S NOTE: COMMAS REPRESENT DECIMAL POINTS

The numerical values of parameters for comparing spectral instruments of several types are listed in Table 14, taken from /306/. The table shows the significantly higher efficiency of Fourier-spectrometers compared with other devices, especially when thermal receivers are used.

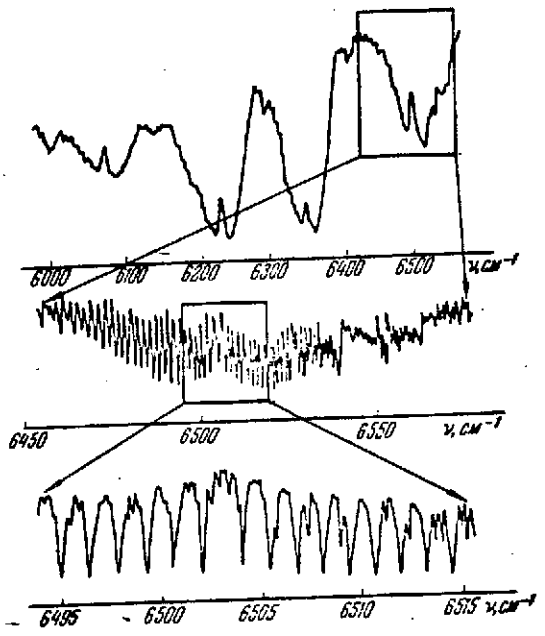

Fig. 39. On the problem of the capabilities of the Fourier-spectrometer. Above -- the spectrum of Venus recorded by Kuiper on a diffraction spectrometer in 1962, in the center -- a portion of the upper spectrum (enclosed in a rectangle) obtained by the husband and wife team Connes in 1964 on a Fourier-spectrometer. Below -- a portion of the central spectrum obtained by the same workers, on an improved Fourier-spectrometer.

The high efficiency of the Fourier-spectrometer permits its use in investigating spectra of weak luminescence with extremely high resolution. In particular, /15 the Connes, husband and wife, and Maillard compiled, based on observations using a Fourier-spectrometer, an atlas of the infrared spectra of Venus, Mars, Jupiter, and Saturn /307/. The dispersion and resolving power attained were at such a high level that formerly these values could be achieved with classical instruments only in observations of the solar spectrum.

Enormous possibilities of Fourier-spectrometry are illustrated by Fig. 39, taken from /295/, which shows the spectrum of Venus in the interval between 6000 and 6600 cm^{-1}, obtained by Kuiper with a diffraction spectrometer, and a portion of this interval obtained by the Connes husband-and-wife team using Michelson interferometers.

Virtually all modern studies of the far IR solar spectral region and the transparency of the terrestrial atmosphere employ Fourier-spectrometers -- cf. Section 4, Chapter Five.

CHAPTER FOUR

/151

EFFECT OF LIMB DARKENING OF THE SOLAR DISK AND THE EFFECT OF ABSORPTION LINES ON THE DISTRIBUTION OF ENERGY IN THE SOLAR SPECTRUM

1. Limb Darkening

The distribution of energy F_λ in the continuous spectrum of the entire solar disk, of the sun as a star, occurs below the distribution of energy measured at the center of the solar disk I_λ (0), which is due to the decrease in brightness in the direction from the center to the limb in the broad spectral region from 1600-1700 angstroms to 0.2-0.5 mm. In contrast, limb brightening of the disk is observed in the far UV spectrum and in the radio range.

Limb darkening in the continuous spectrum is caused by the fact that radiation from the center and from the limb arrives at the observer from layers at different depths. The unit optical thickness in a given wavelength determines, to the first approximation, the geometrical depths of the observed layer; owing to the effect of projection at the disk limb, it will be attained at lesser geometrical depth where owing to the decrease in temperature in the photosphere in the direction toward the outer layers the brightness will be less. The center-limb contrast depends on the wavelength just as the absorption coefficient of the photospheric plasma.

Based on data of solar disk limb darkening, one can investigate the change in physical parameters (T, p, ρ) with depth in the photosphere, which permits devising photosphere models. Observations of limb darkening have been taken since early in the 20th century (Abbot, Chalonge, Pierce, Peyturaux, and so on), but essential for models is information about the actual disk limb, and such observations are complex owing to the tremor of

the solar limb and the effect of light scattered both in the atmosphere and in the instrument. Reliable observations of this kind have been successfully performed only from balloons /308/ or during solar eclipses. However, and this bears special mention, for our purposes of finding a relationship between the distribution of energy in the spectrum of the entire solar disk and of its center, the limb zone is not as essential, since it enters with a small weight (proportional to the area) into the transition formula (67). Therefore in describing the series of limb darkening observations we used (cf. below), we limit ourselves only to the briefest information on technique and apparatus. /15

In making limb darkening measurements, photometric profiles are plotted along the radius of the solar disk and the following quantities are determined:

$$j_\lambda(\theta)=\frac{I_\lambda(\theta)}{I_\lambda(0)}, \tag{66}$$

which are presented in tabular or graphical form for different λ and θ. But we are interested in the coefficients of transition from the radiation intensity of the disk center $I_\lambda(0)$ to the radiation intensity averaged over the entire disk F_λ, and conversely -- since absolute solar spectrometry is performed differently by different workers: some measured $I_\lambda(0)$, while others measured F_λ. The transition coefficient would obviously be determined by the expression

$$\gamma_\lambda=\frac{1}{\beta_\lambda}=\frac{F_\lambda}{I_\lambda(0)}=$$
$$=\sum\frac{j_\lambda(\theta_i)+j_\lambda(\theta_{i-1})}{2}(\sin^2\theta_i-\sin^2\theta_{i-1}). \tag{67}$$

Using this formula, we calculated β_λ (γ_λ) in the interval from 1950 angstroms to 25 microns (more than 150 values). They are plotted in Fig. 40 a - d, which also gives the mean smoothed functions of γ_λ and β_λ obtained by graphical averaging of the data. The results of individual observational series are denoted as follows: 1 -- Bonnet, 2 -- Bonnet and Blammont, 3 -- Lacis and Matsuchima, 4 -- Peyturaux, 1952, 5 -- Peyturaux, 1955, 6 -- Canavaggia and Chalonge, 7 -- Pierce, McMath, Goldberg, and Mohler, 8 -- Pierce, corrected by David and Elste, 9 -- T. V. Krat, 10 -- Rogerson, 11 -- Kozhevnikov, 12 -- Saiedy, and 13 -- Lena. The initial quantities $j_\lambda(\theta)$ used in calculating β_λ are taken from the studies /308-321/, which appeared to us to be most correct; a brief characterization of these studies is given below [26]. In all the studies we utilized, limb darkening was measured in the continuous spectrum (more exactly, in the quasicontinuum). /15

/Footnote 26 on following page/

1. In his first study, R. Peyturaux /309/ obtained $j_\lambda(\theta)$ for 15 wavelengths from 6790 to 23,110 angstroms and nine θ values. A double quartz monochromator served as the spectral instrument, and a lead-sulfide cell was the radiation receiver. The amplifier exhibited a nonlinear dependence between input and output signals, which requires corrections to be made (and is, of course, a drawback of the study).

2. The second work by Peyturaux /310/ is more detailed and precise. The observations were also made with a double quartz monochromator (working region 2800-30,000 angstroms); a photomultiplier was used as the receiver for the visible and ultraviolet radiation, and a lead sulfide cell for the red and infrared regions. Another amplifier was used, providing strict proportionality of input and output signals. The observations were taken at 31 points on a wavelength scale from 3190 to 23,130 angstroms. Independent series of measurements with the photomultiplier and with the photocell in the same wavelength in an overlapping region, and also measurements in different observational seasons afforded quite consistent results. However, agreement with the preceding work /309/ is poorer; the new β_λ values are systematically 1-2 percent higher (Fig. 40, b and c).

3. In the study by R. Canavaggia and D. Chalonge /311/, the measurements were taken at 26 wavelengths in the ultraviolet spectral region (3149-3692 angstroms) and at 17 wavelengths of the visible (4006-5955 angstroms) spectral region. In spite of the fact that these authors used the photographic method, their results are of great value for our problem, especially in the UV region where observations are few. The agreement of the results in the studies /311/ and /310/ is excellent.

4. In their observations in the region 5000-20,000 angstroms, A. Pierce, R. McMath, L. Goldberg, and O. Mohler /312/ used a tower solar telescope with a spectrometer featuring double monochromatization. These authors also made observations in the IR region at 3.5, 8.3, and 10.2 microns, using a spectrometer mounted on a 24-inch reflector. /155

26 Unfortunately, we could not use the numerous limb darkening observations made by Abbot et al.: owing to low spectral resolution of the spectrometer they used, the effect of absorption lines on their results is unclear.

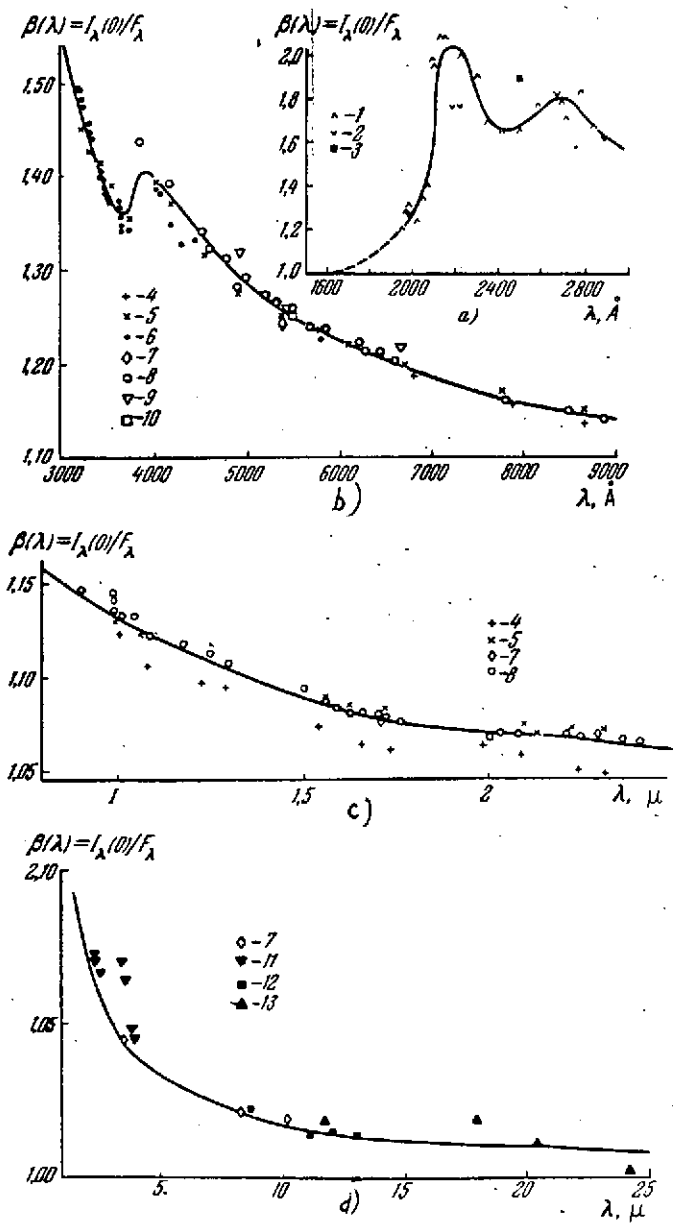

Fig. 40. Limb darkening of solar disk. Ratio of radiation intensity at center of solar disk to radiation intensity averaged over the disk $\beta = I_\lambda(0)/F(0)$ for several spectral regions: a) 1500-3000 angstroms, b) 3000-9000 angstroms, c) 0.9-2.5 microns, and d) 2.5-25 microns.

5. Pierce conducted, in addition, measurements of limb darkening using the photoelectric method in the region 3811-25,000 angstroms. His results are partially published in the work /313/, and partially in an article by W. Mitchell /314/. Subsequently it was found that when the observations were interpreted, scattered light in the terrestrial atmosphere was not fully accounted for. K. David and G. Elste /315/ re-interpreted Pierce's observational data, by excluding (analytically) the effect of scattered atmospheric light; Fig. 40, b and c gives only these corrected data. In drawing the mean curve β_λ in the corresponding wavelength interval, the results in /315/ were assigned the highest weight (cf. Fig. 40, b and c).

6. Three β_λ values derived from the photographic observations of T. V. Krat /316/ agree well with the data of other workers.

7. The observations of J. Rogerson /308/ were made from a balloon. The solar disk was photographed through an interference filter; the effective wavelength of the system was 5400 angstroms. Though the observations were made only in a single wavelength, we used the results as a kind of control, since balloon observations are significantly free of the distortions introduced by the tremor of the limb of the solar image and by scattered atmospheric light. The Rogerson point agrees splendidly (cf. Fig. 40, b) with remaining results, especially with those obtained by Peyturaux /310/ and Pierce (after their correction by David and Elste /315/). The following data were used, moreover, in the infrared region:

8. The observations of P. Lena /317/ were taken at the McMath observatory in the wavelength 10.7, 17.9, 20.4, and 24.2 microns with a telescope equipped with a 158 cm diameter principal mirror. For λ 20 microns, the telescope provided a spatial resolution of 3".4. A grating with 40 rulings per millimeter was the dispersing component of the spectrometer, and the acousticooptical Golay receiver was the detector.

9. Observations of F. Saiedy /318/ in thewavelengths 8.63, 11.10, 12.02, and 12.95 microns (a more detailed description of the study is given in Chapter Five). /156

10. Results of N. I. Kozhevnikov /319/ obtained for a large number of points in the interval 1-4 microns. The observations were made on the horizontal solar telescope of the Kuchino Observatory of the GAISh with a IKS-11 spectrometer.

11. Finally, in the rocket ultraviolet region use was made of the results of R. Bonnet /320/, who based on rocket spectrographic observations obtained $j_\lambda(\theta)$ values for 21 wavelengths in the interval 1946-2839 angstroms, inclusively, and also the data of R. Bonnet and J. Blammont /321/ (cf. also Chapter Five). The results presented in the very first publication by Bonnet /322/ for the region 2100-2800 angstroms, used by us in our 1967 study /120/, are not plotted in Fig. 40 a, since obviously they are erroneous. We regard as unreliable also the single point in the work by A. Lacis and S. Matsuchima /323/ (Fig. 40 a), though the investigation itself is interesting from a technical standpoint, since the authors carefully corrected results for scattered light.

Fig. 40 a and b clearly shows the jumps in β_λ near the limits of the Balmer series of hydrogen, aluminum, and silicon (cf. Section 3, Chapter Five); they are caused by an abrupt increase in the coefficient of absorption of solar plasma in these spectral regions.

In the region 1600-1900 angstroms, Fig. 40 a has no observational data; an interpolation is made between the region of the temperature minimum where $\beta_\lambda = 1$ by definition (cf. Chapter Five) and the region $\lambda > 1900$ angstroms.

Fig. 40 a-d presents all β values calculated based on the data of the above-described studies, and also an averaged curve smoothing the point scatter. It is drawn quite confidently, especially in the visible and near infrared spectral regions: the mean square-root error estimated by the deviation of individual points from the mean proves to be less than 0.5 percent.

The mean β_λ values derived are presented in the composite Fig. 41 and also in Tables 25-27. As already noted, they refer to the continuous spectrum or the quasicontinuum, which is distorted as little as possible by absorption lines. However, in addition to β_λ values, for our problem we are interested in similar β_λ^{in} values for the integrated spectrum. Unfortunately, limb darkening over fairly wide wavelength intervals extending, for example, 25, 50, or 100 angstroms, and including lines and the continuous spectrum, has not been measured, and the β_λ^{in} value has to be derived by combining data on the measurement of equivalent widths from the center to the limb and known β_λ^c values (Section 3). /157

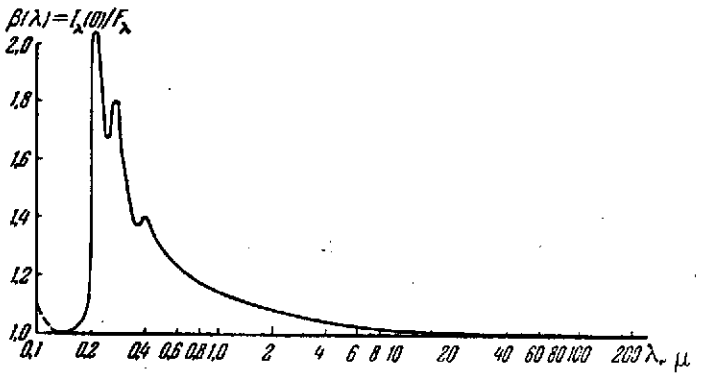

Fig. 41. Limb darkening of solar disk for the solar photosphere. Composite graph.

2. Intensity of Solar Radiation in the Continuous and Integrated Spectra. Coefficients of Conversion Between These Spectra

The integrated solar spectrum is conveniently represented as a histogram with step length $\Delta\lambda$; in this representation averaging ("integration") of intensities is performed at each step, regardless of whether these intensities belong to the continuum or to lines, wings, or the central portions of the latter.

By the concept "true continuous spectrum" we define the level of intensities which would be present if the absorption lines were altogether absent. By selecting in a relatively long-wave spectral region, with $\lambda \geq 5000$ angstroms, sections altogether /158
free of absorption lines, one can quite confidently recover the curve of the true continuous spectrum from them. However, in the short-wave region where the number of lines is extremely large, even for $\lambda \leq 4300$ angstroms there are virtually no such sections of undistorted continuum. Even the highest intensity peaks in this region recorded with the best spectral apparatus are understated owing to two factors: a) the combined effect of superimposed far wings of intense lines, and b) lines that are extremely faint, which even with high resolution remain invisible, since they blend with more intense lines, but their number is in the many hundreds over a wavelength interval λ of 100 angstroms /324/. It is scarcely possible to correct the observed intensity maxima with sufficient precision for these two effects. To do this, we must know, first of all, the true profiles of the intense lines, which in the short-wave region overlap and therefore are amenable to experimental determination only with difficulty, and secondly, we must know the exact values of the equivalent widths and the wavelength of a large number of faint lines.

Some authors circumvent these difficulties by taking as the continuum the intensities obtained through computation, that is, by ignoring the possible deviations of the calculated absorption coefficient in the solar photosphere from the actual coefficient. By this approach, for example, R. Michard /325/, P. P. Kozak /326/, and D. Labs and H. Neckel /113/, relating the sums of equivalent widths of absorption lines to the theoretical continuum, obtained explicitly overstated values of these sums.

Other authors, using spectrograms with high resolution, present the continuous spectrum in the short-wave region as an envelope of the highest intensity peaks. For example, data under the name "continuum 1" were thus obtained in a recent work by J. Houtgast and O. Namba /327/. Though this curve, the "quasicontinuum", lies below the true continuous spectrum, it does have a certain advantage -- complete independence of any assumptions and presuppositions. G. A. Shajn /228/ and G. Mulders /329/ determined /159
their corrections for absorption lines with respect to the quasicontinuum; their studies are evidently the first attempts to estimate the effect of Fraunhofer lines on the distribution of energy in the solar spectrum. The work of Mulders, based on calibration in equivalent widths of visual estimates of line intensities in the corrected addition of the Rowland Tables /330/ has been frequently used for various reductions.

In the following, by continuous spectrum we will mean specifically the quasicontinuum -- the envelope of the highest intensity peaks that have not been subject to any theoretical corrections.

The quasicontinuum practically coincides with the true continuous spectrum in the region $\lambda \geqslant$ 5000 angstroms.

The coefficient for converting from intensity in the continuous spectrum to intensity in the integrated spectrum and vice versa, can be expressed in terms of equivalent widths w_λ of the lines in the interval $\Delta\lambda$ of interest with its center at λ :

$$\eta_\lambda = \frac{1}{\zeta_\lambda} = \frac{I(\eta(0))}{I(0)} = 1 - \frac{\sum_{\Delta\lambda} w_\lambda}{\Delta\lambda}. \qquad (68)$$

Here we must make two remarks. First of all, in the case of blending lines, here the values of the equivalent widths of precisely the blends, and not the components corrected for blending, must enter the picture. Secondly, expression (68) provides the coefficient η_λ^{ce} relating to the emission of the center of the solar disk. It must differ somewhat from the coefficient η_λ^{d} relating to the entire disk, since the equivalent widths of the Fraunhofer lines vary from the center of the disk to the limb. Most studies that can be used in determining the sums of equivalent line widths $\sum_{\Delta\lambda} w_\lambda$ present data only for the disk's center, therefore we must first find η_λ^{ce}, and in the next section we will attempt to estimate how the sums $\sum_{\Delta\lambda} w_\lambda$ must be modified in order to arrive at η_λ^{d} .

Below we briefly characterize studies used in determining η_λ^{ce} in various spectral regions.

1. Ultraviolet region 3000-4050 angstroms. A study by Houtgast and Namba /327/ is used; in particular, this work presents /1
the values of the "total absorption" calculated for each 100 angstroms in the interval 3000-4050 angstroms, that is, in other words precisely the sums of equivalent widths of all lines we need in sections of 100 angstroms, where the lines with overlapping profiles -- the blends -- are not corrected for the blending effect. The data were obtained based on observations made in 1965 at the Mount Wilson Observatory /331/, and also based on planimetry of the Utrecht /189/ and Goettingen /190/ atlases, which were first standardized based on 1965 observations.

In the ultraviolet region, the data of Houtgast and Namba appear most reliable and correct, since first of all, they are based on a great deal of material, and secondly, when the atlases /189, 190/ were subject to planimetry, Houtgast and Namba, in contrast with authors, for example, J. Wempe /332/, adopted as the quasicontinuum level not the "100" level of each atlas map,

but the highest intensity peaks reliably measured by Houtgast /331/ in absolute units. Thus, individual atlas sections proved to be related to each other.

2. The region 4050-8500 angstroms. Use was made of a study by Wempe /332/ and the second corrected edition of the Rowland Tables /333/. Wempe separated the solar spectrum covered by the Utrecht Atlas /189/ (from 3440 to 8500 angstroms) into individual nonoverlapping sections, 6-12 angstroms in extent. The boundaries between intervals occur at wavelengths that are more or less free of absorption lines. By planimetry, for each interval the sum of equivalent widths of all lines in it was determined, without correcting the lines for blending. The above-noted deficiency of the Wempe study, to the effect that the "100" level was taken as the continuum level for the atlas sheets, poses a danger only for the ultraviolet region, but for $\lambda > 4050$ angstroms Wempe's data are quite correct.

The Rowland Tables /333/ in the interval 2935-8772 angstroms give equivalent width of each line revealed for the spectral /161
equipment resolving power of $(4\text{-}5) \cdot 10^4$, that is, the same power as shown in the atlases /189, 190/. Most of the blends have been corrected for the effect of overlapping line profiles.

In determining $\frac{\Sigma w_\lambda}{100 \text{ A}}$ based on the Wempe tables and direct summation of equivalent widths of individual lines taken from the Rowland Tables that in the region 4500-8500 angstroms, the sums found from both sources are close to each other, and we use the mean value of η_λ of both sources. An exception is represented by spectral sections with centers at $\lambda\lambda$ 4800, 4850, 4900, 6500, and 6600 angstroms, that is, near the H_β and H_α lines. In the Utrecht Atlas /189/, elongated wings of these lines are not completely developed; the corresponding error is found also in the Wempe tables. But in the Rowland Tables /333/, the values of the equivalent widths of H_α and H_β evidently are closer to the true values, since to determine them the spectrograms serving as the basis for compilation of the Utrecht Atlas (cf. foreword to /333/) underwent a new photometric treatment. Therefore the quantities Σw_λ and η_λ for these five sections were determined only based on the Rowland Tables.

In the region $\lambda < 4500$ angstroms, the lines are intensely blended and it proves difficult to use the Rowland Tables, for as already noted, the tabulated w_λ values are corrected for the blending effect; but for our purpose we must know precisely the equivalent widths of the blends. Therefore in the interval $4050 < \lambda < 4500$ angstroms, only Wempe's data satisfying our condition were used.

3. In the region 8500 angstroms $< \lambda <$ 2.5 microns we made use of the tables of H. Babcock and C. Moore [87], which give the equivalent widths of all lines in the interval 6600 - 13,495 angstroms, and the analogous tables of O. Mohler [89] covering the interval 11,984 - 25,578 angstroms [27], as well as individual measurements of equivalent hydrogen line widths in the Paschen and Brackett series made by Ts. Khetsuriani [334], C. de Jager, L. Neven, and M. Migeotte [335], C. de Jager [336], and C. Allen [337]. [Footnote 27 is on the next page] [16]

4. In the region $\lambda \geqslant 2.5$ microns there are very few absorption lines, and the coefficients $\eta_\lambda \approx 1$ [338].

5. It is very complicated to calculate the absorption lines in the rocket ultraviolet region. A comparison of the atlas of McAlister [339] compiled for the wavelengths 1800-2965 angstroms, with the Goettingen and Utrecht atlases shows that the apparently continuous "palisade" of lines which are observed in the near, "ground" UV region, beginning at 2900 angstroms, gradually thins out somewhat and the corrections for the lines must be reduced. It proves possible to select broad enough, up to 10 angstroms wide, spectral sections for which the line corrections will be very small. Thus, for example, Heath (cf. Section 3, Chapter Five) made observations in six intervals of rocket ultraviolet with a 10 angstroms instrument passband; two of these intervals (with centers at 2557.0 and 2830.7 angstroms) were selected so that their intensities virtually exactly correspond to the quasicontinuum determined by Bonnet for narrow intervals $\sim$ 0.5 angstrom (for details, cf. Chapter Five). However, it was not possible to determine Σw_λ and the correction of η_λ using the McAlister atlas for $\lambda <$ 2900 angstroms, since in this atlas the logarithmic scale of intensities on the Y axis varies from one edge of each sheet to the other, which is a serious interference in planimetry, especially when determining sums of equivalent line widths for fairly extended sections of 50 or 100 angstroms.

3. Variations in Equivalent Line Widths From Solar Disk Center to Limb. Corrections for Absorption Lines for the Entire Disk.

In the wavelength interval from 3000 to 13,500 angstroms, about 26,000 absorption lines have been recorded in the solar spectrum, while massive data on changes in equivalent line widths from the solar disk center to its limb contained in the works of H. Holweger [340], M. Bretz [341], B. Page [342], M. Adam [343], and Ts. Khetsuriani [334] embrace about a thousand lines, that is, roughly 4 percent of their total number in the visible and near-visible spectral regions. Naturally, the use of these data permits only a very approximate estimate of the variation from center to limb of the sums $\sum_{\Delta\lambda} w_\lambda$ and the coefficients η_λ. [16]

The concept of this estimate amounts to the following. The total sum of equivalent widths of all lines in this section $\Delta\lambda$: $W = \sum_{\Delta\lambda} w_\lambda$ is divided into four components: $W = W_1 + W_2 + W_3 + W_4$, respectively, for the faint lines $\{(w_\lambda)_1 \leqslant 40$ m angstroms$\}$, medium lines $\{40 < (w_\lambda)_2 \leq 250$ m angstroms$\}$, intense lines $\{(w_\lambda)_3 > 250$ m angstroms$\}$, and the lines of hydrogen and ionized calcium. These four categories behave differently in the transition from center to limb. Therefore in order to obtain the total sum W^{li} /li = limb/ for the limb of the disk, each component W_i^{ce} must be multiplied by $\mu_i = w^{li}/w^{ce}$ -- a coefficient that allows for the variation of equivalent widths of a given group of lines from the center to the limb:

$$W^{li} = \mu_1 W_1^{ce} + \mu_2 W_2^{ce} + \mu_3 W_3^{ce} + \mu_4 W_4^{ce} \qquad (69)$$

The mean values of the coefficients μ were determined based on the studies /334, 340-343/, which give the equivalent widths of lines at the disk center and near the limb, for $\cos\theta = 0.3$ ($\sin\theta = 0.954$). The conversion coefficient μ was found for each line contained in these works, which made it possible to plot the graph $\mu(w_\lambda^{ce})$ reproduced in Fig. 42. It shows that the equivalent widths of the faint and medium lines generally grow toward the limb, and this growth is greater for the faint lines. In addition, some slight dependence of μ on the excitation potential was noted. Though the scatter of the points in Fig. 42 is very large, the averaged quantities $\mu(w^{ce})$ were found quite reliable. They are presented for various intervals of w^{ce} in Table 15.

A small decrease in equivalent widths at the disk limb is observed for intense lines, in addition to hydrogen and calcium lines. We can assume that on the average $\mu_1 = 1.49$, $\mu_2 = 1.012$, and $\mu_3 = 0.96$.

TABLE 15. MEAN DEPENDENCE OF THE RATIO $\mu = w^{li}/w^{ce}$ ON w^{ce} /164

w^{ce}, mÅ	μ	w^{ce}, mÅ	μ	w^{ce}, mÅ	μ	w^{ce}, mÅ	μ
5	2,0	15÷20	1,25	30÷40	1,11	75÷100	1,02
5÷10	1,6	20÷25	1,19	40÷50	1,08	100÷250	1,0
10÷15	1,33	25÷30	1,15	50÷75	1,05		

[27] Telluric lines and bands are noted in the tables [87, 89, 333]. They naturally have been excluded for finding Σw_λ from these tables. They are also excluded in works [327] and [332].

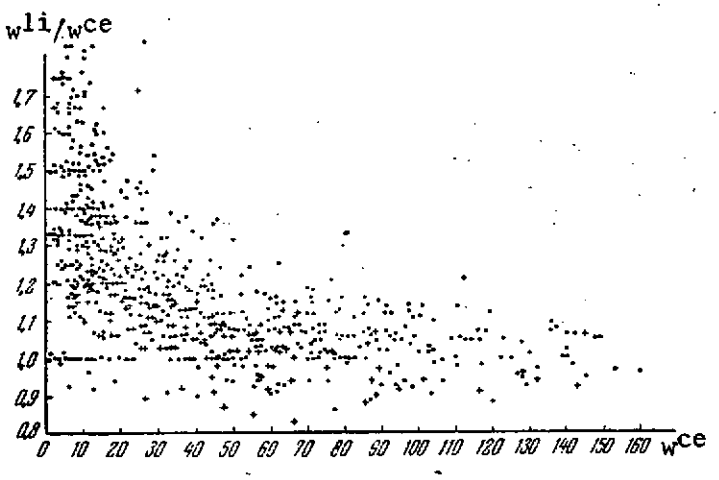

Fig. 42. Dependence of the ratio of equivalent line widths near the solar limb ($\cos\theta \approx 0.3$) to the equivalent widths in the solar disk center, w^{li}/w^{ce} on the equivalent widths in the center w^{ce}. Lines with excitation potential < 3 ev are denoted with dots, and lines with excitation potential > 3 ev -- with crosses.

Finally, the behavior of hydrogen and calcium lines recorded individually for each interval $\Delta\lambda$ is shown in Table 16, which gives data for the most intense representatives of this component, taken from the studies /9, 334/. The hydrogen lines in which the broadening of profiles occurs mainly due to the Stark effect vary very intensely from the disk center to its limb: equivalent widths of the Balmer series lines decrease toward the limb by approximately a factor of two, and by a factor of 3-4 -- for the Paschen and Brackett series. /1

TABLE 16* EQUIVALENT WIDTHS w AND THE VALUES $\mu = w^{li}/w^{ce}$ FOR LINES OF HYDROGEN AND IONIZED CALCIUM

λ, Å	Line, element	w^{ce}, Å	μ	λ, Å	Line, element	w^{ce}, Å	μ
3934	K, Ca II	19,00	0,855	8542	Ca II	3,26	0,80
3968	H, Ca II	14,50		8662	Ca II	2,52	0,79
4101	H_δ	2,86	0,50	10049	H_{3-7}	1,95	0,22
4341	H_γ	3,13	0,47	10938	H_{3-6}	3,46	0,23
4861	H_β	3,68	0,63	12818	H_{3-5}	5,51	0,24
6563	H_α	4,02	0,48	21655	H_{4-7}	8,54	0,29
8498	Ca II	1,22	0,78				

* TRANSLATOR'S NOTE: COMMAS REPRESENT DECIMAL POINTS

To find the sum of equivalent widths of faint lines W_I^{ce}, we made use of the study /324/, which estimates the total number of lines of different intensities with w < 40 m angstroms in various

spectral regions. The effect of blending with numerous intense lines leads to the actual number of faint lines in the ultraviolet having to be much larger than the number of actually observed lines. This effect is particularly evident for the faintest lines. Thus, in the interval 3300-3500 angstroms only 13 lines with $0.5 < w < 2.0$ angstroms is observed, while according to /324/ there must be approximately 2200 of these lines in this interval; 64 lines with $2.0 < w < 5.0$ angstroms are observed, but they must be about 1700, and so on. The estimate is made on the assumption that the relative number of intense and faint lines is independent of wavelength.

The remaining components, W_2^{ce}, W_3^{ce}, and W_4^{ce}, are found relatively simple: W_3^{ce} and W_4^{ce} are the direct summation of equivalent widths of these lines in each interval, and W_2^{ce} is the difference $W_2^{ce} = W^{ce} - (W_1^{ce} + W_3^{ce} + W_4^{ce})$. In the latter case we took account of the fact that when $\lambda < 4500$ angstroms the total sums of W^{ce}, which we set out to find in the last section, are the sums of blends, while the components W_1^{ce}, W_3^{ce}, and W_4^{ce}, owing to the /166
actual method of obtaining them, were corrected for the blending effect. This allowance was made by means of the "deblending coefficient" we found, which averages 1.16 (± 10 percent). It is the ratio of sums W found from Rowland Tables and from Wempe's tables for $\lambda < 4500$ angstroms /120/.

Thus, all data were determined for estimation based on expression (69) of the sums W^{li} of equivalent line widths at the disk limb. To make the corresponding estimate for the entire disk and to obtain W^d, it was assumed that the variation in equivalent widths of all lines from the center to the limb occurs linearly with $\cos\theta$:

$$w(\theta) = w^{li} - (w^{li} - w^{c}) \cos\theta, \qquad (70)$$

from whence we can easily proceed to w^d and W^d. Equality (70) is based on the data of a study by C. Allen /344/, who investigated in detail the variation of a number of lines along a radius of the solar disk.

The values of the equivalent line widths found in the spectrum of the entire solar disk by the above-described procedures, $W^d = \sum_{\Delta\lambda} w^d$, are presented in Table 26, as are the quantities $W^{ce} = \sum_{\Delta} w_\lambda^{ce}$, which was discussed in Section 2.

In conclusion let us return to the coefficient $\beta_\lambda = I_\lambda(0)/F_\lambda$ for converting from the intensity of radiation averaged over the disk to the intensity of radiation from the center. In Section 1 we derived values of this coefficient for the continuum β_λ^c. By uncomplicated calculations we can easily see that $\beta_\lambda^{in} = I_\lambda^{in}/F_\lambda$

-- the coefficient characterizing limb darkening for the integrated spectrum, can be found by the formula

$$\beta_\lambda^{cc}=\beta_\lambda^c\frac{\tau_\lambda^{cc}}{\tau_\lambda^c}=\beta_\lambda^c\frac{1-W^{cc}}{1-W^c}. \qquad (71)$$

4. Integral "Line Blanketing" Effect

We can calculate the sum of equivalent line widths over the entire photospheric spectrum from its UV- to its IR-limits for the entire solar disk, as well as for the center. This sum characterizes the fraction of energy abstracted by absorption lines from the continuous spectrum emitted by the sun. /16

The calculations were made individually for the disk center and for the entire disk based on the following formulas

$$\overline{\eta^{cc}}=\frac{\sum(1-\sum w_\lambda)\,I_\lambda^c(0)}{\sum I_\lambda^c(0)}=\frac{\sum I_\lambda^{cc}(0)}{\sum I_\lambda^c(0)} \qquad (72)$$

and

$$\overline{\eta^d}=\frac{\sum(1-\sum w_\lambda^d)\,F_\lambda^c}{\sum F_\lambda^c}=\frac{\sum F_\lambda^{cc}}{\sum F_\lambda^c} \qquad (73)$$

according to the data in Tables 28, 29, and 31.

In the region $\lambda < 3000$ angstroms, the corrections were not determined for individual intervals of 50 or 100 angstroms (cf. preceding section). The overall correction was determined for the entire section 2100-3000 angstroms according to the data in Table 28 for $I_\lambda(0)$ and F_λ; there are practically no absorption lines in the region $\lambda < 2100$ angstroms.

Integrated corrections due to the blanketing effect were found to be

$$\overline{\eta^{cc}}=0.878,\quad \overline{\eta^d}=0.90.$$

Thus, the absorption lines abstract ~ 12.2 percent from the total radiation of the disk center, and ~ 10 percent from the radiation of the entire disk.

CHAPTER FIVE /168

DISTRIBUTION OF ENERGY IN THE SPECTRUM OF THE SOLAR PHOTOSPHERE

We would assume, as already emphasized in the introduction, that only data obtained by averaging the most reliable modern series of measurements of the intensity of radiation from the solar photosphere as a function of wavelength can represent the most dependable information on the distribution of energy in the spectrum of the quiescent solar photosphere.

Measurements of the energy distribution in the solar spectrum, which we are examining, were made for the center of the disk or else for the entire sun (the sun as a star). In referring to the spectrum of the quiescent photosphere, naturally we mean only the spectrum of the disk's center; in such observations special precautions are always taken in order that active formations do not enter the slit of the spectral apparatus. In investigating the distribution of energy in the spectrum of the sun as a star, it does not appear possible to segregate the spectrum of the quiescent photosphere, since even during the years of the lowest minima of solar activity there are always active formations present on the sun: protuberances, and faculae, whose spectra differ widely from the spectrum of the quiescent photosphere.

As shown in Section 5, Chapter Two, even if the integrated flux of solar radiation from the entire solar disk (solar constant) does vary with the solar activity cycle, these changes lie currently beyond the limit of precision for modern measurements, and in this sense we can identify the intensity of radiation from the entire solar disk for the quiescent photosphere with the intensity for the sum of the quiet and active components. However, for the region of the far UV-spectrum of the photosphere at $\lambda < 3000$ angstroms, this identification may possibly not be wholly legitimate; some observations afford grounds for assuming that in this spectral region marked changes in the intensity of radiation from

the entire solar disk with the solar activity cycle occur (cf. Sections 3 and 4), though this is virtually not reflected in the /16
total value of the solar constant. Evidently, for a dependable study of this kind of variability we need homogeneous observations at least during one more solar activity cycle. For the time being, to the first approximation the assumed identity of the distribution of energy in the spectrum of the entire solar disk for the quiescent photosphere with the spectrum of the sum of the quiet and active components evidently is acceptable.

In deriving mean data on the distribution of energy, the critical stage is selecting observational series or sections of this series suitable for averaging. Naturally we endeavored to adhere to objective criteria: we selected studies conducted with a reliable absolutization of results, with adequate spectral resolution, and with correct reductions for light losses in the earth's atmosphere as well as in the optical system. The weights were assigned mainly as a function of these characteristics, and, moreover, depending on the number of reductions that had to be introduced in order to reduce the series to a given form (the center of the disk or of the entire disk); of course, the volume of observational material entering into a given series was also taken into account.

In several limited cases we had to reject this approach -- when a particular series (or part of a series) yielded results differing widely from all other series, these results were rejected, though the reasons for the deviation, with the initial observational data not at hand, could not always be indicated. For example, in the far UV-spectrum we did not use the data of Parkinson and Reeves for averaging (cf. Section 3), since it appeared to us that these results contain an explicit systematic error: the intensities they measured were three to four times smaller than in all the remaining series.

Below we present a brief critical review of studies dealing with the investigation of the distribution of energy in the solar spectrum, on the basis of which the reader can judge how well-grounded is our selection of series for averaging. This review also is of some independent interest from the standpoint of methods. Brief characteristics of all results selected for constructing mean data are given in Tables 17, and 20-22.

Most of the investigations assembled in these tables are /17C
reduced to absolute units by comparison with given standard sources of radiation, that is, they are ultimately coupled to the radiation of a blackbody in the system of the International Practical Temperature Scale (IPTS).

Since in 1968 the IPTS-48 system was modified and new values of the melting point of gold T_{au} and the constant c_2 were adopted,

and the new system IPTS-68 was introduced (cf. Section 2, Chapter 3, Introduction, and /20/), we also had to make suitable corrections in the results of all the European studies we employed: Peyturaux, G. F. Sitnik, Ye. A. Makarova, and Houtgast (cf. below), with the exception of the work by Labs and Neckel, in which the corrections were taken into account by the authors themselves /113, 345/. The American studies we used (performed at the National Bureau of Standards, the Goddard Center, the Naval Research Laboratory, the Eppley, and the Jet Propulsion Laboratories) evidently were all reduced to the IPTS-68 system, including also the 1967 study, according to a private communication by M. P. Thekaekara /346/. Thus, in the calculation of the brightness temperature of the sun based on 1957 observational data of Thekaekara's group, which he most graciously sent us, T_{Au} and c_2 are used based on IPTS-68.

Corrections for T_{Au} and c_2 are the largest in the UV-region and decrease with increase in wavelength. For example, for 3000 angstroms they are +3.6 and -1.8 percent, respectively; for 5000 angstroms -- +2.2 and -1.2 percent; and for 1 micron -- +1.1 and 0 percent. We did not introduce these corrections into results for $\lambda > 2$ microns; they are smaller than 1 percent.

1. First Investigations of the Distribution of Energy in the Solar Spectrum

1) The works of Langley, Abbot, and other scientists at the Smithsonian Institution. Attempts to record the solar spectrum in a wide wavelength region, including the near infrared, were made more than 130 years ago. In 1840 J. Herschel /347/ and later in the 1870's, M. Lamanski, using a thermocouple as the radiation receiver, recorded the spectrum up to 1 micron and concluded that infrared solar radiation is strongly absorbed by the terrestrial atmosphere.

The pioneering studies by S. Langley were a great step forward /348/; he used a then unprecedented radiation receiver -- a bolometer. His investigations showed that the solar spectrum can be recorded over a broad wavelength range only at higher altitudes above sea level when most of the water vapor in the atmosphere remains below the observer (cf. Section 4, Chapter One), therefore the observations were transferred to California at Mount Whitney (4420 m). The recording of the solar spectrum made by Langley is shown in Fig. 7. For the level of development of astrospectroscopy of the time the tracing is exceptionally good. The main features of the line spectrum of the sun and the absorption bands of the terrestrial atmosphere can be readily seen. The principle of the apparatus Langley developed for spectral investigation of solar radiation remained nearly unchanged in subsequent observations at the Smithsonian Institution embracing several decades. The first systematic long-term observations, with a carefully thought-out

/171

method, of the distribution of energy in the solar spectrum, as well as systematic determinations of the solar constant were begun in the Smithsonian Institution by Langley and his student C. Abbot at the beginning of the 1900's, and were then extended and developed by Abbot and his coworkers L. Aldrich, W. Hoover, F. Fowle, and so on. Spectral observations covered the periods 1902-1910, 1916-1919, and 1920-1922 /132/.

The method of observation and interpretation of results used by the Smithsonian Institution is described in detail in Section 3, Chapter One. Let us note several features involving spectral observations. A spectrobolometer with replaceable prisms for different spectral regions (quartz, glass, and rock salt) permitted the solar spectrum to be recorded in the region from 0.295 to 2.5 microns. The spectrobolometer slit was illuminated directly or else with coelostat mirrors (silvered or metallic -- stellite) or were sighted directly on the sun in a device mounted on the equatorial; the solar image was not formed; the spectrum of the entire solar disk was recorded.

Investigation of selective light losses was made by a complicated and laborious method employing an auxiliary system consisting of a spectral apparatus and mirrors exactly the same as the working ones. Extinction in the earth's atmosphere was determined by the Bouguer method. As a result of the reductions, Abbot obtained the distribution of energy in the spectrum of the entire sun in relative units. The resolving power of the spectrobolometer was so low that only the most intense Fraunhofer lines and bands of water vapor could be reliably distinguished. Abbot recorded a smoothed spectrobologram between the maxima and minima of the Fraunhofer lines, excluding the H and K lines and the lines with Rowland intensity greater than 20. Thus, his distribution was closer to the integrated solar spectrum than to the integral solar spectrum, together with all the absorption lines. But corrections allowing for the effect of absorption lines had to be introduced to bring Abbot's data to any form of distribution. Based on Abbot's data, Minnaert /349/ found the distribution of energy in the integrated spectrum of the entire solar disk in absolute units, by integrating Abbot's relative distribution by wavelength and equating the resulting integral to the corresponding fraction of the solar constant found by Abbot (here the distance of the earth from the sun was taken into account and corrections were made for absorption lines that allow for the method of plotting the smoothed curve used by the Smithsonian Institution). Minnaert used observations of the limb darkening of the solar disk also made by Abbot and his coworkers /132/ to construct the distribution of energy in the continuous spectrum of the solar center. Corrections for absorption in the lines in this case were found by Mulders /329/. The solar constant used by Minnaert in absolutizing Abbot's data, close to 1.94 cal/cm^2 · sec, differs

/17

by less than 1 percent from the modern value, determined at high altitudes.

Results obtained by Abbot and his coworkers played a major role in the advancement of solar astrophysics; they served as the basis for theoretical investigations and as a standard, for example, in studying the spectrum of active formations over more than half a century. These results were taken as the foundation of the mean data on the distribution of energy in the solar spectrum obtained by Mulders /329/, P. Moon /350/, and by more recent workers -- M. Nicolet /118/, F. Johnson /119/, M. P. Thekaekara /351/, and by the authors of this book /120/. /173

Only few years ago, up to 1968, more or less reliable mean data on the distribution of energy in the solar spectrum could not be derived if the results of Abbot and his coworkers were not used. But now, with a long series of more exact and detailed modern studies available (cf. Sections 2-4), in deriving the mean we are able to avoid having to use Abbot's results, obtained with a very low spectral resolution of the order of 100 angstroms/mm and requiring the introduction of substantial reductions, which were not determined rigorously enough.

However, this does nct at all mean that the unique homogeneous material obtained by the Smithsonian Institution covering observations of several decades was utilized in full. The data of Abbot and his coworkers continue to be actively employed in several interesting investigations of a statistical nature, for example, in a series of studies by A. Angstrom /127, 352/.

2) Investigations of the distribution of energy in the solar spectrum bearing only historical interest at the present time. The studies by J. Wilsing /353/ are remarkable in that he was the first to use, in investigating the distribution of energy in the solar spectrum, the method of comparing its spectrum with the spectrum of a standard radiation source -- the absolute blackbody. This method, developed by Wilsing jointly with I. Sheiner for stars /354/ obviates performing cumbersome (and therefore quite unreliable) reductions which necessitate constructing a duplicate of the entire optical system used, as in Abbot's method (for more detail on the two spectrophotometric methods, cf. Section 1, Chapter Three). Wilsing performed observations at the Potsdam Observatory in 1913, 1914, and 1917; the aim was the investigation of the continuous spectrum of the entire solar disk over a wide spectral region from 4000 to 23,000 angstroms; the interval to 6600 angstroms was studied photographically; the region of long wavelengths was studied with a bolometer. The comparison source for the bolometric measurements was directly a blackbody at 1560° K; a tantalum lamp calibrated based on the blackbody was /174 used for the photographic work. The distribution of energy was obtained in relative units; observations at all chosen wavelengths

were coupled to observations at points with λ 6600 and λ 10,260 angstroms. E. Milne /355/ reduced Wilsing's results to absolute units using the same technique as Minnaert employed for Abbot's observations; here the solar constant of 1.932 cal/cm^2 · min was used.

Besides the low resolving power of the instrument Wilsing used, the value of his work suffered appreciably by the fact that he selected a transparency coefficient determined at Potsdam by G. Muller and E. Kron, averaged for each wavelength /356/ in extrapolating observational data beyond the terrestrial atmosphere.

G. Muller and E. Kron /356/ obtained the distribution of energy in the solar spectrum as a by-product of studying the transparency coefficient of the earth's atmosphere on the island of Tenerife. Observations were made with a spectrophotometer using the Wilsing method, but visually, in the spectral region 4300-6790 angstroms with extremely low resolution, and the results required substantial additional reductions to find the true distribution of energy in the solar spectrum.

C. Fabry and H. Buisson /252/ photographically studied the sun's ultraviolet spectrum from λ 2900 to λ 4000 /angstroms/. The spectrum of the center of the solar disk was compared with the spectrum of the positive crater of a carbon arc; the energy distribution in the latter is assumed to be Planckian (T = 3750° K). Sections relatively free of absorption lines, 1-2 angstroms wide, were selected for measurement. A total of five sections were chosen: $\lambda\lambda$ 3940, 3620, 3143, 3022, and 2922 angstroms. According to the estimate of Fabry and Buisson, solar radiation at the last point is attenuated, on traversing the earth's atmosphere, by a factor of 70,000 (it is obvious in this case how unreliable the actual measurements of solar radiation intensity are). The first two points, as noted by Mulders /329/, lie in the wings of intense lines; the consequent understatement of the intensities at these points led Fabry and Buisson to an untrustworthy conclu- /17
sion on the Planckian nature of the distribution of energy in the spectral region studied, corresponding to temperature of 6000° K. Though Mulders /329/ did correct the results of Fabry and Buisson, by allowing for the influence of intense lines, the corrections are so large (up to 50 percent) that these data cannot be regarded as reliable. Also uncertain is the assumption of the Planckian distribution in the spectrum of the carbon arc crater (cf. Fig. 29). Still it must be noted at that time this study was most new and interesting -- the first research on the distribution of energy in the solar spectrum in the ultraviolet region conducted in absolute units.

Plaskett investigated in 1921 /253/, just as Fabry and Buisson, the continuous spectrum of the center of the solar disk in sections freest of distortion by absorption lines. The

observations were made photographically in the spectral region 4000-6700 angstroms using a spectrograph with low dispersion from 23 to 125 angstroms/mm; the method of comparing solar radiation with the carbon arc spectrum was used. Radiation of the arc was tied in via intermediate standards to the radiation of a laboratory absolute blackbody at 1373° K. Data on the distribution of energy were obtained in relative units; they are the results of interpreting one day of observations.

Mulders also reduced Plaskett's data to absolute units /329/, by combining Plaskett's curve in optimal fashion with Abbot's curve (1920-1922 observations). As the first step, Mulders introduced corrections for the absorption in the Fraunhofer lines that was neglected by Plaskett.

The disadvantages of the study, which were in fact noted by Plaskett himself: low resolving power of the instrument, the single day of observations, and the unreliability of standardization, make it impossible to incorporate Plaskett's data in the summary mean result.

But Plaskett's work is extremely interesting from the standpoint of the technique of photographic spectrophotometry. He developed in detail the so-called wedge method, which proved to be highly productive: nowadays virtually all photographic spectrophotometric research uses a stepped attenuator, which is a modification of the neutral Plaskett wedge. /176

E. Pettit /188/ investigated the distribution of energy in the solar spectrum for a number of years (1931, 1934, 1937, and 1939), beginning with the ultraviolet transparency cut-off of the terrestrial atmosphere at 2900, to 7000 angstroms, in 22 sections. The distribution of energy was investigated both in the continuous spectrum of the sun's center, as well as of the entire sun. A double quartz monochromator was the spectral instrument and the feeding system was of the mirror-lens type. Measurements were made by the constant dispersion technique: the spectral region with constant width of 100 angstroms was incident on a vacuum thermocouple. To make corrections for the absorption of light in the Fraunhofer lines, Pettit undertook a special study to determine these corrections and entered them into his results. Dufay /357/ noted, however, that a series of depressions in distribution was due to the absorption in the telluric lines of the terrestrial atmosphere that were not taken into account; also neglected was the effect of the wings of the H and K lines of Ca^+. Pettit obtained his data in relative units; complex deductions had to be introduced to exclude selective absorption in the instrument's optics, since Pettit did not use the method of comparison with a standard radiation source. These reductions were moreover not reliable enough, since losses of light were investigated only for some of the components of the optical system;

for the rest either literature data were adopted, or else the equivalence of one component to another was postulated. The data were absolutized by combining the resulting distribution curve with Abbot's distribution up to optimum coincidence.

The inadequate reliability of the reductions introduced by Pettit for extinction in the terrestrial atmosphere and for absorption lines, taken together with the complicated and unreliable reductions for attenuation in the optical system compels the rejection of Pettit's data in deriving the mean distribution, though his work earlier was of considerable interest, since it was the first research based on long-term observations of the center of the solar disk in the photovisual spectral region.

R. Canavaggia and D. Chalonge [311, 358] and other workers investigated the continuous spectrum of the center of the solar disk and limb darkening using the photographic method in the spectral region 3150-6000 angstroms. Observations were made at the observatory of Upper Provence in 1943-1946, during the Nazi occupation of France, therefore the technical execution of the work encountered major difficulties. A two-prism quartz spectrograph was used with a relative aperture 1/60 and with low dispersion: the entire spectrum from λ 3100 to the H_α line occupied 18.2 cm. The resolving power was quite low, of the order of 1 angstrom, because the effective aperture of the collimator objective was only 2 cm. The diameter of the solar image was 3 cm. The spectrum of the solar center was investigated by comparison with the spectrum of a standard tungsten incandescent lamp enclosed in a quartz envelope. The distribution of energy in the lamp spectrum had been determined earier, in a study of stellar spectra. "Windows" relatively free of absorption lines ("Chalonge windows") were selected as the sections of the continuous spectrum. The resulting distribution was coupled at the point 4900 angstroms to Mulders'distribution [329] to absolutize data. /17

Besides the unreliable absolutization of the results, objections are raised also to two aspects of the method of interpreting observations. First of all, the dependence of the transparency coefficient of the terrestrial atmosphere on wavelength was assumed to be Rayleighian, which can scarcely hold for the nonhigh-elevation site of the observations; secondly, equating the brightnesses of the sun and the standard lamp was done by varying the spectrograph slit width without allowing for diffraction by the slit. Both these causes can lead to systematic errors which are wavelength-dependent, which compels us to avoid using the results of Chalonge and Canavaggia for mean data.

L. Dunkelman and R. Scolnik [254] measured the intensity of radiation from the entire solar disk in high-elevation conditions

using a double quartz monochromator, in the spectral region from 3030 to 7000 angstroms. One day of observations with good atmospheric transparency was selected for interpretation. The solar spectrum was compared with the spectrum of a standard lamp. /178
However, the actual lamp calibration raised doubts, even though it was performed in two ways: 1) based on a not-at-all clearly determined "true" temperature of the lamp, found from its color temperature and assuming the emissivity of tungsten as known; 2) by comparison with the spectrum of a carbon arc, where the distribution of energy was found by D. Packer and C. Lock in absolute units. These data were later corrected by F. Johnson /255/ (the pattern of intensity with wavelength was modified). Standardization by the first method is also somewhat doubtful; one can scarcely regard the emissivity of tungsten to be some constant for all experiments. Either calibration approach could have, evidently, actually introduced errors into the distribution of energy found by Dunkelman and Scolnik, since virtually all subsequent measurements made in this spectral region showed systematic deviations with the data of the study /254/.

We have dwelt at some length on this work and especially on the technique of calibrating data because the results of Dunkelman and Scolnik represent a key link in the construction, for example, of the Johnson mean distribution of energy and the solar constant of 2.0 cal/cm^2 · min corresponding to it /119/. The study /254/ was used in standardizing the data of measurements made in the rocket ultraviolet in relative units, and tying in them to results obtained in the visible region. The overstated value of the Johnson solar constant was to a significant extent "specified" by the study of Dunkelman and Scolnik.

2. Distribution of Energy in the Photospheric Spectrum in the Region 0.3-3 Microns

All studies on the distribution of energy considered in this section were conducted by the method of comparing the sun's spectrum with the spectrum of a standard radiation source (cf. Chapter Three). It is difficult to construct systems that are entirely optically identical when comparing a blackbody (or reference standard lamp) with the sun because usually the brightnesses of the sources being compared differ by two to three orders; further, to ensure the /179
identical path of rays in the optical system we must, for example, when measuring radiation intensities, insert a collimating system for the standard source -- a mirror, and light losses at the mirror must be investigated. Below we will try to mention all cases of auxiliary studies of light losses that always detract from the precision of the end results. The attenuation of light in the terrestrial atmosphere in all studies conducted in this wavelength range was recorded with the Bouguer method,

therefore as a rule this is not specifically stated in the text and is assumed to be understood.

In describing some studies we mainly try to take note of their features with the aim of attempting to estimate their merit and disadvantages. The main characteristics of each experiment are assembled in Tables 17 and 20.

Several investigators undertook observations in the continuous spectrum of the center of the solar disk, $I_\lambda(0)$, and others -- in the integrated spectrum of the entire disk. In the latter case usually the illumination S_λ produced by the sun was measured, and from this F_λ was determined. Only in the work by Labs and Neckel /113/ was the integrated spectrum (that is, the spectrum together with the absorption lines) of the center of the solar disk measured. To bring all studies into a single system, either the system $I_\lambda(0)$ or the system F_λ, coefficients were used that allow for the limb darkening of the solar disk β_λ and the effect of absorption lines η_λ, which were derived in Chapter Four and summarized in Tables 25-27. A compilation of results in the system $I_\lambda(0)$ is given in Table 18, and in the system F_λ -- in Table 19 and partially in Figs. 44 and 45.

The first completely modern research, from the standpoint of the method used and its technical execution, can apparently be regarded as the work of R. Peyturaux /309/ and in particular, A. K. Pierce /313/. The continuous spectrum of the center of the solar disk was investigated in the red and near IR spectral regions up to 2.5 microns in relative units. The observations were made in Upper Provence and at the Mount Wilson Observatory (Pierce); the solar spectrum was compared directly with a blackbody in the case of Pierce, and via a reference standard lamp in the case of Peyturaux. Also studied were light losses in reflection from /18 mirrors in both studies, transmission of the gray filter (Peyturaux) and of the quartz window (Pierce).

Pierce compared his data with Peyturaux's data; the wavelength dependence of solar radiation intensity proved to be in good agreement [313]; both studies revealed an increase in radiation intensity in the 1.6 micron region (cf. Fig. 60), caused by a decrease in the coefficient of absorption by negative hydrogen ions; this fact was independently confirmed by the presence of lines of metals with a relatively high excitation potential of about 5 ev, while in neighboring sections only faint lines of the CO molecule are observed with a low excitation potential.

The combined results of Pierce and Peyturaux were used in numerous studies in deriving mean data on the distribution of energy, as well as in computing the solar constant; they were employed in extrapolating series of observations obtained in the visible region and in the near IR spectral region. We used this

TABLE 17. COMPILATION OF OBSERVATIONS USED IN PLOTTING MEAN DATA ON THE DISTRIBUTION OF ENERGY IN THE SPECTRUM OF THE SOLAR PHOTOSPHERE IN THE REGION 0.3-3 MICRONS

Authors, observational pd.	What was observed; spectral region and instrument	Method of absolutizing measurements	Radiation receiver	Precision in est. of authors
Peyturaux 1. /309/	Cont. spec. of disk ctr., 0.6-2.3 μ (relative data) Monochromator w/resolution 70 A for 1.5 μ	Ref. std. lamp, calibrated w/bl. body at 2000° K, T det. w/pyrom.	Photocell	Not indicated
2. Pierce/313/ 1949,9 days	Cont. spec. of disk ctr., 1-2.5 μ (rel. data) Pfund mirror spectrometer, pass band 0.30 A	Bl. body at 2700° K or carbon arc, T from pyrometer	Cooled photocell	±1.5%
3. Peyturaux /359,360/ 196 -1965 (h=1600 m)	Cont. spec. of disk ctr., 4400-8640 A. Double quartz monochromator, disp. 13 A/mm at 3000 A and 75 A/mm at 1 μ	Bl. body at 2600° K, T from pyrometer	PEM/photoelectric multiplier and photocell	±3%
4. Sitnik [109-111] a) 1952-1956	Cont. spec. of disk ctr., 3500-12,400 A. Diff. spectrometer w/passband 0.33 A for λ≤6200; 3.6-5.2A for λ>5357 A	Ref. std. lamp, calibrated w/bl. body	a) PEM w/ antimony-cesium cathode, sulfur-silver photocell	from 6-10 % in var.sp. regions

TABLE 17. /CONTINUATION/

Authors, observational pd.	What was observed; spectral region and instrument	Method of absolutizing measurements	Radiation receiver	Precision in est. of authors
4. Zitnik b) 1957-1959 (h = 3000 m)	Diff. spectrometer with passband 0.2-0.4 A		b) PEM w/ antimony-cesium & oxygen-cesium cathode	
5. Makarova /362, 112, 83/ a) 1954 11 days	Cont. spec. of disk ctr., diff. spectrograph, used resolution -- from 0.1-0.3 A	As above	Photographic plate	from 6-11% in var. sp. regions
b) 1958, 8 days (h = 3000 m)	As above			
6. Houtgast /331/, 1960 6 days (h=1600 m)	Spectrum of ctr. of solar disk, 2962-4087 A. Diff. spectrograph, 3d order, resolving power ~ 100,000	Philips ref.std. lamp	PEM	±18% at 3000 A, ±8% at 4000 A

TABLE 17. /CONCLUSION/

Authors, observ. period	What was observed; spectral region and instrument	Method of absolutizing measurements	Rad. rec'r	Precision in est. of authors
7. Labs & Neckel /364/ 1961-1964 (h=3600 m)	Integr. spec. of ctr. of solar disk, 3300 A - 1.25 μ. Diff. spectrometer, pass band 20 A	Ref. std. lamp, calibrated with bl. body of Heidelberg	PEM	±2% for λ 5000 Å
8. Stair & Ellis /117/ 1966, 3 days (h=3400 m)	Integr. spec. of entire solar disk, 3100-5300 A. Two instruments: double quartz spectrometer w/ pass band 100 A; spectroradiometer w/interference filters with 100 A half-width (λλ 3100-4000 A)	Quartz-iodine lamp, calibrated with black body	PEM	±5%

series in the same manner, by "tying it" to a preliminary mean over the section 0.9-1.25 microns, overlapping with data in the shorter-wave region. The absolutizing factor was 0.574; the Pierce-Peyturaux results are given in column three of Table 18; they agree well with the independent data of the US Solar committee and Arvesen (cf. Table 18).

Peyturaux extended his work on the continuous spectrum of the center of the solar disk into a shorter-wave region, from 4477 to 8638 angstroms /359, 360/. The observations were made in the Eastern Pyrenees, at an elevation of 1600 m, in 1960-1965. The solar spectrum was compared directly with the spectrum of a blackbody at T = 2600° K; temperature was determined with a pyrometer.

The work is marked by thoroughly executed experiments set up to refine reduction corrections that allow for the coefficient of reflection of the auxiliary collimator mirror, polarization at the mirrors of the optical system, and the passband of the monochromator. Also introduced were corrections that cancel out the effect of absorption lines in all 15 spectral sections in which measurements were taken; the largest correction was 9.4 percent /184
for the point 4477 angstroms; on the average, they lie within the limits 2-6 percent. The correction for polarization at the mirrors did not exceed 1 percent. The results of Peyturaux's measurements are given in column two of Table 18, and results reduced to the integrated spectrum of the entire solar disk are given in Table 19 and in Fig. 44.

The work of G. F. Sitnik in absolute spectrophotometry of the solar spectrum is the only research of its kind in the Soviet Union. To accomplish the research, several complex and extremely laborious experiments had to be performed in building a high-temperature blackbody model, developing a spectrophotometric system for calibrating reference standard lamps over a wide spectral range, and the like. These efforts are described in Sections 2 and 3, Chapter Three; a detailed bibliography is also presented.

Building the spectral radiation standard -- an incandescent ribbon lamp calibrated by the radiation of a blackbody -- made it possible to conduct photoelectric measurements of the distribution of energy in the continuous spectrum of the center of the solar disk in absolute units. The observations were made at the Kuchino Astrophysical Observatory in 1952-1955 in the region from 3500 to 12,400 angstroms (close to sea level) and also at the High-Elevation Expedition of the GAISh (h = 3000 m) in 1957-1959, spectral region 3284 angstroms -- 1 micron (cf. Table 17).

An indisputable merit of the research and its advantage compared with other work conducted at stations close to sea level is the fact that in parallel with the main observations, observations

were made of the intensity of the relative solar aureole during the day, which made it possible to select periods of time with optically stable atmospheric conditions (cf. Section 5, Chapter One). Also studied were problems of the effect of scattered light and polarization characteristics of the optical system used on results; it was shown that using the method of comparison with a standard source and following certain precautions, these effects introduce an error not exceeding 1 percent.

Additionally investigated were losses due to reflection by one spherical mirror inserted in making measurements of the radiation of the reference standard lamp. Differential light losses in the comparison of the sun and the lamp, which are wavelength-dependent, also arose during the equating of source intensities by means of varying the spectrometer slit widths. This effect was not directly explored in the 1952-1955 observations and somewhat distorted the initially published results /361/. Later /109/ the reduction for this effect was considered, but was not described, and from a comparison of /361/ and /109/ the method of introducing the correction is unclear. In the 1957-1959 observations the reductions were determined experimentally. /185

G. F. Sitnik reduced the results of his two observational series to one /111/, by correcting the results first for the effect of absorption lines lying in the passband of the spectrometer; these data are given in Table 18, and the data we reduced to F_λ are given in Table 19. Noteworthy is the fact that the maximum of radiation in the continuous spectrum $I_\lambda(0)$ lies at λ 4600 angstroms, while for all observers the maximum lies quite strictly in the interval 4150-4300 angstroms, but according to photospheric models it must enter an even shorter-wave region. Therefore we judged that this shift in the maximum was due to the above-mentioned reduction effect in the region of overlapping observations with two radiation receivers that had different slit widths /361/, and we made use of the results in /111/ in the region 4350-4950 angstroms with a reduction factor derived by comparing G. F. Sitnik's data with the results of all other studies outside the spectral region.

Ye. A. Makarova, working in the group led by G. F. Sitnik, also studied the continuous spectrum of the center of the solar disk, following mainly the same method, but using the photographic approach. The observations were made in 1954 at the Kuchino Observatory ($\lambda\lambda$ 3700-8000 angstroms) /362, 112/ and in the High-Elevation Expedition of the GAISh in 1958 ($\lambda\lambda$ 3100-6600 angstroms) /83/. In order to select spectral regions that were as free as possible of absorption lines, the spectrograms were photographed with narrow spectrograph slits, of the order of the normal width. Reductions of measurements were mainly analogous for the series of G. F. Sitnik and Ye. A. Makarova [28]. Differential losses due /186

/Footnote 28 on following page/

to diffraction by a slit of different widths for the sun and the reference standard lamp were computed based on experimental data. Evidently, owing to the discrepancy in these reductions, the data of G. F. Sitnik and Ye. A. Makarova, gathered with the same instrument and with the same comparison source, do not agree very well. The maximum of the curve in the work of Ye. A. Makarova falls at λ 4300 angstroms, but the actual course of the distribution as a function of wavelength differs somewhat from the results of G. F. Sitnik.

Table 18 gives the mean of two series of observations /112, 83/. Here results with $\lambda <$ 3675 angstroms are admitted as unreliable owing to overly large and unreliable reduction corrections both when the sun was compared with the lamp, as well as in the actual reference standardization of the lamp based ultimately on the melting point of gold; the intensity of blackbody emission at the melting point of gold is low.

The observations of Houtgast /331/ embrace a relatively small spectral region from 2962 to 4087 angstroms; still, they were very useful for data on the distribution of energy in the spectrum of the photosphere, since generally there are few observations in the section and before Houtgast there were practically no reliable results in its short-wave end. This spectral region, moreover, serves as a connecting link between observations in the visible and rocket spectra.

Houtgast set out to take measurements of intensities in the spectrum of the solar disk center at many points (about 200) of the atlases of Minnaert /189/ and Bruckner /190/ in order then to more precisely measure the equivalent widths of spectral lines. /18
The observations were taken at Mount Wilson observatory; the high resolving power of the Snow telescope-spectrograph, about 10^5, permitted discriminating narrow sections relatively free of absorption lines. The envelope drawn along the intensity peaks

---

[28] Perhaps we must recall the condition of the aperture angles. D. Labs and H. Neckel /113/ raised doubts about the coordination of the aperture angles of the telescope and spectrograph used in the studies of G. F. Sitnik and Ye. A. Makarova. Of course, this condition was satisfied and specifically stipulated in all the above-mentioned investigations. But even the assumption that there is a possibility of formulating a problem in absolute spectrophotometry by the method of comparison without coordinating solid angles, which is the primary and fundamental necessary condition for solving this problem appears to be very strange. It is the equivalent, for example, to the assumption that the physicists decided to solve some problem and neglected the law of conservation of energy in the process.

corresponds to the continuous spectrum or, more exactly, to the quasicontinuum in this spectral region. Absolute intensity values of the continuous spectrum of the disk center were obtained by comparing the spectra of the sun and a Phillips reference standard ribbon lamp, calibrated in the Phillips laboratory, and are presented in the works /327, 363/ (cf. Table 18).

Based on the observational materials /331/, Houtgast together with Namba /327/ determined the fraction of radiation absorbed in the lines of the solar spectrum in the narrow spectral regions as well as on the average, computed for a 100-angstrom interval; we used these correction coefficients in Chapter Four.

In an article published in 1970 /363/, Houtgast scrupulously analyzed his own work on the determination of absolute intensities from the standpoint of possible errors and estimated them, from our point of view, quite realistically. Table 3 of this work presents estimates of 12 error sources (as the function of wavelength); we present the estimates of five errors, of largest value, as well as the overall estimate in Fig. 46 at the end of this section, where we take up the question of the precision of individual series of observations and mean data.

The results of long-term observations by D. Labs and H. Neckel /364, 113, 345/ appear to be some of the most reliable as far as observational data are concerned, but not where the authors used the doubtful approximation of observations by a "model" continuum which leads them to several, in our view, erroneous conclusions recorded in tabular form (cf. below).

Labs and Neckel made observations in high-elevation conditions (3.6 km) at the Jungfraujoch Station; this permitted selecting days with good and stable atmospheric transparency. The spectrometer was mounted on the equatorial unit of a Cassegrain telescope and thus the necessity of allowing for time-variable /193
polarization effects at the coelostat mirrors was avoided. The spectrometer slits were selected so that from the spectrum of the solar disk center each time a rectangular passband 20.0 angstroms wide for $\lambda > 4000$ angstroms, and 20.5 angstroms wide for $\lambda < 4000$ angstroms was cut out. Scattered light in the instrument was reduced to a negligibly small value. The reference standard ribbon lamp was calibrated relative to the blackbody of the Heidelberg laboratory. In addition, the lamp was compared with reference standards of other national laboratories (United States, Great Britain, and Canada); the results agree within the limits 3 percent /113/, however the procedure was not described, and moreover, for example, lamps at the US National Bureau of Standards are calibrated based on flux (specified distance of radiation source), while the authors' lamps are calibrated based on brightness, and the method of comparison is not obvious.

TABLE 18.* INTENSITY OF RADIATION FROM THE CENTER OF THE SOLAR DISK IN THE CONTINUOUS SPECTRUM BASED ON MODERN STUDIES IN THE REGION 0.3-3.0 MICRONS

Author / λ, μ	$I_\lambda(0)$ in 10^{13} erg/cm^2·sec·sterad·cm									
	Peytu-raux [360]	Pierce-Peytu-raux [309,313]	Sitnik [111]	Maka-rova [83,112]	Labs & Neckel [345]	Hout-gast [363]	Stair &Ellis [117]	US Solar Comm. [142]	Arve-sen [373]	Heath [375]
Weight	2	2	2	2	2	2	1	2	1	1
0,295	—	—	—	—	—	17,7	—	—	—	25,3
0,300	—	—	—	—	—	22,1	25,2	24,0	26,3	27,0
0,305	—	—	—	—	—	24,4	27,8	28,2	27,8	29,3
0,310	—	—	—	—	—	26,1	31,5	31,8	30,7	31,5
0,315	—	—	—	—	—	27,1	32,5	34,5	33,0	35,0
0,320	—	—	—	—	—	27,9	32,5	36,3	34,0	36,0
0,325	—	—	—	—	—	28,5	31,3	36,7	34,5	35,0
0,330	—	—	25,4	—	—	29,5	31,2	36,8	34,8	33,0
0,335	—	—	25,5	—	30,0	30,1	31,3	36,7	34,7	32,0
0,340	—	—	25,6	—	30,3	30,2	31,6	36,5	34,7	32,0
0,345	—	—	26,0	—	30,4	30,3	32,1	36,3	34,3	—
0,350	—	—	26,4	—	31,0	30,7	32,8	36,3	34,1	—
0,355	—	—	26,7	—	32,3	31,4	34,0	36,5	34,3	—
0,360	—	—	27,2	—	33,3	32,3	36,0	37,2	34,9	—
0,3625	—	—	27,5	—	33,7	32,8	36,0	37,2	35,3	—
0,3675	—	—	28,1	28,0	35,0	33,4	37,5	39,0	37,4	—
0,370	—	—	28,4	31,4	36,2	33,6	38,2	40,3	39,0	—

* TRANSLATOR'S NOTE: COMMAS REPRESENT DECIMAL POINTS

TABLE 18. /CONTINUATION/

Author / λ, μ	I_λ (0) in 10^{13} erg/cm^2·sec·sterad·cm									
	Peytu-raux /360/	Pierce Peytu-raux /309,313/	Sitnik /111/	Maka-rova /83,112/	Labs& Neckel /345/	Hout-gast /363/	Stair& Ellis /117/	US Solar Comm. /142/	Arve-sen /373/	Heath /375/
Weight	2	2	2	2	2	2	1	2	1	1
0,375	—	—	31,8	33,1	37,6	33,8	40,6	41,5	42,0	—
0,380	—	—	36,5	34,8	39,0	39,0	42,4	43,3	43,7	—
0,385	—	—	40,0	37,0	40,6	39,2	44,2	44,5	45,0	—
0,390	—	—	42,6	38,6	42,2	39,4	45,7	45,8	46,6	—
0,395	—	—	45,0	41,6	44,0	40,0	47,3	46,8	48,8	—
0,400	—	—	47,1	43,2	45,2	43,7	48,5	47,8	49,6	—
0,405	—	—	48,1	44,3	46,3	43,8	49,2	48,5	50,5	—
0,410	—	—	49,1	45,8	46,9	—	49,6	48,9	51,4	—
0,415	—	—	49,9	47,5	47,7		49,9	49,0	52,0	—
0,420	—	—	50,7	49,2	48,3		49,8	49,0	52,0	—
0,425	—	—	51,3	50,0	48,6	—	49,0	49,0	51,8	—
0,430	—	—	51,8	50,8	48,8	—	47,5	48,7	50,7	—
0,435	—	—	(52,3)	50,2	48,4	—	46,3	48,0	50,0	—
0,440	—	—	(52,8)	49,9	47,3	—	45,3	47,3	49,7	—
0,445	—	—	(53,1)	49,1	46,3	—	44,5	46,7	49,0	—
0,450	52,8	—	(53,2)	48,3	45,5	—	43,5	46,3	48,0	—
0,455	50,3	—	(53,4)	47,1	44,8	—	42,8	45,8	47,4	—
0,460	49,5	—	(53,4)	46,4	43,9	—	42,0	45,1	46,7	—
0,465	50,0	—	(52,7)	46,4	43,2	—	41,5	44,5	46,0	—
0,470	50,6	—	(51,9)	46,5	42,5	—	41,1	44,0	45,3	—

TABLE 18. /CONTINUATION/

Author / λ, μ	I_λ (0) in 10^{13} erg/cm^2·sec·sterad·cm									
	Peytu-raux /360/	Pierce Peytu-raux /309,313/	Sitnik /111/	Maka-rova /83,112/	Labs& Neckel /345/	Hout-gast /363/	Stair &Ellis /117/	US Solar Comm. /142/	Arve-sen /373/	Heath /375/
Weight	2	2	2	2	2	2	1	2	1	1
0,475	50,3	—	(51,1)	46,9	42,0	—	40,8	43,8	45,1	—
0,480	47,4	—	(50,5)	47,0	41,5	—	40,6	43,4	44,8	—
0,485	45,9	—	(49,7)	47,1	41,5	—	40,4	43,0	43,8	—
0,490	45,3	—	(49,1)	47,2	41,5	—	40,3	42,5	43,4	—
0,495	45,3	—	(48,5)	47,2	41,5	—	40,3	41,8	42,7	—
0,500	45,5	—	47,9	47,4	41,2	—	40,3	41,0	42,3	—
0,510	45,1	—	46,4	46,8	40,2	—	40,4	40,0	41,5	—
0,520	41,9	—	44,9	46,3	39,1	—	40,5	39,3	40,7	—
0,530	39,0	—	43,4	45,2	38,2	—	40,5	38,0	39,5	—
0,540	38,4	—	42,3	43,6	37,3	—	—	35,5	38,2	—
0,550	38,8	—	41,1	41,1	36,5	—	—	33,8	36,9	—
0,560	36,5	—	40,0	38,9	35,0	—	—	33,2	36,0	—
0,570	35,6	—	38,9	36,7	35,1	—	—	32,8	35,7	—
0,580	35,2	—	37,7	34,9	34,1	—	—	32,1	35,5	—
0,590	35,1	—	36,6	34,3	33,4	—	—	31,9	34,6	—
0,600	35,0	—	35,7	33,5	32,6	—	—	30,9	33,5	—
0,610	34,8	—	34,65	32,4	32,0	—	—	30,3	33,4	—
0,620	34,3	—	33,9	31,9	31,1	—	—	29,7	32,1	—
0,630	33,6	—	33,1	30,9	30,3	—	—	28,9	31,6	—
0,640	32,9	—	32,5	30,4	29,4	—	—	28,2	30,8	—

TABLE 18. /CONTINUATION/

Author / λ, μ	I_λ (0) in 10^{13} erg/cm^2·sec·sterad·cm									
	Peytu-raux /360/	Pierce Peytu-raux /309,313/	Sitnik /111/	Maka-rova /83,112/	Labs& Neckel /345/	Hout-gast /363/	Stair &Ellis /117/	US Solar Comm. /142/	Arve-sen /373/	Heath /375/
Weight	2	2	2	2	2	2	1	2	1	1
0,650	32,3	—	31,7	29,4	28,3	—	—	27,4	29,5	—
0,660	31,5	—	31,2	29,0	28,3	—	—	27,5	29,0	—
0,670	30,8	—	30,5	28,4	27,5	—	—	26,0	28,5	—
0,680	30,2	—	29,8	28,1	26,7	—	—	25,4	28,2	—
0,690	29,6	—	29,1	29,4	26,2	—	—	24,9	26,8	—
0,700	28,9	—	28,5	30,1	25,6	—	—	24,4	26,9	—
0,720	27,8	—	27,2	28,4	24,3	—	—	23,3	24,9	—
0,740	26,6	—	25,5	25,4	23,1	—	—	22,3	23,7	—
0,760	25,4	—	24,6	22,7	21,8	—	—	21,0	22,6	—
0,780	24,2	—	23,3	21,1	20,7	—	—	19,9	21,1	—
0,800	22,9	—	22,2	20,3	19,9	—	—	19,1	20,3	—
0,850	19,8	—	19,2	—	17,5	—	—	17,1	16,9	—
0,900	—	16,2	16,8	—	15,5	—	—	15,7	15,8	—
0,950	—	14,4	14,8	—	13,2	—	—	14,2	13,7	—
1,00	—	12,6	13,2	—	11,8	—	—	12,7	12,7	—
1,05	—	11,3	11,7	—	11,2	—	—	11,4	11,7	—
1,10	—	10,0	10,5	—	10,1	—	—	10,1	10,3	—
1,15	—	9,04	9,29	—	8,96	—	—	8,94	9,23	—
1,20	—	8,07	8,17	—	8,23	—	—	8,07	8,33	—
1,25	—	7,32	7,37	—	7,31	—	—	7,12	7,44	—
1,30	—	6,58	—	—	—	—	—	6,52	6,96	—

TABLE 18. /CONCLUSION/

Author / λ, μ	I_λ (0) in 10^{13} erg/cm^2·sec·sterad·cm									
	Peytu-raux /360/	Pierce-Peytu-raux /309,313/	Sitnik /111/	Maka-rova /83,112/	Labs & Neckel /345/	Hout-gast /363/	Stair &Ellis /117/	US Solar Comm. /142/	Arve-sen /373/	Heath /375/
Weight	2	2	2	2	2	2	1	2	1	1
1,35	—	5,99	—	—	—	—	—	5,91	6,20	—
1,40	—	5,40	—	—	—	—	—	5,43	5,69	—
1,45	—	4,98	—	—	—	—	—	5,05	5,21	—
1,50	—	4,56	—	—	—	—	—	4,64	4,83	—
1,55	—	4,23	—	—	—	—	—	4,35	4,44	—
1,60	—	3,90	—	—	—	—	—	3,98	4,16	—
1,65	—	3,57	—	—	—	—	—	3,58	3,78	—
1,70	—	3,24	—	—	—	—	—	3,25	3,49	—
1,80	—	2,61	—	—	—	—	—	2,53	2,73	—
1,90	—	2,13	—	—	—	—	—	2,00	2,23	—
2,0	—	1,77	—	—	—	—	—	1,62	1,89	—
2,1	—	1,48	—	—	—	—	—	1,55	1,50	—
2,2	—	1,24	—	—	—	—	—	1,25	1,22	—
2,3	—	1,05	—	—	—	—	—	1,07	1,02	—
2,4	—	0,895	—	—	—	—	—	1,004	0,910	—
2,5	—	0,763	—	—	—	—	—	0,844	0,839	—
2,6	—	0,660	—	—	—	—	—	0,748	—	—
2,7	—	—	—	—	—	—	—	0,668	—	—
2,8	—	—	—	—	—	—	—	0,606	—	—
2,9	—	—	—	—	—	—	—	0,557	—	—
3,0	—	—	—	—	—	—	—	0,479	—	—

To relate the intensity of solar radiation with that of lamp radiation, transmission of neutral filters attenuating solar radiation, and the reflectivity of the collimator mirror had to be additionally allowed for (in addition to extinction in the terrestrial atmosphere).

The results of measurements [29] are summed up in the form of 196 values /113, 345/, each of which, in the region 3288-6550 angstroms, represents the integral (together with absorption lines) intensity of emission from the solar disk center in the 20-angstrom band; these values continuously cover the entire region studied. For λ > 6550 angstroms to 12,460 angstroms, the measurements were taken in individual sections and here they must determine the intensity of radiation of the continuous solar spectrum $I_\lambda(0)$, since there are few absorption lines. All the quantities are reduced to the IPTS-68 system /345/.

In the region 3288-6550 angstroms, in order to reduce Labs-Neckel data obtained for the disk center to the integrated spectrum of the entire solar disk F_λ, corrections had to be introduced that allow for the limb darkening of the solar disk and the variation of equivalent widths of absorption lines of the disk. These procedures were carried out by Labs and Neckel /113/; conversion factors differed only slightly from those used in this book; Table 19 presents directly the F_λ values from /345/. /194

To convert to the continuous spectrum of the center of the solar disk, $I_\lambda(0)$, Labs and Neckel introduced corrections η_λ that allow for absorption in lines, but it is precisely these corrections that were, in our view, found in principle unreliably. We believe it necessary to dwell on this problem in more detail, since the data of Labs and Neckel have gained quite extensive acceptance; for example, recently H. Wohl, A. Wittmann, and E. Schroter /366/ used incorrect $I_\lambda(0)$ data for the photosphere, taken from Labs and Neckel, as the standard for determining the intensity of the continuous spectrum of a spot.

Labs and Neckel, in comparing their observations with the distribution of energy yielded by the modern photospheric models

---

29 In 1957 Labs /365/ published the results of a study of the distribution of energy in the continuous solar spectrum in the region 3300-6600 angstroms which he made at Pic du Midi. The intensities he obtained were found much higher than subsequent results of Labs and Neckel /364/; they were then somewhat reduced by allowing for the variation in the intensity of the standard -- a carbon arc, however they remain 5-10 percent above the data in /364/; no satisfactory explanation was found, and Labs and Neckel did not take these data into consideration.

of H. Holweger [340] and Bilderberg [367], found that observations and models agree if the latter are "normalized" to the authors' data at the point 5000 angstroms (later the authors preferred normalizing over the region from 6000 angstroms to 1.25 microns [345], but this does not essentially change the situation).

Since for $\lambda < 5500$ angstroms, it is still more difficult to fix the continuous spectral level owing to clustering of absorption lines, Labs and Neckel believed that one must use not observations but the model. It must be observed, however, that the "normalized" models begin to diverge for $\lambda \leq 5000$ angstroms, and the deviation reaches $\sim$ 10 percent for λ 3700 angstroms. The authors, not specifically emphasizing this, selected the model in [340] for the interval $4200 < \lambda < 5000$ angstroms, and in the shorter-wave region, based on the data in Fig. 2 and Table 6 in [113], adopted some mean between the models.

By identifying the continuous solar spectrum with the "normalized" model, Labs and Neckel drew the following conclusions: 1) the continuous solar spectrum extends smoothly everywhere, not deviating anywhere from the theoretically calculated course; [19] it has no "waves" not predicted by theory; 2) corrections for absorption lines η_λ in the spectral region from $\lambda < 5500$ angstroms must be determined simply as the difference between the level of the "normalized" model (Table 6 in [113]) and the data of Labs and Neckel on the emission level of the integrated solar spectrum (Table 4 in [113], corrected for c_2 in [345]). Let us examine whether these two conclusions are valid, by using the actual authors' data to do this.

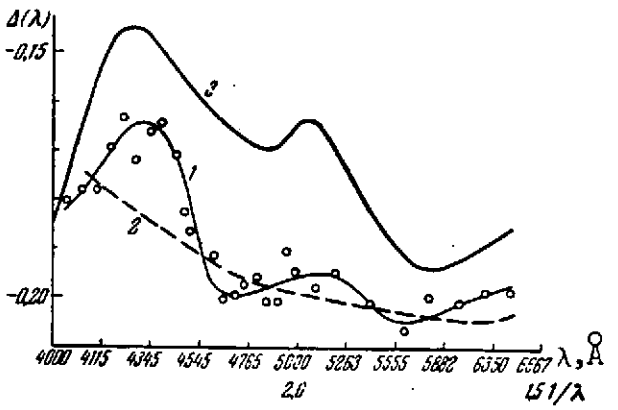

Fig. 43. Waves in continuous spectrum of the solar disk center. $\Delta = \lg [I_\lambda(0)/B(7000^\circ\ K)]$ as a function of λ:
1 -- based on the data of Labs and Neckel
2 -- based on the model
3 -- based on average data of nine independent series of observations

To determine the level of the continuous spectrum from the observational results of Labs and Neckel, we took their data on the integral solar spectrum for 20-angstrom intervals in the region $\lambda < 6400$ angstroms, summed over 100-angstrom intervals, and introduce corrections for absorption lines by using Wempe's results [332] instead of corrections obtained by the authors, as the difference between the "normalized" model and data on the integral

spectrum. (Labs and Neckel also used Wempe's data for longer wavelength). Fig. 43 shows the corresponding two functions of emission intensity of the continuous spectrum of the solar center in the region 4000-6400 angstroms based on the same starting data, /196 but for the cases when 1) the corrections for the absorption lines were introduced after Wempe, and 2) the "model" continuous spectrum was utilized (Table 6 in /113/). The radiation intensity of the continuous solar spectrum relative to blackbody radiation at 7000° K was plotted along the Y axis; the course of distribution appears more distinct in this form, used earlier by Labs and Neckel /364/. The picture clearly demonstrates the unsoundness of determining the corrections η_λ based on the model. Actually, the continuous spectrum determined with the aid of Wempe corrections proved to be higher than the spectrum of the "normalized" model [29]; still, by definition it could only be below the true continuous spectrum, since Wempe's corrections are determined (cf. Chapter Four) based on a construction of the envelope of the solar spectrum drawn along the intensity peaks, but these peaks can only be lowered by unresolved absorption lines or wings of intense lines. But adapting as the continuous spectrum the "normalized" model, we reach a nonsensical conclusion: from the observed energy distribution in the quasi-continuous solar spectrum plotted based on intensity peaks we must further subtract some quantity in order to arrive at the "true" (model) continuous spectrum. It is understandable why Labs and Neckel selected the Holweger model /340/ for the region of energy maximum and not the Bilderberg /367/ model. The "normalized" Bilderberg model lies below for $\lambda < 5000$ /angstroms/; for this model the nonsensicality would extend to the absurd: even the integral solar spectrum, even sections with intense absorption lines would have to be reduced still further in order to reach the level of the "theoretical" continuous spectrum.

For $\lambda < 4000$ angstroms, the "theoretical" continuous spectrum lies, conversely, above the observed spectrum drawn based on intensity peaks: the deviation is $\sim$ 25 percent for $\lambda\lambda$ 3650-3700. And here the attempt to use the theory leads to strange results: for example, even if for maximum majorizing conditions (in the favor of Labs and Neckel) the equivalent width is determined for any of /197 the high terms of the Balmer series; in particular, H_{2-15}, then it will prove to be equal at least to 6 angstroms, that is, for then 1.5 times greater than the equivalent width of the H_α lines -- the most intense line of this series; this could scarcely be plausible.

Fig. 43 plotted from Labs' and Neckel's own data shows waves in the continuous spectrum. In order to judge how realistic they are, we plotted on the same figure a curve (3) that represents the mean data we constructed (cf. below) for $I_\lambda(0)$ from

[29] In Fig. 43 a model is normalized along λ 5000 angstroms; normalization over the region 6500 angstroms -- 1.25 microns /345/ does not alter the situation: curve 2 is raised only slightly.

Table 29. The agreement of the course of the distributions (1) and (3) exceeded our expectation; it is difficult to assume that a fourfold agreement of the positions of the maxima and minima is fortuitous.

The attempt of Labs and Neckel to replace observations with the model is clearly unsuccessful: for $\lambda < 6000$ angstroms models do not adequately represent observations and the shorter the wavelength, the greater the deviation (cf. also Section 3 of this chapter). There are "waves" in the energy distribution in the continuous solar spectrum that are not predicted by models of the solar photosphere. The observations cannot be "fitted" to the model; this leads to nonsensical results; rather, the models must be corrected according to observations. The discussion must end with these elementary truths no matter how much, obviously, there is that is excellent in the experimental techniques of the work by Labs and Neckel. Nonetheless, the data of these authors in the region $\lambda < 5000$ angstroms for $I_\lambda(0)$ (Table 6 in /113/) and η_λ presented in /113/ and corrected in /345/ cannot be used; they are in error. The fact that data published only two years ago and characterized by the authors themselves as "uniquely correct" and "data which in the near future cannot be improved on" (pages 21 and 54 in /113/) have to be corrected by adjusting to new considerations with respect to the model (there are no new observations) speaks for itself [31].

To determine the solar constant, Labs and Neckel supplemented /19 their observational results in the region 3288 angstroms -- 1.25 microns with data from other authors. They "coupled" the results obtained in relative units by Tousey and Detwiler's data on the ultraviolet, by reducing these authors' results by 10 percent, and Pierce's data /313/ -- in the region 1.25-1.5 microns. Further, they used the results of absolute measurements in the IR region by Saiedy and Goody, Murcray and Farmer and Todd (cf. Section 4). The normalized Bilderberg model was adopted for the region 10-100 microns. The solar constant in the system was 1.947 cal/cm^2 · min or 135.8 mw/cm^2.

The study of R. Stair and H. Ellis /117/ was performed, as to technique, very much like the work of Labs and Neckel. The observations were made in high-elevation conditions (h = 3.4 km) in the Hawaiian Islands, in good atmospheric conditions. Spectral instruments were also mounted on the equatorials. But it was not the spectrum of the solar center that was measured, but of the entire disk in the region 3100-5300 angstroms.

---

[31] We stress that here we refer to corrections caused in principle by the undetermined "normalization site" of the model; corrections that allow for variation in c_2 according to IPTS-68, introduced in /345/, are naturally valid and necessary.

TABLE 19* DISK-AVERAGED INTENSITY OF SOLAR RADIATION IN THE INTEGRATED SPECTRUM BASED ON MODERN STUDIES IN THE REGION 0.3-3.0 MICRONS

Author / λ, μ	F_λ (0) in 10^{13} erg/cm^2·sec·sterad·cm									
	Peytu-raux [360]	Pierce Peytu-raux [309,313]	Sitnik [111]	Maka-rova [83,112]	Labs & Neckel [345]	Hout-gast [363]	Stair &Ellis [117]	US Solar Comm. [142]	Arve-sen [373]	Heath [375]
Weight	1	1	1	1	2	1	2	4	1	1
0,295	—	—	—	—	—	7,46	—	—	—	8,78
0,300	—	—	—	—	—	6,92	7,94	7,56	8,30	8,28
0,305	—	—	—	—	—	7,69	8,68	8,87	8,75	8,68
0,310	—	—	—	—	—	8,33	9,85	10,13	9,79	10,04
0,315	—	—	—	—	—	8,64	10,59	11,24	10,82	11,21
0,320	—	—	—	—	—	9,07	11,0	12,2	11,1	12,4
0,325	—	—	—	—	—	11,20	12,2	14,3	13,2	13,1
0,330	—	—	11,3	—	—	13,1	13,7	15,6	15,4	13,6
0,335	—	—	10,9	—	13,2	12,9	13,4	15,9	15,1	14,0
0,340	—	—	11,0	—	13,2	13,0	13,5	15,8	14,8	14,2
0,345	—	—	11,5	—	13,1	13,4	14,1	15,7	15,0	—
0,350	—	—	12,0	—	13,5	13,9	14,9	16,1	15,4	—
0,355	—	—	11,6	—	14,0	13,7	15,4	15,9	15,1	—
0,360	—	—	11,3	—	14,6	13,5	15,3	15,7	14,5	—
0,3625	—	—	12,1	—	15,0	14,4	15,6	16,2	15,7	—
0,3675	—	—	12,9	12,8	15,4	15,3	16,4	17,0	17,1	—
0,370	—	—	11,8	13,4	15,3	14,3	16,0	17,4	17,1	—
0,375	—	—	12,3	12,8	15,3	13,1	16,6	17,0	16,8	—

* TRANSLATOR'S NOTE: COMMAS REPRESENT DECIMAL POINTS

TABLE 19. /CONTINUATION/

Author / λ, μ	F_λ (0) in 10^{13} erg/cm^2·sec·sterad·cm									
	Peytu-raux /360/	Pierce-Peytu-raux /309,313/	Sitnik /111/	Maka-rova /83,112/	Labs& Neckel /345/	Hout-gast /363/	Stair &Ellis /117/	US Solar Comm. /142/	Arve-sen /373/	Heath /375/
Weight	1	1	1	1	2	1	2	4	1	1
0,380	—	—	14,0	13,3	14,6	14,9	16,9	16,5	16,5	—
0,385	—	—	14,2	13,2	13,9	14,0	15,7	16,1	15,6	—
0,390	—	—	14,2	12,9	15,3	13,1	15,9	16,1	16,3	—
0,395	—	—	16,5	15,2	16,7	14,6	16,0	17,5	17,9	—
0,400	—	—	21,9	20,0	20,2	20,3	22,1	21,0	22,8	—
0,405	—	—	25,2	23,2	24,0	23,0	26,5	24,2	26,2	—
0,410	—	—	26,0	24,2	24,5	—	26,2	25,8	27,1	—
0,415	—	—	26,7	25,5	25,0	—	26,2	26,1	27,9	—
0,420	—	—	26,9	26,1	24,7	—	26,0	25,7	27,4	—
0,425	—	—	26,0	25,4	24,4	—	25,1	24,9	26,1	—
0,430	—	—	25,6	25,1	24,5	—	23,1	24,1	24,8	—
0,435	—	—	(27,3)	26,1	24,6	—	24,0	24,5	25,9	—
0,440	—	—	(30,1)	28,5	26,3	—	25,6	26,6	28,5	—
0,445	—	—	(32,0)	29,6	28,4	—	27,4	28,3	29,8	—
0,450	33,7	—	(33,8)	30,8	28,9	—	28,2	29,5	30,5	—
0,455	33,0	—	(35,1)	30,9	29,5	—	28,1	30,3	31,1	—
0,460	33,2	—	(35,8)	31,1	29,4	—	27,9	30,4	31,3	—
0,465	34,1	—	(35,8)	31,6	29,2	—	27,9	30,1	30,8	—
0,470	34,4	—	(35,2)	31,6	29,2	—	27,9	29,9	30,7	—
0,475	34,6	—	(35,2)	32,3	29,3	—	28,5	30,1	31,3	—
0,480	32,9	—	(35,0)	32,6	28,5	—	28,7	30,5	31,1	—
0,485	31,2	—	(33,8)	32,0	27,8	—	27,1	29,1	29,4	—
0,490	30,2	—	(32,7)	31,5	28,5	—	26,9	28,7	29,1	—
0,495	31,2	—	(33,5)	32,5	28,8	—	27,9	28,8	29,7	—
0,500	31,4	—	33,1	32,7	28,4	—	27,9	28,6	29,1	—
0,510	31,8	—	32,7	33,0	27,5	—	28,2	27,7	29,2	—
0,520	28,4	—	30,4	31,4	27,1	—	28,1	27,0	27,4	—
0,530	27,8	—	30,9	32,2	27,7	—	28,7	27,1	28,5	—
0,540	28,1	—	31,0	32,0	27,7	—	—	26,2	28,0	—
0,550	29,2	—	30,9	30,9	27,1	—	—	25,4	27,9	—
0,560	27,6	—	30,3	29,4	26,9	—	—	24,9	27,1	—
0,570	27,3	—	29,8	28,1	26,9	—	—	25,2	27,4	—
0,580	27,7	—	29,6	27,4	26,8	—	—	25,2	27,9	—
0,590	27,5	—	28,7	26,9	26,2	—	—	25,0	27,1	—
0,600	27,7	—	28,2	26,5	25,8	—	—	24,4	26,5	—
0,610	27,5	—	27,4	25,6	25,3	—	—	24,0	26,4	—
0,620	27,2	—	26,9	25,3	24,7	—	—	23,6	25,5	—
0,630	26,8	—	26,4	24,7	24,2	—	—	23,1	25,2	—
0,640	26,5	—	26,2	24,5	23,7	—	—	22,7	24,8	—
0,650	26,2	—	25,7	23,8	22,9	—	—	22,2	23,9	—

TABLE 19. /CONCLUSION/

Author / λ, μ	F_λ (0) in 10^{13} erg/cm^2·sec·sterad·cm									
	Peytu-raux /460/	Pierce Peytu-raux /309,313/	Sitnik /111/	Maka-rova /83,112/	Labs & Neckel /345/	Hout-gast /363/	Stair &Ellis /117/	US Solar Comm. /142/	Arve-sen /373/	Heath /375/
Weight	1	1	1	1	2	1	2	4	1	1
0,660	25,0	—	24,8	23,1	22,5	—	—	21,9	23,1	—
0,670	25,3	—	25,1	23,3	22,6	—	—	21,4	23,4	—
0,680	25,0	—	24,6	23,2	22,1	—	—	21,0	23,3	—
0,690	24,4	—	24,0	24,3	21,6	—	—	20,6	22,1	—
0,700	23,8	—	23,5	24,8	21,1	—	—	20,1	22,2	—
0,720	23,0	—	22,5	23,5	20,1	—	—	19,3	20,6	—
0,740	22,0	—	20,0	21,0	19,1	—	—	18,5	19,6	—
0,760	21,4	—	20,7	19,1	18,4	—	—	17,7	19,0	—
0,780	20,6	—	19,8	17,9	17,6	—	—	16,9	17,9	—
0,800	19,4	—	18,8	17,2	16,9	—	—	16,2	17,2	—
0,850	16,8	—	16,2	—	14,8	—	—	14,5	14,3	—
0,900	—	13,3	14,0	—	12,9	—	—	13,1	13,2	—
0,950	—	12,0	12,8	—	11,4	—	—	12,3	11,8	—
1,00	—	10,6	11,4	—	10,2	—	—	10,97	10,99	—
1,05	—	9,55	9,92	—	9,50	—	—	9,68	9,92	—
1,10	—	8,50	9,10	—	8,74	—	—	8,71	8,93	—
1,15	—	7,74	8,15	—	7,87	—	—	7,85	8,10	—
1,20	—	6,98	7,23	—	7,26	—	—	7,12	7,35	—
1,25	—	6,36	6,60	—	6,57	—	—	6,40	6,69	—
1,30	—	5,74	—	—	—	—	—	5,82	6,21	—
1,35	—	5,28	—	—	—	—	—	5,35	5,62	—
1,40	—	4,81	—	—	—	—	—	4,94	5,17	—
1,45	—	4,44	—	—	—	—	—	4,59	4,74	—
1,50	—	4,07	—	—	—	—	—	4,22	4,39	—
1,55	—	3,76	—	—	—	—	—	3,94	4,02	—
1,60	—	3,45	—	—	—	—	—	3,59	3,75	—
1,65	—	3,18	—	—	—	—	—	3,26	3,45	—
1,70	—	2,91	—	—	—	—	—	2,97	3,19	—
1,80	—	2,36	—	—	—	—	—	2,34	2,52	—
1,90	—	1,94	—	—	—	—	—	1,85	2,06	—
2,00	—	1,61	—	—	—	—	—	1,51	1,76	—
2,10	—	1,35	—	—	—	—	—	1,44	1,40	—
2,20	—	1,13	—	—	—	—	—	1,162	1,13	—
2,30	—	0,963	—	—	—	—	—	1,000	0,955	—
2,40	—	0,822	—	—	—	—	—	0,941	0,853	—
2,50	—	0,704	—	—	—	—	—	794	0,789	—
2,60	—	0,611	—	—	—	—	—	706	—	—
2,70	—	—	—	—	—	—	—	632	—	—
2,80	—	—	—	—	—	—	—	574	—	—
2,90	—	—	—	—	—	—	—	529	—	—
3,00	—	—	—	—	—	—	—	0,456	—	—

The observations were made simultaneously with two instruments: a quartz spectroradiometer and a filter radiometer with interference filters; the set of filters cover the least-studied region 3100-4000 angstroms. An integrating sphere was placed in front of the entrance aperture of the instruments; the internal hollow cavity of the sphere was coated with $BaSO_4$ and MgO layers, which ensure a uniform diffuse reflection of solar light (or light from the comparison lamp).

The solar spectrum was compared with the spectrum of a 1000-watt quartz-iodine standard lamp (cf. Chapter Three) calibrated at the US National Bureau of Standards by comparison with a blackbody.

The Stair group from the US National Bureau of Standards conducted studies of the distribution of energy in the solar spectrum even earlier [115, 368], but at that time they obtained overstated intensities, for example, in the work [115] the solar constant is 2.05 cal/cm^2 · min, which evidently is due to the 4.5 percent overstated intensities of the standard lamp calibrated based on color temperature and the emissivity of tungsten, and not based on a blackbody [117].

Stair and Ellis, just as in the case of Labs and Neckel, determined the solar constant based on their own observations (covering a smaller wavelength interval), by supplementing them with the same rocket UV data, but reducing their values by 13 percent. The authors adopted the Smithsonian observations presented by Johnson [119] in the region with $\lambda > 5300$ angstroms; in this system the solar constant is 1.95 cal/cm^2 · min or 136 mw/cm^2.

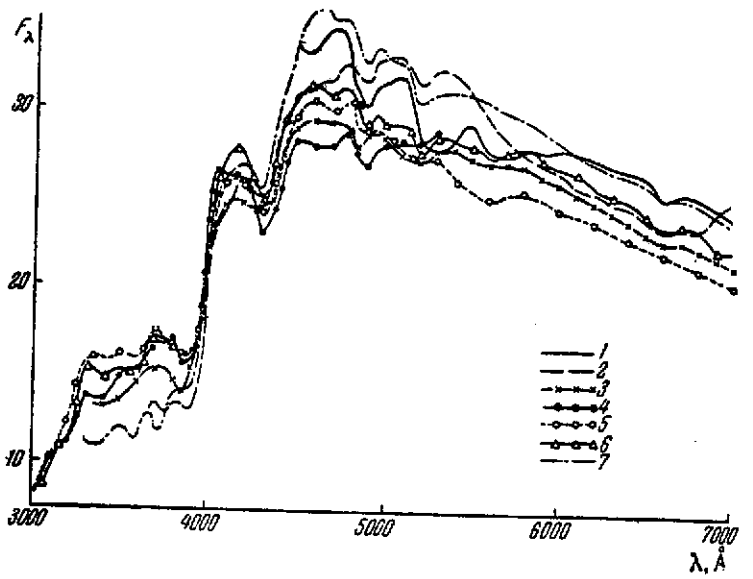

Fig. 44. Integrated spectrum of the entire solar disk based on individual data adopted for averaging.
1 -- Peyturaux
2 -- Makarova
3 -- Labs and Neckel
4 -- Stair and Ellis
5 -- US Committee
6 -- Arvesen
7 -- Sitnik

The distribution of energy in the integrated spectrum of the entire solar disk, based on the data of Stair and Ellis and most other ground data, is given in Fig. 44.

The first (and thus far the only) measurements of the distribution of energy in the solar spectrum taken outside the earth's troposphere were made by the M. P. Thekaekara group from the NASA Goddard Center in August 1967 /122, 157, 369-372/; an instrument was launched together with this group on the same aircraft by researchers from the Jet Propulsion Laboratory, J. Arvesen et al. /205 /373/. Measurements of the solar constant described in Chapter Two were made on the same aircraft. (The guidance accuracy was ~ 1/4°.)

The Goddard Center loaded six spectral instruments on the aircraft; based on the results of measurements made with five of these instruments, M. P. Thekaekara, R. Kruger, and C. Duncan presented the mean distribution curve (observations on the sixth instrument, an electronic scanning spectrometer /369/, were unsuccessful). We found individual tabulated data only for one instrument -- a Leiss monochromator /372/. Since we thus were unable to clearly distinguish results obtained on individual instruments and since the method of observations and subsequent reductions of measurements was common to a large extent, we consider the work of the entire group as a whole, singling out only individual details that are central from our point of view. But the instrumental characteristics of individual experiments for this group and for Arvesen are presented in Table 20.

Absolutization of the data on all the instruments was conducted as in the work of Stair and Ellis, by comparing the solar spectrum with the spectrum of 1000-watt standard quartz-iodine lamps calibrated with a blackbody model, with the exception of the I-4 interferometer, for which the comparison was made directly with a blackbody at T = 1200° K. However, absolute intensity values could be obtained directly from observations for the first, third, and fifth instruments in Table 20. The drift of the intensity of reference lamp radiation was observed with the second instrument during the observational period and absolutization was conducted by coupling to the solar constant value obtained with integral instruments during the same flights -- 135.1 mw/cm^2. The entrance apertures for the sun and the lamp proved to be not reliably enough coordinated on the fourth instrument; absolutization was conducted by coupling to data obtained on a Perkin-Elmer monochromator.

Allowance for absorption of light in the aircraft windows made of different grades of fused quartz and sapphire was common to all instruments; window transmission was carefully investigated (cf., for example, /122, 373/ and Fig.19). Light losses in /208 reflection by auxiliary mirrors had to be investigated only for the Perkin-Elmer monochromator, in which the matte aluminum mirror used for comparing the radiation of the sun and the reference lamp was positioned after the auxiliary mirrors. In all the remaining instruments, either an integrating sphere identically functioning for the light of the sun and of the lamp, or else in the case of

TABLE 20. COMPILATION OF AIRCRAFT OBSERVATIONS OF THE INTEGRATED INTENSITY OF THE ENTIRE SOLAR DISK MADE BY THE THEKAEKARA AND ARVESEN GROUPS IN 1967 AT AN ALTITUDE OF 11.58 KM IN THE REGION 0.3-16 MICRONS

Authors	Spectral region & instrument	Method of absolutizing measurements	Radiation receivers	Precision in authors' est.
1. Thekaekara, Stair, Winker /122, 371/, 6 days	0.2945-2.53 μ Perkin-Elmer monochromator w/LiF prisms, double passage of light. Resolving power 2.7, 11, & 90 A at 0.3, 0.7, & 4 μ, respect.	Quartz-iodine, 1000-w standard lamp	PEM in region 0.3-0.63 μ ; thermocouple from 0.63-2.53 μ	$\pm$ 5 %
2. McIntosh, Park /122, 372/, 4 days	0.3-1.6 μ double two-prism quartz Leiss monochromator	Relative measurement, calibrated with 1000-w quartz iodine lamp. Absolutization based on solar constant	PEM in UV & visible regions; lead sulfide photocell, cooled to 0° in the IR region	$\pm$ 5.5 %

/206

TABLE 20. /CONCLUSION/

Authors	Spectral region & instrument	Method of absolutizing measurements	Radiation receivers	Precision in authors' est.
3. Stair, Webb /122, 372/ 2-3 days in different spectral reg.	0.31-1.1 μ Radiometer with 33 interference filters with half-widths of 100, 500, and 1000 A in UV, visible, and IR spectral regions	Quartz-iodine, 1000-w standard lamp	PEM with electrometer	$\pm$ 5 %
4. Rogers, Ward, Thekaekara /122, 370/, 4 days	0.3-2.5 μ R-4 polarization interferometer, Soleil beam-splitter-prism, resolution 15 A for 0.72 μ, and 170 A for 2.2 μ	Relative calibration based on quartz-iodine standard lamp. Absolutization by coupling with data No. 1 of this Table	Lead sulfide photocell and PEM	Not stated
5. Rogers, Ward, Thekaekara /122/ 4 days	2.6-15 μ Michelson type interferometer I-4	Black body at 1200° K	Bolometer	Not stated
6. Arvesen, Griffin Pearson /373/, 11 days	0.3-2.5 μ Spectrophotometer with double monochromatization, dispersion from 10 to 30 A/mm	1000-w quartz-iodine standard lamp	PEM from 0.3 to 0.7 μ Lead sulfide photocell to 2.5 μ	$\pm$ 5 % at 3000 A, $\pm$ 3 % for $\lambda > 4000$ A

the I-4 interferometer, the aircraft window directly was used to illuminate the entrance aperture, since the flux from the sun in the spectral region studied was the weakest; the comparison was made with a blackbody.

Extinction in the terrestrial atmosphere was allowed for by the classical Bouguer method using observational data obtained on a Perkin-Elmer monochromator for a single day; for the remaining days of observations and for other instruments extinction was calculated from these data.

Extinction in the terrestrial atmosphere (outside the absorption bands) remains substantial even at an altitude of ~ 12 km up to wavelengths of 1-2 microns inclusively; it is more than 10 percent for $\lambda < 4100$ angstroms (cf. [122, 373]). Only for the IR region with $\lambda > 2$ microns was the transparency coefficient of the [209] atmosphere outside the absorption bands assumed to be unity.

All spectral instruments employed in the aircraft observations were standard models, however of particular interest are the Fourier-spectrometers, a polarization and a Michelson interferometer (cf. Chapter Three), first successfully used in studies of the solar spectrum in this spectral region.

Fig. 45 presents the results of measurements made with three instruments of the Thekaekara group. The results of measuring energy distribution obtained on all five instruments were reduced by Thekaekara into a single curve, initially normalized with respect to the solar constant value of 135.1 mw/cm^2 (the data were supplemented, as is usual, by measurements made in the rocket ultraviolet and in the IR region on the assumption that the brightness temperature decreases with wavelength) [122].

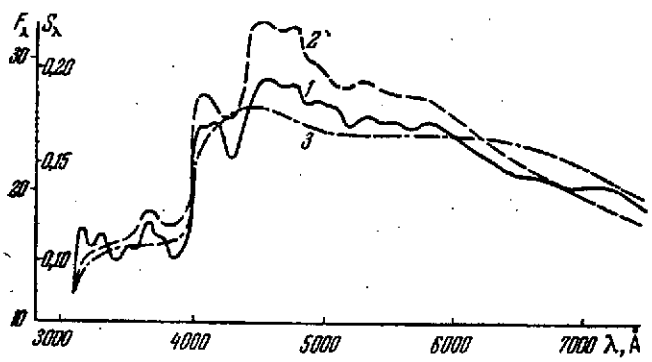

Fig. 45. Integrated spectrum of entire solar disk based on data obtained with three instruments of the Thekaekara group.
1 -- Leiss monochromator
2 -- Perkin-Elmer monochromator
3 -- data obtained with filters (F_λ -- in 10^{13} erg/cm · sterad · cm, S_λ in 10^{11} erg/cm^2 · sec · cm)

Data of the US Solar Radiation Committee [141, 152, 157] [32] (cf. also, Chapter Two) adopted in the United States as the standard for spectral components of integrated solar radiation of the entire disk in 1970, are based on the results of observations made by the Thekaekara group. Thekaekara's data were slightly corrected (cf. [142]), first of all, by being fitted to the solar constant value

[Footnote 32 on following page]

of 135.3 mw/cm^2, adopted by the Committee, and secondly, the data were somewhat changed in the region 0.3-0.7 microns to agree with the observations of the Drummond group /141/, and in the rocket regions -- according to Heath's estimates /374/.

Results of observations made on the same aircraft by the Jet Propulsion Laboratory group, Arvesen et al. /373/ are somewhat of a special case, but they were not adopted in averaging by the US Committee on Solar Radiation, though the method of observations, the spectral radiation standard (1000-watt quartz-iodine lamp), and the method of reductions are all the same for both groups (cf. Table 20). The integrating sphere mounted in front of the instrument was rotated at the rate of 30 rps, so that the standardization of the spectrum was made continuously, which evidently must /210 enhance the precision of the result. Extinction in the terrestrial atmosphere was determined by observations using Bouguer method.

The results of observations made by the Arvesen group are presented as highly detailed tables with steps from 4 to 1 angstrom in the region up to 7000 angstroms, steps of 20 angstroms in the region up to 1 micron, and 50 angstrom steps in the region up to 2.5 microns. Also presented are results averaged based on 100-angstrom intervals for $\lambda < 1$ micron.

The intensity of solar radiation based on Arvesen's data proved to be generally somewhat greater than the value obtained by the Thekaekara group; the solar constant, based on these results, embracing ~ 94 percent of the solar constant value (and supplemented by the usual method in the UV and IR regions), was found to be 1.99 cal/cm^2 · min, or 139 mw/cm^2.

We do not see the reasons why these detailed and evidently quite carefully conducted experiments should have been rejected. A reference to the unreliability of the measurements made of the transparency coefficient of the aircraft window /157/ is not convincing, since the correction is small (cf. Fig. 19), and, in addition, it even further increased the measured intensity values. We corrected Arvesen's data by using the transparency coefficient of the aircraft window determined experimentally as well as by the calculation method of Thekaekara et al. /158/. The correction is small, averaging 1.0083, less than one percent. Arvesen's results for F_λ are presented in Table 19 and, recalculated to $I_\lambda(0)$ in Table 18.

---

[32] In our tables these data are referred to as the US Committee, for brevity. The initial data of the Committee for the integrated spectrum of the entire solar disk (expressed in radiation intensities, and not in illumination values, as in the original) are given in Table 19 and were reduced to the solar center, $I_\lambda(0)$, in Table 18.

The last-performed study, which must enter into the results for this spectral region is the work of Heath /375/, which he performed on the Nimbus-4 AES /artificial earth satellite/ in the region 2550-3400 angstroms. It is discussed in the next section dealing with investigations in the rocket UV spectrum, since by method and main results it is close to rocket observations.

Before proceeding to deriving the mean values for $I_\lambda(0)$ and F_λ, let us see how far the results of individual studies are harmonized.

First of all, of course it is most interesting to compare the internal convergence of the results of ground studies of the distribution of energy with those made outside the earth's tropo- /2
sphere. Both are shown in Figs. 44 and 45 (for the intensity of the integrated spectrum of the entire solar disk, F_λ). The result of the comparison is somewhat discouraging: in both figures individual series differ in roughly the same limits from each other and these limits are large: up to 20 percent(sometimes even higher). Thus, in the UV spectral region the quantities obtained on the aircraft using the Leiss monochromator (based on the tabulated data in /372/) differed from the mean (!) derived in /122/ by 20 and even 30 percent, and close to the curve maximum -- by 3-7 percent. Aircraft observations were made simultaneously; spectral radiation standards calibrated in the same organization -- the US National Bureau of Standards -- were used. The differential effect of the terrestrial atmosphere was completely excluded. And still the deviation in individual observational series was as great as in the ground results.

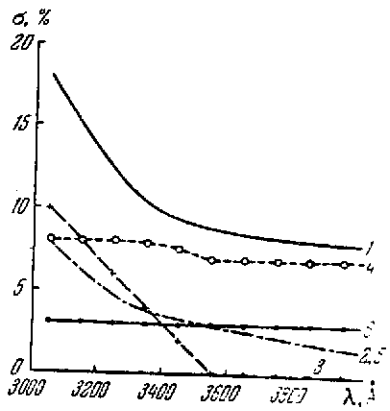

Fig. 46. Components of errors in observations made on the distribution of energy based on the Houtgast estimate. Errors:
1 -- overall
2 -- in determining extinction in the terrestrial atmosphere
3 -- absorption in the ozone layer
4 -- calibration of the reference standard lamp
5 -- equipment noise
6 -- in determining polarization effects

The cause of this paradoxical phenomenon must evidently be sought for in the estimate of the significance of individual observational errors. Houtgast made the most reliable estimate of this kind, in our view. Fig. 46 presents these estimates based on the data in Table 3 of the 1970 study /363/. The figure quite clearly shows that in the overall estimate the error (1) for extinction in the terrestrial atmosphere plays the paramount role only in

the spectral region where there is absorption in the ozone layer, up to 3400 angstroms (the ozone layer in fact remained over the aircraft), and further the error in reference standardization of /212 the spectral standard with which the solar spectrum was compared plays a fundamental role; curve (4) apparently served as the asymptote for the overall error. Only thus can the disparity of the aircraft results be accounted for.

The same conclusion was reached independently by American researchers /372, 373/. The error in standardizing the lamp includes the following: a) error in building the blackbody model, b) error in comparing lamp with the model, and c) instability of reproducing the radiant flux from one firing of the lamp to another. Evidently, only building a new, reliable international spectrophotometric standard (lamp) can substantially improve the convergence of series of energy distribution measurements. An excellent internal convergence can be obtained, as Labs and Neckel did, but here the deviation with other data sometimes is as much as 20 percent and there is no certainty about which of the series is the best.

Examination of the problem of the main error in all results affords us grounds to believe that when weights are distributed in the averaging of individual results we must not give a larger weight to altitude observations (but, of course, only in the spectral region under study). The weights are indicated in Tables 18 and 19. In plotting the mean for the continuous solar spectrum $I_\lambda(0)$, the larger weight 2 was assigned to those observations which were made in the system $I_\lambda(0)$ and which thereby did not require supplementary reductions; in the system F_λ all these results were assigned the weight of 1, since reductions were introduced for β_λ and η_λ. Similarly, in the system F_λ the predominant weight was specified for those observations where the integrated spectrum of the entire solar disk was measured. A weight of 2 was assigned to the data of Labs and Neckel in both systems, since they did not need complete reductions, and in addition, the internal precision of the results was in their favor. A weight of 4 in the system F_λ was assigned the Committee's results, since they were based on the data of several instruments; it is dangerous to give a large weight, since the results were already fitted to the solar constant value of 135.3 mw/cm^2. It is difficult to say how substantially this procedure can distort the energy distribution.

Table 29 presents mean values of $I_\lambda(0)$, F_λ, and S_λ in the region 0.3-3 microns, derived from the data in Tables 18 and 19, with allowance for weights.

3. Rocket Region of Ultraviolet Radiation of the Solar Photosphere, 1400-3000 Angstroms /213

As noted above a number of times, study of the solar spectrum in the short-wave region for wavelength shorter than 3000 angstroms

is possible only outside the earth's ozonosphere at great altitudes, of the order of 100 km and higher. The solar spectrum was first recorded in the region up to 2100 angstroms during the flight of a captured V-2 rocket by the US Naval Research Laboratory (NRL) in 1946. The hydrogen line L_αH 1216 angstroms, the most intense in the spectral region $\lambda < 2000$ angstroms, was recorded in 1948 [235], and in 1952 W. Rense [377] photographed it and it was shown that it is an emission line.

Further advances in UV spectroscopy occurred at startlingly vigorous rates, especially if one considers that this is the most "expensive" region of solar studies. Each ascent of a spectral instrument on a rocket or satellite (balloons and aircraft do not reach the required altitude) is expressed in expenditures in "astronomical" figures.

Excellent reviews of progress in this field of study over its first 17 years are given in the review articles by R. Tousey and H. Friedman, leading researchers at the Naval Research Laboratory [378-380]. Interesting results, especially in the far UV spectrum, extending to hard x-rays began to be obtained nearly simultaneously by two other groups of US workers: the group of H. Hinteregger at the Cambridge Air Force Research Center [381, 382], and the Rense group at the University of Colorado [383]. In the Soviet Union, successful observations began in 1956; much work in identifying lines in the UV spectrum was done by V. P. Kachalov and A. V. Yakovleva et al. [384, 385]. Then the S. L. Mandel'shtam group [386] undertook important and interesting observations of the x-ray spectral region. Reviews of research on the UV spectrum are presented in the Russian language in the collections [383, 7] and in a book by G. S. Ivanov-Kholodnyy and G. M. Nikol'skiy [5], dealing mainly with the line solar spectrum as of 1967-1968.

The reviews also contain a description of equipment and methods of absolutizing results, with essential features in the UV region. Several problems are considered above, in Chapter Three. Diffraction gratings in normal or grazing incidence are used as dispersing components for the spectrographs.

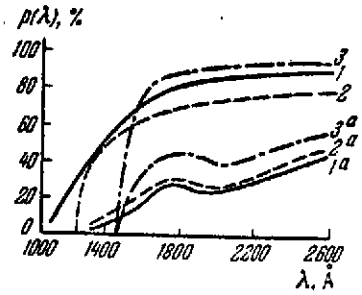

Fig. 47. Transparency coefficient of various substances in the UV spectral region before and after (a) irradiation, based on the data of Gerasimova [185]:
1 -- lithium fluoride
2 -- fluorite
3 -- quartz

The feeding optics in most cases is of the mirror type. Prisms and lenses are ordinarily not used, except for rare special cases,

since first of all there are no transparent materials in the region $\lambda < 1100$ angstroms, and secondly, transmission of crystals sometimes used in the longer-wave ultraviolet varies widely with time, deteriorating on exposure to radiation, as shown, for example, by Fig. 47. The reflection coefficients of most mirror coatings are low, and the amount of scattered light is large, therefore often multiple layer coatings are used: for example, layers of germanium or magnesium fluoride, acting as filters cutting off long-wave radiation, are deposited on a layer of sputtered aluminum. Filter measurements are widely used: combinations of transmission regions of the optical window and the spectral sensitivity of the photocathode or filling of the ionic chamber are selected. Absolutization of measurements is especially difficult, since the measurements themselves and their calibrations as a rule are performed at different times and the standard radiation sources are lacking. One must resort to multistage calibration, briefly described in Chapter Three.

Equipment problems will be discussed below only very briefly, when we describe the main investigations of the distribution of energy in the solar UV spectrum.

The far UV solar spectrum has several remarkable features. In the region from 3000 to ~ 2075 angstroms it is similar to the longer-wave spectrum: a palisade of Fraunhofer absorption lines /215 is visible against the background of the continuous spectrum, but in the spectrum of the solar limb, beginning at 2900 angstroms, distinct emission lines are present and they become stronger with the transition to the shorter-wave region (tables of emission lines with identification and estimates of intensity are presented, for example, in the work of W. Burton and A. Ridgeley /387/).

In the narrow section 2100-2085 angstroms, an "unexpected and dramatic change in the appearance of the spectrum occurs," as Tousey writes /379/. The continuum intensity falls off abruptly, almost by a factor of 4, over an extent of 25 angstroms; the corresponding brightness temperature is reduced roughly from 5500 to 5000° K. This abrupt drop is due to the inclusion of new intense absorbing agents: the series limits, first of all, of Al (2076 angstroms), and then of Ca and of Si -- at 2000 angstroms, and of Fe (a^3F) at 1875 angstroms (several limits of the series have been noted in Fig. 48). Below 2085 angstroms even though absorption lines are present, they are significantly attenuated. Elementary theory shows that as long as absorption lines are present, the continuous spectrum must originate in the deeper layers of the photosphere where temperature drops off with increasing distance from the sun's center. But if the continuous spectrum is produced where the temperature increases in the direction toward the outer layers, formation of absorption lines becomes impossible (with the exception of cases of the abrupt deviation from thermodynamic equilibrium conditions). There must be a minimum-temperature region in the transitional zone from the photosphere to the chromosphere. In the UV spectrum, the temperature

minimum occurs in the region near 1525-1682 angstroms and is due to intense absorption within the limits of the silicon series SiI3P and SiI^1D_2, respectively. The absorption coefficient of silicon increases by a factor of 40 at the limit 1682 angstroms, and by a factor of 15 at the limit 1525 angstroms /388/. A transition from the absorption spectrum to the emission spectrum is visible in spectrograms obtained by D. Garrett, J. Purcell, and R. Tousey /389, 390/ and in a microphotogram (Fig. 49) of one of the spectra. The continuous spectrum is greatly attenuated and in the region with $\lambda \lesssim 1682$ angstroms absorption lines disappear (with the exception of the heads of the CO bands noted in Fig. 49).

Another characteristic feature of the minimum-temperature region is the absence of noticeable variation in the intensity of emission from the center toward the limb in the continuous spectrum; the latter is easily visible in Fig. 48 taken from a study by R. Bonnet /320/. All emission lines show, moreover, limb brightening, which confirms their chromospheric origin. However the fact that the above-mentioned absorption lines of CO near 1540 angstroms exist remains unexplained. Judging from theoretical considerations, they should not be there. We will return to this problem and to the question of the reliability with which the temperature minimum was determined at the end of the next section. /21

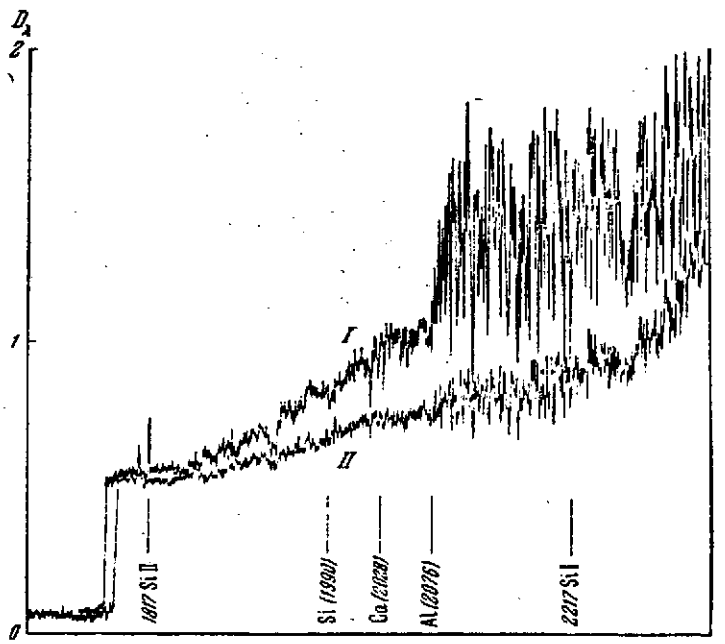

Fig. 48. Densitogram of the spectra of the center (I) and limb (II) of the solar disk in the region 2500-1800 angstroms. Series limits with intense absorption are noted.

It bears mentioning that the minimum temperature in the transitional region from the photosphere to the chromosphere can also be observed in the infrared spectral region, in the interval from 50 to 300 microns (cf. Section 4), where absorption by free-free transitions of negative hydrogen ions is so intense that radiation exits only from the uppermost layers of the solar photosphere. However, determination of /2

the brightness temperature in the ultraviolet end of the spectrum has, it would appear, some fundamental advantages. Thus, in determining the temperature with a specified precision of 100° K, the corresponding precision in measuring the intensity of the ultraviolet spectrum can be restricted by approximately 40 percent, while to attain the same precision in the infrared region we must measure the intensity with an error of not more than 2 percent, which directly follows from the Planck's law for temperatures of the order of 5000-6000° K. /218

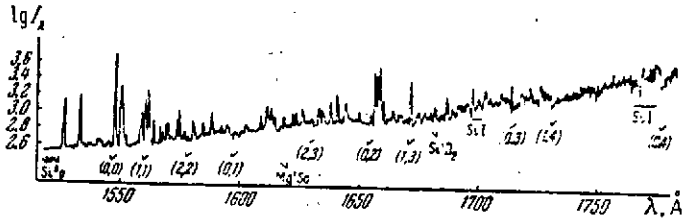

Fig. 49. Microphotogram of solar spectrum in the minimum temperature region

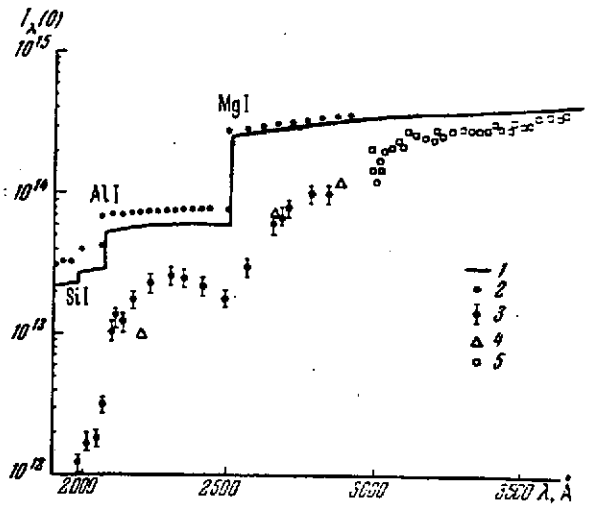

Fig. 50. Intensity of radiation in the continuous solar spectrum in the UV region.
1, 2 -- based on the models of Holweger and Bilderberg,
3 -- Bonnet's spectral observations
4 -- Bonnet's filter observations
5 -- Houtgast's data

Let us proceed to briefly characterizing the investigations of the rocket solar UV spectrum from which we can extract data on the distribution of energy in the region 3000-1500 angstroms.

Unquestionably, the investigations by the US Naval Research Laboratory are the first, both as to the time the research began as well as in the volume of material of interest to us. The results and presentation of the methods of studies completed up to 1963 inclusively are quite adequately summed up in the same articles of Tousey /278, 279/ and in an article by Detwiler et al. /391/.

In the region 3000-1400 angstroms the overall results are based on four series of observations. N. Wilson, R. Tousey, J. Purcell, F. Johnson, and C. Moore /392/ obtained photographs of

the solar spectrum in the region 2900-2635 angstroms using a spectrograph with a concave grating (Table 21); the solar image came through the spectrograph slit. H. Malitson, Purcell, Tousey, and Moore /393/ used a similar spectrograph; they photographed the spectrum of the solar center in the region 2635-2085 angstroms; a second low-dispersion spectrograph with a matte plate positioned in front of a wide entrance slit was employed to determine the intensity of radiation at a given wavelength for the entire solar disk.

The spectral section from 2085 to 1750 angstroms was obtained using a similar technique by Purcell, Packer, and Tousey /394/ in March 1959; it was not possible to do this in a shorter-wave region owing to intense light scattering. These three series of measurements were made in relative units. The selective sensitivity of the receiving equipment was cancelled out by calibration in the laboratory based on the spectrum of a carbon arc; its energy distribution was investigated by F. Johnson /255/ and was absolutized using data of D. Packer and C. Lock /395/ (cf. Fig. 29).

Detwiler, Purcell, and Tousey /383/ used a telescope-spectrograph with two diffraction gratings in investigating the region 1550-500 angstroms, to reduce the scattered light. The first grating formed the solar image at the entrance slit and served as a predispersing component of the optical scheme. An Aerobee-Hi rocket lifted the instrument to an altitude of about 180 km on 19 April 1960. To standardize the results, simultaneous measurements of the intensity of emission in the line L_α of hydrogen was used; the measurements were taken with an ionization chamber filled with nitrogen oxide, and with a lithium fluoride optical window; this combination made it possible to cut out the spectral section 1075-1275 angstroms. Measurement results were reduced by 15 percent in order to consider the emissions of the continuous spectrum and of other lines besides $L_\alpha H$ falling in this wavelength interval. Naturally, it was assumed that the emission $L_\alpha H$ is quite stable with time, which evidently has been confirmed by recent measurements carried out for over a year by A. and J. Timothy /396/. Simultaneous measurements of the line L_αHeII moreover showed intense fluctuations.

Results of measuring the emission intensity of the entire solar disk together with absorption lines made by the Naval Research Laboratory up to 1963 were compiled into a single system in articles by Tousey /378/ and Detweiler /391/ for the spectral regions 2900-1700 and 1500-500 angstroms. These data reduced to absolute units by the coupling to ground observatories performed by Dunkelman and Scolnik proved to be highly overstated, just as the results of Dunkelman and Scolnik (cf. Section 1, Chapter Five). Table 28 presents the data of Naval Research Laboratory absolutized now based on new, more reliable observations, adjoining the result of the NRL in the near UV region and overlapped by Heath's results (cf. below). The spectral region from 1700 to 1520 angstroms was

TABLE 21. COMPILATION OF OBSERVATIONS USED IN PLOTTING MEAN DATA ON THE DISTRIBUTION OF ENERGY IN THE ROCKET REGION OF THE UV SPECTRUM OF THE SOLAR PHOTOSPHERE, 1400-3000 ANGSTROMS

Authors and period of observations	What was observed, spectral region & instrument	Method of absolutizing measurements	Radiation receiver	Precision in authors' est.
1. Tousey /378/ Detwiler [391] as per following material 1) Willson et al. [392], 1950, 1952	Entire disk, integrated spectrum2635-2990 A. Spectrograph w/concave normal-incidence grating, R = 40 cm resol. power ~0.5 A	Calibration w/carbon arc for $\lambda >$ >1950 A, determination of eff. of grating and sensitivity of photographic materials. Absolutization based on ground data $\lambda > 3000$ A	Photographic plates	± 20%
2) Malitson et al. /393/, 1952, 1955, 1956	Entire disk, integ. spec.2085-2635 A. Spectrogr. as in 1)	As above	As above	± 20%
3) Purcell et al. /394/, 1959	Entire disk, integ. spec.1700-2035 A. Spectrogr. as in 1)	As above	As above	± 20%
4) Detwiler et al. /383/, 1960	Entire disk, integ spectrum 850-1550 A. Telescope-spectrograph w/two diffraction gratings, R = 40 m	Based on line $L_\alpha H$, measurement of grating efficiency, film sensitivity	Photographic film	± 20%

TABLE 21. /CONCLUSION/

Authors and period of observations	What was observed, spectral region & instrument	Method of absolutizing measurements	Radiation receiver	Precision in authors' est.
2. Bonnet /320/, 1964 (filters), 1967 (spectrograph)	Center of disk, quasicont. 1984-2885 A spectrogr. w/two concave gratings (resol. 0.4 A) and filter (43 A band)	Based on mercury lamp, high-pres., Phillips, calibrated w/bl. body model after Heidelberg	Photographic film	±26-30 %
3. Widing, Purcell, Sandlin /389/, July 1966	Center of disk, quasicont. 1450-2100 A. Telescope-spectrograph w/two diffrac. gratings resol. ~0.2 A	Absolutization w/ carbon arc for $\lambda >$ > 1935 A, calculation of grating eff. for $\lambda <$ 1950 A	S-5 photo. film sensitivity independent of	±30% for $\lambda >$ 1950 A ±40% for $\lambda <$ 1950 A
4. Heath /374,375/ 1966, 1969-1970, 1970 (monochromator)	Entire solar disk I. 1100-3000 A, wide-band photometer a) λ_{ef} 1216 A, $\Delta\lambda$ 200 A; b) λ_{ef} 1750 $\Delta\lambda$ 200 A; c) λ_{ef} 2950 A, $\Delta\lambda$ 500 A II. 2550-3400 A, double monochromator, passband width 10 A	Based on standard CsTe vacuum photodiode with Al_2O_3 window	Photodiodes: a) tungsten, MgF window b) CuI, SiO_2 window; Al_2O_3 window c) CsTe, $CaCO_3$ window	±15% (40° K)

not observed, and in the table shown in /391/ was obtained by interpolating between two observational series; we did not take these data into consideration.

A group of researchers at the State Optical Institute -- V. P. Kachalov and A. V. Yakovleva et al. /384, 385/ obtained photographs of the solar spectrum in the interval from 2471 to 2635 angstroms in 1956, and in the interval from 2700 to 3100 angstroms in 1959. Rockets lifted equipment to altitudes of about 100 km. A concave grating, 600 rulings/mm with a radius of curvature of 1 m, was used in the normal light incidence device, with a resolving power in the shorter-wave section of 0.3 angstrom, and 0.15 angstrom in the longer-wave section. A third flight was launched in 1960 to determine the scale of absolute intensities, the spectrum was recorded with a smaller resolution (0.3 angstrom); the photographs were compared with the spectra of a carbon arc and a krypton lamp standardized with a blackbody. However, since the solar image was constructed at the spectrograph slit and the reports did not indicate how much of the image entered the spectrograph, we cannot state with certainty whether the measured absolute intensities apply only to the center of the disk or to the sum of the center and the limb. Limb darkening in this spectral region is very great, therefore owing to the impossibility of performing the appropriate reductions, the data of V. P. Kachalov and A. V. Yakovleya are not included in the table for deriving the mean, but are plotted in Fig. 58. /222

Studies by the French authors R. Bonnet, J. Blammont, G. Courtes and their coworkers (cf., for example, /320, 398, 397/, and so on) aimed at solving two problems: absolute spectrophotometry of the center of the solar disk and a detailed study of limb darkening at various wavelengths (Chapter Four). The main results are presented in the Bonnet article /320/. Absolute spectrophotometry was performed during two launches of the Veronique rocket in November 1964 and in January 1967; altitudes of 98 and 124 km, respectively, were reached. During the first flight quasimonochromatic solar images 5 mm in diameter were photographed in three wavelengths: 2190, 2665, and 2885 angstroms. The photograph was performed through a multiband filter with adjustable passbands, described in detail in the report /397/. It is a modification of the monochromator with a concave grating in which the entrance and several of the exit windows are arranged on a Rowland circle. The filter had a 43-angstrom passband in carrying out absolute spectrophotometry (and an 80-angstrom passband in studying limb darkening -- cf. Table 21).

During the second flight the stigmatic spectrum of the solar disk center was photographed with a spectrograph equipped with two concave gratings with crossed dispersion. The maximum resolvable interval in the spectrograms was about 0.4 angstrom; in making measurements, points with maximum intensities were selected; the /223

envelope drawn along these points corresponds to the quasicontinuum in our understanding of the term.

In spite of the appreciably different resolution, Bonnet's data obtained with the spectrograph and with the filter agree very closely with each other. This is not completely understandable since even though the filter observations were taken in sections that were more free of lines compared with adjoining sections, still for several of these sections the correction ζ_λ is 1.25-1.30, as can be estimated from the McAlister atlas [339].

W. Parkinson and E. Reeves [399] attempted to obtain more reliable data on the UV region of the temperature minimum in the UV end of the spectrum, in the interface between the photosphere and the chromosphere. A telescope with an Ebert type spectrograph was launched in September 1968 on the Aerobee-150 rocket (cf. Table 21). The telescope system consisted of an off-axis paraboloid and two plane mirrors; all mirrors were coated with a layer of sputtered aluminum, 400 angstroms thick, with an overlayer of magnesium fluoride, which provides a reflection maximum at about 1400 angstroms. The entire system was evacuated to the state of high vacuum prior to flight in order to ensure the temperature stability of the optical parts.

The spectrum of the solar center was scanned in the region 1400-1875 angstroms. The combination of a photomultiplier with a cesium-iodine cathode and a lithium fluoride window permitted a total cut-off of radiation outside the region 2000-1300 angstroms.

The spectrometer was calibrated on earth in a vacuum tank; the intense lines of iodine in a discharge in a mixture of hydrogen and iodine crystal vapor was used; absolute standardization was performed with a four-element bismuth-tellurium and bismuth-antimony thermocouple calibrated with three sources for which the radiation intensity was known in absolute units. Two of these standard sources with carbon and tungstem filaments were [2] calibrated in the Eppley Laboratory, and the third -- a mercury lamp -- was calibrated in the 2537 angstroms line at the National Bureau of Standards.

The results of Parkinson and Reeves are shown in Fig. 58, but we do not include them in the composite table and in the mean data since they obviously carry a substantial systematic error (cf. end of the section). Based on the data in [399], the temperature in the minimum-value region drops to 4300° K.

Widing, Purcell, and Sandlin [389, 390], in continuing the series of investigations at Naval Research Laboratory, also set out to determine the minimum brightness temperature in the solar UV spectrum.

The reports [389, 390] present the results of interpreting ten solar spectra obtained by Garrett, Schneider, Purcell, and Tousey on 27 July 1966 using a spectrograph placed in a rocket lifted to an altitude of 187-202 km. The main characteristics of the equipment and the measurement method are given in Table 21.

Thirty sections relatively free of lines were selected for the measurements: for $\lambda > 1682$ angstroms -- between intense absorption lines; in the shorter-wave region -- in the quite broad intervals between emission lines.

The calibration and standardization of the spectra were carried out in a laboratory. For the region $\lambda > 1935$ angstroms, a standard source was used -- a hydrogen tube and, as in earlier studies of the NRL, the positive crater of a carbon arc. For $\lambda < 1935$ angstroms, the efficiency of the grating used was determined and it was assumed that the sensitivity of the SC-5 photoemulsion was independent of wavelength. This spectral region was "coupled" to the carbon arc at λ 1935 angstroms in order to arrive at absolute flux values.

The results of the absolute measurements of solar radiation intensity in the temperature-minimum region are given in Table 28 and in Fig. 58. The minimum temperature of 4670 $\pm$ 100° K occurs in the region 1525-1682 angstroms, where as already remarked absorption occurs beyond the limits of the silicon series.

D. Heath [374, 375] measured the solar radiation flux, within the framework of Monitor of Ultraviolet Solar Energy program (MUSE) in the region 1100-3400 angstroms in absolute units in order to find possible variations in the long-period intensity associated with solar activity. The problem is of vital importance from the geophysical point of view, since solar radiation in this spectral region supplies energy to the lower thermosphere, mesosphere, and the upper stratosphere, by being nearly entirely absorbed in these layers of the terrestrial atmosphere, and makes possible the process of photodissociation of oxygen and ozone (cf. Chapter One). /225

Using identical equipment, measurements were made in 1966 on an Aerobee rocket lifted to an altitude of 210 km, and then on the Nimbus-3 and Nimbus-4 satellites, launched in April 1969 and in April 1970, respectively, to altitudes of about 1100 km. Both satellites will continue making observations for a number of years.

Measurements were conducted in the region 1100-3000 angstroms with a broad-band photometer provided with three kinds of vacuum diodes as radiation receiver. The passband of each individual receiver was cut off on the short-wave side with an optical filter, and by the photocathode material -- on the long-wave side (cf. Table 21).

Since the ultimate aim of the MUSE program was to investigate the variability of solar UV emission and to establish its relationship to the 11-year cycle, absolute calibration of measurements and the temporal stability of this calibration must be extremely reliable. The basis for the direct comparison of the UV solar radiation flux measured during the 1966 rocket flight and then on the Nimbus-3 and Nimbus-4 satellites was a standard vacuum photodiode, a semitransparent cesium-tellurium (CsTe) photodiode deposited on an Al_2O_3 window. Initially, in 1966 the photocathode was calibrated in the wavelength 2537 angstroms based on a calibrated Eppley Laboratory thermocouple. This calibration of the diode was used in calibrating a newly sputtered film of sodium salicylate placed in front of the photomultiplier, calibrated in turn at the point 1216 angstroms. If it is assumed that the efficiency of sodium salicylate remains constant within the calibration limits, then it turns out that the two calibration points agree within the limit 15 percent, and the photomultiplier calibration is thus transferred to the standard CsTe-diode. Late in 1970 the diode calibration was repeated at the US National Bureau of Standards; the agreement of the 1966 and 1970 calibration results at the point 2537 angstroms, performed by independent methods, was within the limits 5 percent.

However, in order to determine the intensity of solar radiation in absolute units when making observations with broad filters, one must know the distribution of energy in the solar spectrum, which is a fundamental restriction on the precision of the end results. A study by Heath adopted as the starting data distributions in the region 1027-1775 angstroms according to Hinteregger /381/, from 1800 to 2600 angstroms -- according to Detwiler /391/, and from 2600 to 4000 angstroms -- according to Tousey /378/. The signals calculated with this distribution differ from those actually observed. For a filter with λ_{eff} = 1750 angstroms, that is, a spectral region near the temperature minimum, the observed intensity was considerably below the calculated value; it differs somewhat less, but still appreciably, from the computed intensity also for the other two spectral sections.

The solar brightness temperature computed for λ_{eff} 1750 angstroms was found to be 4485° K in 1966, 4715° K in 1969, and 4635° K in April 1970, where the error of determination did not exceed ± 40° K. Naturally, Heath drew the conclusion: the brightness temperature in the region of the photosphere-chromosphere interface varies markedly depending on the solar activity phase; it is a minimum near the minimum (1966), rises sharply around the maximum (April 1969), and then again decreases with the decline in activity (April 1970). The pattern of the radiation (temperature) intensity is also noticeabl in the longer-wave passband with λ_{eff} 2950 angstroms, as a function of the solar activity phase, but with a much smaller amplitude; observations made with a receiver separating radiation from the hydrogen L_α line did not show this course.

Based on the observational data of the Nimbus-3 and Nimbus-4 tellites, periodic changes in UV radiation with the 27-day rota- /227 onal period of the sun were also reliably detected, however the mplitude of the change as a function of wavelength showed a differ- t course: it dropped off more rapidly with increase in wavelength.

TABLE 22*. ORIGINAL MEASUREMENT DATA OF HEATH, S_λ, OBTAINED WITH A 10 ANGSTROM INSTRUMENT PASSBAND AND WITH CORRECTIONS INTRODUCED FOR ABSORPTION LINES*

λ, Å	S_λ, 10^9 erg/cm²·sec	* α_λ
2557,0	10,7	—1,0
2736,8	23,5	1,38
2830,7	39,1	1,0
2876,7	39,0	1,28
2922,6	63,8	1,25
2976,2	61,9	—2,0

*) Heath's data for $I_\lambda(0)$ given in Table 28 -- were corrected also for limb darkening by using coefficient β_λ (Table 25).

* TRANSLATOR'S NOTE: COMMAS REPRESENT DECIMAL POINTS

Heath made observations, at a number of wavelengths, of the diation intensity from the entire solar disk in the region 2550- 00 angstroms on the Nimbus-4 satellite using a double monochromator th a 10-angstrom passband. The original results of these observa- ons for $\lambda < 3000$ angstroms are given in Table 22, in column 2; the ird column gives the correction factors that allow for the effect absorption lines on the selected 10-angstrom section; these rrections were determined by us based on the spectral trace in Alister's atlas /339/; the continuous spectrum level was drawn ng points selected by Bonnet /320/ for the determination of the asicontinuum. After the intensity of the radiation from the center the solar disk in the quasicontinuum was determined, a correction r limb darkening was made in the Heath data, besides the correc- ns for absorption lines (cf. Table 25 and Chaper Four); averaged (0) values for the 50-angstrom interval are presented in the mposite Table 28.

For $\lambda > 3000$ angstroms, Heath's data correspond to the integrated /228 ectrum of the entire solar disk; averaged over a 100-angstrom terval, they are given in Table 19.

Prag and Morse /400/, just as Heath, investigated changes in the UV solar radiation flux in the region 300-2100 angstroms, using photodiodes as radiation recievers. Combinations of observations made with titanium photodiodes and MgF_2 and SiO_2 windows made it possible to single out the following spectral sections: 300-1150, 1150-1600, and 1600-2100 angstroms. The observations were made on the OV1-15 geophysical satellite in July-August 1968, at altitudes of 130-400 km.

Just as in the case of Heath, intense variations in the radiation flux appeared with the 27-day period. In the section 1600-2100 angstroms the measured flux varied more than 50 percent. These changes correlate best of all with the index of the area of calcium flocculi and much worse -- with radio observations of the integral flux at the wavelength 10.7 cm. Assuming that radiation in this spectral region is caused mainly by radiation in the continuous spectrum and that its variation is caused by the appearance of calcium flocculi, Prag and Morse estimated the brightness temperature in the region of the transition from the spectrum of the photosphere to the spectrum of the chromosphere for the "quiet sun" (with no calcium flocculi) and individually for the calcium flocculi. The temperature of the minimum region for the "quiet sun" was found to be 4450° K with an error of ±100° K, and about 5700° for only the calcium flocculi, which yields an estimate of the brightness temperature for the entire sun near the activity maximum of about 4700° K (depending on the area occupied by the calcium flocculi); this agrees quite well with Heath's estimates.

Measurement series we used in the region of the rocket ultraviolet are compiled in Table 28 and Fig. 58 [33].

The distribution of energy in the integrated spectrum of the entire solar disk F_λ is represented by a single series of observations from the Naval Research Laboratory /378, 391/. It was obtained in relative units and was absolutized by us using coupling to mean data (Table 29) based on the spectral region 3000-3600 angstroms overlapping with Tousey's data /378/; the coefficient for converting from the NRL results to the mean is 0.867. Thus, the NRL results given in /378/ in the Dunkelman-Scolnik system must be reduced by ~ 13 percent.

To determine the mean intensities of radiation in the quasicontinu $I_\lambda(0)$, three partially overlapping series (cf. Fig. 58, Table 28) were used: Widing et al. /389/, Bonnet /320/, and Heath /374/ (the last

33 In Fig. 58 (text page 254 /translation page 202/) the disk-averaged intensity F_λ is given according to Tousey-Detwiler (1), V. P. Kachalov and A. P. Yakovleva (2), and $I_\lambda(0)$ is given according to Widing (3), Parkinson and Reeves (4), Bonnet (5), Heath (6), and Houtgast (7); (8) represents Drummond's filter data. All the quantities are in the units erg/cm^2 · sec · sterad · cm.

series was reduced for the effect of absorption lines and for limb darkening; cf. above). These three series show an average mutual agreement within the limits 5 percent, which must doubtless be regarded as an excellent agreement, considering the difficulty of making the observations in this spectral region. The techniques of absolutizing all three series differ and are not interrelated, which significantly increases the reliability of the results that are in agreement.

We regard as clearly erroneous the fourth series of measurements by Parkinson and Reeves [399], also shown in Fig. 58. These results are three to four times smaller than the others, though they pertain to the year of maximum solar activity and might have been only somewhat higher than the remaining values [cf. Fig. 4 at the end of Section 4 dealing with IR measurements].

Even though the data of Tousey and Detwiler is unique, their reliability has been confirmed by other results in the "blue" and "red" ends of this series. In the region of the temperature minimum the radiation intensity, in the continuous spectrum of the center as well as in the integrated spectrum of the entire solar disk, must coincide, since limb darkening is not involved here, there are nearly no absorption lines, and the emission lines are few. Actually, the data of Detwiler and Widing show excellent agreement (both series of observations were made at roughly equal distance from the phase of maximum solar activity). For the "red" end of the spectrum where the comparison of Tousey's results with the data for the quasicontinuum is difficult owing to the absence of reliable corrections for absorption results for intervals as wide as 50 angstroms, there are data of V. P. Kachalov and A. V. Yakovleva [384, 385]. These data must be only somewhat higher, since even though the integrated spectrum was recorded, it was not of the entire disk, but only with a somewhat larger weight for the central portion of the disk, but whose value is not precisely specified (cf. above). /230

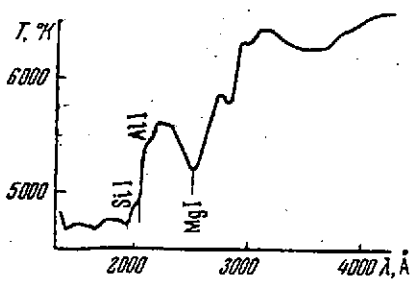

Fig. 51. Wavelength function of brightness temperature in the UV spectral region

Tousey's results were confirmed by yet another independent source -- observations with narrow interference filters made by the Drummond group [141, 142]. The agreement of these results within the limits 10 percent must (cf. Fig. 58) be regarded in this case as good, since the profile of the passband of the Drummond system was not precisely known; in recomputing, we assume it to be rectangular, which of course is quite a rough approximation.

Interestingly, rocket UV data on the energy distribution in the solar spectrum agree internally better than series of observations made in the near UV spectrum and even in the visible region where the deviations sometimes are 20 percent (cf., for example, Table 19). But if, for example, we couple the relative data of Tousey and Detwiler to the data of the US committee, we find that in the temperature-minimum region Widing's absolute data for the continuous spectrum of the center will be 20 percent smaller than Detwiler's data for the integrated spectrum of the entire disk. Then by using the derived mean intensities, we obtained an agreement of the results in the ultraviolet within the limits that actually exist between the individual data and it appears to us that this serves as an unnecessary argument in favor of the mean data on the distribution /2
of energy being the more reliable.

The results of determining the brightness temperature for the center of the solar disk in the quasicontinuum in the near and rocket UV spectrum are shown in Fig. 51. The temperature drops off from ~ 6500° K at 4000 angstroms down to ~4700° K in the region 1400-1700 angstroms. Wavelengths of several limits of series causing distinct "waves" in the pattern of the brightness temperature curve are noted in the figure.

We place the discussion of the temperature minimum and possible variability of UV radiation at the close of the following section, since data of UV as well as IR measurements are important to this matter.

4. Infrared Spectrum of the Photosphere, 3-300 Microns

Measurements in the IR spectral region, just as in the UV region, are severely complicated by intense absorption in the telluric bands of the terrestrial atmosphere (cf. Chapter One). Thus, the region 23-900 microns is completely blocked to observations from the earth owing to the presence of the complex rotational spectrum of water vapor containing a mass of lines distributed rather uniformly over the spectrum; at sea level the wings of these lines broadened by pressure overlap. In high-elevation conditions the situation markedly improves owing to the drop in pressure and the decrease in water vapor content. However, here also measurements are possible only in the short-wave and long-wave limits of this section and in a window of relative transparency at about 350 microns, admitting less than 30 percent of the flux. Naturally, investigations of this spectral region are made now mainly from aircraft and balloons at altitudes of 12-32 km. Even at balloon altitudes most rotational lines of water vapor remain saturated, though the amount of precipitable water in the optical path of a ray is many times less than 1 micron, but because the pressure is negligible the lines become very narrow and therefore with high resolution one can either make measurements in the windows between lines or else with moderate resolution

one can integrate over broad sections; overall absorption by the water vapor proves to be negligibly small in this case.

In the region 3-23 microns there are several windows of relative transparency in which measurements are possible from ground level, chiefly in high-elevation conditions, however in these windows as well observations from aircraft and balloons are to be preferred. /232

The intensity of solar radiation falls off abruptly in the IR spectral region, which significantly simplifies the problem of devising a standard radiation source in reducing observational data to absolute values. Thus, even in the region of about 10 microns the solar brightness is weaker in the visible region, by roughly a factor of 10,000, and radiation intensity of the order of 10^{10} erg/cm^3 · sec · sterad can be ensured by constructing a model of an absolute blackbody with relatively low temperature, of about 1500° K. The low-temperature model is much simpler in design and therefore can be compared directly, without intermediate secondary standards (lamps), with the sun.

The radiation flux in the IR region of the solar spectrum is virtually proportional to the brightness temperature, therefore to reliably determine the latter one needs high-precision measurements of the radiation intensity with errors not more than ~3 percent, if we must know the temperature with an error not greater than 100° K, and more precisely, the higher the wavelength at which the study is made. However, interpretation of measurements in this spectral section is much simpler compared with the far UV spectrum, since here only one appreciable absorption source in the solar atmosphere predominates -- free-free transitions of negative hydrogen ions. Opacity increases in proportion to the square of the wavelength quite monotonely, without jumps, and the drawing nearer to the surface layers of the photosphere and then the transition to the chromosphere takes place slowly; the minimum-temperature region is reached somewhere beyond 20-50 micons and has a shallow slope.

Observational series of several authors in the IR region of the spectrum agree with each other and generally better than in the visible and UV spectral regions (with the exception of the region 3-4 microns where the agreement is poor, but clearly owing to the random error allowed by the US Solar Radiation Committee; cf. end of section). The superior agreement of the results is evidently explained first of all by the possibility of a direct comparison of solar radiation with blackbody radiation, which ensures a reliable intensity scale. In addition, the virtually complete absence of reductions that allow for the effect of Fraunhofer lines for different widths of the passbands of the receivers used by various workers also reduces the disparity of results. There are very few Fraunhofer lines in the IR region. /233

Below we present brief characteristics of the studies made of the IR spectrum on the subject of interest to us. As earlier, the investigations we utilized in deriving mean data are complied in a table; cf. Table 23.

A few words are in order concerning the submillimeter and millimeter spectral sections. For $\lambda > 300$ microns observed radiation exits from the chromosphere, and then from the corona. Here the measurements are usually made by radio astronomical methods. However, in order to grasp the nature of the transition of emission intensity and brightness temperature of the sun from the photospheric layers to the higher layers, we present also purely radio astronomical data, using the very complete and detailed review by A. G. Kislyakov /71/. Here, though all points plotted in Fig. 61 for $\lambda > 300$ microns are taken from Table 5 in /71/, still the average trend (cf. Fig. 5) of the review by A. G. Kislyakov and our own (cf. further, Fig. 61) differs somewhat as the result of the fact that in the two years elapsing between when the reviews were written the "blank space" in the IR region between 13 and 300 microns began to be filled; new data appreciably modify our concepts of the trend of the brightness temperature in the far IR and submillimeter regions.

F. Saiedy and R. Goody /96/ were the first to measure the solar radiation intensity in the atmospheric window at 11.1 microns lying between the strong bands of ozone at 9.6 microns and of carbon dioxide gas at 15 microns.

The solar spectrum was compared directly with the spectrum of a blackbody (cf. Table 23); alternately a 17 mm diameter solar image or the image of a blackbody was projected onto the spectrometer slit 7 x 1.9 mm in size using a siderostat and a parabolic mirror; the fluxes were equalized with a sector diaphragm; the solar flux had to be weakened only by a factor of 6. The region 8-14 microns was scanned; scattered light was blocked by inserting an /2 indium antimonide filter with a lead chloride layer cutting off only the wavelength interval under study.

The blackbody was a sphere made of sillimanite (Al_2SiO_5) and heated with a current passing through a wire wound over the surface of this sphere. The temperature of the radiator was 1300° K; it was monitored with a calibrated platinum-platinum-rhodium thermocouple with a precision of ±2° C; the uniformity of the temperature in the radiating cavity was kept within the limits ±1°.

The atmospheric transparency coefficient was determined by the Bouguer method; it fluctuated within the limit 0.83-0.97 and depended heavily on the water vapor content in the atmosphere. Two corrections were made in the measurement results to allow for the following factors: 1) the coefficient of reflection of the supplementary mirror collimating the light leaving the blackbody

TABLE 23. COMPILATION OF OBSERVATIONS USED IN CONSTRUCTING MEAN DATA ON THE DISTRIBUTION OF ENERGY IN THE FAR IR SPECTRAL REGION OF THE SOLAR PHOTOSPHERE, 3-300 MICRONS

Authors, observational period, el. above sea level	What was observed, spectral region, & instrument	Method of absolutizing measurements	Radiation receiver	Precision in authors' estimate
1. Saiedy, Goody [96] 1958, 5 days, sea level	Disk center, 11.1 μ double diffraction monochromator	Blackbody, T 1300° K	Acoustico-optical	$\pm$ 0.8 % ($\pm$30° K)
2. Saiedy [318] sea level	Disk center, 8.63 and 12.02 μ, double diff. monochromator			$\pm$(1-2) % $\pm$(40-80)° K
3. Farmer, Todd [401] compilation of 10 sources 1948-1960, from 0 to 14.7 km	Entire disk, integrated spectrum, 3.5-5 μ, various spectral instru.	Not described	Various	$\pm$3%, $\pm$100°K
4. F. Murcray et al. [402], 28 May 1963, balloon, 31 km	Entire disk, integrated spectrum, 4-5 μ, Littrow spectrometer, CaF_2 prism, filter cut-off of emission, $\lambda < 3.4$ μ	Blackbody, T 2500° K	Bolometer	$\pm$2 %, $\pm$70° K
5. Kondrat'yev et al. [73,403], 1961-1963, 3.1 km	Disk center, 3-13 μ spectrophotometer, NaCl prism, germanium filter	Blackbody T 712 and 802° K	Acoustico-optical	$\pm$(70-100)°K

TABLE 23. /CONCLUSION/

Authors, observational period, el. above sea level	What was observed, spectral region, & instrument	Method of absolutizing measurements	Radiation receiver	Precision in authors' estimate
6. Lena /317/, 1969 cf. Ch. IV	Disk center, 10-60 μ			
7. Koutchmy, Peyturaux /97/, 1968, 1.6 km	Disk center, 5, 10-13, 20-24 μ ; double monochromator, prisms: quartz, NaCl, KBr, CsI	Two blackbody models T 800 and 1200° K	Schwartz thermocouple	$\pm$(1-3) %
8. Eddy, Lena, MacQueen /406, 407/, 1968, aircraft, 12.8 km	Entire disk, integ. spectrum, 80-400 μ, Michelson interferometer, beam splitter, metal grid, polyethylene filters & optics	Blackbody T 700° K	Germanium bolometer at T 2.2° K	+260° K
9. Gay /410/, 1967-1968, balloon, 25-30 km	Central part of solar disk, 50-200 μ Michelson interferometer, polyethylene beam splitter, optics, filters	Sky and Dewar flask containing liquid He and N	Pneumatic detector	$\pm$500°°K
10. US Solar Radiation Committee, cf. Table 20	Entire disk, integ. spectrum, 3-15 μ			

adiator; it was 0.979 for λ 11.1 microns; 2) variations within ıe limits 5 percent of the reflectivity of the siderostat mirror ; a function of the angle of incidence of the rays.

The radiation intensity of the center of the solar disk based ı the Saiedy and Goody measurements was found to be :.408 $\pm$ 0.016) $\cdot$ 10^{10} erg/cm^2 $\cdot$ sec $\cdot$ sterad $\cdot$ cm, and the corres- ɔnding blackbody temperature was 5036 $\pm$ 30° K.

Saiedy /318/ continued the work of Saiedy and Goody ıd, employing the same technique, Saiedy determined the ıtensity of radiation from the center of the solar disk in the ındows of relative terrestrial atmospheric transparency at 8.63 ıd 12.02 microns; measurements were conducted at the same time f solar limb darkening (cf. Chapter Four) in the region from 8.63 ɔ 12.95 microns. The 8.63-micron window contains lines of nitrogen :ide N_2O, which do not permit direct use of Bouguer's law. There- ɔre the departures from Bouguer's law had to be determined first ased on data of the transparency of N_2O for different air masses, ıd then the extra-atmospheric radiation intensities were determined. ıe radiation was found to be 6.530 $\cdot$ 10^{10} and 1.774 $\cdot$ 10^{10} g/cm^2 $\cdot$ sec $\cdot$ sterad $\cdot$ cm for 8.63 and 12.02 microns, respectively, ɔr the center of the solar disk, and the brightness temperatures ere (5160 $\pm$ 40)° and (5050 $\pm$ 80)° K (cf. Fig. 60).

C. Farmer and S. Todd /401/ gathered data on measurements of ·lar radiation intensity taken at different altitudes above sea level ɔ to 14.7 km in the spectral region 3.5-5.5 microns. Ten studies /237 ıre critically analyzed, half of which were not published, and in ıly three were the results presented in absolute units. All observa- ions were reduced to a single system in which the envelope plotted ased on observations at the altitudes 5.2-14.7 km is dopted as the distribution of energy in the spectrum of the entire ɔlar disk outside the atmospheric limits (Fig. 52). The error in etermining absolute intensities was assumed to be $\pm$3 percent (or 100° K). Some of the studies of the authors discussed in the /238 eview of the observations investigated the center of the solar isk, while others investigated the entire disk. Whether solar imb darkening attaining values of the order of 3 percent in this egion were considered in reducing all data to the single system as not indicated. Also not described was the method of absolutizing ased on unpublished data of Talbert and Templin.

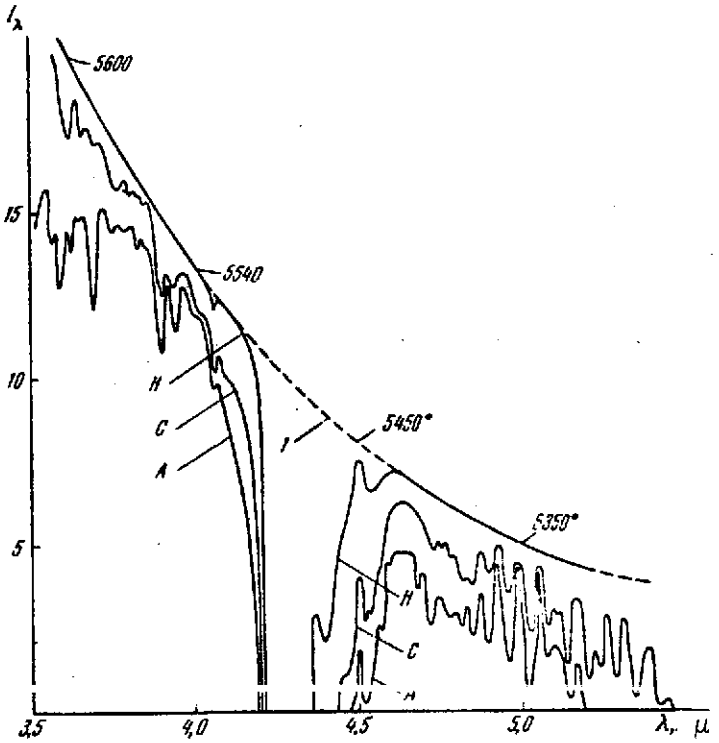

Fig. 52. Spectrum of the sun in the region 3.5-5.5 microns from observations at various altitudes. A = sea level, C = altitude of 5.2 km, H = 13.5-14.7 km, 1 -- outside atmospheric limits. Based on the data of Farmer and Todd /401/. Brightness T values are indicated based on mean data (Table 30).

F. Murcray, D. Murcray, and W. Williams /402/ made observations on a balloon on 28 May 1963 at an altitude of 31 km in the spectral region from 4 to 5 micron. They used a Littrow type spectrometer with CaF_2 prism; the selected region was scanned each 2 minutes; the radiation receiver was a bolometer; measurement with $\lambda < 3.4$ microns was cut off with a filter. The solar image was formed at the spectrometer slit; the slit subtended 18' for the solar diameter of 31' and the guidance precision was $\pm 6'$. After the flight, a comparison was made with the spectrum of a blackbody radiator (the stability of the spectral and receiver systems was checked by recording the spectrum of an uncalibrated, but time-stable radiation source). The blackbody was a cylinder of tungsten foil, heated with electric current, with a lens-diameter ratio of about 10:1. The entire system with supplementary envelope to reduce reflection losses was mounted inside a copper shell with a CaF_2 window cooled with water. A vacuum of the order of 0.1 mm was maintained in a nitrogen or mercury atmosphere. The working temperature of the blackbody (about 2500° K) was measured with an optical pyrometer; the reproducibility of pyrometer readings was ensured within the limits $\pm 10^\circ$ K. An auxiliary parabolic mirror was used to compare the blackbody radiator with the sun and fill the spectrometer aperture. Calibration of recordings wavelength was carried out using coupling to the absorption band of carbon dioxide CO_2, 4.28 microns, with known instrument dispersion. A correction factor 0.953 x 0.99 x 0.98 was introduced into the results of measuring blackbody radiator intensity; this factor allowe

or, successively, the transmission coefficients of the blackbody indow, the emissivity of tungsten, and the coefficient of reflection f the aluminized mirror in the spectral region studied. The bolo- eter sensitivity depends strongly on ambient temperature; tracings t which the bolometer temperature was identical were selected, both /239 n recording solar emission as well as in recording blackbody radi- on. The measurement results of these authors are given in Fig. 0. Formally, they pertain to measurement of the entire solar isk (Fig. 2 in /402/), but since during guidance the spectrometer lit subtended the center and some part of the boundary zone (gui- ance precision ±6'), it remained unclear how the reduction to he entire disk was done.

A group of researchers from Leningrad University: I. Ya. adinov, S. V. Ashcheulov, S. D. Andreyev, and A. V. Poberovskiy 73, 403/, led by K. Ya. Kondrat'yev, investigated absorption in he terrestrial atmosphere in the region 3-13 microns in 1961-1963, t sea level as well as in high-elevation conditions (Peak Terskol, 100 m in elevation; cf. Fig. 8). These observations were used to etermine the radiation intensity of the center of the solar disk utside the terrestrial atmosphere.

The studies were made with an automatic thermostated spectro- hotometer constructed on the basis of the IKS-12 series-built pectrometer with rock-salt prisms as the dispersing component cf. Table 23). A Cassegrain mirror system formed the solar image t the spectrophotometer slit; the guidance precision was about 0"; the slit subtended the disk center. The radiation receiver as of the acoustico-optical type; at its input was placed a germanium ilter cutting out short-wave radiation and thus reducing the level f scattered light.

The tracing of the solar spectrum took 9 minutes; at the begin- ing and the end of the observations a signal from a reference tandard lamp was recorded in the wavelength corresponding to the aximum equipment sensitivity. The intensity of solar radiation in he wavelength interval studied varied by nearly three orders; this ariation was to some extent automatically compensated by the pre- alculated variation in slit width with wavelength.

In reducing the results to absolute units, a specially designed lackbody was employed at two temperatures: 712 and 802° K (cf. hapter Three). The image of its aperture was formed at the entrance lit of the spectrophotometer by means of the same Cassegrain system /240 s for the solar image; this did away with the necessity of additional studies of the optics.

In processing observations, the extension beyond atmospheric limits was carried out with the Bouguer method for sections relatively free of absorption in the bands of the terrestrial atmospheric olecules. Time intervals with the smallest water vapor content ere selected. Measurement results are presented in Figs. 60 and 61.

One must remember that the data in the interval 4-7.5 microns were obtained by interpolating between results for points at approximately 3.7 and 8 microns, since this interval is nearly entirely overlapped by intense absorption in the CO_2 band at 4.2 microns and the H_2O band at 6.3 microns. The point at 3 microns is evidently extrapolated.

The results of the observations made by R. Beer [40] are at present, one must admit, only of historical importance, though the spectral region 20-50 microns selected for investigation is extremely interesting since before Beer no one had studied close to the region of the temperature minimum in the IR solar spectrum. The observations were made with a Michelson interferometer launched on a balloon in August 1965. The results were obtained only in relative units and were absolutized by extrapolation to the data of Saiedy and Goody [96]. Beer's data extrapolated by him also to 100 microns are plotted in Fig. 61. The agreement with other observational results performed by the method of comparison with a standard emission source is poor and in deriving the mean curve of energy distribution we did not take these data into consideration.

G. F. Sitnik [40] observed the IR spectrum of the sun in the region 2.5-5 microns in the High-Elevation Expedition of the Astronomical Institute imeni Shternberg (h ~ 3 km) for 10 days in 1958. A IKS-6 spectrometer was used; extra-atmospheric values of the radiation intensity of the entire solar disk were determined by the Bouguer method, however the stability of optical properties of the terrestrial atmosphere was checked in the visible spectral region where there are no water vapor bands, therefore this monitoring may not have been effective enough. The absence of a record of residual absorption in the water vapor bands somewhat detracts from the reliability of the results. Sitnik's data are plotted in Fig. 60.

The results of P. Lena [31], who measured the brightness temperature in the region 10-60 microns, are actually a by-product of measurements he carried out in 1969 of solar limb darkening in these wavelengths and are discussed in greater detail in Chapter Four; the results are also included in Fig. 61. /2

In the work by S. Koutchmy and R. Peyturaux [97], a double monochromator with replaceable prisms made of quartz and the salts NaCl, KBr, and CsI was used. A Schwartz thermocouple was used as the receiver. The observations were made in 1968 in the Pyrenees (h = 1.6 km) in the relative atmospheric windows at $\lambda \sim 5$, 10-13, and 20-24 microns. The water vapor content during the observational period was monitored by a spectroheliograph[34], adjusted for the water vapor Φ band; its calibration curve yielding the dependence of H_2O content on the ratio $T = I_\Phi/I_o$ was plotted from literature data.

[Footnote 34 on following page]

Two absolute blackbody models were used in standardizing the observations -- graphite and metal. The disk center was observed; six intensity values were obtained for it, shown in the composite graph (Figs. 60 and 61).

Investigations made by a group of French scientists -- J. Eddy, P. Lena, and R. MacQueen /406, 407/, are of interest for a somewhat closer examination: the experiment was carried out in the far IR region 80-400 microns (125-25 cm^{-1}) on an altogether modern level, both in technical terms as well as in the well-thought-out method. The observations were made on the same NASA-711 aircraft as was used by the Drummond and Thekaekara groups (cf. above). The series of flights in August 1968 took place at an altitude 12.8 km; the flight velocity was selected so that the elevation of the sun was kept constant, 65 $\pm$ 2°, during the observations.

A Michelson interferometer was used and the spectrum of the entire solar disk was investigated in the region 80-400 microns (125-25 cm^{-1}). A metal grid served as the beam splitter in the /242
interferometer, affording a maximum instrument efficiency in the region about 400 microns. All mirror surfaces of the interferometer were gold-coated. The modulator, both of whose surfaces were mirrored, alternately fed to the interferometer with a germanium bolometer as the radiation receiver, a signal from the sun and sky, then from the sky, then from the blackbody (see Table 23 and Fig. 53). The blackbody was a cylindrical hollow with stainless steel walls with a reflection coefficient of ~ 43 percent for λ 337 microns; the dimensions of the cavity provided an emissivity of 0.99 $\pm$ 0.005. The blackbody temperature of 700° K was /243
selected so that the signals from the sky and the blackbody were approximately equal.

---

34 A photometer with filters, one of which cut out the water vapor Φ band, and the others -- spectral regions alongside it, made it possible to obtain the ratio of $T = I_\Phi / I_\Psi$, which is dependent on the equivalent band width.

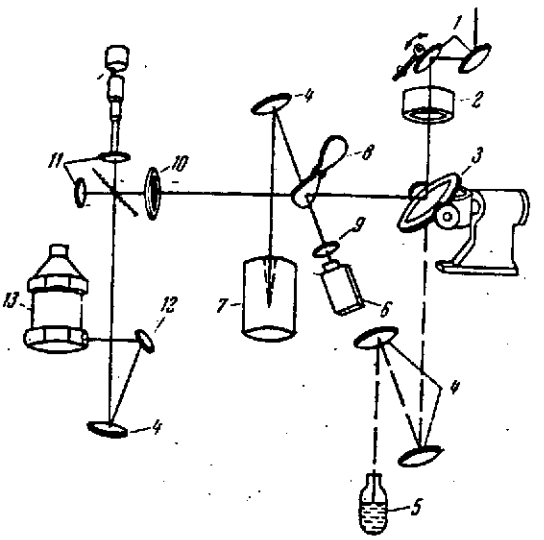

Fig. 53. Optical scheme used by the Eddy group for observing solar radiation in the region 80-400 microns.
1 -- two "coelostat mirrors"
2 -- crystalline quartz window
3 -- mirror of the heliostat
4 -- plane and concave off-axis parabolic mirrors
5 -- Dewar vessel containing liquid nitrogen
6 -- Golay detector
7 -- source of "black" radiation
8 -- modulator
9 -- polyethylene condenser lens with black polyethylene filter
10 -- three-layer filter of black polyethylene
11 -- Michelson interferometer with 12-micron thick nickel grid with lattice constant 127 microns
12 -- plane matte mirror
13 -- germanium bolometer cooled to 2.2° K at a pressure of 21 mm

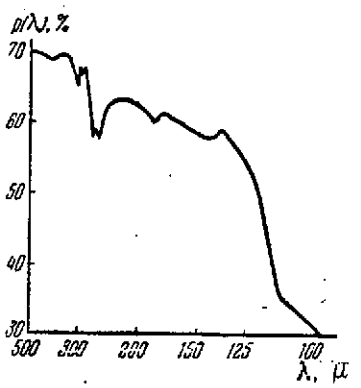

Fig. 54. Spectral coefficient of transparency of aircraft window made of crystalline quartz, 7 mm thick, in the spectral region 100-500 microns

To monitor the stability of atmospheric transparency and the constancy of blackbody modulation, the modulated signa were fed also to the Golay detector (cf. Fig. 53) equipped with a broad-band filte cutting off short-wave radiation.

The difference between the signals from the sun I_0 and from th sky I_s /s = sky/ (both signals were calibrated based on the blackbo signal; the optical path length for the blackbody and the sun within the instrument were selected to be identical) permitted cancelling out radiation of the sky and the instrument. The solar temperature was determined from the relation

$$T_o = I_o - I_s / \alpha \beta \gamma G R_{123} ;$$

the coefficients $\alpha\beta\gamma G$ were determined as follows: α is atmospheric transparency from the analysis of the atmospheric spectrum; β is

ıe transparency of the aircraft quartz window investigated in the aboratory; the measurement results are presented in Fig. 54; the roduct γG, where γ is the transparency of air along the path from ıe aircraft window to the modulator and G is a factor that allows for adiation constants and the wavelengths, was determined y means of calibration measurements of the blackbody relative to he emission of liquid nitrogen in the Dewar vessel (cf. Fig. 53).

The intensity of solar radiation was measured n the atmospheric windows with a transparency coefficient not less ıan 97 percent (cf. Table 24). Absorption was too high in the pectral region studied for $\lambda < 238$ microns; reliable measurements roved to be impossible. On the average, T in the region 238-312 icrons was 4370° K, with an error of ±260° K. The precision of easurements was restricted mainly by the fact that the water vapor /244 ontent in the atmosphere varied appreciably; the layer of recipitated water averaged 2.9 ± 1.2 microns, hence the error in he determination was $\Delta\alpha/\alpha = 0.009$ and $\Delta T/T = 0.06$.

TABLE 24* ATMOSPHERIC WINDOWS IN THE REGION 230-315 MICRONS FOR THE ALTITUDE ~ 13 KM AND BRIGHTNESS TEMPERATURE OF THE SUN BASED ON THE DATA OF EDDY ET AL. /406/

λ, μ	ν, cm⁻¹	Transparency			T_b
		H_2O	N_2O_2	total	
238	42,05	0,99	0,985	0,98	4401
288	34,70	0,99	0,988	0,98	4438
298	33,60	0,98	0,988	0,97	4294
312	32,10	0,98	0,989	0,97	4338

* TRANSLATOR'S NOTE: COMMAS REPRESENT DECIMAL POINTS

T could not be measured also for the region with $\lambda > 333$ microns, lthough the sensitivity of the measurement system was adequate. ın anomalous depression of solar radiation was observed in this spectral egion; sky brightness was greater than solar brightness. The same epression was observed by Gebbie et al. /408/, and by J. Biraud et l. /409/. A satisfactory explanation for this fact has not been ound.

Gay /410, 411/ measured the brightness temperature in the spec- ral region from 50 to 200 microns. The equipment was lifted on a tabilized gondola of a stratospheric balloon to elevations of 5-30 km. The mirror of a Cassegrain telescope with a 40 cm diameter and with a elative aperture variable within the limits f/1 - f/5 (with polished

nickel coating) formed the solar image, from which 26' was subtended by the diaphragm (guidance precision ±10"). Then a polyethylene field lends sent a beam of light to a mirror modulator and then to the Michelson interferometer (cf. Table 23). A Mylar polyethylene film was used as the beam-splitting plate in the interferometer. A second polyethylene lens formed the image of the principal mirror at the quartz window of the pneumatic detector. Radiation with $\lambda < 50$ microns was cut off, moreover, by two polyethylene filters.

To cancel out intrinsic equipment radiation and to standardize /245 the spectrogram, sky light was also sent to the modulator; the temperature of the sky in the vicinity of the sun was assumed to be -50° C. After the flights the spectra were standardized, in addition, in the laboratory: the entire instrument was placed in a vacuum chamber, a Dewar flask filled with liquid helium or nitrogen served as the source of "black" radiation.

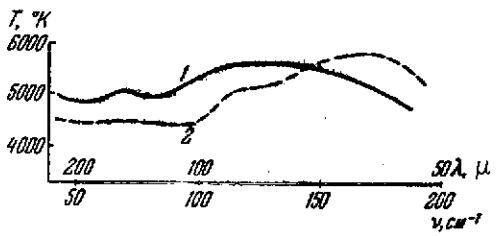

Fig. 55. Brightness temperature of the entire solar disk in the region 50-200 microns based on the data of Gay /410/. Results obtained by coupling to sky measurement -- 1, and by coupling to the laboratory source -- 2.

Three flights were made from June 1967 to January 1968; the author regards the third flight as the most reliable; the results of measuring the brightness temperature of the central portion of the solar disk (which is practically equal to the temperature of the entire solar disk, since limb darkening is very slight in this region) are presented in Fig. 55 and in the composite graph (Fig. 61) for this ascent. The temperature has an appreciable maximum in the region ~ 150 cm^{-1} (~ 70 microns), though there is no complete certainty that it is the actual one. The deviations in temperature values determined by coupling to sky radiation or to radiation from the laboratory source are large, sometimes more than 700° K. Even larger are the deviations between the results of the first and third flights and results presented in the preliminary publication /411/.

Gay also determined the water content in the atmosphere over the balloon; it was found to be 0.022 micron for the atmosphere over 28.4 km and 0.077 micron over 25 km; this is much less than in measurements made by other authors.

The most detailed data for the integrated spectrum of the entire solar disk in the region 3-15 microns are presented by the US Committee on Solar Radiation /142, 157/; we described the method of /24

observations and the interpretation of the results in Section 1, together with observations made in the shorter-wave region, since the Committee presented mean-weighted results of observations for all five instruments, covering the region 0.3-15 microns, and it was difficult to single out a spectral section owing to the absence of all the initial data (cf. Section 1).

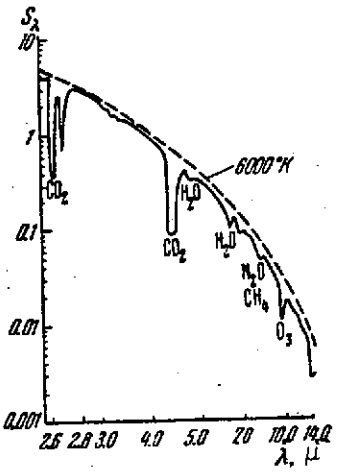

Fig. 56. Solar spectrum in the region 2.6-14 microns for M = 1.13 according to the data of Thekaekara et al.

Still, there are grounds to assume that the Committee's data in the region 2.5-5 microns are erroneous. Actually, in the composite graph Fig. 60 the Committee's results formed two strange humps, which are of low probability from what we know about the trend of the absorption coefficient in the solar atmosphere in this spectral region. The results are based on observations made with a Perkin-Elmer monochromator in the section up to 4 microns and on a Michelson interferometer in the interval 3-15 microns; recent results are shown in Fig. 56, taken from /122/. As we can see in the figure and as has been stressed by the authors in the text of an article comparing observations with the mean data of Johnson /119/ and Moon /350/, the intensity of the radiation from the entire solar disk at approximately 2-3 microns is close to the level corresponding to blackbody radiation at 6000° K, but not above it, and then, with increase in wavelength, decreases smoothly below this limit, while the mean of Johnson and Moon is assumed to persist at the 6000° K level.

Still, the "hump" of the Committee's data at 3 microns reaches a height of 6570° K for the brightness temperature of the entire solar disk (6780° for the solar center) and 5940° K for 4 microns. This is ~ 800 and 400° K, respectively, above what we can obtain based on the data in Fig. 56.

To plot mean data on the wavelength dependence of the intensity of radiation in the far IR spectrum, we cannot, as was done in the visible region, perform averaging at individual discrete wavelengths, at a certain specified step, since over the enormous interval of this spectral region, roughly 100 times greater (on the wavelength scale) than the section of the visible spectrum, individual observation points are separated from each other sometimes by a distance greater than the extreme points of the visible and near IR regions. /247

Therefore, to plot mean data, use was made of graphical averaging of individual results, where the brightness temperature (of the entire solar disk) was plotted on graphs (cf. Figs. 60 and 61), since it is extremely sensitive to variation in intensity in this wavelength interval. In the construction of the mean, the data of the studies which determine the intensity of radiation from the center of the solar disk /96, 318, 73, 317/ are reduced, using the coefficient β that allows for solar limb darkening (cf. Table 27), to the intensity of the entire solar disk. In plotting the mean curve, the reliability of a result was taken into account, as far as possible. The most reliable for the region with $\lambda > 3$ microns were assumed to be the data of Saiedy and Goody /96/, Saiedy /318/, the Kondrat'yev group /73/ (with the exception of points obtained by interpolation and extrapolation), Lena /317/, Koutchmy and Peyturaux /97/ for $\lambda\lambda$ 21 and 24 microns, a group of Eddy, Lena, and MacQueen /406/, and the data of the US Solar Radiation Committee, but with the exception of the section 2.5-5 microns where the Committee's results were evidently erroneous and we did not take them into consideration.

Less reliable were assumed to be the data of Farmer and Todd /401/, since we did not know the method of absolute calibration used in this compilation in averaging individual results; also, it is not clear how the observations made for the center of the solar disk were reduced for the entire disk. The single day of observations and the indeterminacy of reductions to the entire solar disk also diminish the reliability of the result of Murcray and coworkers /402/.

In the works by Gay /410, 411/, first of all confusion is raised by the large deviation between the results of the first and subsequent studies, and also by the disparity in the temperature values determined relative to the brightness of the laboratory source and of the sky, amounting to 700° K and changing sign with wavelength (cf. Fig. 55). /2

The study by Beer /404/, as already remarked, was not taken into account (though the data are plotted in Fig. 61), owing to the law of decrease in temperature with wavelength proposed by Beer, clearly not in agreement with subsequent observations.

Mean data on the distribution of energy in the spectrum of the entire solar disk F_λ and of the solar center $I_\lambda(0)$, illumination S_λ produced at the distance of 1 astronomical unit, and the brightness temperature of the entire solar disk T_δ in the region 3 microns -- 4 mm are presented in Table 30. For wavelengths longer than 25 microns, the limb darkening of the solar disk is very slight (cf. Table 27 and Chapter Four), and we adopted the same value for the intensity of radiation from the disk center as well as from the entire disk, and for the corresponding brightness temperatures.

ccording to a recent study by Shimabukuro /412/, up to 1.4 mm
nclusively, and perhaps even for a longer-wave region, limb
ightening is not observed (it is less than 1 percent). There-
re in the submillimeter and millimeter regions, the mean plotted
noted above, based on the review data of A. G. Kislyakov /71/,
s assumed to be identical for the center as well as for the
ntire disk of the sun.

The results and their reliability are more graphically illus-
ated by Figs. 60 and 61. In Fig. 60 the brightness temperature
the entire solar disk is presented beginning at 0.8 micron.
e local temperature maximum at λ 1.6-1.7 microns is 6350° K [35]
mpared with 5750° K for λ 0.9 micron; it naturally is accounted
r by the minimum in the absorption coefficient of negative
drogen ions in this spectral region. Beyond 3 microns, T decreases
ite smoothly all the way to 5000° K at 12 microns, then follows
abrupt decline, by nearly 500° K at 20-25 microns in the "well"
the temperature minimum (recall that Beer's data smoothing this
op evidently are unreliable and were not taken into consideration;
. above). The region of the temperature minimum encompasses a
ry broad wavelength interval from 25 microns to 300 microns.
tween the data of Eddy, Lena, et al. /406/ for 330 microns, and
e data of L. I. Fedoseyev et al. /68/ for λ 740 microns, there
e no observations; the attempt by Eddy, Lena, and MacQueen to /249
easure the temperature in the region > 330 microns was unsuccess-
ul.

Beyond the region of the minimum, at a point with wavelength
any case not larger than 500-600 microns, an abrupt rise in
ightness temperature begins. The observed radiation is generated
the sun's chromosphere.

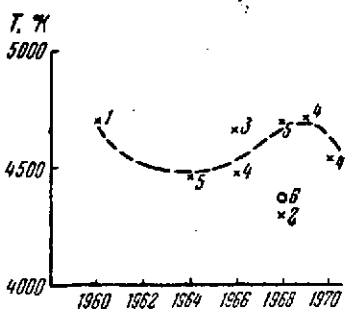

Fig. 57. Brightness temperature in the region of minimum values based on the results of observations in the UV region (crosses) and in the IR region (circle). Results:
1 -- Detwiler
2 -- Parkinson and Reeves
3 -- Widing
4 -- Heath
5 -- Prag and Morse
6 -- Results of IR region observations

35 T_{max} will be 6680° K for the center of the solar disk; cf. able 29.

Fig. 57 presents data on temperature values in the UV and IR spectral regions, where there are grounds to assume that the temperature must pass through minimum values. For the UV region this is the spectral section $1300 < \lambda < 1800$ angstroms; the figure shows the determinations of T for different years. For the IR region, this is the interval $50 < \lambda < 500$ microns; unfortunately, the determinations in this interval began to be conducted only near the last solar activity maximum in 1968, and no time dependence could be established, therefore only the mean taken from Fig. 61 is shown for the IR region.

For the period close to the last solar activity maximum a significant systematic difference shows up clearly between the results of the minimum temperature determination for the UV region, which is close to 4700° K, while it is roughly 300° K less for the IR region, about 4400° K [36].

The reliability of the value T_{min} in the IR region is apparently confirmed, for example, by the estimate of the excitation temperature made by L. Goldberg and E. Muller, based on the variation in equivalent CO line widths in the IR region from 2.3 to 2.5 microns; T_{min} is approximately 4300° K /413/.

The assumption has been advanced that perhaps T_{min} is reached somewhere below 1450 angstrom in in the UV region; apparently favoring this view is the existence of the CO absorption bands /413/, but on the other hand, even from 1350 angstroms the temperature determined from the continuous spectrum increases and apparently is of clearly chromospheric origin.

A final solution to the question of the minimum temperature in the UV as well as the IR spectra, and the site of its localization (as to wavelength) can be provided by further observations; determinations of the actual temperature values and more reliable measurements of limb darkening of the solar disk. For the present we must admit that T_{min} in the IR spectral region is below T_{min} in the UV region, and this discrepancy is greater, the higher the possible error of determination.

Judging from Fig. 57, the dependence of T_{min} on the solar activity cycle based on UV region observations would apparently be evident, but of course, for reliable conclusions we need long-term observations with extremely dependable and, which is the most

---

[36] As noted above, we regard the results of Parkinson and Reeves /399/ as unreliable, since four other completely independent sources using fundamentally different methods of data absolutization yield extremely close results in the UV region (cf. Fig. 58).

iifficult aspect, time-constant calibration of the results in bsolute units.

.. Mean Data on the Distribution of Energy in the Spectrum of the uiet Photosphere in the Region 1400 Angstroms -- 0.3 mm

Mean data on the distribution of energy in the spectrum of he quiet photosphere of the sun in the region 1400 angstroms - .4 mm [37] are based on series of observations, whose characteristics re summed up in Tables 17, 20, 21, and 23, and the actual results f observations -- in Tables 18, 19, 22, 28, and in Figs. 60 and 61.

Mean-weighted values of the spectral characteristics of solar adiation are given, for convenience of use, at the end of the book, n Tables 28-33 and are illustrated by Figs. 51, and 58-61. Tables /251 5-27 present coefficients $\beta_\lambda = 1/\gamma_\lambda = I_\lambda(0)/F_\lambda$ and $\eta_\lambda = 1/\zeta_\lambda$ [38], hich permit converting from the intensity of the continuous spectrum of the solar disk center, $I_\lambda(0)$, to the integrated (together ith absorption lines) intensity of the entire disk (that is, of he sun as a star), F_λ, and vice versa. These coefficients also nable us to derive the intensity characteristics of the integrated pectrum of the disk center $I^{in}(0)$ and the continuous spectrum of he entire solar disk F^c_λ /c = continuum/ (Table 31, cf. below).

Tables 28-30 present, moreover, values for the spectral components of ie solar constant or, in other words, the monochromatic illumination produced by the sun at the mean earth-sun distance, S_λ [39]. he brightness temperature values corresponding to the intensities $_\lambda(0)$ and F_λ are given in the last columns of these tables.

All the results are expressed in the IPTS-68 system (cf. hapter Three and the beginning of Chapter Five). Intensity is iven everywhere in the units erg/cm^2 · sec · sterad · cm, illumination -- in erg/cm^2 · sec · cm, and temperature -- in degrees Kelvin, K.

---

[37] Table 30 presents radiation characteristics to 4 mm inclusively, o afford an idea of the photosphere-to-chromosphere interface.

[38] Table 26 presents for each wavelength interval $\Delta\lambda$, indicated t the end of the table, not the values η_λ and ζ_λ, but the sums of he equivalent widths of the lines occurring in this interval Σw_λ in ngstroms. The coefficients that allow for the effect of lines re: $\eta_\lambda = 1 - \frac{\Sigma w_\lambda}{\Delta\lambda}$, $\zeta_\lambda = \frac{1}{\eta_\lambda}$ (cf. Chapter Four).

[39] $S_\lambda = (\pi R_\odot^2/\Delta^2)F_\lambda = 6{,}8000 \cdot 10^{-5} F_\lambda$ (cf. "Introduction" and /9/).

The mean square-root errors in the determination of $I_\lambda(0)$, F_λ, and S_λ (Tables 28-30), found by the deviation of individual result from the mean-weighted value, are about 4 percent for the interval 3000-4000 angstroms; 3-2.5 percent for $\lambda\lambda$ 4000-8000 angstroms; and further in the IR region are reduced to 1-2 percent. The mean square-root error could not determined in the UV spectral region owing to the small number of series of observations; the deviation between these was within the limits 5 percent, with the exception of the results of Parkinson and Reeves; cf. Section 3. (for a more detailed discussion of the precision of results, cf. "Conclusions".)

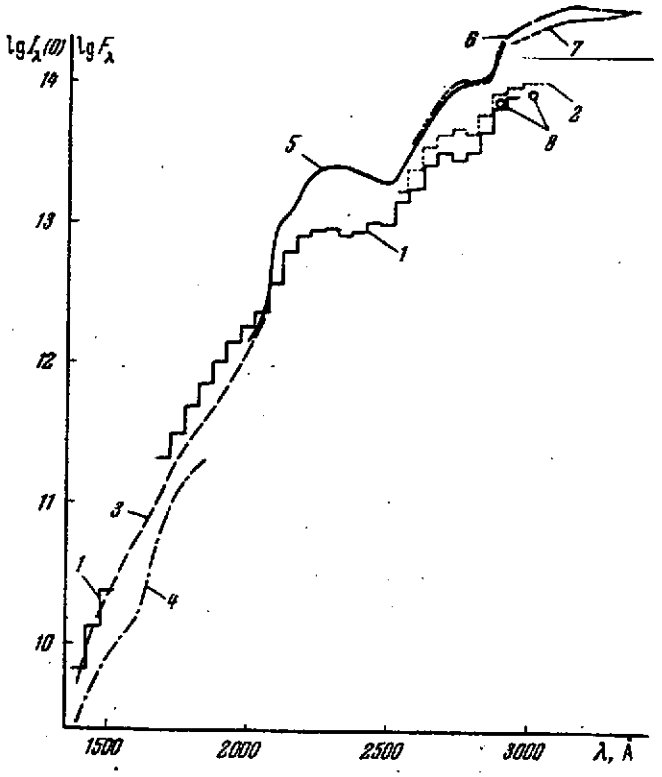

Fig. 58. Results of measuring radiation from the solar photosphere in the rocket ultraviolet region (cf. Footnote 33 on page 182 for symbols) /2

Data given in Tables 31 and 32 were obtained in a different fashion than the remaining data, not by averaging of individual results. In Table 31, the quantities $I_\lambda^{in}(0)$ and F_λ^c in the spectral region 0.3-3 microns are each calculated from the pair of obvious equalities (a) and (b):

$$\text{(a) } I_\lambda^{in}(0) = I_\lambda^c(0)\,\eta_\lambda^{ce}; \quad \text{(b) } I_\lambda^{in}(0) = F_\lambda^{in}\beta_\lambda^{in}, \tag{74}$$

$$\text{(a) } F_\lambda^c = \frac{F_\lambda^{in}}{\eta_\lambda^{ce}} = F_\lambda^{in}\gamma_\lambda^{ce}; \quad \text{(b) } F_\lambda^c = \frac{I_\lambda^c(0)}{\beta_\lambda^c} = I_\lambda^c(0)\,\gamma_\lambda^c. \tag{75}$$

The agreement between $I_\lambda^{in}(0)$ values found from equalities (74) and F_λ^c values found from equalities (75) is good; for nearly the entire spectral region the deviations are less than 1 percent, and only at certain wavelengths in the UV spectrum does the deviation sometimes amount to 2-5 percent (Table 31 presents mean values). /2

Small discrepancies between values obtained based on relations (a) and (b) evidently show that the conversion factors characterizing the degree of solar limb darkening and the fraction of radiation "removed" by the lines from the continuous spectrum are not very far from the true values; otherwise, in converting from the system $I_\lambda(0)$ to the system F_λ, and back again, significant discrepancies would emerge. There must not be complete agreement of the quantities (a) and (b), since the weights of individual series varied within either system, depending on how these quantities were obtained (cf. Section 2).

Table 32 presents the distribution of energy in the integrated spectrum of the entire solar disk in the spectral region 3050-6600 angstroms in the form of the illumination value S_λ (from whence we can easily find the quantities F_λ proportional to it) with small wavelength step of 10 angstroms. These data proved to be necessary in order to solve several problems in comparing the spectra of stars and the sun, in determining the effective wavelength of passbands of narrow-band filters, and so on. There is no special need for these quantities for $\lambda > 6600$ angstroms, since there are very few solar absorption lines. Thus far there is no reliable basis for constructing these tables for $\lambda < 3050$ angstroms.

Table 32 was compiled from results of observations made by the Arvesen group (cf. Section 2, Chapter Five). These results, presented with a step of 4-1 angstrom, were averaged initially based on 10-angstrom intervals, and then based on 100-angstrom sections; the latter were compared with the mean data (Table 29); the normalizing factor was found for expressing Arvesen's data in absolute values that agree with the mean values. The normalizing factor varies with wavelength; it averages 0.94 for $\lambda < 4200$ angstroms, and 0.98 for longer wavelengths. The factors were used to reduce each 10-angstrom interval to our system.

Table 33 is auxiliary in nature: it permits estimating the fraction of the solar contant belonging to the wavelength interval of interest to a reader. The second column of the table presents the quantities $A_{\lambda_1} = \int_0^{\lambda_1} S_\lambda d\lambda$, where λ_1 is given in the first table column; the third column shows what fraction in percent the quantity A_{λ_1} is of the entire spectrophotometric solar constant $S_0 = 137.4$ mw/cm^2. /254

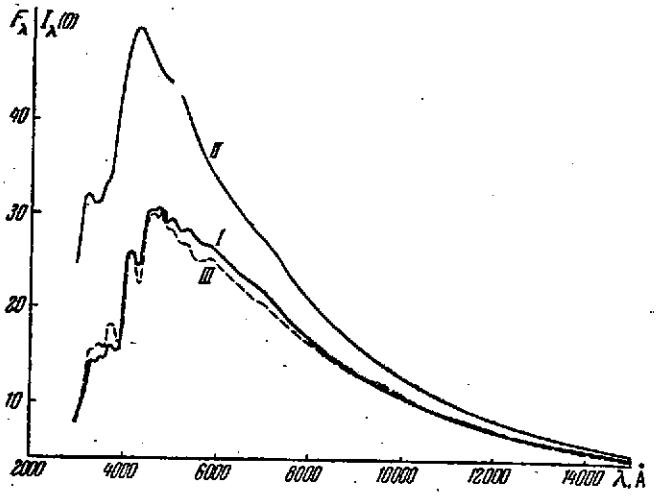

Fig. 59. Distribution of energy in the spectrum of the photosphere based on modern studies; mean data in the region 0.3-1.5 microns (cf. Table 29). cf. text for symbols.

Our mean data F_λ and $I_\lambda(0)$ in the region 3000-14,000 angstroms are given in Fig. 59, where standard F_λ values of the US Solar Radiation Committee are also shown, for comparison. Agreement between our own and the American data is satisfactory on the average, but the sets of data differ most widely in the visible spectral region (the difference is about 3-4 percent). The symbols in Fig. 59 are as follows: I - F_λ, II -- $I_\lambda(0)$; both quantities are given according to Table 29, and III -- F_λ according to /142/; all data are given in the units 10^{13} erg/cm^2 · sec · sterad · cm.

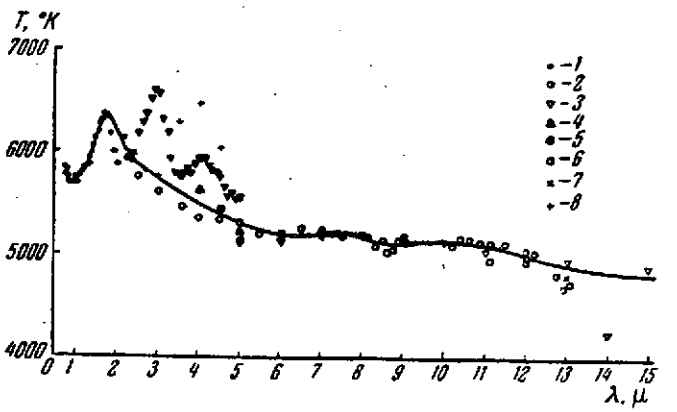

Fig. 60. Results of measuring the brightness temperature of the sun in the region 1-15 microns.
1 -- mean-weighted according to Table 29 data
2 -- Leningrad State University
3 -- US Solar Radiation Committee
4 -- Murcray
5 -- Farmer and Todd
6 -- Saiedy and Goody
7 -- Koutchmy and Peyturaux
8 -- G. F. Sitnik

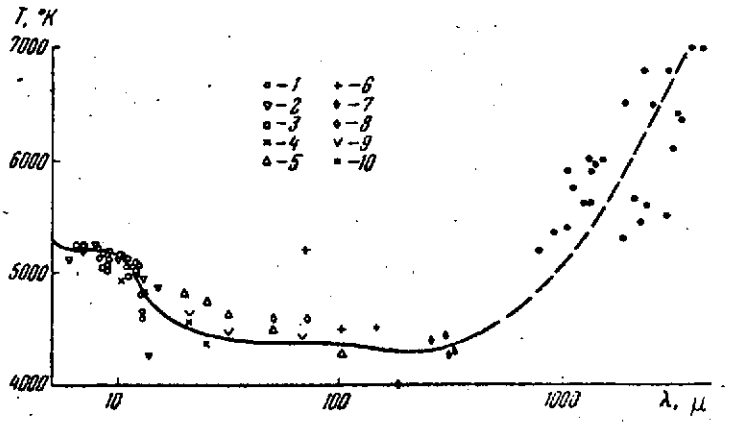

Fig. 61. Results of measuring the brightness temperature of the sun in the region 10 microns to 4 mm.
1 -- Leningrad State University
2 -- US Solar Radiation Committee
3 -- Saiedy and Goody
4 -- Koutchmy and Peyturaux
5 -- Beer
6 -- Gay
7 -- Eddy and Lena
8 -- Mankin
9 -- Lena
10 -- A. G. Kislyakov

Knowing the distribution of energy in the integrated spectrum of /256
he photosphere for the entire solar disk, F_λ, and thus, S_λ (Tables 8-32) in the region from 1350 angstroms to 0.4 mm, we can determine he spectrophotometric solar constant

$$(S_0)_{s.c.} = \int_{0{,}135\,\mu}^{0{,}4\ \text{mm}} S_\lambda d\lambda.$$

s.c. = solar constant/. Solar radiation outside this interval is o more than 0.001 S_0, which thus lies far beyond the limits f the precision in determining S_0. The spectrophotometric solar onstant was found to be

$$(S_0)_{s.c.} = 1.969 \text{ cal/cm}^2 \cdot \text{min} = 137.4 \text{ mw/cm}^2.$$

he precision of this determination can be estimated in two ways, nd they give different results. If we make the estimate based on he scatter of the quantities $\Delta S_\lambda/(S_\lambda)_{av}$ as a function of wavelength, he mean square-root error of determination will be ~ 2.5 percent. n contrast to this, we can compute the solar constant for each eries of measurements in Table 19 (Sitnik's data have been corrected; f. Section 2), by coupling to them the mean distributions for $\lambda > 3$ microns and for $\lambda < 0.3$ micron. In this case the mean square-oot error of the deviation of individual S_0 values from the mean ill be less than 1 percent. This disparity in determinations of he precision of S_0 also evidently points to the fact that errors in tudying the distribution of energy are "specified" to a larger xtent by the error in calibrating the reference standard lamps cf. Section 2 and Conclusions). Integrally, over a wide spectral egion, the reference standard lamps were calibrated well and afforded faithful representation of the total radiation flux. However,

significant systematic errors of the lamp calibration in various spectral regions do exist, which lead to marked errors in deriving the spectral components of total flux.

CONCLUSIONS /257

1. Reliability of data on total flux emitted by the photosphere d its spectral components. Prospects for refining these data. A estion naturally arises: however timely the summing up of results d the derivation of mean values, will they not have to be signifi- ntly modified after 2-3 years? Obviously, we can state with strong surance that in the immediate future significant changes are arcely possible for the following reasons.

On the one hand, the solar constant values determined by two dependent methods are close: direct measurements from high alti- des give 1.94 cal/cm^2 · min, and based on mean data on the distribu- on of energy in the solar spectrum, the constant is 1.97 cal/cm^2·min. reement within the limits 1.5 percent can be regarded as very good; ite recently the mean data alone afforded a spectrum of values thin the limits 5 percent, and individual results -- within the mits ~9 percent (cf. Chapter Two).

The precision which was achieved in determining the solar nstant permits us to hope that we are close to the limit which the variability of the solar constant as a function of the -year solar activity cycle can now come into play. These changes st occur, since the intensity of emission by chromospheric forma- ons, the corona and, possibly, the photosphere in the far UV region, d finally the sunspot-forming activity of the sun vary with the cle. However, discovering the variability necessitates, first of l, observations that are uniform as to method over an extended riod and, secondly, the precision of pyrheliometric measurements st be appreciably enhanced while obviously they are not precise /258 ough for these investigations (cf. Chapter Two). From this reason- ng, we can scarcely anticipate appreciable changes in the value of e solar constant in the near future.

On the other hand, despite the good agreement of the results of easuring the integrated flux of solar radiation, measurements of the pectral components of this flux converge much more poorly. And orest of all is the agreement in the spectral region most accessible observations, from 0.3 to 1.5 microns (in which about 90 percent

of the total flux is generated; cf. Tables 18 and 19 and Figs. 44 and 45). Thus, solar constant values determined by Labs and Neckel, Stair and Ellis and the US Committee from their own measurements are very close: 1.947, 1.950, and 1.940 cal/cm^2 · min; at the same time data on the distribution of energy, used as the basis for determining the solar constant, systematically deviate by up to 15 percent for the region from $\lambda < 4000$ angstroms and up to 8 percent for $\lambda > 5500$ angstroms.

Even more revealing is the example of aircraft observations made by the Thekaekara group, on the basis of which the Committee on the Electromagnetic Radiation of the Sun (US) proposed the standard distribution of energy (cf. Chapters Two and Five). For the same solar constant, 1.940 cal/cm^2 · min, the results of measuring the spectral components of this constant using five individual instruments systematically deviate, sometimes by up to 20 percent. The total identity of conditions and methods of observations as well as the methods of reduction should seemingly exclude differential errors in allowing for losses of light along the path to the radiation receiver (cf. Section 4, Chapter Five). The divergence of the results can evidently be explained in this case only on the assumption that the main error is the total error arising in the calibration of the spectrophotometric standard -- the reference lamp. (Sometimes different lamps, often of the same model calibrated in the same laboratory, were used for different spectral instruments). By Houtgast's estimate (cf. Fig. 46), the mean square-root error in lamp calibration is about $\pm$8 percent for 3000 angstroms and decreases slowly with wavelength, down to $\pm$7 percent at 4000 angstroms. This error significantly exceeds all others, including the error in determining light losses in the terrestrial atmosphere for ground /2 observations at $\lambda > 3400$ angstroms. In the estimate of American investigators /372, 373/, averaged over the spectrum, the lamp calibration error is $\pm$5 percent, which agrees closely with Houtgast's estimate for the UV end of the spectrum.

It is difficult to appreciably lower the errors in calibrating the reference standard lamp at each wavelength. New types of spectrophotometric standards are being developed, but the fundamental solution of the problem evidently is possible only when a single international standard (lamp?) is built, just as reliable as existing reference standards for determination of wavelength, temperature, and so on. Thus, in the near future as long as there is no such standard, one can scarcely anticipate any significant decrease in the error of determining assumed mean data on the distribution of energy in the spectral region 0.3-1.5 microns, where the precision is poorest, and a significant change in the quantities we derived for F_λ and $I_\lambda(0)$ is hardly possible.

In the far UV spectrum, contrary to expectations, observations converge better than in the visible spectrum, but since the series are few in number, there is the danger that this is a random agreement.

Observations in this range are important both for the purposes of astrophysics (for example, the region of minimum temperatures) as well as for geophysics, and are intensively underway.

In the IR spectrum of the photosphere for $\lambda > 2$-3 microns, the departure from the mean is smaller, which evidently is due to the possibility of comparing the solar spectrum directly with the blackbody spectrum. New observations must refine results, especially in the region of the transition from photospheric radiation to chromospheric, in the section of minimum temperatures.

Summing up the discussion of the problem of how precise proposed mean data on the distribution of energy are, we must once more note that they evidently have one significant advantage compared with preceding mean data. They do not carry significant hidden systematic errors of absolutization exceeding the limits of their precision estimates. Actually, the mean square-root error determined by the deviations of individual observations from the mean-weighted value remains approximately the same (2-4 percent) as it was in the earlier-derived mean values of Minnaert, Nicolet, Johnson, and the authors of /1, 118-120/.

However, agreement of solar constant values determined both /260
from individual series of observations as well as from the mean derived from these series, with the solar constant independently found from direct measurements at high altitudes precludes, evidently, the assumption that significant errors in the absolutization of data as a whole are present.

2. Solar constant value. There are grounds to assume that the mean of the solar constant values measured at higher altitudes, 1.943 cal/cm^2 · min, is more properly the lower limit of the true value owing to the fact that light losses in the aerosol layer at higher altitudes were not adequately allowed for (cf. Chapter Two). There are some arguments in favor of the idea that the spectrophotometric solar constant, 1.969 cal/cm^2 · min is somewhat overstated[40]. Therefore, we will assume that the most probable solar constant value is the weighted mean of direct and spectrophotometric determinations with weights inversely proportional to their mean errors (that is, equal to 2 and 1, respectively), and the precision of this value is about 1 percent: $S_0 = 1.95 \pm 0.02$ cal/cm^2 · min = 136 ± 1.4 mw/cm^2. Precisely the same value $S_0 = 1.95$ cal/cm^2 · min was assumed to be the most probable by Labs and Neckel /414/, based on an examination of modern direct and spectrometric determinations, though they used approximately three times fewer series of energy distribution measurements somewhat different data on extra-atmospheric determinations.

---

[40] On the average, measurements made initially in the system of the continuous spectrum, $I_\lambda(0)$, yield somewhat greater values than the data in the system F_λ.

Knowing the solar constant

$$S_0 = 1.95 \pm 0.02 \text{ cal/cm}^2 \cdot \text{min} = 136 \pm 1.4 \text{ mw/cm}^2,$$

we can present several other parameters of the total radiation of the sun [41]:

Effective temperature of the sun, /2

$$T_{eff} = 5770 \pm 10^{\circ} \text{ K}.$$

Mean intensity of radiation,

$$F = (2.00 \pm 0.02) \cdot 10^{10} \text{ erg/cm}^2 \cdot \text{sec} \cdot \text{sterad}.$$

Radiation flux,

$$\pi F = (6.28 \pm 0.06) \cdot 10^{10} \text{ erg/cm}^2 \cdot \text{sec}.$$

Luminosity of the sun,

$$L = (3.81 \pm 0.04) \cdot 10^{33} \text{ erg/sec}.$$

Bolometric stellar magnitude, visible,

$$m_{bol} = -26^m.82 \pm 0^m.01.$$

Bolometric stellar magnitude, absolute,

$$M_{bol} = 4^m.75 + 0^m.01.$$

3. We recommend our derived mean data as the standard energy distribution in the solar spectrum (Tables 28-33). Thus far the obsolete data of Johnson /119/ have been used in a number of studies. The energy distribution compiled by Johnson is such that, for example, it yields the lowest values of the efficiency of solar batteries and the highest fractions of energy absorbed by various spacecraft coatings, compared with many other distributions.

4. Comparing results with models of the solar photosphere. Though this problem was not specifically explored, we still can indicate the spectral regions where modern models, for example, those of Bilderberg or Holweger /367, 340/, agree or do not agree with

[41] In spite of the fact that this most probable S_0 value is 1 percent smaller than the spectrophotometric solar constant, we did not believe it necessary to "fit" the mean data on the energy distribution (Tables 28-30) to agree with the new S_0 value. Introducing a correction over the entire spectrum does not refine our information on the energy distribution, and we do not know what portion of the spectrum actually is responsible for the corrections in S_0.

he trend of mean data on the energy distribution in the continuous pectrum of the solar photosphere. Good agreement is observed in he interval from ~ 6600 angstroms to ~ 20 microns. In the far R region of the temperature minimum and the transition from photo-pheric emission to chromospheric, the agreement is worse; the models redict the onset of the transition to the chromosphere and the imb brightening of the solar disk at a shorter-wave section than s actually observed; the region of the minimum is broader and /262 eeper-lying than the models indicate.

Deviations from the course predicted by the models also xist in the visible spectral region. One can doubt the existence f "waves" in the continuous spectrum in the region 4000-5500 ngstroms (cf. Fig. 43), since the precision of observations is s yet low for final judgment. However, beyond question is the act that in the spectral section close to the distribution maximum, rom ~ 4100 to 4500 angstroms, the models clearly do not correspond o observations, since even the intensity of the observed quasi-ontinuum (somewhat reduced by the wings of intense absorption lines nd faint lines indistinguishable against the background) proves o be higher than the intensity of the model continuous spectrum, hich by definition must not be (cf. Section 2, Chapter Five, and ig. 43). In the UV spectral region the model, yields excessively arge intensity values for $\lambda < 4000$ angstroms and, especially, or $\lambda < 3000$ angstroms (cf., for example, Fig. 50).

5. Devising an international spectrophotometric reference standard. he International Practical Temperature Scale of 1968 proved ossible to put into effect to a large extent due to studies on he precise determination of the melting point of gold made at the nstitute of Metrology imeni Mendeleyev (cf. Chapter Three). We ill hope that colleagues of the VNIIM will also take the initiative n building an international spectrophotometric reference standard hat will ensure the reproducibility of emission intensity over a ide spectral region with a precision not worse than at least 0.5 per-ent. Then we can anticipate obtaining refined data on the distribu-ion of energy in the solar spectrum.

TABLES OF MEAN DATA

TABLE 25.* LIMB DARKENING COEFFICIENTS $\beta_\lambda = I_\lambda(0)/F_\lambda$ (CONTINUUM) IN THE REGION 1400-3000 ANGSTROMS *)

λ, Å	β_λ	λ, Å	β_λ	λ, Å	β_λ	λ, Å	β_λ
1400	1,0	1850	1,124	2300	1,870	2750	1,778
1450	1,0	1900	1,168	2350	1,736	2800	1,730
1500	1,000	1950	1,220	2400	1,674	2850	1,664
1550	1,000	2000	1,292	2450	1,668	2900	1,605
1600	1,000	2050	1,420	2500	1,688	2950	1,570
1650	1,014	2100	1,752	2550	1,728	3000	1,545
1700	1,036	2150	1,968	2600	1,770		
1750	1,060	2200	2,012	2650	1,800		
1800	1 089	2250	1,980	2700	1,800		

*) For region 1600-1900 angstroms, data from interpolation are presented.

* TRANSLATOR'S NOTE: COMMAS REPRESENT DECIMAL POINTS

TABLE 26.** COEFFICIENTS β_λ^c AND β_λ^{in} AND SUM *) OF EQUIVALENT WIDTHS $\sum_{\Delta\lambda} w_\lambda^{ce}$ AND $\sum_{\Delta\lambda} w_\lambda^{d}$ FOR THE SOLAR CENTER AND THE ENTIRE SOLAR DISK (ANGSTROMS) IN THE REGION 0.30-2.6 MICRONS

λ, μ	β_λ^c	β_λ^{in}	$\sum_{\Delta\lambda} w_\lambda^{ce}$	$\sum_{\Delta\lambda} w_\lambda^{d}$	λ, μ	β_λ^c	β_λ^{in}	$\sum_{\Delta\lambda} w_\lambda^{ce}$	$\sum_{\Delta\lambda} w_\lambda^{d}$
0,300	1,545	—	—	51,7	0,315	1,485	1,584	49,4	52,6
0,305	1,525	1,537	51,6	52,0	0,320	1,468	1,566	49,1	52,3
0,310	1,506	1,596	49,1	52,0	0,325	1,450	1,524	40,1	43,0

*) Interval $\Delta\lambda$=100 A for $\lambda < 0.700\ \mu$, $\Delta\lambda$=200 A for $0.700 < \lambda < 0.800\ \mu$, $\Delta\lambda$= 500 A for $0.800 < \lambda < 1.70\ \mu$, $\Delta\lambda$= 1000 A for $\lambda < 1.70\ \mu$

TABLE 26. /CONCLUSION/ /264

λ, μ	β_λ^c	β_λ^{in}	$\sum_{\Delta\lambda} w_\lambda^{ce}$	$\sum_{\Delta\lambda} w_\lambda^{cd}$	λ, μ	β_λ^c	β_λ^{in}	$\sum_{\Delta\lambda} w_\lambda^{ce}$	$\sum_{\Delta\lambda} w_\lambda^{cd}$
0,330	1,434	1,496	33,8	36,5	0,590	1,230	1,235	3,2	3,6
0,335	1,420	1,481	36,8	39,4	0,600	1,226	1,232	2,6	3,1
0,340	1,407	1,468	37,3	39,5	0,610	1,222	1,227	2,9	3,3
0,345	1,396	1,446	36,2	38,4	0,620	1,219	1,224	2,8	3,2
0,350	1,386	1,432	35,0	37,1	0,630	1,216	1,221	2,5	2,9
0,355	1,375	1,420	38,0	40,0	0,640	1,212	1,216	2,1	2,4
0,360	1,366	1,411	41,2	43,1	0,650	1,207	1,209	2,0	2,2
0.3625	1,364	1,405	38,3	40,1	0,660	1,203	1,190	5,4	4,3
0.3675	1,367	1,403	35,9	37,5	0,670	1,199	1,200	1,3	1,4
0.370	1,373	1,409	39,8	41,3	0,680	1,194	1,195	1,2	1,3
0,375	1,395	1,434	44,5	46,0	0,690	1,190	1,192	1,6	1,8
0,380	1,406	1,448	44,5	46,1	0,700	1,186	1,190	1,9	2,2
0,385	1,406	1,423	49,3	49,9	0,720	1,178	1,182	4,4	5,0
0,390	1,405	1,450	51,7	53,2	0,740	1,172	1,177	5,2	6,0
0.395	1,402	1,443	47,2	48,7	0,760	1,168	1,170	2,8	3,2
0,400	1,399	1,423	34,0	35,1	0,780	1,163	1,164	2,2	2,4
0,405	1,394	1,429	25,1	26,9	0,800	1,159	1,161	2,8	3,2
0.410	1,390	1,416	25,0	26,4	0,850	1,150	1,147	15,0	13,5
0.415	1,384	1,417	24,0	25,8	0,900	1,144	1,151	19,5	22,5
0,420	1,377	1,414	25,0	27,0	0,950	1,138	1,140	7,5	8,5
0,425	1,370	1,410	28,6	30,6	1,00	1,132	1,126	14,5	12,0
0,430	1,364	1,386	31,5	32,6	1,05	1,127	1,132	19,0	21,0
0,435	1,357	1,379	28,3	29,4	1,10	1,123	1,126	12,5	14,0
0,440	1,350	1,381	21,0	22,8	1,15	1,119	1,121	8,0	9,0
0,445	1,344	1,374	17,1	18,9	1,20	1,114	1,117	7,5	9,0
0,450	1,337	1,364	13,0	14,7	1,25	1,110	1,110	1,2	1,0
0,455	1,330	1,358	10,8	12,6	1,30	1,106	1,105	6,5	7,0
0,460	1,324	1,349	9,6	11,3	1,35	1,102	1,102	0,85	1,0
0,465	1,318	1,340	8,6	10,1	1,40	1,098	1,098	0,8	1,0
0,470	1,313	1,335	9,3	10,8	1,45	1,095	1,096	2,0	2,5
0,475	1,308	1,329	8,7	10,1	1,50	1,091	1,092	3,4	4,0
0,480	1,303	1,319	8,1	9,5	1,55	1,087	1,090	6,4	8,0
0,485	1,299	1,305	11,3	11,7	1,60	1,084	1,084	11,0	11,0
0,490	1,295	1,303	13,1	13,6	1,65	1,082	1,082	7,0	7,0
0,495	1,290	1,309	9,8	11,1	1,70	1,080	1,080	12,0	12,0
0,500	1,286	1,304	10,1	11,3	1,80	1,076	1,076	7,0	7,0
0,510	1,279	1,294	8,8	9,9	1,90	1,073	1,073	8,0	8,0
0,520	1,271	1,286	12,9	13,9	2,00	1,071	1,071	4,0	4,0
0,530	1,264	1,277	8,9	9,8	2,10	1,069	1,069	4,0	4,0
0,540	1,257	1,270	7,0	7,9	2,20	1,067	1,065	8,54	6,0
0,550	1,250	1,259	5,3	6,0	2,30	1,065	1,065	3,0	3,0
0,560	1,244	1,253	5,2	5,9	2,40	1,063	1,063	4,0	4,0
0,570	1,239	1,246	4,3	4,9	2,50	1,061	1,061	2,0	2,0
0,580	1,234	1,241	3,4	3,0	2,60	1,058	1,058	1,0	1,0

** TRANSLATOR'S NOTE: COMMAS REPRESENT DECIMAL POINTS

TABLE 27.* COEFFICIENTS β_λ IN THE SPECTRAL REGION 3-25 MICRONS /265

λ, μ	β_λ	λ, μ	β_λ	λ, μ	β_λ	λ, μ	β_λ
3,0	1,051	7,0	1,026	11,0	1,016	17,0	1,012
3,5	1,044	7,5	1,0245	11,5	1,015	18,0	1,012
4,0	1,039	8,0	1,023	12,0	1,015	19,0	1,011
4,5	1,036	8,5	1,022	12,5	1,014	20,0	1,011
5,0	1,033	9,0	1,021	13,0	1,014	25	1,008
5,5	1,031	9,5	1,019	14,0	1,013		
6,0	1,029	10,0	1,018	15,0	1,013		
6,5	1,027	10,5	1,017	16,0	1,013		

* TRANSLATOR'S NOTE: COMMAS REPRESENT DECIMAL POINTS

TABLE 28. INTENSITY OF SOLAR RADIATION F_λ AND $I_\lambda(0)$ AND ILLUMINATION S_λ BASED ON EXTRA-ATMOSPHERIC OBSERVATIONS BY SEVERAL AUTHORS, MEAN VALUES OF INTENSITY $I_\lambda(0)$ AND BRIGHTNESS TEMPERATURE T_{ce} OF THE DISK CENTER IN THE REGION 1350-3000 ANGSTROMS *)

Author / λ, Å	F_λ **)	S_λ **)	$I_\lambda(0)$ **)				T_{ce} °K
	Tousey [378, 391]		Widing [359]	Bonnet [320]	Heath [373]	mean	
1350	66 8	45 4	—	—	—	66 8	4820
1400	66 8	45 4	50 8	—	—	58 8	4670
1450	13 9	90 4	13 9	—	—	13 9	4710
1500	24 9	16 5	22 9	—	—	22 9	4720
1550	—	—	35 9	—	—	35 9	4700
1600	—	—	55 9	—	—	55 9	4700
1650	—	—	80 9	—	—	80 9	4680
1700	21 10	14 6	13 10	—	—	13 10	4700
1750	31 10	21 6	22 10	—	—	22 10	4750
1800	48 10	33 6	30 10	—	—	30 10	4750
1850	71 10	48 6	42 10	—	—	42 10	4750
1900	10 11	70 6	59 10	—	—	55 10	4730
1950	14 11	95 6	86 10	—	—	75 10	4710
2000	18 11	12 7	13 11	15 11	—	14 11	4860
2050	23 11	16 7	22 11	22 11	—	22 11	4940
2100	37 11	25 7	—	94 11	—	94 11	5420
2150	61 11	41 7	—	126 11	—	126 11	5470
2200	79 11	54 7	—	193 11	—	193 11	5600
2250	89 11	61 7	—	230 11	—	230 11	5600
2300	92 11	63 7	—	256 11	—	256 11	5600
2350	82 11	56 7	—	250 11	—	250 11	5520
2400	87 11	59 7	—	230 11	—	230 11	5420
2450	100 11	68 7	—	210 11	—	210 11	5300
2500	97 11	66 7	—	190 11	—	190 11	5200
2550	143 11	97 7	—	240 11	—	240 11	5250
2600	179 11	122 7	—	370 11	385 11	378 11	5440
2650	255 11	173 7	—	575 11	560 11	568 11	5600
2700	319 11	217 7	—	770 11	825 11	798 11	5750
2750	281 11	191 7	—	950 11	100 12	975 11	5850
2800	306 11	208 7	—	100 12	985 11	992 11	5810
2850	434 11	295 7	—	108 12	100 12	104 12	5790
2900	663 11	451 7	—	182 12	187 12	184 12	6160
2950	803 11	546 7	—	—	236 12	218 12	6320
3000	—	—	—	—	271 12	247 12	6310
3050	—	—	—	—	293 12	—	
3100	—	—	—	—	315 12	—	
3150	—	—	—	—	350 12	—	

*) Averaging interval 50 angstroms

**) F_λ, $I_\lambda(0)$, and S_λ are written in the form "66 8", which means $66 \cdot 10^8$. The dimension for F_λ and $I_\lambda(0)$ is erg/cm^2·sec·sterad·cm, and erg/cm^2·sec·cm for S_λ.

TABLE 29.** MEAN CHARACTERISTICS OF SOLAR RADIATION: INTENSITY OF RADIATION OF THE ENTIRE DISK F_λ IN THE INTEGRATED SPECTRUM AND OF DISK CENTER $I_\lambda(0)$ IN THE CONTINUUM (10^{13} erg/cm^2 · sec · sterad · cm), ILLUMINATION S_λ IN THE INTEGRATED SPECTRUM (10^9 erg/cm^2 · sec · cm), AND BRIGHTNESS TEMPERATURES T_d AND T_{ce} CORRESPONDING TO F_λ AND $I_\lambda(0)$ IN THE REGION 0.3-3.0 MICRONS *)

λ,	F_λ	$I_\lambda(0)$	S_λ	T_d, °K	T_{ce}, °K
0,295	8,34	21,8	5,67	—	—
0,300	7,79	24,7	5,30	5480	6320
0,305	8,66	27,1	5,89	—	—
0,310	9,82	29,9	6,68	5560	6420
0,315	10,76	31,5	7,32	—	—
0,320	11,5	32,1	7,82	5600	6420
0,325	13,2	32,0	8,98	—	—
0,330	14,3	31,4	9,72	5690	6340
0,335	14,1	31,1	9,59	—	—
0,340	14,1	31,1	9,59	5620	6280
0,345	14,3	31,2	9,72	—	—
0,350	14,8	31,6	10,06	5600	6250
0,355	14,8	32,2	10,06	—	—
0,360	14,7	33,1	10,00	5550	6260
0,3625	15,3	33,4	10,4	—	—
0,3675	15,8	33,5	10,7	—	—
0,370	15,9	34,7	10,8	5560	6260
0,375	15,6	37,0	10,6	—	—
0,380	15,6	39,3	10,6	5510	6370
0,385	15,05	41,0	10,2	—	—
0,390	15,3	42,5	10,4	5460	6430
0,395	16,6	44,2	11,3	—	—
0,400	21,1	45,5	14,3	5700	6480
0,405	24,6	46,8	16,7	—	—
0,410	25,6	48,2	17,4	5850	6540
0,415	26,1	49,0	17,7	—	—
0,420	25,9	49,6	17,6	5840	6560
0,425	25,1	49,9	17,1	—	—
0,430	24,3	49,8	16,5	5760	6570
0,435	24,9	49,5	16,9	—	—
0,440	26,9	48,9	18,3	5850	6570
0,445	28,6	48,4	19,4	—	—
0,450	29,9	47,8	20,3	5950	6520
0,455	30,3	47,2	20,6	—	—
0,460	30,4	46,7	20,7	5960	6500
0,465	30,3	46,2	20,6	—	—
0,470	30,2	45,8	20,5	5950	6490
0,475	30,6	45,4	20,8	—	—
0,480	30,5	45,0	20,7	5960	6460
0,485	29,2	44,5	19,9	—	—
0,490	29,0	44,3	19,7	5900	6450
0,495	29,5	44,1	20,1	—	—
0,500	29,4	44,0	20,0	5910	6440
0,505	29,2	43,7	19,9	—	—
0,510	29,1	43,2	19,8	5900	6420
0,520	28,0	42,0	19,0	5860	6400
0,530	28,4	40,6	19,3	5880	6340
0,540	27,9	39,3	19,0	5870	6340
0,550	27,5	38,0	18,7	5860	6310

/267

TABLE 29. /CONCLUSION/

λ, μ	F_λ	$I_\lambda(0)$	S_λ	T_d, °K	T_{ce}, °K
0,560	26,8	36,8	18,2	5840	6290
0,570	26,7	35,8	18,2	5840	6260
0,580	26,7	34,9	18,2	5860	6250
0,590	26,3	34,2	17,9	5860	6250
0,600	25,8	33,5	17,5	5850	6240
0,610	25,4	32,9	17,3	5870	6240
0,620	24,9	32,1	16,9	5840	6230
0,630	24,4	31,4	16,6	5830	6220
0,640	24,0	30,7	16,3	5830	6220
0,650	23,4	30,0	15,9	5820	6220
0,660	22,9	29,3	15,6	5810	6210
0,670	22,8	28,7	15,5	5830	6210
0,680	22,4	28,2	15,2	5840	6220
0,690	22,0	27,7	15,0	5840	6230
0,700	21,7	27,2	14,8	5850	6240
0,720	20,7	26,1	14,1	5840	6240
0,740	19,5	24,6	13,3	5790	6220
0,760	18,8	23,1	12,8	5780	6190
0,780	17,9	21,8	12,2	5770	6170
0,800	17,1	20,8	11,6	5760	6170
0,850	15,0	18,2	10,20	5700	6140
0,900	13,2	16,0	8,97	5700	6130
0,950	12,1	14,1	8,23	5750	6110
1,00	10,8	12,6	7,35	5690	6130
1,05	9,68	11,4	6,58	5770	6180
1,10	8,75	10,2	5,95	5800	6200
1,15	7,91	9,08	5,38	5820	6200
1,20	7,17	8,16	4,87	5860	6220
1,25	6,48	7,30	4,41	5880	6230
1,30	5,87	6,63	3,99	5930	6280
1,35	5,38	6,00	3,66	5990	6310
1,40	4,96	5,47	3,37	6050	6350
1,45	4,59	5,05	3,12	6130	6430
1,50	4,22	4,65	2,87	6190	6500
1,55	3,92	4,32	2,67	6270	6600
1,60	3,59	3,98	2,44	6310	6670
1,65	3,28	3,62	2,23	6360	6680
1,70	3,00	3,29	2,04	6350	6680
1,8	2,45	2,64	1,67	6280	6550
1,9	1,99	2,14	1,35	6160	6420
2,0	1,64	1,76	1,115	6080	6330
2,2	1,154	1,23	0,785	5950	6190
2,4	0,843	0,896	0,573	5880	6110
2,6	0,633	0,670	0,430	5830	6050
2,8	0,483	0,509	0,328	5780	5980
3,0	0,374	0,393	0,254	5730	5950

*) Averaging interval is 100 A for $\lambda \leq 0.7\mu$, 200 A for $0.7 < \lambda \leq 0.8\mu$, 500 A for $0.8 \leq \lambda \leq 1.65\mu$, and 1000 A for $\lambda \geq 1.7\mu$.

**TRANSLATOR'S NOTE: COMMAS REPRESENT DECIMAL POINTS

TABLE 30+ FLUX CHARACTERISTICS OF THE SOLAR RADIATION IN THE WAVELENGTH REGION 3.0 MICRONS TO 4 mm: INTENSITIES F_λ AND $I_\lambda(0)$, ILLUMINATION S_λ, AND BRIGHTNESS TEMPERATURE OF ENTIRE DISK T_d *)

λ, μ	F_λ **)	$I_\lambda(0)$ **)	S_λ **)	T_d, °K
3,0	374 10	393 10	254 6	5730
3,5	211 10	220 10	143 6	5640
4,0	127 10	132 10	864 5	5540
4,5	808 9	837 9	549 5	5450
5,0	535 9	553 9	364 5	5350
5,5	366 9	377 9	249 5	5240
6,0	260 9	268 9	177 5	5170
6,5	193 9	198 9	131 5	5200
7,0	146 9	150 9	993 4	5210
7,5	113 9	116 9	768 4	5230
8,0	876 8	896 8	596 4	5180
8,5	681 8	696 8	463 4	5100
9,0	549 8	561 8	373 4	5110
9,5	446 8	455 8	303 4	5120
10,0	366 8	373 8	249 4	5110
10,5	301 8	306 8	205 4	5080
11,0	250 8	254 8	170 4	5050
11,5	209 8	212 8	142 4	5020
12,0	176 8	179 8	120 4	4980
12,5	146 8	148 8	993 3	4860
13,0	122 8	124 8	830 3	4750
13,5	104 8	106 8	707 3	4700
14,0	896 7	908 7	609 3	4650
14,5	774 7	784 7	526 3	4620
15,0	676 7	685 7	460 3	4590
16	519 7	525 7	353 3	4550
17	407 7	412 7	277 3	4530
18	324 7	328 7	220 3	4510
19	261 7	264 7	177 3	4490
20,	212 7	214 7	144 3	4480
21	177 7	179 7	120 3	4470
22	150 7	151 7	102 3	4470
23	123 7	124 7	836 2	4460
24	104 7	105 7	711 2	4460
25	884 6	890 6	601 2	4460

*) Averaging interval is 0.5 μ in the region 3.0-15.0 μ, 1.0 μ in the region 16-25 μ, 5 μ in the region 30-50 μ, 10 μ in the region 50-100 μ, 50 μ in the region 100-300 μ, 100 μ in the region 300-600 μ, 200 μ in the region 600 μ - 1 mm, and 1 mm in the region 1-4 mm.

+ TRANSLATOR'S NOTE: COMMAS REPRESENT DECIMAL POINTS

TABLE 30. /CONCLUSION/

λ, μ	F_λ **)	$I_\lambda(0)$ **)	S_λ **)	T_d, °K
30***)	430 6		292 2	4450
35	234 6		159 2	4440
40	137 6		932 1	4430
45	860 5		585 1	4420
50	568 5		386 1	4420
60	273 5		186 1	4410
70	147 5		100 1	4400
80	865 4		588 0	4390
90	544 4		370 0	4380
100	361 4		245 0	4375
150	713 3		485 −1	4350
200	219 3		149 −1	4340
250	917 2		624 −2	4340
300	408 2		277 −2	4360
400	143 2		972 −3	4450
500	606 1		412 −3	4550
600	300 1		204 −3	4680
800	981 0		667 −4	4890
1000	425 0		289 −4	5100
2000	310 −1		211 −5	6050
3000	710 −2		483 −6	6900
4000	248 −2		169 −6	7500

**) F_λ, $I_\lambda(0)$, and S_λ are written in the form "374 10", which means $374 \cdot 10^{10}$. The dimension for F_λ and $I_\lambda(0)$ is erg/cm^2·sec·sterad·cm, and erg/cm^2·sec·cm for S_λ.

***) Beginning at wavelength 30 μ, F_λ and $I_\lambda(0)$ -- as for T_d & T_{ce} -- virtually coincide.

TABLE 31.* MEAN CHARACTERISTICS OF SOLAR RADIATION: INTENSITY OF RADIATION OF DISK CENTER IN THE INTEGRATED SPECTRUM $I_\lambda^{in}(0)$ AND OF THE ENTIRE DISK IN THE CONTINUUM F_λ^c IN THE REGION 0.3-3.0 MICRONS (10^{13} erg/cm^2 · sec · sterad · cm)

λ, μ	$I_\lambda^{in}(0)$	F_λ^c	λ, μ	$I_\lambda^{in}(0)$	F_λ^c
0,295	13,0	14,0	0,325	19,6	22,6
0,300	12,0	16,0	0,330	21,1	22,6
0,305	13,2	17,9	0,335	20,3	22,6
0,310	15,0	20,2	0,340	20,0	22,7
0,315	16,0	22,0	0,345	20,3	22,9
0,320	17,2	22,8	0,350	20,8	23,2

TABLE 31. /CONCLUSION/

λ, μ	$I_\lambda^{(0)}$	F_λ^C	λ, μ	$I_\lambda^{(0)}$	F_λ^C
0,355	20,5	24,0	0,610	31,6	26,6
0,360	20,0	25,0	0,620	30,8	26,0
0,3625	21,0	25,0	0,630	30,2	25,4
0,3675	21,8	24,9	0,640	29,7	24,9
0,370	21,6	26,2	0,650	28,9	24,4
0,375	21,4	27,3	0,660	27,5	24,0
0,380	22,2	28,4	0,670	27,8	23,6
0,385	21,1	29,6	0,680	27,4	23,2
0,390	21,4	30,8	0,690	26,8	22,8
0,395	23,6	32,0	0,700	26,2	22,5
0,400	30,0	33,0	0,720	25,0	21,7
0,405	35,1	33,9	0,740	23,4	20,4
0,410	36,2	34,7	0,760	22,2	19,2
0,415	35,2	35,3	0,780	21,0	18,2
0,420	35,0	35,8	0,800	20,0	17,6
0,425	35,5	36,2	0,850	17,3	15,4
0,430	33,9	36,3	0,900	15,2	13,8
0,435	34,9	36,2	0,950	13,8	12,2
0,440	38,0	36,0	1,00	12,1	11,05
0,445	39,8	35,7	1,05	10,9	10,0
0,450	41,4	35,4	1,10	9,84	8,99
0,455	41,6	35,1	1,15	8,84	8,04
0,460	41,6	34,8	1,20	7.98	7,28
0,465	41,4	34,6	1,25	7,21	6,50
0,470	40,9	34,5	1,30	6.51	5,97
0,475	41,1	34,3	1,35	5,96	5,42
0,480	40.8	34,1	1,40	5,46	4,98
0,485	38,8	34,0	1,45	5,03	4,61
0,490	38,2	33,9	1,50	4,62	4,26
0,495	39,2	33,7	1,55	4,26	3,98
0,500	39,0	33,6	1,60	3,89	3,67
0,505	38,8	33,4	1,65	3,56	3,34
0,510	38,6	33,2	1,70	3,24	3.04
0,520	36,3	32,7	1,80	2,63	2,46
0,530	36,6	31,8	1,90	2,12	2,00
0,540	36,0	30,8	2,0	1,76	1,64
0,550	35,3	29,8	2,2	1,22	1,16
0,560	34,2	29,0	2,4	0,894	0,844
0,570	33,8	28,4	2,6	0,670	0,634
0,580	33,6	27,9	2,8	0,509	0,483
0,590	32,8	27,5	3,0	0,393	0,374
0,600	32,2	27,0			

* TRANSLATOR'S NOTE: COMMAS REPRESENT DECIMAL POINTS

TABLE 32* DETAILED COURSE OF SPECTRAL ILLUMINATION S_λ PRODUCED BY THE SUN, OUTSIDE THE TERRESTRIAL ATMOSPHERE AT A DISTANCE OF 1 ASTRONOMICAL UNIT (10^3 erg/cm^2 · sec · 10 ANGSTROMS)

λ, Å	S_λ	λ, Å	S_λ	λ, Å	S_λ	λ, Å	S_λ	λ, Å	S_λ	λ, Å	S_λ
3005	0,514	3415	0,985	3825	0,676	4235	1,662	4645	2,022	5055	2,075
3015	0,661	3425	1,066	3835	0,666	4245	1,831	4655	2,070	5065	2,010
3025	0,526	3435	1,085	3845	0,996	4255	1,686	4665	1,977	5075	1,986
3035	0,604	3445	0,762	3855	1,065	4265	1,771	4675	2,051	5085	1,981
3045	0,542	3455	1,035	3865	0,909	4275	1,614	4685	2,032	5095	2,036
3055	0,607	3465	0,906	3875	0,989	4285	1,706	4695	2,053	5105	2,014
3065	0,570	3475	0,986	3885	0,913	4295	1,404	4705	1,970	5115	2,083
3075	0,720	3485	0,924	3895	1,215	4305	1,103	4715	2,096	5125	1,930
3085	0,635	3495	0,922	3905	1,122	4315	1,707	4725	2,122	5135	1,943
3095	0,526	3505	1,076	3915	1,345	4325	1,623	4735	2,057	5145	1,902
3105	0,605	3515	0,960	3925	1,054	4335	1,791	4745	2,095	5155	1,975
3115	0,773	3525	0,925	3935	0,501	4345	1,697	4755	2,088	5165	1,724
3125	0,703	3535	1,070	3945	1,120	4355	1,806	4765	2,085	5175	1,795
3135	0,751	3545	1,137	3955	1,299	4365	1,971	4775	2,143	5185	1,714
3145	0,720	3555	1,033	3965	0,716	4375	1,778	4785	2,091	5195	1,857
3155	0,773	3565	0,888	3975	0,953	4385	1,593	4795	2,167	5205	1,948
3165	0,653	3575	0,851	3985	1,590	4395	1,835	4805	2,097	5215	1,945
3175	0,862	3585	0,616	3995	1,602	4405	1,795	4815	2,135	5225	1,907
3185	0,704	3595	1,095	4005	1,607	4415	1,986	4825	2,083	5235	1,927
3195	0,798	3605	0,960	4015	1,783	4425	1,982	4835	2,090	5245	1,986
3205	0,865	3615	0,794	4025	1,715	4435	1,906	4845	2,052	5255	2,002
3215	0,773	3625	1,003	4035	1,621	4445	1,986	4855	1,887	5265	1,761
3225	0,791	3635	1,023	4045	1,538	4455	1,858	4865	1,636	5275	1,839
3235	0,629	3645	0,960	4055	1,564	4465	1,968	4875	1,914	5285	1,949
3245	0,673	3655	1,217	4065	1,538	4475	2,072	4885	1,954	5295	1,959
3255	0,776	3665	1,229	4075	1,743	4485	2,016	4895	2,014	5305	2,073
3265	1,136	3675	1,241	4085	1,798	4495	2,017	4905	2,119	5315	2,002
3275	1,079	3685	1,121	4095	1,762	4505	2,173	4915	1,979	5325	1,840
3285	0,964	3695	1,223	4105	1,561	4515	2,134	4925	1,946	5335	1,965
3295	1,096	3705	1,019	4115	0,819	4525	1,940	4935	2,024	5345	1,930
3305	1,110	3715	1,103	4125	1,817	4535	1,985	4945	2,134	5355	2,045
3315	1,004	3725	1,004	4135	1,818	4545	2,028	4955	1,952	5365	1,872
3325	1,039	3735	0,811	4145	1,880	4555	2,040	4965	2,061	5375	1,879
3335	1,027	3745	0,794	4155	1,730	4565	2,099	4975	2,129	5385	1,968
3345	1,062	3755	0,993	4165	2,029	4575	2,124	4985	1,915	5395	1,862
3355	1,073	3765	1,103	4175	1,651	4585	2,075	4995	2,014	5405	1,816
3365	0,842	3775	1,255	4185	1,722	4595	2,048	5005	1,951	5415	1,848
3375	0,863	3785	1,149	4195	1,932	4605	2,063	5015	1,935	5425	1,913
3385	0,973	3795	0,963	4205	1,774	4615	2,084	5025	1,988	5435	1,881
3395	1,007	3805	1,201	4215	1,905	4625	2,131	5035	1,968	5445	1,919
3405	1,093	3815	1,059	4225	1,574	4635	2,102	5045	1,976	5455	1,869

* TRANSLATOR'S NOTE: COMMAS REPRESENT DECIMAL POINTS

TABLE 32. /CONCLUSION/ /273

λ, Å	S_λ	λ, Å	S_λ	λ, Å	S_λ	λ, Å	S_λ	λ, Å	S_λ	λ, Å	S_λ
5465	1,965	5655	1,809	5845	1,857	6035	1,745	6225	1,689	6415	1,622
5475	1,873	5665	1,811	5855	1,788	6045	1,676	6235	1,658	6425	1,692
5485	1,887	5675	1,830	5865	1,828	6055	1,776	6245	1,664	6435	1,627
5495	1,903	5685	1,778	5875	1,840	6065	1,782	6255	1,657	6445	1,626
5505	1,850	5695	1,859	5885	1,785	6075	1,812	6265	1,731	6455	1,675
5515	1,884	5705	1,729	5895	1,574	6085	1,682	6275	1,672	6465	1,619
5525	1,787	5715	1,804	5905	1,813	6095	1,725	6285	1,658	6475	1,604
5535	1,884	5725	1,930	5915	1,794	6105	1,749	6295	1,656	6485	1,580
5545	1,871	5735	1,835	5925	1,790	6115	1,701	6305	1,644	6495	1,485
5555	1,906	5745	1,849	5935	1,767	6125	1,693	6315	1,646	6505	1,621
5565	1,855	5755	1,855	5945	1,809	6135	1,643	6325	1,736	6515	1,651
5575	1,806	5765	1,864	5955	1,735	6145	1,699	6335	1,636	6525	1,621
5585	1,788	5775	1,817	5965	1,814	6155	1,685	6345	1,685	6535	1,679
5595	1,811	5785	1,786	5975	1,762	6165	1,604	6355	1,638	6545	1,597
5605	1,797	5795	1,814	5985	1,755	6175	1,695	6365	1,672	6555	1,476
5615	1,767	5805	1,787	5995	1,750	6185	1,705	6375	1,655	6565	1,377
5625	1,856	5815	1,822	6005	1,789	6195	1,764	6385	1,725	6575	1,559
5635	1,865	5825	1,808	6015	1,697	6205	1,711	6395	1,658	6585	1,596
5645	1,834	5835	1,836	6025	1,704	6215	1,728	6405	1,605	6595	1,587

TABLE 33+. FRACTION OF SPECTROPHOTOMETRIC SOLAR CONSTANT A_{λ_1} (mw/cm^2) BELONGING TO SPECTRAL INTERVAL FROM 0 TO λ_1

λ_1, μ	$A_{\lambda_1}=\int_0^{\lambda_1} S_\lambda d\lambda$	$\frac{A_{\lambda_1}}{S_0}$, %	λ, μ	$A_{\lambda_1}=\int_0^{\lambda_1} S_\lambda d\lambda$	$\frac{A_{\lambda_1}}{S_0}$, %
0,14	0,00084*)	0,0006	1,60	122,1	88,92
0,20	0,0190	0,014	1,80	126,2	91,90
0,25	0,260	0,189	2,00	129,0	93,89
0,30	1,546	1,13	2,40**)	132,2	96,27
0,346**)	5,295	3,85	3,00	134,6	97,98
0,40	11,03	8,03	3,50	135,6	98,70
0,45	$19,78_5$	14,40	4,0	$136,1_5$	99,12
0,50	29,97	21,82	5,0	136,7	99,55
0,55	39,62	28,84	6,0	137,02	99,75
0,60	48,67	$35,43_5$	7,0	137,12	99,83
0,65	57,06	41,54	8,0	137,19	99,877
0,70	64,72	47,12	9,0	137,248	99,919
0,80	77,81	56,65	10,0	137,278	99,941
0,90	$88,06_5$	64,11	20,0	137,349	99,992
1,00	96,26	70,08	50,0	137,355	99,997
1,20	108,3	78,82	100,0	137,3488	$99,999_4$
1,40	116,4	84,71		137,3598	100%

*) The value A = 0.0006 mw/cm^2 is assumed for $\lambda < 0.135\ \mu$. **) Wavelengths 0.346 and 2.40 μ are singled out, since as a rule UV and IR corrections in Smithsonian observations were determined for them (K_u and K_i; see Sec. 3, Chapter Two).

/274

+ TRANSLATOR'S NOTE: COMMAS REPRESENT DECIMAL POINTS.

REFERENCES

1. Minnaert, M., in "Solntse" (The Sun), ed. by G. Kuiper, IL, Moscow, 1955.

2. Jäger, C. de., "Stroyeniye i dinamika atmosfery Solntsa" (Structure and Dynamics of the Solar Atmosphere), IL, Moscow, 1962.

3. Shklovskiy, I. S., "Fizika solnechnoy korony" (Physics of the Solar Corona), Fizmatgiz, Moscow, 1962.

4. Smith, G., and Smith, E., "Solnechnyye vspyshki" (Solar Flares), Mir, Moscow, 1966.

5. Ivanov-Kholodnyy, G. S., and Nikol'skiy, G. M., "Solntse i ionosfera" (The Sun and the Ionosphere), Nauka, Moscow, 1969.

6. Zheleznyakov, V. V., "Radioizlucheniye Solntsa i planet" (Radio Emission of the Sun and the Planets), Nauka, Moscow, 1964.

7. "Kosmicheskaya astrofizika" (Outer Space Astrophysics), ed. by W. Liller, IL, Moscow, 1962.

8. Livshits, M. A., "Fizika Solntsa", "Itogi nauki" series (Physics of the Sun, Advances in Science series), Astronomiya, 1967, Moscow, 1970.

9. Allen, C. W., "Astrophysical Quantities," 2nd ed., Univ. London, Athlone Press, 1962.

10. Aller, L., "Rasprostranennost' khimicheskikh elementov" (Abundance of Chemical Elements), IL, Moscow, 1963.

11. Aller, L., "Astrofizika" (Astrophysics), Vol. 2, IL, Moscow, 1957.

12. Martynov, D. Ya., "Kurs obshchey astrofiziki" (Course on General Astrophysics), Nauka, Moscow, 1965.

13. Unsol'd /Unsold/, A., "Fizika zvezdnykh atmosfer" (Physics of Stellar Atmospheres), IL, Moscow, 1947.

14. Ambartsumyan, V. A., Mustel', E. R., Severnyy, A. B., and Sobolev, V. V., "Teoreticheskaya astrofizika" (Theoretical Astrophysics), Gostekhizdat, Moscow, 1952.

15. Sobolev, V. V., "Kurs teoreticheskoy astrofiziki" (Course on Theoretical Astrophysics), Nauka, Moscow, 1967.

16. Zirin, G., "Solnechnaya atmosfera" (The Solar Atmosphere), Mir, Moscow, 1969.

17. Artsimovich, L. A., "Elementarnaya fizika plazmy" (Elementary Plasma Physics), 3rd ed., Atomizdat, Moscow, 1969.

18. Mustel', E. R., Uspekhi astron. nauk 3, 155 (1947).

19. Trans. I.A.U., XII B, 591 (1966).

20. Barber, C. R., Nature 222, 929 (1969).

21. Glagolev, Yu. A., "Spravochnik po fizicheskim parametram atmosfery" (Handbook on Physical Parameters of the Atmosphere), Gidrometeoizdat, Leningrad, 1970.

22. Astapovich, I. S., "Meteornyye yavleniya v atmosfere Zemli" (Meteoric Phenomena in the Terrestrial Atmosphere), Fizmatgiz, Moscow, 1958.

23. Vasil'yev, O. B., "Astrofizicheskiye issledovaniya serebristykh oblakov" (Astrophysical Research on Noctilucent Clouds), pub. by the Astronomical Council of the USSR Academy of Sciences, Moscow, 1967.

24. Goody, R., "Atmosfernaya radiatsiya" (Atmospheric Radiation), Mir, Moscow, 1966.

25. Gushchin, G. P., "Issledovaniye atmosfernogo ozona" (Research on Atmospheric Ozone), Gidrometeoizdat, Leningrad, 1963. /276

26. Danilov, A. D., "Khimiya ionosfery" (Chemistry of the Ionosphere), Gidrometeoizdat, Leningrad, 1967.

27. Zuyev, V. Ye., "Prozrachnost' atmosfery dlya vidimykh i infrakrasnykh luchey" (Transparency of the Atmosphere for Visible and Infrared Rays), Sov. radio, Moscow, 1966.

28. Caidle, R., "Tverdyye chastitsy v atmosfere i v kosmose" (Solid Particles in the Atmosphere and in Space), Mir, Moscow, 1969.

29. Mirtov, B. A., "Gazovyy sostav atmosfery Zemli i metody yego analiza" (Gaseous Composition of the Earth and Methods of Its Analysis), USSR Academy of Sciences, Moscow, 1961.

30. Nicolet, M., "Aeronomiya" (Aeronomy), Mir, Moscow 1964.

31. "Okolozemnoye kosmicheskoy prostranstvo" (Near-Earth Outer Space), ed. by Johnson, F. S., Mir, Moscow, 1966.

32. Rozenberg, G. V., "Sumerki" (Twilight), Fizmatgiz, Moscow, 1963.

33. Feygel'son, Ye. M., "Radiatsionnyye protsessy v sloisto-obraznykh oblakakh" (Radiative Processes in Stratiform Clouds), Nauka, Moscow, 1964.

34. Khvostikov, I. A., "Fizika ozonosfery i ionosfery" (Physics of the Ozonosphere and Ionosphere), USSR Academy of Sciences, Moscow, 1963.

35. Khrgian, A. Kh., "Fizika atmosfery" (Physics of the Atmosphere), Gidrometeoizdat, Leningrad, 1969.

36. Yunge, Ch., "Khimicheskiy sostav i radioaktivnost' atmosfery" (Chemical Composition and Radioactivity of the Atmosphere), Mir, Moscow, 1965.

37. Landsberg, G. S., "Optika" (Optics), 2nd ed., Gostekhizdat, Moscow, 1952.

38. Ditchburn, R., "Fizicheskaya optika" (Physical Optics), Nauka, Moscow, 1965.

39. Bouguer, P., "Opticheskiy traktat o gradatsii sveta" (Optical Treatise on the Gradation of Light), USSR Academy of Sciences, Moscow, 1950.

40. Gershun, A. A., "Izbrannyye trudy po fotometrii i svetotekhnike" (Selected Works on Photometry and Light Engineering), Fizmatgiz, Moscow, 1958.

41. Vavilov, S. I., "Mikrostruktura sveta" (Microstructure of Light), "Sobr. soch." (Collected Works), 2, USSR Academy of Sciences, Moscow, 1952.

42. Bemporad, A., Mitt. Sternw. Heidelberg (Astron. Inst.), 4 (1904).

43. "Kurs astrofiziki i zvezdnoy astronomii" (Course on Astrophysics and Stellar Astronomy), ed. by Mikhaylov, A. A., Gostekhizdat, Moscow-Leningrad, 1951.

44. Kondrat'yev, K. Ya., "Luchistaya energiya Solntsa" (Radiant Energy of the Sun), Gidrometeoizdat, Leningrad, 1954.

45. Kondrat'yev, K. Ya., "Aktinometriya" (Actinometry), Gidrometeoizdat, Leningrad, 1965.

46. Townes, Ch., UFN 8 (3), 461 (1966).

47. Prokhorov, A. M., UFN 85(4), 599 (1965).

48. Bunin, F. V., and Prokhorov, A. M., ZhETF 48(4), 1084 (1965).

49. Ishchenko, Ye. F., and Klimkov, Yu. M., "Opticheskiye kvantovyye generatory" (Lasers), Sov. radio, Moscow, 1968.

50. Klimontovich, Yu. L., "Kavantovyye generatory sveta i nelineynaya optika" (Lasers and Nonlinear Optics), Prosveshcheniye, Moscow, 1966.

51. "Kvantovaya elektronika" (Quantum Electronics), "Malen'kaya entsiklopediya" (Short Encyclopedia) series, Sov. Entsiklopediya, Moscow, 1969.

52. Rozenberg, G. V., UFN 71(2), 173 (1960).

53. Shtaude, N. M., "Photometric Observations of Twilight as a Method of Studying the Upper Stratosphere," Tr. Komissii po izuch. stratosfery (Works of the Commission on the Investigation of the Stratosphere), USSR Academy of Sciences, Moscow-Leningrad, 1936.

54. Vol'kenshteyn, M. V., "Molekulyarnaya optika" (Molecular Optics), Gostekhizdat, Moscow-Leningrad, 1951. /277

55. Mandel'shtam, L. I., "Sobr. trudov" (Collected Works), 1, p. 109, USSR Academy of Sciences, Moscow, 1948.

56. Smoluchowski, M., Ann. Physik 25, 205 (1908).

57. Einstein, A., Ann. Physik 33, 1275 (1910).

58. Kondrat'yev, K. Ya., "Luchistyy teploobmen v atmosfere" (Radiative Heat Exchange in the Atmosphere), Gidrometeoizdat, Leningrad, 1956.

59. Penndorf, R., J. Opt. Soc. Amer. 47, 176 (1957).

60. Mikirov, A. Ye., Iskusstv. sputniki Zemli 13, 97 (1962); Kosmicheskiye issled. 3(2), 284 (1965).

61. Elterman, L., AFCRL Environments Res. Papers, 46 (1964); in "Handbook of Geophysics and Space Environments," ed. Valley, S. L., New York, 1965.

62. "Handbook of Geophysics and Space Environments," ed. Valley S. L., New York, 1965.

63. Kagan, V. K., and Kondrat'yev, K. Ya., "Osnovy informatsionnoy teorii vidimosti v atmosfere" (Essentials of the Information Theory of Visibility in the Atmosphere), Gidrometeoizdat, Leningrad, 1968.

64. Shifrin, K. S., "Rasseyaniye sveta v mutnoy srede" (Scattering of Light in a Turbid Medium), Gostekhizdat, Moscow-Leningrad, 1951.

65. Penndorf, R. B., J. Opt. Soc. Amer. 47, 603 (1957); 1010 (1957).

66. Kalitin, N. N., "Aktinometry" (Actinometry), Gidrometeoizdat, Moscow-Leningrad, 1938.

67. Vasil'chenko, I. V., Kardashev, N. S., Moroz, V. I., Morozov, I. K., Repin, A. N., and Khromov, G. S., AZh 44, 897 (1967). /AZh = Astron. Zh./

68. Fedoseyev, L. I., Lubyako, L. V., and Kukin, L. M., AZh 44, 1191 (1967).

69. Kukin, L. M., Lubyako, L. V., and Fedoseyev, L. I., Izv. vuzov, Radiofizika 10(6), 747 (1967).

70. Kislyakov, A. G., and Stankevich, K. S., op. cit., 10(9-10) 1244 (1967).

71. Kislyakov, A. G., UFN 101(4), 607 (1970). /UFN = Uspekhi fiz. nauk/

72. Makarova, Ye. A., Sitnik, G. F., and Kozhevnikov, N. I., AZh 40, 359 (1963).

73. Kondrat'yev, K. Ya., Badinov, I. Ya., Ashcheulov, S. V., and Andreyev, S. D., Fiz. atm. i okeana 1(4), 363 (1965)

74. Kislyakov, A. G., and Naumov, A. I., op. cit. 6(3), 239 (1970).

75. Frish, S. E., "Opticheskiye spektry atomov" (Optical Spectra of Atoms), Fizmatgiz, Moscow-Leningrad, 1963.

76. Yel'yashevich, M. A., "Atomnaya i molekulyarnaya spektroskopiya" (Atomic and Molecular Spectroscopy), Fizmatgiz, Moscow, 1962.

77. Herzberg, G., "Atomnyye spektry i stroyeniye atomov" (Atomic Spectra and the Structure of Atoms), IL, Moscow, 1948.

78. Gertsberg, G., "Spektry i stroyeniye dvukhatomnykh molekul" (Spectra and the Structure of Diatomic Molecules), IL, Moscow, 1949.

79. Gertsberg, G., "Kolebatel'nyye i vrashchatel'nyye spektry mnogoatomnykh molekul" (Vibrational and Rotational Spectra of Polyatomic Molecules), IL, Moscow, 1949.

80. Inn, E. C. Y., and Tanaka, Y., J. Opt. Soc. Amer. 43, 870 (1953).

81. Vigroux, E., Ann. Physik 8, 709 (1953). /278

82. "The Earth as a Planet," ed. Kuiper, G. P., Univ. Chicago Press, Chicago and London, 1954.

83. Makarova, Ye. A., Tr. GAISh 34, 36 (1966); AZh 42, 681 (1965).

84. Hulst, H. C. Van de., Ann. Ap. 8, 12 (1945).

85. Herzberg, L., and Herzberg, G., Ap. J. 105, 353 (1947)

86. Babcock, H. D., and Herzberg, L., Ap. J. 108, 167 (1948).

87. Babcock, H. D., and Moore, C. E., "The Solar Spectrum λ 6600 to λ 13,495 /angstroms/," Washington, Carnegie Institute of Washington Publication 579, 1947.

88. Mohler, O. C., Pierce, A. K., McMath, R. R., and Goldberg, L., "Photometric Atlas of the Near-Infrared Solar Spectrum λ 8465 to λ 25,242 /angstroms/," Univ. Michigan Press, 1950.

89. Mohler, O. C., "A Table of Solar Spectrum Wavelengths 11,984-25,578 A," Univ. Michigan Press, 1955.

90. Shaw, J. H., Chapman, R. M., Howard, J. N., and Oxholm, M. L., Ap. J. 113, 268 (1951).

91. Shaw, J. H., Oxholm, M. L., and Classen, H. H., Ap. J. 116, 554 (1952).

92. Migeotte, M., Neven, L., and Swensson, Y., "The Solar Spectrum from 2.8 to 23.7 microns, Part I: Photometric Atlas, Part II: Measures and Identifications," Inst. d'Astrophys., Univ. Liege, 1956.

93. Vigroux, E., Migeotte, M., Neven, L., and Swensson, J., "An Atlas of Nitrous Oxide, Methane, and Ozone Infrared Absorption Band, Part I: The Photometric Record, Part II: Measures and Identifications," Inst. d'Astrophys., Univ. Liege, 1957.

94. Farmer, C. B., and Key, P. J., Appl. Optics 4, 1051 (1965).

95. Williams, R. A., and Chang, W. S. C., Proc. IEEE 54 (4), 462 (1966).

96. Saiedy, F., and Goody, R. M., MN 119, 213 (1959).

97. Koutchmy, S., and Peyturaux, R., C. R. Acad. Sci. 267, Ser. B, 905 (1968); Astron. Astrophys. 5 (3), 470 (1970).

98. Zhevakin, S. A., and Naumov, A. P., Izv. vuzov, Radiofizika 10(9-10), 1214 (1967).

99. Naumov, A. P., "Molekulyarnoye pogloshcheniye i refraktsiya santimetrovykh, millimetrovykh i submillimetrovykh radiovoln v atmosferakh Zemli i planet" (Molecular Absorption and Refraction of Centimeter, Millimeter, and Submillimeter Radio Waves in the Atmospheres of the Earth and the Planets), Candidate's Dissertation, Gor'kiy State University, Gor'kiy, 1968.

100. Nikonov, V. B., Byull. Abastumanskoy Astrofiz. obs. 14, (1953).

101. Kotova, Ye. N., "Razrabotka novogo metoda opredeleniye spektral'nogo koeffitsiyenta nochnoy prozrachnosti atmosfery" (Development of a New Method for Determining the Spectral Coefficient of Nighttime Atmospheric Transmission), Candidate's Dissertation, Moscow State University and the GAISh, Moscow, 1954.

102. Sarychev, A. P., in "Atmosfernaya optika" (Atmospheric Optics), Nauka, Moscow, 1968.

103. Pyaskovskaya-Fesenkova, Ye. V., "Issledovaniye rasseyaniya sveta v zemnoy atmosfere" (Investigation of the Scattering of Light in the Terrestrial Atmosphere), USSR Academy of Sciences, Moscow, 1957.

104. Livshits, G. Sh., "Scattering of Light in the Atmosphere," Tr. Astrofiz. in-ta AN Kaz. SSR 6, (1965).

105. Boyko, P. N., and Livshits, G. Sh., Izv. Astrofiz. in-ta AN Kaz. SSR 11, 97 (1960).

106. Ivanov, A. I., Livshits, G. Sh., Pavlov, V. Ye., Tashenov, B. T., and Teyfel', Ya. A., "Scattering of Light in the Atmosphere," Tr. Astrofiz. in-ta AN Kaz. SSR 10, (1968). /279

107. Fesenkov, V. G., AZh 10, 3 (1933).

108. Sitnik, G. F., and Khmeleva, R. N., AZh 35, 932 (1958).

109. Sitnik, G. F., Soobshch. GAISh 113, 19 (1961).

110. Murasheva, M. S., and Sitnik, G. F., AZh 40, 819 (1963).

111. Sitnik, G. F., AZh 42, 59 (1965).

112. Makarova, Ye. A., AZh 34, 539 (1957).

113. Labs, D., and Neckel, H., Z. Ap. 69, 1 (1968).

114. Yanishevskiy, Yu. D., "Aktinometricheskiye pribory i metody izmereniy" (Actinometric Instruments and Measurement Techniques), Gidrometeoizdat, Leningrad, 1957.

115. Stair, R., and Johnston, R. G., J. Res. NBS 57, 205 (1956).

116. Sitnik, G. F., ATs No 444, 1 (1967).

117. Stair, R., and Ellis, H. T., J. Appl. Meteorol. 7(4), (1968).

118. Nicolet, M., Arch. f. Met., Geoph. u. Biokhim., Ser. B. 3, (1951); Ann. Ap. 14, 3 (1951).

119. Johnson, F. S., J. Meteorol. 11(6), 431 (1954).

120. Makarova, Ye. A., and Kharitonov, A. V., ATs No 435, 3 (1967); AZh 45, 752 (1968); Izv. SAO AN SSSR 1, 33 (1970).

121. Makarova, Ye. A., and Kharitonov, A. V., in "Rasseyaniye sveta v zemnoy atmosfere" (Scattering of Light in the Terrestrial Atmosphere) ("Materialy Vsesoyuznoy konferentsii po rasseyaniyu sveta, noyabr' 1969 g." /Materials of the November 1969 All-Union Conference on the Scattering of Light/), Nauka, Kazakh SSR Academy of Sciences, Alma-Ata, 1972.

122. Thekaekara, M. P., Kruger, R., and Duncan, C. H., Appl. Optics 8, 1713 (1969); Report X-332-68-304 GSFC, Greenbelt, Maryland, 1968.

123. Drummond, A. J., Hickey, J. R., Scholes, W. J., and Laue, E. G., J. Spacecraft Rockets 4, 1200 (1967).

124. Drummond, A. J., and Hickey, J. R., Sol. Energy 12, 217 (1968).

125. Drummond, A. J., and Laue, E. G., In-t Astronaut. Fed. Congress, 19th, No 9, 1968, preprint AS 176, 1968.

126. Wilson, R., J. Geophys. Res. 76, 4325 (1971).

127. Angstrom, A., Tellus 22(2), 205 (1970).

128. Golikov, V. I., Tr. GGO 237, 23 (1969); 237, 40 (1969).

129. Sena, L. A., "Yedinitsy fizicheskikh velichin i ikh razmernosti" (Units of Physical Quantities and Their Dimensions), Nauka, 1969.

130. Thekaekara, M. P., Sol. Energy 9, 7 (1965).

131. Langley, S. P., and Abbot, C. G., Ann. Smithson. Inst. Astrophys. Obs. 1, (1900); 2, (1908).

132. Abbot, C. G., Fowle, F. E., Aldrich, L. B., and Hoover, W. H., Op. cit. 3, (1913); 4, (1922); 5, (1932); 6, (1942); 7, (1954).

133. Aldrich, L. B., and Hoover, W. H., Science 116, 3 (1952).

134. Sitnik, G. F., AZh 42, 996 (1965).

135. Fesenkov, V. G., Uspekhi astron. nauk 3, 147 (1947).

136. Kondratyev, K. Ya., Nikolsky, G. A., Badinov, I. Ya., and Andreev, S. D., Appl. Optics 6, 197 (1967).

137. Kondratyev, K. Ya., and Nikolsky, G. A., Quart. J. Roy. Meteorol. Soc. 96(409), 509 (1970).

138. Murcray, D. G., Kyle, T. G., Kosters, J. J., and Gast, P. R., /2
Report AFGRL-68-0452, 1968.

139. Laue, E. G., and Drummond, A. J., Science 161, 188 (1968).

140. Drummond, A. J., Hickey, J. R., Scholes, W. J., and Laue, E. G., Nature 218, 15138 (1968).

141. Drummond, A. J., COSPAR XIII, Paper A-27, Leningrad, May 1970.

142. Thekaekara, M. P., and Drummond, A. J., Nature 229, 6 (1971).

143. NASA News Release 69-69, 8 (May 1969).

144. Kondrat'yev, K. Ya., Gayevskaya, G. N., and Nikol'skiy, G. A., in "Problemy fiziki atmosfery" (Problems in Atmospheric Physics), No. 1, p. 17, Leningrad State University, 1963.

145. Kondratiev, K. Ya., Badinov, I. Ya., Gaevskaya, G. N., Nikolsky, G. A., and Fedorova, M. P., Pure Appl. Geophys. 58(2), 187 (1964).

146. Kondrat'yev, K. Ya., Badinov, I. Ya., Ashcheulov, S. V., and Andreyev, S. D., Fiz. atm. i okeana 1(2), 175 (1965).

147. Nikol'skiy, G. A., "Aerostatnyye issledovaniya radiatsionnogo rezhima troposfery i nizhney stratosfery" (Aerostatic Research on the Radiation Regime of the Troposphere and the Lower Stratosphere), Candidate's Dissertation, Leningrad State University, Leningrad, 1970.

148. Menon, M. P., Menon, K. K., and Kuroda, P. K., J. Geophys. Res. 68, 4495 (1963).

149. Willard, R., and Kenney, J. I., J. Geophys. Res. 68, 2053 (1963).

150. Kuroda, P. K., Miyake, V., and Nemoto, J., Science 150, 1289 (1965)

151. Radhavan, S., and Jadov, B. R., Ind. J. Meteorol. Geophys. 17(4), 607 (1966).

152. Fesenkov, V. G., Meteoritika 24, 177 (1964).

153. Angstrom, A., Ap. J. 55, 24 (1922).

154. Murcray, D. G., Kyle, T. G., Kosters, J. J., and Gast, P. R., Tellus 21(5), 620 (1969).

155. Willson, R., J. P. L. Techn. Report 32-1365, Feb. 1969.

156. Drummond, A. J., Karoli, A.R., and Hickey, J. R., E.S.S.A. Contract Report E-66-70, 1970.

157. Thekaekara, M. P., Proc. 16th Ann. Techn. Meet., April 12-16, 1970.

158. Thekaekara, M. P., and Winker, A. R., Report X-322-69-399, GSFC, Greenbelt, Maryland, Sept. 1969.

159. Gutnick, P., and Prager, R., Veroff Berlin-Babelsberg 1, 1(1914); 2, 3 (1918).

160. Stebbins, J., and Jacobsen, T., Pop. Astr. 35, 494 (1924).

161. Stebbins, J., Lick Observ. Bull. 13(385), 1 (1927-1928).

162. Johnson, H. L., and Iriarte, B., Lowell Observ. Bull. 4, No. 8(36), 99 (1959).

163. Serkowski, K., Lowell Observ. Bull. 5, 157 (1961).

164. Jerzykiewicz, M., and Serkowski, K., Lowell Observ. Bull.6, No. 18(137), 295((1966).

165. Harris, D. L., in "Planety i sputniki" (Planets and Satellites), ed. by Kuiper, G., IL, Moscow, 1963.

166. Rakosch, K. D., Mitt. Astron. Ges. 27, 177 (1969).

167. Sharov, A. S., AZh 40, 754 (1963).

168. Abbot, C. G., Smithson. Miscell. Coll. 146, 3 (1963); Proc. /28 Nat. Acad. Sciences 56(6), 1627 (1966).

169. Angstrom, A., Tidskriff for Elementar Matematik, Fysik och Kemi, 5 (1921).

170. Lundblad, R., Arkiv for Matematik, Astronomi och Fysik 17, 14 (1922).

171. Rodhe, B., "Swedish Meteorological and Hydrological Institute," Notiser och prelimara rapporter, No. 19, 1969.

172. "Metody astronomii" (Methods in Astronomy), ed. by Hiltner, V. A., Mir, Moscow, 1967.

173. Wood, R., "Fizicheskaya optika" (Physical Optics), ONTI, Leningrad-Moscow, 1936.

174. Frish, S. E., "Tekhnika spektroskopii" (Techniques of Spectroscopy), Leningrad State Univ., Leningrad, 1934.

175. Sawyer, R., "Eksperimental'naya spektroskopiya" (Experimental Spectroscopy), IL, Moscow, 1953.

176. Toporets, A. S., "Monokhromatory" (Monochromators), Gostekhizdat, Moscow-Leningrad, 1955.

177. Tolanskiy, S., "Spektroskopiya vysokoy razreshayushchey sily" (High-Resolution Spectroscopy), IL, Moscow, 1955.

178. Namioka, T., in "Kosmicheskaya astrofizika" (Space Astrophysics), ed. by Liller, U./W./, IL, Moscow, 1962.

179. Zaydel', A. N., and Shreyder, Ye. A., "Spektroskopiya vakuumnogo ul'trafioleta" (Vacuum Ultraviolet Spectroscopy), Nauka, Moscow, 1967.

180. Tarasov, K. I., "Spektra'nyye pribory" (Spectral Instruments), Mashinostroyeniye, Leningrad, 1968.

181. Peysakhson, I. V., "Optika spektral'nykh priborov" (Optics of Spectral Instruments), Mashinostroyeniye, Leningrad, 1970.

182. Martynov, D. Ya., "Kurs prakticheskoy astrofiziki" (Course on Practical Astrophysics), 2nd ed., Nauka, Moscow, 1967.

183. Nagibina, I. M., and Prokof'yev, V. K., "Spektral'nyye pribory i tekhnika spektroskopii" (Spectral Instruments and Techniques of Spectroscopy), Mashgiz, Moscow-Leningrad, 1963.

184. Lekont, Zh., "Infrakrasnoye izlucheniye" (Infrared Radiation), Fizmatgiz, Moscow, 1958.

185. Gerasimova, N. G., OMP, No. 6, 2 (1964).

186. Gerasimov, F. M., OMP, No. 11, 33(1965).

187. Liller, W., Appl. Optics 2, 187 (1963).

188. Pettit, E., Ap. J. 91, 159 (1940).

189. Minnaert, M., Mulders, G. F. W., and Houtgast, J., "Photometric Atlas of the Solar Spectrum," Amsterdam, 1940.

190. Bruckner, G., "Photometrischer Atlas des Nahen Ultravioletten Sonnenspectrums 2988-3629 A," Gottingen, 1960.

191. Karpinskiy, V. N., Soln. dannyye 1, 70 (1961); 7, 73 (1961); Optika i spektroskopiya 8, 401 (1960).

192. Delbouille, L., Neven, L., and Roland, G., J. Quant. Spectrosc. Radiat. Transfer 3, 189 (1963).

193. Garbuni, M., "Fizika opticheskikh yavleniy" (Physics of Optical Phenomena), Energiya, Moscow, 1967.

194. Chechik, N. O., Faynshteyn, S. M., and Livshits, T. M., "Elektronnyye umnozhiteli" (Electronic Multipliers), Gostekhizdat, Moscow, 1957.

195. Morse, F., "Teplofizika" (Heat Physics), Nauka, Moscow, 1968.

196. Kirenkov, I. I., "Razrabotka i issledovaniye metodov absolyutnykh izmereniy i etalonov vysokikh temperatur" (Development and Investigation of Methods of Absolute Measurements and Reference Standards at High Temperatures), Doctoral Dissertation, VNIIM, Leningrad, 1965.

197. Kirenkov, I. I., Tr. VNIIM, No. 71(131), 5 (1963).

198. Brodskiy, A. D., and Savateyev, A. V., Izmer. tekhn., 5 (1960). /28

199. Brodskiy, A. D., op. cit., 6 (1961).

200. Solov'yev, V. I., and Brodskiy, A. D., Pribory i tekhn. eks., 2 (1962).

201. Brodskiy, A. D., "Novyye methody izmereniya nizkikh temperatur" (New Methods of Measuring Low Temperatures), Standartgiz, Moscow-Leningrad, 1962.

202. Lounasmaa, O., Uzpekhi fiz. nauk 103(2), 367 (1971).

203. Aref'yeva, N. V., Diykov, U. V., Dobrokhotov, A. G., Izrailov, K. S., Kirenkov, I. I., Nikitenko, L. V., and Shemetillo, N. V., Tr. VNIIM, No. 71(131), 14 (1963).

204. Kubo, R., "Termodinamika" (Thermodynamics), Mir, Moscow, 1970.

205. Hall, J., in "Temperatura i yeye izmereniye" (Temperature and Its Measurement), IL, Moscow, 1960.

206. Aliyeva, F. Z., Tr. VNIIM, No. 87(147), 5 (1966).

207. Beklemishev, A. V., "Mery i yedinitsy fizicheskikh velichin" (Measures and Units of Physical Quantities), Moscow, 1963.

208. Izmer. tekhn. 2, 24 (1970).

209. Aliyeva, F. Z., Tr. VNIIM, No. 87(147), 29(1966).

210. Gordov, A. N., Arzhanov, A. S., and Diykov, U. V., DAN SSSR 133, 4 (1960). /DAN SSSR = Doklady Akademii Nauk SSSR/

211. Kirenkov, I. I., Izmer. tekhn., 6 (1960).

212. Arzhanov, A. S., Gordov, A. N., and Diykov, U. V., Tr. VNIIM, No. 49 (109), 1 (1960).

213. Moser, H., "Symposium on Temperature, Its Measurement and Control in Science and Industry," Columbus, Ohio, USA, 1961.

214. Oishi, J., Awano, M., and Mochizuki, J. Phys. Soc. Japan 11, (3), 31 (1956).

215. Krakhmal'nikova, G. A., Tr. VNIIM, No. 71(131), 46 (1963).

216. Krakhmal'nikova, op. cit., No. 87(147), 48 (1966)

217. Sitnik, G. F., AZh 37, 1176 (1960).

218. Sitnik, G. F., op. cit., 39, 116 (1962)

219. Ribo, G., "Opticheskaya pirometriya" (Optical Pyrometry), GTTI, 1934.

220. Gordov, A. N., Tr. VNIIM, No. 9(69), 5 (1950).

221. Sitnik, G. F., Soobshch. GAISh (100), 56 (1957).

222. Sitnik, G. F., AZh 37, 75 (1960).

223. Kirenkov, I. I., Tr. VNIIM, No. 105 (165), 5 (1969).

224. De Vos, J. C., Physica 20 (10), 669 (1954).

225. Brounshteyn, A. M., Tr. GGO, No. 100, 93(1960).

226. Quinn, T. J., Brit. J. Appl. Phys., 18, 1105 (1967).

227. Krakhmal'nikova, G. A., and Lapina, E. A., Izmer. tekhn. 1, 44 (1970).

228. Stair, R., Johnston, R. G., and Halbach, E. W., J. Res. NBS 64A (4), 291 (1960).

229. Stair, R., Schneider, W. E., and Fussell, W. B., Appl. Optics 6, 101 (1967).

230. Epshteyn, M. I., Pribory i tekhn. eks. 3, 118 (1961).

231. Samson, J. A. R., J. Opt. Soc. Amer. 54, 6 (1964).

232. Knapp, R. A., and Smith, A. M., Appl. Optics 3, 637 (1964).

233. Kazachevskaya, T. V., and Ivanov-Kholodnyy, G. S., Isskusstv. sputniki Zemli 15, 81 (1963).

234. Kazachevskaya, T. V., Arkhangel'skaya, V. A., Ivanov-Kholodnyy, G. S., Medvedev, V. S., Razumova, T. K., and Chudaykin, A. V., op. cit., No. 15, 71 (1963). /283

235. Tousey, R., Watanabe, K., and Purcell, J., Phys. Rev. 83, 792 (1951).

236. Hinteregger, G. Ye., in "Nauchnoye ispol'zovaniye ISZ" (Scientific Applications of Artificial Earth Satellites), IL, Moscow, 1960.

237. Matsunaga, T. M., Jackson, R. S., and Watanabe, K., J. Quant. Spectr. Rad. Transfer 5, 329 (1965).

238. Rumsh, M. A., Lukirskiy, A. P., Karpovich, I. A., and Shchemelev, V. N., Pribory i tekhn. eks. (5), 67 (1960).

239. Lukirskiy, A. P., Rumsh, M. A., and Smirnov, L. A., Optika i spektroskopiya 9, 505 (1960).

240. Severnyy, A. B., Vestn. AN SSSR (11), 91 (1969).

241. Ivanenko, D. D., and Pomeranchuk, I. Ya., DAN SSSR 44, 343 (1944).

242. Schwinger, J., Phys. Rev. 75, 1912 (1949).

243. Tomboulian, D. H., and Hartman, P. L., Phys. Rev. 102, 1423 (1956).

244. Korolev, F. A., and Kulikov, O. F., Optika i spektroskopiya 8, 1 (1960).

245. Kodling, K., and Madden, R. P., J. Appl. Phys. 36, 380 (1965

246. Kinle, G., Izv. Kr. AO 16, 223 (1956).

247. Levshin, V. L., Panasyuk, Ye. I., and Pakhomycheva, L. A., Izv. AN SSSR, ser. fiz. 21(4), 612 (1957).

248. Bolotovskiy, B. M., Uspekhi fiz. nauk 62(3), 201 (1957).

249. Pariyskiy, N. N., and Gindilis, L. M., AZh 36, 539 (1959).

250. Mehlteretter, J. P., Ann. Apl. 24, 40 (1961).

251. Peytremann, E., Publ. Obs. Geneva 69, 84 (1964).

252. Fabry, Ch., and Buisson, H., C. R. Acad. Sci., Paris 175 (1), 156 (1922).

253. Plaskett, H. H., Publ. Dom. Astr. Obs. 2, 242 (1923).

254. Dunkelman, L., and Scolnik, R., J. Opt. Soc. Amer. 49, 356 (1959).

255. Johnson, F. S., J. Opt. Soc. Amer. 46, 101 (1956).

256. Yakovlev, S. A., and Shishatskaya, L. P., OMP 36, 53 (1969).

257. Kruger, M. Ya., Panov, V. A., Kulagin, V. V., Pogarev, G. V., Kruger, Ya. M., and Levinzon, A. M., "Spravochnik konstruktora optiko-mekhanicheskikh priborov" (Manual for the Designer of Mechanical-Optical Instruments), Mashinostroyeniye, Leningrad, 1968.

258. Drummond, A. J., and Hickey, J. R., Sol. Energy 11, 14 (1967).

259. "Kosmonavtika, Ser. Malen'kaya entsiklopediya" (Astronautics, Short Encyclopedia Series), Sov. Entsiklopediya, Moscow, 1970.

260. Koval'skiy, V. Ya., and Shklover, D. A., Geliotekhnika 1, 35 (1967).

261. Latil, J. P., Missiles and Space 11(5), 18 (1963).

262. Neuder, S. M., Appl. Optics 9, 1014 (1970).

263. Bartera, R. E., Inst. Environm. Sci. Annual Techn. Meet. Proc., Washington, D.C., 1967; Mt. Prospect, III, 681, 1967.

264. Castle, J. A., Inst. Environm. Sci. Annual Techn. Meet. /284
Proc., Washington, D.C., 1967; Mt. Prospect, III, 687, 1967.

265. Sitnik, G. F., AZh 36, 375 (1959).

266. Gordov, A. N., "Osnovy pirometrii" (Essentials of Pyrometry), Metallurgiya, 1964.

267. Lapina, E. A., Tr. VNIIM, No. 105(165), 115 (1969).

268. Thekaekara, M. P., Winker, A. R., and Riley, T. A., Preprint X-322-70-23, Jan. 1970, GSFC, Greenbelt, Maryland.

269. Hickey, J. R., Eppley Lab. Reprint Ser. No. 49, March-April 1969.

270. Sitnik, G. F., Soobsh. GAISh 109, 18 (1960).

271. Kharitonov, A. V., Izv. AN Kaz. SSR, ser. fiz.-matem., No. 1 (Astrofizika, Vol. 16), 78 (1963).

272. Arnulf, A., Barbier, D., Chalonge, D., and Canavaggia, R., J. Observat. 19(9-10), 149 (1936).

273. Glushneva, I. N., AZh 41, 212 (1964); 43, 80 (1966); Tr. GAISh 34, 53 (1966).

274. Sitnik, G. F., Tr. GAISh 22, 3 (1953).

275. Petrov, V. A., "Izluchatel'naya sposobnost' vysokotemperaturnykh materialov" (Emissivity of High-Temperature Materials), Nauka, Moscow, 1969.

276. Tijen, I. W., Philips Techn. Rev. 23(8/9), 1961/62.

277. Kirenkov, I. I., and Krakhmal'nikova, G. A., Tr. VNIIM, No. 105(165), 125 (1969).

278. Michelson, A. A., Phil. Mag., Ser. 5, 31, 256 (1891).

279. Maykel'son /Michelson/, A. A., "Svetovyye volny i ikh primeneniye" (Light Waves and Their Uses), Gostekhizdat, Moscow-Leningrad, 1934.

280. Maykel'son, A. A., "Issledovaniya po optike" (Investigations in Optics), Gosizdat, Moscow-Leningrad, 1937.

281. Fellgett, P., Thesis, Cambridge Univ., 1951; Symposium, Ohio State Univ., 1952; J. Phys. et Radium 19, 187 (1959); 19, 237 (1958).

282. Gebbie, H., and Vanasse, G., Nature 178, 432 (1956).

283. Gebbie, H., Phys. Rev. 107, 1197 (1957); J. Phys. et Radium 19, 230 (1958).

284. Jacquinot, P., XVII^{eme} Congres du GAMS, 1954; J. Phys. et Radium 19, 223 (1958).

285. Connes, J., Rev. Optique 40, 45 (1961); 40, 116 (1961); 40, 171 (1961); 40(5), 231 (1961).

286. Connes, J., and Connes, P., J. Opt. Soc. Amer. 56, 896 (1966)

287. Strong, J., J. Opt. Soc. Amer. 44, 352 (1954); 47, 354 (1957)

288. Strong, J., and Vanasse, G., J. Opt. Soc. Amer. 49, 844 (1959); 50, 113 (1960).

289. Merts, L., "Integral'nyye preobrazovaniya v optike" (Integral Transforms in Optics), Mir, Moscow, 1969.

290. Zhakino /Jacquinot/, P., Uzpekhi fiz. nauk 72(4), 799 (1960). 78(1), 123 (1962).

291. Gebbi /Gebbie/, G. /H./, and Tviss, R., Uspekhi fiz. nauk 99(1), 87 (1969).

292. Hunten, D. M., Science 1962 (3851), 313 (1968).

293. Richards, P., in "Dlinnovolnovaya infrakrasnaya spektroskopiya" (Long-Wave Infrared Spectroscopy), Mir, Moscow, 1966.

294. Connes, J., and Connes, P., in "Infrakrasnaya astronomiya" (Infrared Astronomy), Mir, Moscow, 1971

295. Connes, P., Ann. Rev. Astron. Astroph. 8, 209 (1970).

296. Nyuberg, N., DAN SSSR 4, 278 (1934).

297. Kiselev, B. A., and Parshin, P. F., Optika i spektroskopiya /285 12, 311 (1962).

298. Parshin, P. F., Op. cit. 16, 507 (1964).

299. Shnyrev, G. D., "Pribory dlya fur'ye-spektrometrii" (Instruments for Fourier Spectrometry), Candidate's Dissertation, Institute of Crystallography of the USSR Academy of Sciences, Moscow, 1966.

300. Petrov, I. P., "O poluchenii i registratsii interferogramm v fur'ye-spektrometrii" (Obtaining and Recording Interferograms in Fourier Spectrometry), Candidate's Dissertation, Institute of Crystallography of the USSR Academy of Sciences, Moscow, 1967.

301. Taranova, O. G., "Infrakrasnyye spektry sobstvennogo izlucheniya verkhney atmosfery Zemli" (Infrared Spectra of the Intrinsic Emission of the Upper Terrestrial Atmosphere), Candidate's Dissertation, Moscow State University-GAISh, Moscow, 1969.

302. Gorskiy, S. M., and Zverev, V. A., Izv. vuzov, Radiofizika 11(8), 1205 (1968).

303. Kiselev, B. A., and Pushkin, Yu. D., OMP 8, 33 (1966).

304. Shnyrev, G. D., Grechushnikov, B. N., and Moroz, V. I., ATs /Astron. tsirk./, No. 302 (1969).

305. Bakhshiyev, N. G., Optika i spektroskopiya 2, 815 (1957).

306. Kiselev, B. A., and Parshin, P. F., op. cit. 17, 940 (1964).

307. Connes, J., Connes, P., and Maillard, J. P., "Atlas des spectres dans le proche infraronge de Venus, Mars, Jupiter et Saturne" (Atlas of the Spectra of the Far Infrared of Venus, Mars, Jupiter, and Saturn), C.N.R. Sci., Paris, 1969.

308. Rogerson, J. B., Ap. J. 130, 985 (1959).

309. Peyturaux, R., Ann. Ap. 15, 302 (1952).

310. Peyturaux, R., op. cit., 18, 34 (1955).

311. Canavaggia, R., and Chalonge, D., Ann. Ap. 9, 143 (1946).

312. Pierce, A. K., McMath, R. R., Goldberg, L., and Mohler, O. C., Ap. J. 112, 289 (1950).

313. Pierce, A. K., Ap. J. 120, 221 (1954).

314. Mitchell, W. E., Ap. J. 129, 93 (1959).

315. David, K. H., and Elste, G., Z. Ap. 54, 12 (1962).

316. Krat, T. V., Izv. GAO 17(137), 7 (1948).

317. Lena, P. J., Solar Phys. 3, 28 (1968).

318. Saiedy, F., MN 121, 483 (1960).

319. Kozhevnikov, N. I., AZh 34, 881 (1957).

320. Bonnet, R., Ann. Ap. 31, 597 (1968).

321. Bonnet, R., and Blammont, J. E., Solar Phys. 3, 64 (1968).

322. Bonnet, R., L'Astronomie (225), June 1966.

323. Lacis, A. A., and Matsuchima, S., J. Opt. Soc. Amer. 56, 1239 (1966).

324. Lipayeva, N. A., and Makarova, Ye. A., Soobshch. GAISh 147, 14 (1967).

325. Michard, R., BAN 11, 227 (1950).

326. Kozak, P. P., Soln. dannyye 1962(11), 54 (1964); (8), 56 (1964); (11), 51 (1964).

327. Houtgast, J., and Namba, O., BAN 20 87 (1968).

328. Shajn, G. A., MN 94, 642 (1934).

329. Mulders, G. F. W., Z. Ap. 11, 132 (1935).

330. St. John, C. E., Moore, C. E., Ware, L. M., Adams, E. F., and Babcock, H. D., Publ. Carnegie Inst. Washington, 396, 1928; Mt. Wilson Obs. Papers 3, 1928.

331. Houtgast, J., Proc. Konikl. Nederl. acad. wet. 1368(5), 306 (1965). /286

332. Wempe, J., Astron. Nachr. 275(3), 97 (1947).

333. Moore, C., Minnaert, M., and Houtgast, J., "Second Revision of Rowland's Preliminary Tables of Solar Spectrum, Wave Lengths 2935-8772 Angstroms," Washington, 1966.

334. Khetsuriani, Ts. S., Byull. Abastumanskoy Astrofiz. obs. 36, 57 (1968).

335. Jager, C. de, Neven, L., and Migeotte, M. V., Ann. Ap. 19, 9 (1956).

336. Jager, C. de, Univ. Liege Inst. Astrophys. 2, 151 (1964).

337. Allen, C. W., Ap. J. 89, 165 (1937).

338. Jager, C. de, Mem. Soc. Roy. Sci. Liege 9, 151 (1961).

339. McAlister, H. C., "A Preliminary Photometric Atlas of the Solar Ultraviolet Spectrum from 1800 to 2965 Angstroms," Univ. Colorado Print Service, 1960.

340. Holweger, H., Z. Ap. 65, 365 (1967).

341. Bretz, M., Z. Ap. 38, 259 (1956).

342. Page, B. E. J., MN 115, 493 (1955).

343. Adam, M. G., MN 98, 112 (1937).

344. Allen, C. W., MN 109, 343 (1949).

345. Labs, D., and Neckel, H., Solar Phys. 15, 79 (1970).

346. Thekaekara, M. P., private communication, 1969.

347. Herschel, J., Philos. Trans. 130, 1 (1840).

348. Langley, S. P., Acad. Sci. C.R. 95, 482 (1882).

349. Minnaert, M., BAN 2, 75 (1924).

350. Moon, P., J. Franklin Inst. 230, 583 (1940).

351. Thekaekara, M. P., NASA Sp., 74, Washington, 1965.

352. Angstrom, A. K., and Angstrom, K. H., Sol. Energy 13, 243 (1971).

353. Wilsing, J., Publ. Astroph. Obs. Potsdam 22(66), 1913; 23 (72), 1917.

354. Wilsing, J., and Sheiner, I., Publ. Astroph. Obs. Potsdam 19(56), 1909.

355. Milne, E. A., Phil. Trans. R. Soc. London A223, 201 (1922).

356. Muller, G., and Kron, E., Publ. Astroph. Obs. Potsdam 22(64), 1913.

357. Dufay, J., Ann. Ap. 5, 85 (1942).

358. Canavaggia, R., Chalonge, D., Egger-Morean, M., and Oziol-Pettey, H., Ann. Ap. 13, 355 (1950).

359. Peyturaux, R., C. R. Acad. Sci. 252, 668 (1961); 258, 1159 (1964).

360. Peyturaux, R., Ann. Ap. 31, 227 (1968).

361. Sitnik, G. F., Doctoral Dissertation, Moscow State Univ., Moscow, 1955; ATs (167), 1956.

362. Makarova, Ye. A., Candidate's Dissertation, Moscow State Univ.-GAISh, Moscow, 1956.

363. Houtgast, J., Solar Phys. 3, 47 (1968); 15, 273 (1970).

364. Labs, D., and Neckel, H., Z. Ap. 55, 269 (1962); 57, 283 (1963).

365. Labs, D., Z. Ap. 44, 37 (1957).

366. Wohl, H., Wittman, A., and Schroter, E. H., Solar Phys. 13, 104 (1970).

367. Gingerich, O., and Jager, C. de, Solar Phys. 3, 5 (1968).

368. Stair, R., Johnston, R. G., and Bagg, T. C., J. Res. NBS 53, /2 113 (1954).

369. Webb, J. J., preprint GSFC, 1966.

370. Thekaekara, M. P., and Rogers, J. F., preprint GSFC, 1967.

371. Thekaekara, M. P., Stair, R., and Winker, A. R., preprint GSFC, 1968.

372. Webb, J. J., Duncan, C. H., McIntosh, R., and Lester, D., Appl. Optics 9, 345 (1 70).

373. Arvesen, J. C., Griffin, R. N., and Pearson, B. D., Appl. Optics 8, 2215 (1969).

374 Heath, D. F., J. Atm. Sci. 26, 1157 (1969).

375. Heath, D. F., J. Geophys. Res., 1971, in press; preprint, GSFC X-651, 71-116, 1971

376. Baum, W. A., Johnson, F.S., Oberly, J. J., Rookwood, C. C., Strain, C. V., and Tousey, R., Phys. Rev. 70, 781 (1946).

377. Rense, W. A., Phys. Rev. 1, 299 (1953).

378. Tousey, R., Space Sci. Rev. 2, 35 (1963).

379. Tousey, R., Quart. J. Roy. Astron. Soc. 5, 123 (1964).

380. Friedman, H., "Space Science," ed. by Le Galley, 1963.

381. Hinteregger, H. E., Space Sci. Rev. 4, 461 (1965).

382. Hinteregger, H. E., Hall, L. A., and Schmidtke, G., Space Res. V, 1175 (1965).

383. "Ultravioletovoye izlucheniye Solntsa i mezhplanetnaya sreda" (Ultraviolet Radiation of the Sun and Interplanetary Environment), ed. by Nikol'skiy, G. M., IL, Moscow, 1962.

384. Kachalov, V. P., Pavlenko, N. A., and Yakovleva, A. V., Izv. AN SSSR, ser. geofiz. (9), 1099 (1958).

385. Kachalov, V. P., and Yakovleva, A. V., Izv. Kr. Astron. Obs. 27, 5 (1962).

386. Mandel'shtam, S. L., in "Uspekhi SSSR v issledovanii kosmicheskogo prostranstva" (Advances of the USSR in Investigating Outer Space), Nauka, 1968.

387. Burton, W. M., and Ridgeley, A., Solar Phys. 14, 3 (1970).

388. Gingerich, O., and Rich, T. C., Astron. J. 71, 161 (1966).

389. Widing, K. G., Purcell, J. D., and Sandlin, G. D., Solar Phys. 12, 52 (1970).

390. Sandlin, G. D., and Widing, K. G., Ap. J. Letters 149, L 129 (1967).

391. Detweiler, C. R., Garrett, D. L., Purcell, J. D., and Tousey, R., Ann. Geoph. 17, 9 (1961).

392. Wilson, N., Tousey, R., Purcell, J. D., Johnson, F. S., and Moore, C. E., Ap. J. 119, 590 (1954).

393. Malitson, H. H., Purcell, J. D., Tousey, R., and Moore, C. E., Ap. J. 132, 746 (1960).

394. Purcell, J. D., Packer, D. M., and Tousey, R., Space Res. 1, 581 (1960).

395. Packer, D. M., and Lock, C., J. Opt. Soc. Amer. 42, 879 (A) (1952).

396. Timothy, A. F., and Timothy, J. C., J. Geophys. Res. 75, 6950 (1970).

397. Bonnet, R. M., and Courtes, G., Ann. Ap. 25, 367 (1962).

398. Bonnet, R. M., Blammont, J. E., and Gildwarg, P., Ap. J. Letters 148, 115 (1967).

399. Parkinson, W. H., and Reeves, E. M., Solar Phys. 10, 342 (1969).

400. Prag, A. B., and Morse, F. A., J. Geophys. Res. 75, 4613 (1970).

401. Farmer, C. B., and Todd, S. J., Appl. Optics 3, 453 (1964).

402. Murcray, F. H., Murcray, D. G., and Williams, W. J., Appl. Optics 3, 1373 (1964).

403. Badinov, I. Ya., Andreyev, S. D., and Poberovskiy, A.V., in "Problemy fiziki atmosfery" (Problems of Atmospheric Physics), No. 3, p. 189, Leningrad State University, 1965.

404. Beer, R., Nature 209, 1266 (1966).

405. Sitnik, G. F., ATs, No 344, 1965.

406. Eddy, J., Lena, P. J., and MacQueen, R. M., Solar Phys. 10, 330 (1969).

407. Eddy, J. A., Lee, R. H., Lena, P. J., and MacQueen, R. M., Appl. Optics 9, 439 (1970).

408. Gebbie, H., Nature 220, 893 (1968).

409. Biraud, J., Gay, J., Verdet, J. P., and Zeau, J., Astron. Astroph. 2, 413 (1969).

410. Gay, J., Astron. Astroph. 6, 327 (1970); 7, 24 (1970).

411. Gay, J., Leguex, J., Verdet, J. P., Turon-Laccarien, P., Bardet, M., Roucher, J., and Zeau, J., Ap. Letters 2, 169 (1968).

412. Shimabukuro, F. J., Solar Phys., 18, 247 (1971).

413. Goldberg, L., and Muller, E. A., Ap. J. 118, 397 (1953).

414. Labs, D., and Neckel, H., Solar Phys. 19, 3 (1971).

415. Baluteau, J. P., Astron. Astroph. 14, 428 (1971).

416. Clark, T. A., Courts, G. R., and Jennings, R. E., Phil. Trans. Roy. Soc. London A270 (1202), 55 (1971).

417. Sacotte, D., and Bonnet, R. M., Astron. Astroph. 17, 60 (1972).

418. Thekaekara, M. P., Optical Spectra 6(3), 32 (1972).

419. "Pretsizionnyye radiatsionnyye izmereniya v meteorologii" (Precision Radiation Measurements in Meteorology), revised under the editorship of K. Ya. Kondrat'yev and L. V. Krasil'shchikov, Gidrometeoizdat, Leningrad, 1972.

420. New Techn. Space Astron. Int. Astron. Union Symp., No. 41, Munich, 1970, Dordrecht, 1971

421. Zuyev, V. Ye., "Rasprostraneniye vidimykh i infrakrasnykh voln v atmosfere" (Propagation of Visible and Infrared Waves in the Atmosphere), Sov. radio, Moscow, 1970.

422. "Modelirovaniye teplovykh rezhimov kosmicheskogo apparata v okruzhayushchey yego sredy" (Modeling of a Spacecraft and the Environment Surrounding It), ed. by G. I. Petrov, Mashinostroyeniye, Moscow, 1971.

423. Koval'skiy, V. Ya., Geliotekhnika 3, 46 (1972).

424. "Infrared Detection Techn. Space Res.," Dodrecht, 1972.

☆ U.S. GOVERNMENT PRINTING OFFICE: 1974—739-161/139